LATERAL WEB BEHAVIOR OF INTERACTIVE WEB SYSTEMS

By

BIN FANG

Bachelor of Science
Fuxin Mining College
Fuxin, Liaoning, P. R. China
1982

Master of Science
Oklahoma State University
Stillwater, Oklahoma
1985

Submitted to the Faculty of the
Graduate College of the
Oklahoma State University
in partial fulfillment of
the requirements for
the Degree of
DOCTOR OF PHILOSOPHY
December, 1990

LATERAL WEB BEHAVIOR OF INTERACTIVE

WEB SYSTEMS

Thesis Approved:

Gary E. Young

Thesis Adviser

John J. Shelton

James L. [illegible]

G. Steven Gipson

Norman N. Durham

Dean of the Graduate College

ACKNOWLEDGEMENTS

During the working of this research project I have had the pleasure and privilege of interacting with my committee. It has been indispensable during the course of this research that my committee members have been showing their understanding, encouragement, and direction. As the thesis advisor Dr. Gary Young has shown his interest, trust, and support. With his deep understanding and great expertise on the web handling problem Dr. J. J. Shelton spent long hours of conscientious work and gave me a lot of guidance and many invaluable advises on doing this research work. Dr. J. K. Good and Dr. G. S. Gipson have offered many advises and given careful attention to the details of the analysis. I sincerely appreciate the efforts of the committee members.

I would like to take this opportunity to thank the Web Handling Research Center for giving and supporting me to work on this project. Many of my friends and fellow students have shown their understanding and help. I am very grateful to all of them. Special thanks are due to Dr. C. Kardamilas for his kind permission in using the data acquisition system he developed, which has had a great help in the experimental study. The patience and support of my family during my long college-attending years is greatly appreciated.

TABLE OF CONTENTS

Chapter Page

LIST OF TABLES

LIST OF FIGURES

Figure Page

Figure Page

Figure Page

Figure		Page

NOMENCLATURE

A	pre-entering roller or span
a_i	scaled coefficients, $a_i = \dfrac{C_i}{L\theta_L}$, i = 1, 2, 8
B	entering roller or span
b_i	scaled coefficients, $b_i = \dfrac{C_i}{LQ_l/T}$, i = 1, 2, 8
C	guide roller, post-entering roller, or air-drum
C_i	coefficients in governing equation, i = 1, 2, ..., 12
ch	hyperbolic cosine, cosh
d_i	scaled coefficients, $d_i = \dfrac{C_i}{M_l/T}$, i = 1, 2, 8
E	modulus of elasticity, moving dam, or light-emitting sensor
F	moving web
f	a function
f_1, f_2, f_3	functions of KL
g	acceleration of gravity; a function
H_{gl}	half gap length, one half of the quantity of $(W_s - W)$
H_{md}	gap length of moving dam to the nominal position of near side web edge
I	moment of inertia of the web $(tW^3/12)$
K	a parameter, $(T/EI)^{1/2}$
L	web span length
l	location of lateral load disturbance source from upstream roller
M	bending moment; oscillation magnitude in lateral web motion

M_l	lateral moment at disturbance location
M_r	friction related lateral moment at entering roller
M_{y_0}	oscillation magnitude in lateral web motion at upstream roller
M_{y_L}	oscillation magnitude in lateral web motion at downstream roller
M_{y_0}/H_{gl}	input ratio (IR)
$(M_{y_0}/H_{gl})_{cr}$	critical input ratio
M_{y_L}/M_{y_0}	amplitude factor (AF)
m	distributed lateral moment
N	shear force
N_r	friction related shear force at entering roller
p	pressure
p_i	web system parameters, i = 1, 2, ..., 8
Q	volume air flow rate; lateral force
Q_1	friction related lateral force parameter, N_r/TK
Q_2	friction related lateral moment parameter, M_r/T
Q_3	steering related parameter, θ_L/K
Q_4	disturbance related lateral force parameter, Q_l/TK
Q_5	disturbance related lateral moment parameter, M_l/T
Q_l	lateral force at disturbance location
r	radius of air drum
r_{m1}, r_{m2}	moment ratios
r_{n1}, r_{n2}, r_{n3}	shear force ratios
s	Laplace transform variable
sh	hyperbolic sine function, sinh
T	total tension in web
T_1	web span time constant, L/V
t	web thickness; time

V longitudinal web velocity

V_o valve opening

W web span width

W_s slot width on air drum

w distributed lateral force function

x longitudinal coordinate for web span

y lateral web displacement

z lateral displacement of guide roller; Z-transform variable

δ Dirac delta function

θ guide roller steering angle

ω oscillation frequency

ω^* normalized oscillation frequency, $T_1\omega$

ξ normalized longitudinal coordinate of web span, x/L

CHAPTER I

INTRODUCTION

Definition of a Web System

In order to introduce a general definition for a web system, one has to know what is meant by a "web". A common definition for a web is that it is any material in continuous flexible strip form. The characteristics of a web are either endless or very long in relation to its width, and very wide in relation to its thickness. There are a variety of web materials, such as paper, textiles, plastics, metals, composites, food products, fiberglass, and combinations of above.

Many products and devices in various industries can be included in the above definition even though they may be called different names such as "film", "belt", "strip", "felt", "foil" and "fabric". The moving of materials in web form is called web handling. There is a variety of interests in web handling research. A common web handling or storage form is to wind onto or unwind from a roll. The mechanical behavior of a web during winding is important in controlling the quality of a wound roll. In trying to investigate this mechanical behavior a web system for winding must be formed. A winding model for the web system can then be constructed. The problems such as the effect of a nip roll on the winding roll, winding roll defect analysis, and web stresses during roll winding can be investigated in detail through the web system for winding. Other analyses which need corresponding web systems include web wrinkling, dynamic coefficient of traction between web media and rollers, control and measurement of web rolling and winding air films, control of web handling processes incorporating uncertainty and web stresses induced by spreading devices, to name only a few.

In web handling, the lateral web position at a certain location is often pre-specified. To keep a moving web at its desired position, guiding devices are required to effectively control the lateral web position. In order to make the control accurate and stable, the dynamics of lateral web motion should be well understood. By doing so a web system for lateral web motion and control must be selected. A simple web system consists of a moving web passing between two parallel rollers. Such a system can be used to analyze the lateral web motion under the parallel roller condition. In order to investigate both the lateral web motion and the control of the lateral web position, the simple web system must be modified. For example one may put a guide roller at the downstream roller location instead of a parallel one. This modified web system can be used to investigate the lateral web motion under the control of a guide roller provided there is sufficient friction between web and both rollers [1]. When the friction is not large enough, the lateral moment and shear force in the web span may be transferred to the web span upstream. Under such a condition interaction in terms of lateral force and moment occurs between two adjacent web spans. To investigate the lateral web behavior under interaction an interactive web system should be considered. Besides insufficient friction, considerable lateral load disturbances such as those from an air-bar in the process line, may also cause interaction. Unlike the friction which causes the interaction between two web spans, the lateral load disturbances cause interaction between different portions of a web span. The subject for this project is to investigate the effect of the interaction of lateral moment and shear force on the lateral web behavior. Thus the focal point of the research is the analysis of the lateral web behavior in interactive web systems.

An interactive web system may consist of two web spans. As mentioned above the insufficient friction between the web and the entering roller can cause interaction between two web spans. For the sake of identification, this type of interactive systems can be defined as a type I interactive system. A schematic representation for such a web system is shown in Fig. 1. In this figure the three rollers are, from left to right, pre-entering roller, entering roller, and guiding roller. The two spans are, also from left to right, the pre–entering span and the entering span. When there are considerable lateral loads acting on a web span, even in the cases without interaction between spans due to insufficient friction, the interaction still exists between portions of the web span divided by those loads. One such interactive web system is the web span supported by an air flotation device. One can name this type of system a type II interactive system. In Fig. 2 such a system with a pair of concentrated side loads is schematically illustrated. In this system only the entering and guiding rollers with the entering span are present. The friction between the web and rollers is large enough to isolate adjacent web spans from interaction in the lateral moment and shear force. A pair of loads, a moment and a force, act at the location l from the upstream roller. A more complicated interactive web system has the interaction induced by both insufficient friction and side load disturbances, i.e., the combination of interactive systems of type I and type II. Such a system is schematically shown in Fig. 3, in which the insufficient friction at the entering roller causes interaction between two web spans and the concentrated side loads on the pre-entering span cause interaction between two portions of the span. This type of interactive web system may be categorized as a type III interactive system. In addition to the one shown in Fig. 3, other forms of a type III interactive system exist. For example the lateral load disturbances may act on the entering span. Another one is where both web spans have lateral load disturbances. Thus in comparison type III interactive systems are more complicated than each of type I or type II interactive systems.

State of the Art of Web System Investigation

Only a few published articles can be found in dealing with web handling theory on lateral web motion. One of the pioneers is Shelton [1, 2, 3]. In his thesis [1], the fundamental theory for lateral web motion has been established. Based on the theory, an extensive investigation on the statics and dynamics of a single moving web span has been performed.

Soong and Li [4] have proposed a procedure for analyzing a multiroll endless web system. In their approach the web is divided into endless, parallel strips which are longitudinally elastic and possess shear rigidity. For each individual strip between rollers, the string approximation has been made. Using such an approach, the problems concerning edge guide force, steering moment, pivoting cylinders, rate of drift and effect of conicity of web, taper of cylinder, and initial unstretched length of the web can be analyzed.

Sievers, et. al.. [5] have investigated the lateral web dynamic behavior of a moving web using a model as either a string, a Bernoulli-Euler beam, or a Timoshenko beam. They have found that the agreement with experimental results can be found only when the web is modeled as a Timoshenko beam, i.e., the one including the shearing effect on the lateral web motion.

Young, Shelton, and Kardamilas [6] constructed a new model for lateral web dynamics using the theory established by Shelton [3]. A parameter estimation scheme is further used to tune the model for imperfections not originally incorporated. The modeling of lateral web dynamics through a stochastic approach has been further investigated by Kardamilas and Young [16].

At high speed, air can be entrained between the web and rollers. Extensive investigations have been done for such air entrainment problems, termed as foil bearing problems. The self-acting foil bearings were first investigated by Van Rossum [7]. Among other later researchers, Eshel and Elrod [8] have investigated such bearings for a perfectly flexible web. The effect of introducing externally pressurized fluid into a foil bearing has been examined by Wildmann [9] for foils of finite stiffness and finite width grooves, but limited to small changes in gap so that linearization about an average gap could be done, and by Barlow [10] for perfectly flexible foil and finite width grooves, but not limited to small gap changes.

The theory for foil bearing assumes that the flow field involved can be described using the Reynolds equation, which is applicable only for those flow fields with small Reynolds numbers. Basheer [11] has done an experimental study on the air entrainment problem in web handling research based on the foil bearing theory. When an air flotation device is introduced for non-contact web handling, the web is supposed to be totally supported by pressurized air. The flow fields can be very complicated ranging from laminar to turbulent flow. No working model has been found in the literature to describe adequately an air flotation device.

The analyses of both statics and dynamics for the type I interactive system performed by Young, Shelton, and Fang have been published [12, 13]. A model for the system has been developed which expends Shelton's work [1] to this case and utilizes beam theory which is valid when the web is not in a wrinkled or slack edge state. The boundary conditions and static solutions for the three different types of interaction are established. In the circumferential slippage mode a negative steering effect has been identified. A steering effect description function is established which allows prediction of this phenomenon which can be avoided by proper choice of system parameters. The dynamic equations for web span interaction are derived. Due to the three different possible interaction modes the analysis relies heavily on the static analysis of the type I interactive system. A Fourier analysis has also been included. The frequency analysis reveals that if both web spans are in the under-damped mode, large oscillations will occur in some range of steering frequencies. Experimental verification has been given for both the static and dynamic analyses.

Since the establishment of the Web Handling Research Center (WHRC) at Oklahoma State University (OSU), many fundamental research activities on web handling have been on-going. The research projects include: web winding and unwinding, on-line web tension measurement, web stress induced by spreading devices, web wrinkling, control of web handling processes incorporating uncertainty and delay, distributed control of tension in web handling systems, dynamic coefficient of traction between web media and rollers, dynamic analysis of discrete webs, out-of-plane dynamics of a moving web, tension distribution across a web, the measurement of web stresses during roll winding, fracture mechanics characterization of slit edges in thin sheets and membranes, the regulation of tension during roll winding/unwinding with disturbances, and the control and measurement of web rolling and winding air films. There have been many papers published and a number of reports and theses written on those projects, which represent the state of the art in the public literature of web system investigation. Those papers, reports, and theses can be easily located using the database WEBSCAN developed at WHRC.

Scope of Study

The investigation of the lateral web behavior in interactive web systems is one of the research projects at WHRC. A special interest in this research is to investigate the dynamic interaction of web spans over an air flotation device. The work on the type I interactive system, which is part of this research, has been published [12, 13].

The interest of this research is on lateral web behavior only. Thus the out-of-plane effect due to an air flotation or other type of device is not considered. Some devices, like an air flotation device, are capable of imparting lateral loads to a moving web span. Such a web system becomes a type II interactive system if the friction between the web and rollers is sufficient to isolate adjacent web spans from lateral moment and shear force transfer. On the other hand if the friction is not sufficient the web system is a type III interactive system. This research is concentrated on the analyses of both type II and type III interactive systems. In theoretical analyses, Shelton's work [1] has been extended to including lateral load disturbances. Further investigation is inhibited due to the lack of models for describing the relationship between the lateral load disturbances and the lateral web motion. As in the case involving an air-bar, the model for the lateral load disturbance from the air-bar is currently not available due to the complexity of the air flow field between the web span and air-bar in combination with the elastic characteristics of the web span.

An experimental study has been done on a type II interactive system. The Shelton machine with an air-bar unit mounted is used for the experiments. The detailed experimental set-up will be described in Chapter V of this thesis. A parameter identification technique has been used to establish the condition for the autoregressive and moving average (ARMA) model applicable range. An extensive study on the amplitude factor, which is the ratio of oscillation amplitudes in lateral web displacement at the downstream span to that of the upstream span, has been performed for several system and disturbance factors. The concept of critical input ratio is introduced to establish the amplification-free condition for the web system. This study provides guidelines for a system designer in designing web systems involving a series of air-bar units. The design should guarantee that the web system is always operated in the amplification-free condition. The amplification of lateral web displacement will make either the control of lateral web position at the downstream difficult or break down of the web process line due to the instability in lateral web motion.

When using a narrow web, the web system in the experimental study may become a type III interactive system. With a small difference between the slot length of the air-drum and the web width, which is termed the gap width, the misalignment in the air-bar unit can cause a bistable state for the lateral web position. Even though there is no steering from the downstream roller, the action of the air-drum at one stable state of the web may cause a moment transfer at the upstream roller. As a result, the negative steering of the moment transfer may switch the web to the other stable state. While this process continues, the system enters a limit cycle in the lateral web oscillation. While doing the experiment with both a narrow web and gap, such a limit cycle has occurred. Based on the study from the type I interactive system, important parameters have been identified to eliminate the limit cycle. This result has a practical significance in solving similar problems encountered in industrial applications.

Fundamental Theory and Assumptions

The fundamental theory has been developed by Shelton [1] for lateral web motion. All the analyses done in this research on the lateral web behavior of interactive web systems are based on this theory. The work for the type I interactive systems has been published [12, 13], which will not be included in this thesis. Only the investigation on the type II and type III interactive systems will be reported in the following chapters. The research for the lateral web behavior in type II and type III interactive systems extends this theory to incorporate lateral load disturbances and lateral moment and force transfer due to insufficient friction between the web and rollers. Some major assumptions are given below.

A web is modeled as a Bernoulli-Euler beam in this analysis. Thus most of the common assumptions of beam theory are used. Some other assumptions relating specifically to webs are also made.

It is assumed that the deflection is small enough that the web edge is never slack. The conditions which satisfy this assumption are given by Shelton [1].

It is assumed that the longitudinal velocity in the web spans is constant. The buckling strength of a web in compression is extremely low. It is assumed that this buckling strength is negligible in comparison to the operating tension. The tension is assumed to be constant and great enough that sagging of the web is very small.

The stress distribution in the web is assumed to be linear and the web is elastic in the range of stresses encountered. The deflection due to shear stress is assumed negligible, which is valid for relatively long free web spans.

In considering the lateral load disturbances from an air-bar, it is assumed that the length wrapped around the air-bar is small compared to the web span length in the air-bar unit. This enables one to approximate the finite wrapping length as a line instead of a finite section, therefore the distributed lateral load disturbances are replaced by concentrated ones, which follows from the St. Venant's principle (refer to, for example, [17]). A similar assumption has been made in dealing with the friction force and moment at the entering roller in type I and type III interactive system analyses.

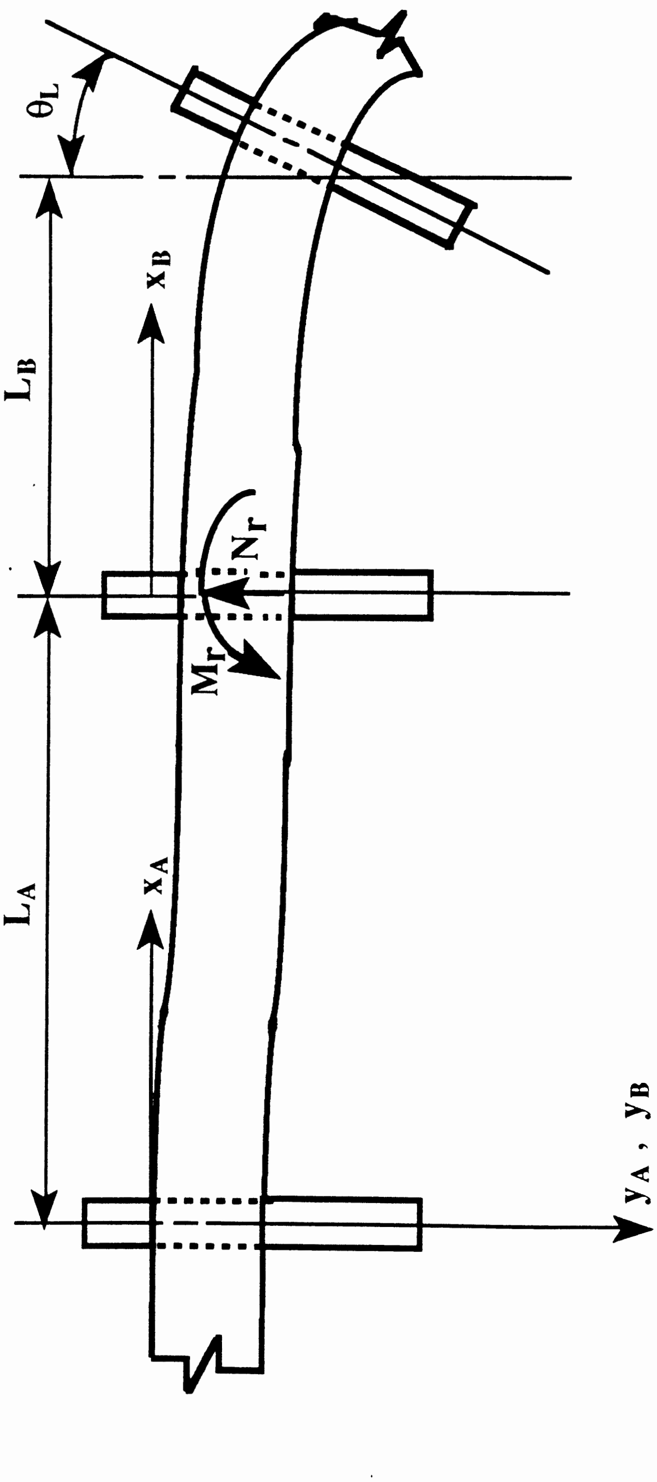

Figure 1. Interactive Web Spans

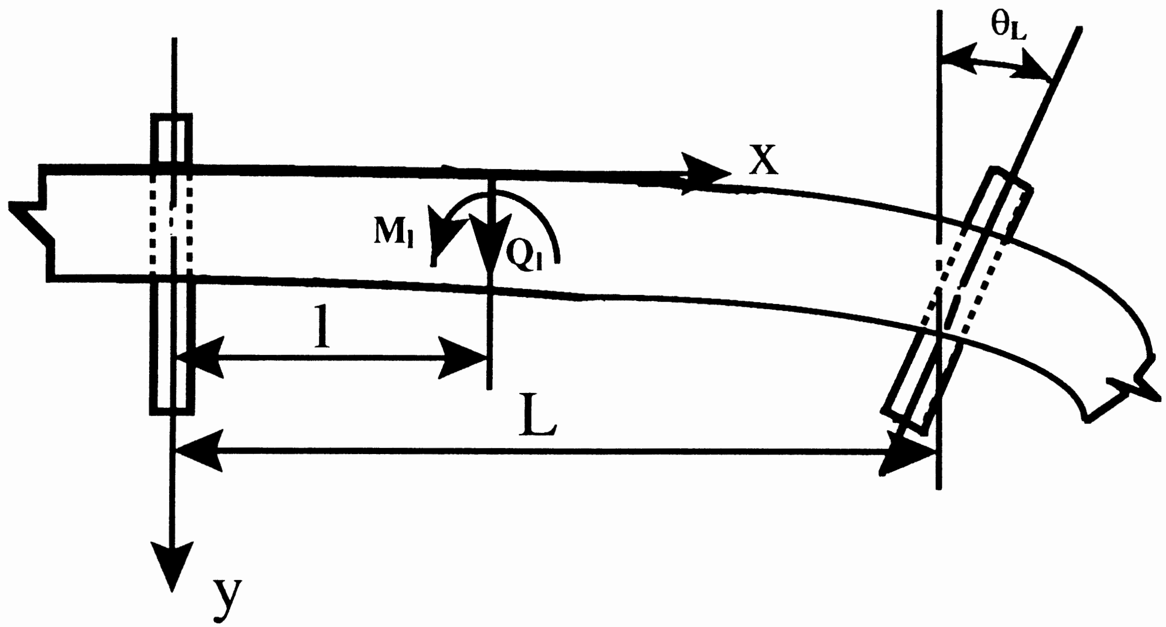

Figure 2. A Web Span With a Pair of Concentrated Lateral Loads

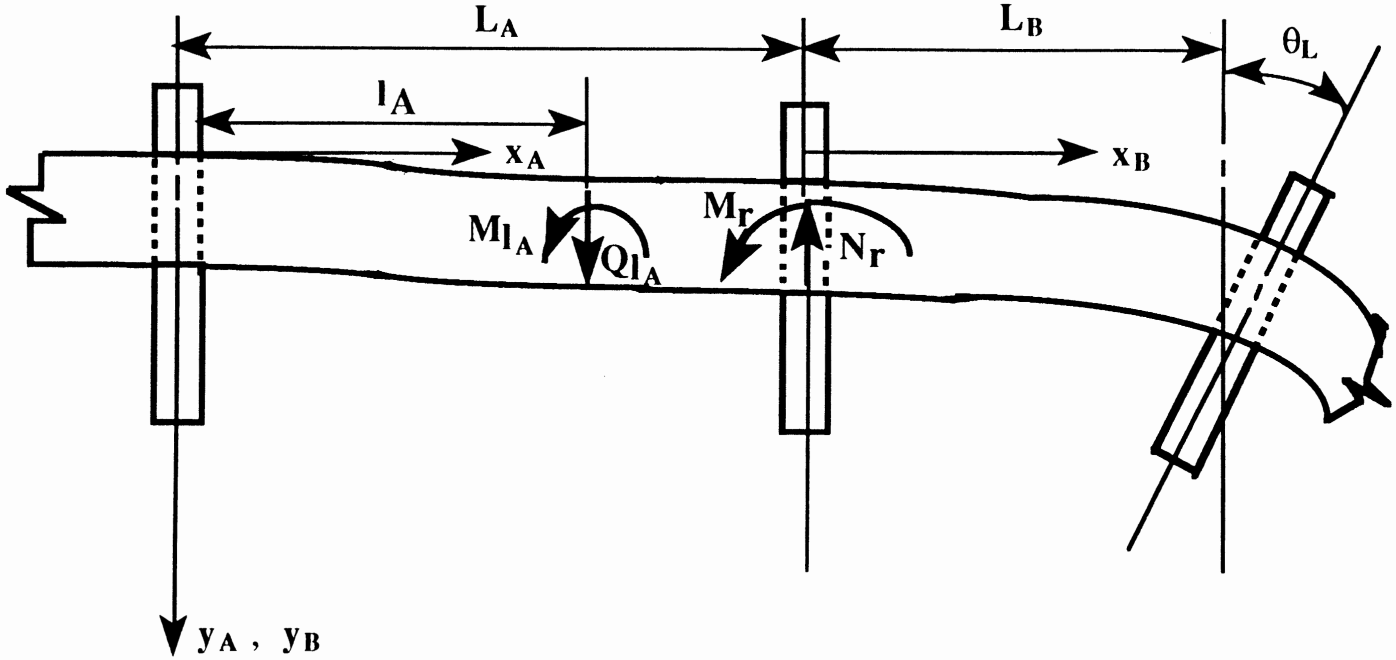

Figure 3. An Interactive Web System With Lateral Loads on Pre-Entering Span

CHAPTER II

STATICS WITH SIDE LOADS ON A MOVING WEB SPAN

A web moves longitudinally in most web systems considering the lateral web position and its control. The terms "static" and "steady state" in the context of lateral web motion do not mean that the web is stationary in longitudinal direction, but that there is no change in lateral web position. Thus statics is the analysis of lateral web behavior under the steady state lateral web condition.

In a process line, a moving web may experience some disturbances laterally, longitudinally, or in the normal direction. When a web goes through a drying process, for example, it passes a series of air drums and supporting rollers. The complex flow field in the oven provides all kinds of disturbances on the web. In non-contact handling, air-turn bars have to be used to support the web and change its direction. The supplied air under such conditions can also generate disturbances on the web. This project investigates the lateral web behavior. Thus only the lateral disturbances are considered. Furthermore, applying St. Venant's principle, the lateral force and moment disturbances can be treated as concentrated lateral forces and moments applied at certain locations along a web span.

Lateral disturbances on the web include lateral linear and angular displacements, lateral forces, and lateral moments. The effects of linear and angular displacements at the end of the span can be easily deduced from the work by Shelton [1]. The effects of lateral forces and moments, however, need more detailed analysis before understanding can be gained. A thorough analysis can relate the lateral web behavior to the system parameters thus providing a system designer with useful information.

Governing Equation and Solution

A web system with side loads on its moving web span is a type II interactive system if the friction between the web and rollers is sufficient to prevent the transfer of moment and shear force between spans. Such a system has been illustrated in Fig. 2. The fundamental theory for lateral web motion will be used to derive the governing equations needed in describing the lateral static behavior of a moving web in a type II interactive system. But one has to deal with the side load effect first so that the theory can be extended to include the case with side loads acting on a moving web span.

The coordinate system describing a web span and the sign convention used for moment and shear force are the same as used by Shelton [1]. Consider a web section loaded with a distributed lateral force, w(x), and a moment, m(x) as shown in Fig. 4. From the summation of the forces in the N direction (shear force normal to web), one has

$$\frac{\partial N}{\partial x} = -w(x) \tag{1}$$

Similarly, a summation of the moments about the center point of the web section, assuming zero moment due to w(x), yields

$$\frac{\partial M}{\partial x} = -m(x) \tag{2}$$

The concentrated load is a special form of a distributed load. A concentrated force acting at a location x = l with a magnitude Q_l can be expressed as

$$w(x) = Q_l\delta(x-l)$$

where $\delta(.)$ is the Dirac delta function. Similarly a concentrated moment acting at x = l with a magnitude M_l can be written as

$m(x) = M_l \delta(x-l)$

Thus for the case of concentrated loads, (1) and (2) have the following forms

$$\frac{\partial N}{\partial x} = Q_l \delta(x-l) \tag{3}$$

$$\frac{\partial M}{\partial x} = M_l \delta(x-l) \tag{4}$$

Using the property of a delta function, (3) and (4) can be easily integrated, which yields

$$N_{l^+} - N_{l^-} = - Q_l \tag{5}$$

$$M_{l^+} - M_{l^-} = - M_l \tag{6}$$

These two equations will be used as boundary conditions to determine the coefficients involved in the general solution for web displacement.

The governing differential equation for a web span from the fundamental theory for lateral web motion is still valid, which is given by [1]

$$y^{iv} - K^2 y^{ll} = 0 \tag{7}$$

where $K^2 = \frac{T}{EI}$.

The general solution for each portion of the web span has the same form but different coefficients. Thus for the two portions of the web span in Fig. 2 one has

$$y = C_1 shKx + C_2 chKx + C_3 x + C_4 \tag{8}$$

$$0 \leq x < l$$

$$y = C_5 shKx + C_6 chKx + C_7 x + C_8 \tag{9}$$

$$l < x \leq L$$

The analysis just made is valid only for one pair of concentrated loads at the same location. As a result, 8 coefficients need to be determined, which requires 8 boundary conditions (BC's). A general case of concentrated loads acting at n locations needs (n + 1) equations to describe (n + 1) portions of web span divided by those loads. Thus 4(n + 1) coefficients need to be determined. The case involving only one pair of concentrated loads acting at the same location is the most common one and very representative. The analysis below thus concentrates solely on this case.

Determination of Coefficients

The solutions for web lateral displacement are given in (8) and (9). As mentioned above, 8 BC's are needed. At the upstream end, the web is normal to the entering roller and the displacement is assumed to be zero, which yields $y_0^1 = 0$, and $y_0 = 0$. From (8), one has $C_4 = -C_2$, and $C_3 = -C_1K$. Thus (8) now has the form

$$y = C_1(shKx - Kx) + C_2(chKx - 1) \qquad (10)$$

$$0 \leq x < l$$

At the downstream end, a guiding roller steered an angle θ_L is assumed. The normal entry rule gives $y_L^1 = \theta_L$, and the zero moment condition yields $y_L^{11} = 0$. From (9), it is easy to obtain that

$$C_5 = \frac{(\theta_L - C_7)chKL}{K}, \text{ and } C_6 = \frac{-(\theta_L - C_7)shKL}{K}$$

(9) then can be written as

$$y = \frac{-\theta_L}{K} shK(L-x) + \frac{C_7}{K}(Kx + shK(L-x)) + C_8 \qquad (11)$$

$$l < x \leq L$$

(10) and (11) involve only 4 arbitrary coefficients. The continuity of the web for both the displacement and the slope at x = l can give two of them, i.e., $y_{l^-} = y_{l^+}$, and $y^1_{l^-} = y^1_{l^+}$. The remaining two are given by (5) and (6). By definition, $M = -EIy^{11}$, and $N = -EIy^{111}$.

$y_{l^-}^{ll}$ and $y_{l^-}^{lll}$ can be obtained from (10), and $y_{l^+}^{ll}$ and $y_{l^+}^{lll}$ from (11). Thus using (5) and $y_{l^-}^{l} = y_{l^+}^{l}$, one has

$$C_1 chKl + C_2 shKl + C_7 \frac{chK(L-l)}{K} = \frac{\theta_L}{K} chK(L-l) - \frac{Q_l}{KT} \tag{12}$$

$$C_1(chKl-1) + C_2 shKl + C_7 \frac{chK(L-l)-1}{K} = \frac{\theta_L}{K} chK(L-l) \tag{13}$$

Combining (12) and (13) yields

$$C_7 = -C_1 K - \frac{Q_l}{T}$$

Using this result, (11) can be further written as

$$y = \frac{-\theta_L}{K} shK(L-x) - (C_1 + \frac{Q_l}{KT})(Kx + shK(L-x)) + C_8 \tag{14}$$

$$l < x \leq L$$

and (12) has the form

$$C_1(chKl - chK(L-l)) + C_2 shKl = \frac{\theta_L}{K} chK(L-l) + \frac{Q_l}{KT}(chK(L-l)-1) \tag{15}$$

Using (6) and the expression for C_7 gives

$$C_1(shKl + shK(L-l)) + C_2 chKl = \frac{-\theta_L}{K} shK(L-l) - \frac{Q_l}{KT} shK(L-l) - \frac{M_l}{T} \tag{16}$$

Solving (15) and (16), C_1 and C_2 are determined as

$$C_1 = \frac{1}{chKL-1}\left(\frac{-\theta_L}{K} chKL + \frac{Q_l}{KT}(chKl - chKL) - \frac{M_l}{T} shKl\right) \tag{17}$$

$$C_2 = \frac{1}{chKL-1}\left(\frac{\theta_L}{K} shKL + \frac{Q_l}{KT}(shKL - shKl - shK(L-l)) - \frac{M_l}{T}(chK(L-l) - chKl)\right) \tag{18}$$

Finally, from $y_{l^-} = y_{l^+}$, C_8 can be obtained as

$$C_8 = \frac{1}{chKL-1}\left(\frac{-\theta_L}{K} shKL + \frac{Q_l}{KT}\ (Kl(chKL-1)+shKl-shKL+shK(L-l)) + \frac{M_l}{T}(chK(L-l)-chKl-chKL+1)\right) \tag{19}$$

Thus the displacement of the web is determined uniquely by (10) and (14). The coefficients involved are given by (17), (18), and (19).

The web displacement, y, can be normalized using the steering parameter, θ_L, the lateral force, Q_l , or the lateral moment, M_l. The effects of these parameters on the web displacement then can be examined. The steering parameter, θ_L, on web displacement without lateral loads has been investigated by Shelton [1]. Further analysis is given here including lateral load effects.

Using ($L\theta_L$), i.e., the steering term, to normalize y, (10) and (14) become

$$\frac{y}{L\theta_L} = \frac{C_1}{L\theta_L}(shKx - Kx) + \frac{C_2}{L\theta_L}(chKx - 1) \qquad 0 \le x < l \tag{20}$$

$$\frac{y}{L\theta_L} = \frac{-1}{KL}\, shK(L-x) - \left(\frac{C_1}{L\theta_L} + \frac{Q_l}{KLT\theta_L}\right)(Kx+shK(L-x)) + \frac{C_8}{L\theta_L} \qquad l < x \le L \tag{21}$$

From (17), (18), and (19), the normalized coefficients are

$$\frac{C_1}{L\theta_L} = \frac{1}{chKL-1}\left(\frac{-1}{KL}chKL + \left(\frac{Q_l}{T\theta_L}\right)\frac{(chKl-chKL)}{KL} - \frac{M_l}{TL\theta_L}shKl\right) \tag{22}$$

$$\frac{C_2}{L\theta_L} = \frac{1}{chKL-1}\left(\frac{shKL}{K} + \left(\frac{Q_l}{T\theta_L}\right)\frac{(shKL-shKl-shK(L-l))}{KL} - \frac{M_l}{TL\theta_L}(chK(L-l)-chKl)\right) \tag{23}$$

$$\frac{C_8}{L\theta_L} = \frac{1}{chKL-1}\left(\frac{-shKL}{KL} + \left(\frac{Q_l}{T\theta_L}\right)\frac{(Kl(chKL-1)+shKl-shKL+shK(L-l))}{KL} + \frac{M_l}{TL\theta_L}(chK(L-l)-chKl-chKL+1)\right) \tag{24}$$

Through (22) to (24), the system parameters and the disturbance parameters normalized by the steering angle, θ_L, can be identified. These parameters are defined as

$$p_1 = KL,\ p_2 = l/L,\ p_3 = \frac{Q_l}{T\theta_L}, \text{ and } p_4 = \frac{M_l}{TL\theta_L}$$

Obviously (0.0, ∞) and (0.0, 1.0) are the domains for parameters p_1 and p_2 respectively. The independent variable is defined as $\xi = x/L$. Also let

$$a_1 = \frac{C_1}{L\theta_L},\ a_2 = \frac{C_2}{L\theta_L},\ a_8 = \frac{C_8}{L\theta_L}, \text{ and } y_{\theta_L} = \frac{y}{L\theta_L}$$

(20) and (21) then become

$$y_{\theta_L} = a_1(sh p_1\xi - p_1\xi) + a_2(ch p_1\xi - 1) \qquad 0 \le \xi < p_2 \tag{25}$$

$$y_{\theta_L} = \frac{-1}{p_1} sh p_1(1-\xi) - (a_1 + \frac{p_3}{p_1})(p_1\xi + sh p_1(1-\xi)) + a_8 \qquad p_2 < \xi \le 1 \tag{26}$$

where a_1, a_2 and a_8 are given by (22) to (24) and are functions of parameters p_1, p_2, p_3, and p_4.

Equations (25) and (26) are plotted in Fig. 5. The curve corresponding to zero p_3 and p_4 is the special case with the negligible side load effect. The plot shows the effect of adding lateral force alone, $(p_1, p_2) = (1.0, 0.0)$, adding lateral moment alone, $(p_3, p_4) = (0.0, 1.0)$, and adding the combinations of both lateral force and moment, $(p_3, p_4) = (1.0, 1.0)$, $(-1.0, -1.0)$, and $(-1.0, 1.0)$. The comparison can be made with the case of steering only, $(p_3, p_4) = (0.0, 0.0)$. The other two parameters for the plot are $(p_1, p_2) = (2.0, 0.5)$. In the second case, a set of curves has been obtained similar to the one in Fig. 5. The only difference is that p_1 is set to be 0.5 instead of 2.0 as in the first case of Fig. 5. If the web cross sections have the same geometry, the webs are the same material, and the tensions in the process line are the same then the above difference in p_1 means that the length of web span in the case of Fig. 5 is 4 times the one in the second case. On the other hand, if only the elasticities of webs are different, then the Young's modulus in the second case is 16 times that of Fig. 5. A comparison of these two sets of curves shows that the effect of lateral force or moment is much less pronounced in the second case than that of Fig. 5. This indicates that a less stiff or a relatively long web span has a lower capability to resist the concentrated lateral force and moment disturbances than a stiff or a relatively short one if other conditions are the same.

Effects of Lateral Force

Most commonly, a moving web passes two parallel rollers. The steering angle, θ_L, in this case then is invariably zero. The normalization scheme using the steering angle is thus not possible. If lateral disturbances exist, it is possible to use lateral force, Q_l, or lateral moment, M_l, to perform the normalization. To see the effects of lateral force on lateral web behavior, Q_l, must be present and nonzero. Thus Q_l can be used to normalize the web displacement, y.

Inspecting the parameters identified in the last section, using (10) and (14), the normalized form can be expressed as

$$\frac{y}{LQ_l/T} = \frac{C_1}{LQ_l/T}(shKx - Kx) + \frac{C_2}{LQ_l/T}(chKx - 1) \qquad 0 \leq x < l \tag{27}$$

$$\frac{y}{LQ_l/T} = \frac{-\theta_L}{Q_l/T}\frac{shK(L-x)}{KL} - \left(\frac{C_1}{LQ_l/T} + \frac{1}{KL}\right)(Kx + shK(L-x)) + \frac{C_8}{LQ_l/T} \qquad l < x \leq L \tag{28}$$

Let $b_1 = \frac{C_1}{LQ_l/T}$, $b_2 = \frac{C_2}{LQ_l/T}$, and $b_8 = \frac{C_8}{LQ_l/T}$, from (17) to (19), one has

$$b_1 = \frac{1}{chKL-1}\left(\frac{-\theta_L}{Q_l/T}\frac{chKL}{KL} + \frac{1}{KL}(chKl - chKL) - \frac{M_l}{LQ_l}shKl\right) \tag{29}$$

$$b_2 = \frac{1}{chKL-1}\left(\frac{\theta_L}{Q_l/T}\frac{shKL}{KL} + \frac{1}{KL}(shKL-shKl-shK(L-l)) - \frac{M_l}{LQ_l}(chK(L-l)-chKl)\right) \quad (30)$$

$$b_8 = \frac{1}{chKL-1}\left(\frac{-\theta_L}{Q_l/T}\frac{shKL}{KL} + \frac{1}{KL}(Kl(chKL-1)+shKl-shKL+shK(L-l)) + \frac{M_l}{LQ_l}(chK(L-l)-chKl-chKL+1)\right) \quad (31)$$

In equations (29) to (31), two parameters in addition to p_1 and p_2 are identified. These two parameters are defined as $p_5 = \frac{\theta_L}{Q_l/T}$ and $p_6 = \frac{M_l}{LQ_l}$; however, because $p_5 = 1/p_3$, actually only one more parameter is introduced from such a normalization scheme.

Similar to (25) and (26), by letting $y_{Q_L} = \frac{y}{LQ_l/T}$, (27) and (28) become

$$y_{Q_L} = b_1(shp_1\xi - p_1\xi) + b_2(chp_1\xi - 1) \qquad 0 \le \xi < p_2 \quad (32)$$

$$y_{Q_l} = \frac{-p_5}{p_1} shp_1(1-\xi) - (b_1 + \frac{1}{p_1})(p_1\xi + shp_1(1-\xi)) + b_8 \qquad p_2 < \xi \le 1 \quad (33)$$

where b_1, b_2, and b_8 are given by (29) to (31), and are functions of parameters p_1, p_2, p_5 and p_6.

Using (32) and (33), 2 plots are obtained. In Fig. 6 the normalized web displacement using a concentrated lateral force at the middle of the web span ($p_2 = 0.5$) for several p_1 values are shown. The two rollers are parallel ($p_5 = 0.0$)and there is no concentrated moment disturbance ($p_6 = 0.0$). It shows that the displacement of the web monotonically increases along the web span. At a fixed point, the web displacement also monotonically increases as the web span becomes less stiff or relatively long, i.e., increasing p_1 values. The plot in Fig. 7 shows the effect of adding steering alone $(p_5, p_6) = (1.0, 0.0)$, adding lateral moment alone, $(p_5, p_6) = (0.0, 1.0)$, and adding the combinations of steering and moment, $(p_5, p_6) = (1.0, 1.0)$, $(-1.0, -1.0)$, and $(-1.0, 1.0)$, on the web displacement normalized using lateral force. It shows that at the given set of parameters, the lateral moment disturbance has an opposite effect at the downstream end of the web span. The parameter p_1 in this plot is set to be 2.0. The results have been obtained from the second case similar to the one in Fig. 7 with the only difference in p_1, which is set to be 0.5. Thus the web span is more stiff or relatively short than in the first case. The effect of steering is still quite significant compared to the previous case. The lateral moment disturbance is, however, much smaller compared to the case in Fig. 7. The strong resistance capability to the lateral loads for a more stiff or relatively short web span is further confirmed.

More often than not, one is interested in the displacement at the downstream end of a web span. It is thus necessary to emphasize the effects of steering and lateral loading on the downstream end. From (14) by setting $x = L$, one has

$$\frac{y_L}{L} = -C_1 K - \frac{Q_l}{T} + \frac{C_8}{L} \tag{34}$$

To see the effect on y_L/L by a related parameter, it is convenient to examine the derivatives of y_L/L with respect to that parameter. Let p represent a parameter (p thus can be θ_L, Q_l, or M_l), then the first derivative of y_L/L with respect to p from (34) is given by

$$\frac{\partial(y_L/L)}{\partial p} = -\frac{\partial(KC_1)}{\partial p} - \frac{\partial(Q_l/T)}{\partial p} + \frac{\partial(C_8/L)}{\partial p} \tag{35}$$

To simplify the notation, one wants to set $Y_p = \dfrac{\partial(y_L/L)}{\partial p}$. First, to examine the effect of steering by setting $p = \theta_L$. From (35) and using (34) and (35) yields

$$Y_{\theta_L} = \frac{p_1 chp_1 - shp_1}{p_1(chp_1 - 1)} \tag{36}$$

which is the curvature factor defined by Shelton [1]. It is a function of p_1 only. One can easily find that Y_{θ_L} (defined as K_C by Shelton [1]) is a monotonically increasing function of p_1 . Y_{θ_L} has a value of 2/3 as p_1 approaches 0.0 and unity as p_1 approaches infinity.

Next, to come back to the effect of concentrated lateral force by setting p = Q_l. Again from (35) and using (17) and (18), one has

$$TY_{Q\,l} = \frac{1}{p_1(chp_1\text{-}1)}(p_1(chp_1\text{-}chp_1p_2)\text{-}p_1(1\text{-}p_2)(chp_1\text{-}1)+shp_1p_2\text{-}shp_1+shp_1(1\text{-}p_2)) \tag{37}$$

It is seen that (TY_{Q_l}) is a function of two parameters p_1 and p_2. Extending the concept of curvature factor by considering (36) as a curvature factor due to steering, then (37) defines the curvature factor due to lateral force. If one plots (TY_{Q_l}) in (37) as a function of p_1 for different p_2, then one can see that for large p_2 values, (TY_{Q_l}) has smaller values than for small p_2 values for the same p_1 value. This indicates that the variation of (TY_{Q_l}) in p_2 for given p_1 is not monotonic. Extreme values for (TY_{Q_l}) as a function of p_2 at given p_1 can be expected. On the other hand, if one plots (TY_{Q_l}) in (37) again as a function of p_2 for given p_1 values, a maximum (TY_{Q_l}) can be clearly seen for some p_2 in the range of (0.0, 1.0) with a given p_1.

For a given p_2 such that $0.0 < p_2 < 1.0$, (TY_{Q_l}) is a function of p_1. At the limiting p_1 it can be found that

$$\lim_{p_1 \to 0} (TY_{Q\,l}) = 0\ , \ and \quad \lim_{p_1 \to \infty} (TY_{Q\,l}) = p_2 \tag{38}$$

For a given $p_1 > 0.0$, (TY_{Q_l}) is a function of p_2. At the limiting p_2 values it can also be shown that

$$\lim_{p_2 \to 0} (TY_{Q\,l}) = 0\ , \ and \quad \lim_{p_2 \to 1} (TY_{Q\,l}) = 0 \tag{39}$$

The monotonic behavior of (TY_{Q_l}) in p_1 for a given $p_1 \in$ (0.0, ∞) has been verified by taking the first derivative of (TY_{Q_1}) with respect to p_1 and showing that its values for all p_1 and p_2 in their valid domain are greater than zero, i. e.,

$$\frac{\partial(TY_{Q_1})}{\partial p_1} > 0 \text{ , for } p_1 \in (0.0, \infty) \text{ and } p_2 \in (0.0, 1.0) \qquad (40)$$

The maximum (TY_{Q_1}) as a function of $p_2 \in (0, 1)$ for a given $p_1 > 0$ can be found by taking the first derivative of (TY_{Q_1}) with respect to p_2 and set it equal to zero. The point p_2 corresponding to the maximum (TY_{Q_1}) for given p_1 can then be obtained by solving the equation of

$\frac{\partial(TY_{Q_1})}{\partial p_2} = 0$. From (37) one has

$$ch\, p_1p_2 - shp_1p_2 + chp_1 - chp_1(1-p_2) - 1 = 0 \qquad (41)$$
$$p_1 \in (0.0, \infty) \text{ and } p_2 \in (0.0, 1.0)$$

By presetting a p_1 in its domain, then solving (41) for p_2, if p_2 is in its domain, the pair of (p_1, p_2) obtained this way corresponds to a maximum point of (TY_{Q_1}), which is a function of p_2 only if p_1 is preset. Fig. 8 shows a curve of p_1 versus p_2, where each point on the curve corresponds to such a pair. If the maximum (TY_{Q_1}) obtained by solving (41) is shown in the plots with p_1 and p_2 as x-axis respectively, one can see clearly that the maximized (TY_{Q_1}) is a monotonically increasing function .

Effects of Lateral Moment

When the lateral moment disturbance is considered to be the major factor, its effect on web span lateral behavior is naturally the subject to be investigated. Similar to the argument for the case of lateral force disturbance, the displacement of a web span can be normalized using the moment term, M_l. The normalized form by using (10) and (14) can be given as

$$\frac{y}{M_l/T} = \frac{C_1}{M_l/T}(shKx - Kx) + \frac{C_2}{M_l/T}(chKx - 1) \qquad (42)$$
$$0 \le x < l$$

$$\frac{y}{M_l/T} = \frac{-L\theta_L}{M_l/T}\frac{shK(L-x)}{KL} - (\frac{C_1}{M_l/T} + \frac{LQ_l}{KLM_l})(Kx+shK(L-x)) + \frac{C_8}{M_l/T} \qquad (43)$$
$$l < x \le L$$

Let $d_1 = \frac{C_1}{M_l/T}$, $d_2 = \frac{C_2}{M_l/T}$, *and* $d_8 = \frac{C_8}{M_l/T}$, then from (17) to (19), one has

$$d_1 = \frac{1}{chKL-1}(\frac{-TL\theta_L}{M_l}\frac{chKL}{KL} + \frac{LQ_l}{M_l}\frac{(chKl-chKL)}{KL} - shKl) \qquad (44)$$

$$d_2 = \frac{1}{chKL-1}(\frac{TL\theta_L}{M_l}\frac{shKL}{KL} + \frac{LQ_l}{M_l}\frac{(shKL-shKl-shK(L-l))}{KL} - (chK(L-l)-chKl)) \qquad (45)$$

$$d_8 = \frac{1}{chKL-1}(\frac{-TL\theta_L}{M_l}\frac{shKL}{KL} + \frac{LQ_l}{KLM_l}(Kl(chKL-1)+shKl-shKL+shK(L-l)) + (chK(L-l)-chKl-chKL+1)) \qquad (46)$$

From the above normalization, two more parameters are identified. These two parameters are defined as

$$p_7 = \frac{TL\theta_L}{M_l}, \text{ and } p_8 = \frac{LQ_l}{M_l}$$

Note $p_8 = 1/p_6$, thus actually only one more independent parameter is added to the previously identified parameters.

Using y_{M_l} to represent $y/(M_l/T)$ and with the parameters and variable defined earlier, (42) and (43) become

$$y_{M_l} = d_1(chp_1\xi - p_1\xi) + d_2(chp_1\xi - 1) \qquad (47)$$
$$0 \le \xi < p_2$$

$$y_{M_l} = -\frac{p_7}{p_1}shp_1(1-\xi) - (d_1 + \frac{p_8}{p_1})(p_1\xi + shp_1(1-\xi)) + d_8 \qquad (48)$$
$$p_2 < \xi \le 1$$

where d_1, d_2, and d_8 are functions of p_1, p_2, p_7, and p_8 are defined by (44) to (46).

From (47) and (48), 2 plots are obtained to see the effects of the lateral concentrated moment on the web span displacement. Fig. 9 corresponds to the effect of moment disturbance only. y_{M_1} is purely a function of p_1 and p_2. The case studied has set $p_2 = 0.5$, thus for a given location, the web displacement is a function of p_1 only. The curves shown in Fig.9 indicate y_{M_1} has negative values for all $\xi \in (0.0, 1.0)$ and $p_1 > 0.0$. In Fig. 10, p_1 and p_2 are set to be (2.0, 0.5). The moment only effect corresponds to $(p_7, p_8) = (0.0, 0.0)$, adding the effect of steering to $(p_7, p_8) = (1.0, 0.0)$, adding the effect of lateral force to $(p_7, p_8) = (0.0, 1.0)$, and adding the combinations of steering and lateral force to $(p_7, p_8) = (1.0, 1.0)$, (-1, -1), and (-1.0, 1.0). It shows clearly that the moment has an opposite effect on the web lateral displacement compared to the steering or lateral force for the given condition in Fig. 9. The second case is almost the same as the one in Fig. 10 except that p_1 is set to 0.5, i. e., a more stiff or a shorter web span is used. If the plot similar to Fig. 10 is obtained, one can see that the effect of disturbances is much smaller than that of the steering. It agrees with the conclusion obtained earlier that the resistance capability is much better for a stiff or a relatively short web span than a less stiff or a relatively long one.

It is equally important to investigate the effect of M_l on the downstream end of a web span. Using (35) by letting $p = M_l$, from (17) and (18), one has

$$\left(\frac{T}{K}Y_{M_l}\right)= \frac{1}{p_1(chp_1\text{-}1)}(p_1shp_1p_2+chp_1(1\text{-}p_2)\text{-}chp_1p_2\text{-}chp_1+1) \qquad (49)$$

Y_{M_1} normalized by (K/T) as shown is a function of p_1 and p_2. Similar to (37), (49) defines the curvature factor due to lateral moment.

$(\frac{T}{K}Y_{M_1})$ in (49) can be plotted versus p_1 for given p_2 values. From those plots, it can be seen that $(\frac{T}{K}Y_{M_1})$ has only one minimum value for a given p_2 if it is small enough. But when p_2 increases to above a certain value, a maximum, a zero, and a minimum exist for $(\frac{T}{K}Y_{M_1})$. It can be found that at limiting values of p_1 for given $p_2 \in (0.0, 1.0)$, $(\frac{T}{K}Y_{M_1})$ are zero, i. e., for $p_2 \in (0.0, 1.0)$, one has

$$\lim_{p_1 \to 0} (\frac{T}{K}Y_{M_1}) = 0, \quad and \quad \lim_{p_1 \to \infty} (\frac{T}{K}Y_{M_1}) = 0 \tag{50}$$

Note in order for $(\frac{T}{K}Y_{M_1})$ to have a minimum only as a function of p_1 for given $p_2 \in (0.0, 1.0)$, the slope of $(\frac{T}{K}Y_{M_1})$ at $p_1 \to 0.0$ has to be less than or equal to zero. The critical p_2, which separates the condition for $(\frac{T}{K}Y_{M_1})$ has only a minimum or has a minimum, a maximum, and a zero at non-limiting p_1 values which can be determined from $\frac{\partial}{\partial p_1}(\frac{T}{K}Y_{M_1}) = 0$ by finding $p_2 \in (0.0, 1.0)$ as $p_1 \to 0.0$. In trying to find such a p_2, it boils down to dealing with a function $g(p_2)$ with the form of

$$g(p_2) = \frac{4p_2^3 + (1-p_2)^4}{1 + p_2^4} - 1 \tag{51}$$

and the conditions are identified as

$$g(p_2) = \begin{cases} > 0\,, & max,\ min,\ \&\ zero; \\ \leq 0\,, & min\ only. \end{cases}$$

It can be found that

$$g(p_2) = \begin{cases} < 0, & for\ 0 < p_2 < 2/3\ ; \\ = 0, & for\ p_2 = 2/3\ ; \\ > 0, & for\ 2/3 < p_2 < 1\ . \end{cases}$$

It is also of interest to find these minimum points of p_1, as well as the maximum and zero points if they exist for $(\frac{T}{K}Y_{M_1})$ at given p_2.

The extreme points of p_1 for a given p_2 can be found by taking the first partial derivative of $(\frac{T}{K}Y_{M_1})$ in (49) with respect to p_1 and setting it to be zero, which yields

$$\begin{aligned} &(shp_1p_2+p_1p_2chp_1p_2+(1-p_2)shp_1(1-p_2)-p_2shp_1p_2-shp_1)p_1(chp_1-1) \\ &\quad - (chp_1-1+p_1shp_1)\,(p_1shp_1p_2 + chp_1(1-p_2) - chp_1p_2 - chp_1 + 1) = 0 \end{aligned} \tag{52}$$

For $p_2 \in (0.0, 2/3]$, only one minimum of $(\frac{T}{K}Y_{M_1})$ exists, thus one root is available for p_1 for a given p_2 in the above specified domain. For $p_2 \in (2/3, 1.0)$, however, both a minimum and a maximum of $(\frac{T}{K}Y_{M_1})$ exist; in this case, there are two roots of p_1 for a given p_2 in the specified domain. If $\bar{p}_1$ corresponds to the maximum of $(\frac{T}{K}Y_{M_1})$ and $\hat{p}_1$ to the minimum, then $\bar{p}_1 < \hat{p}_1$ for the same given p_2.

The zero point $\tilde{p}_1$ of $(\frac{T}{K}Y_{M_1})$ can be found by letting $(\frac{T}{K}Y_{M_1})$ be equal to zero in (49), i. e., solving

$$p_1 shp_1 p_2 + chp_1(1-p_2) - chp_1 p_2 - chp_1 + 1 = 0 \tag{53}$$

From the above analysis, one knows $\tilde{p}_1$ exists only if $p_2 \in (2/3, 1.0)$. It is obvious that $\bar{p}_1 < \tilde{p}_1 < \hat{p}_1$.

In Fig. 11, the (p_1, p_2) pairs by solving (52) and (53) are plotted. Curve 1 corresponds to the minimums of $(\frac{T}{K}Y_{M_1})$ for given p_2, curve 2 to the maximums, and curve 3 to the zeros. The actual minimum and maximum of $(\frac{T}{K}Y_{M_1})$ values are plotted in Figs. 12 and 13 versus p_1 and p_2 respectively. They are functions of p_1 for given p_2 values. It is seen that the overall minimum of $(\frac{T}{K}Y_{M_1})$ is not necessarily corresponding to small p_1 values.

Effects at the Location of a Disturbance Source

A moving web is often seen to oscillate at the location of a disturbance source, such as an air-bar. Thus it is desirable to investigate the effect of side loads on web lateral behavior at the disturbance location.

Let $y_l = y(l)$, then at $x = l$ from (14) one has

$$y_l = - Q_3\, shK(L-l) - (C_1+Q_4)(Kl+shK(L-l)) + C_8 \tag{54}$$

To see the effect of Q_l and M_l on y_l, it is convenient to examine the derivatives of y_l with respect to Q_l and M_l respectively. From (55) one has

$$\frac{\partial y_l}{\partial Q_l} = -\left(\frac{\partial C_1}{\partial Q_L} + \frac{\partial Q_4}{\partial Q_l}\right)(Kl + shK(L-l)) + \frac{\partial C_8}{\partial Q_l} \tag{55}$$

$$\frac{\partial y_l}{\partial M_l} = -\frac{\partial C_1}{\partial M_l}(Kl + shK(L-l)) + \frac{\partial C_8}{\partial M_l} \tag{56}$$

Carrying out the derivatives involved and simplifying, (55) and (56) become

$$\frac{\partial y_l}{\partial Q_l} = \frac{1}{KT(chKL-1)}(Kl(chKL-chKl)-shK(L-l)(chKl-2)+shKl-shKL) \tag{57}$$

$$\frac{\partial y_l}{\partial M_l} = \frac{1}{T(chKL-1)}(shKl(Kl+shK(L-l))+chK(L-l)-chKl-chKL+1) \tag{58}$$

The curvature factors at the location of the disturbance source due to the lateral force and moment can then be defined as $Y_{lQ_l} = KT\frac{\partial y_l}{\partial Q_l}$ and $Y_{lM_l} = T\frac{\partial y_l}{\partial M_l}$ respectively, from (57) and (58) one has

$$Y_{lQ_l} = \frac{1}{chp_1-1}(p_1p_2(chp_1-chp_1p_2)-shp_1(1-p_2)(chp_1p_2-2)+shp_1p_2-shp_1) \tag{59}$$

$$Y_{lM_l} = \frac{1}{chp_1-1}(shp_1p_2(p_1p_2+shp_1(1-p_2))+chp_1(1-p_2)-chp_1p_2-chp_1+1) \tag{60}$$

From (59) and (60), one sees that the effect of Q_l and M_l on y_l involves two system parameters, p_1 and p_2, i.e., the web material property, tension, span length, and the location of the disturbance source. In general, one wants to minimize Y_{lQ_l} and Y_{lM_l} in magnitude, or to avoid the maximized Y_{lQ_l} and Y_{lM_l} in magnitude if possible by adjusting parameters p_1 and p_2.

Before trying to find the extremum and zero Y_{lQ_l} and Y_{lM_l} values, (59) and (60) are plotted as a function of p_1 and p_2 respectively. The plot shows a curve from (59) as a function of p_1 for given p_2 values, on which Y_{lQ_l} is seen as a monotonically increasing function of p_1 for given p_2. In the plot where (59) is plotted as a function of p_2 for given

p_1 values, a maximum Y_{lQ_l} as a function of p_2 for given p_1 can be seen to exist.

Similarly from (60) Y_{lM_l} is plotted as a function of p_1 for given p_2 values and of p_2 for given p_1 values respectively. It is possible for Y_{lM_l} to have a minimum, maximum, or zero value as a function of p_1 for given p_2 and a minimum and a zero Y_{lM_l} exists as a function of p_2 for given p_1 as can be seen from these plots.

To find those extreme Y_{lQ_l} and Y_{lM_l} values, one can take the first derivatives of Y_{lQ_l} and Y_{lM_l} with respect to p_1 and p_2 respectively, then setting them equal to zero and using the root finding technique to obtain the pairs of (p_1, p_2), which are the points corresponding to extreme Y_{lQ_l} and Y_{lM_l} values for different circumstances.

Now examine Y_{lQ_l} and Y_{lM_l} in (59) and (60) for limiting p_1 and p_2 values. As mentioned above, for a given physical web system, p_1 and p_2 are in the range of $p_1 \in (0.0, \infty)$ and $p_2 \in (0.0, 1.0)$. Using L' Hospital rule if necessary, one has

For $p_2 \in (0.0,\ 1.0)$:

$$\lim_{p_1 \to 0} Y_{lQ_l} = 0\ ; \qquad \lim_{p_1 \to \infty} Y_{lQ_l} = \infty$$

For $p_1 \in (0.0,\ \infty)$:

$$\lim_{p_2 \to 0} Y_{lQ_l} = 0\ ; \qquad \lim_{p_2 \to 1} Y_{lQ_l} = 0$$

The previously obtained plots verify the above conclusions.

For $p_2 \in (0.0,\ 1.0)$:

$$\lim_{p_1 \to 0} Y_{lM_l} = 0\ ; \qquad \lim_{p_1 \to \infty} Y_{lM_l} = \infty$$

For $p_1 \in (0.0,\ \infty)$:

$$\lim_{p_2 \to 0} Y_{lM_l} = 0\ ; \qquad \lim_{p_2 \to 1} Y_{lM_l} = \frac{p_1 sh p_1}{ch p_1 - 1} - 2$$

Again the previously mentioned plots confirm the above conclusions.

Taking the first partial derivatives of Y_{lQ_l} from (59) with respect to p_1 and p_2, and after simplifying, one has

$$D_1Y_{lQ_l} = \frac{1}{(chp_1\text{-}1)^2}(p_2(chp_1\text{-}1\text{-}p_1shp_1)(chp_1\text{-}chp_1p_2)\text{-}(chp_1p_2\text{-}chp_1(1\text{-}p_2)$$
$$(p_2(chp_1\text{-}1)+1))(chp_1p_2\text{-}2)\text{-}\ (p_2(chp_1\text{-}1)(p_1p_2+shp_1(1\text{-}p_2))+shp_1)shp_1p_2 \quad (61)$$
$$+(chp_1\text{-}1)(p_2(p_1shp_1+chp_1p_2)+1))$$

$$D_2Y_{lQ_l} = \frac{p_1}{(chp_1\text{-}1)}(chp_1+chp_1(1\text{-}p_2)(chp_1p_2\text{-}2)$$
$$\text{-}shp_1p_2(p_1p_2+shp_1(1\text{-}p_2))) \quad (62)$$

where $D_1Y_{1Q_1} = \frac{\partial Y_{1Q_1}}{\partial p_1}$, and $D_2Y_{1Q_1} = \frac{\partial Y_{1Q_1}}{\partial p_2}$.

Similarly from (60), two more equations are obtained

$$D_1Y_{lM_l} = \frac{1}{(chp_1\text{-}1)^2}(shp_1(1\text{-}p_2)(p_2(chp_1\text{-}1)chp_1p_2+(1\text{-}p_2)(chp_1\text{-}1)\text{-}shp_1shp_1p_2)$$
$$.\ +chp_1(1\text{-}p_2)((1\text{-}p_2)(chp_1\text{-}1)shp_1p_2\text{-}shp_1)\ \text{-}p_1p_2shp_1shp_1p_2$$
$$+chp_1p_2(p_1p_2^2(chp_1\text{-}1)+shp_1))$$
$$(63)$$

$$D_2Y_{lM_l} = \frac{p_1}{(chp_1\text{-}1)}(shp_1(1\text{-}p_2)(chp_1p_2\text{-}1)\text{-}shp_1p_2chp_1(1\text{-}p_2)+p_1p_2chp_1p_2) \quad (64)$$

$D_1Y_{1Q_1}$ in (61) is plotted as a function of p_1 for given p_2 values and of p_2 for given p_1 values respectively. No zero $D_1Y_{1Q_1}$ exists for non-limiting p_1 and p_2 values, which confirms the observation from previously obtained plots that no extreme Y_{1Q_1} as a function of p_1 exists for non-limiting (p_1, p_2). $D_2Y_{1Q_1}$ in (62) is also plotted as a function of p_1 for given p_2 values and of p_2 for given p_1 values respectively. Zero $D_2Y_{1Q_1}$ can be seen in in the plots obtained. $D_2Y_{1Q_1}$ passes a zero from positive value to negative value as p_2 increases, which indicates maximum Y_{1Q_1} exist as a function of p_2 for given p_1. This agrees with the observation in the previously obtained plots.

$D_1Y_{1M_1}$ in (63) is plotted as a function of p_1 for given p_2 values and of p_2 for given p_1 values respectively. Zero $D_1Y_{1M_1}$ can be observed from these plots. As a function of p_1,

Y_{lM_l} can have a minimum or maximum value for different p_2. As a function of p_2, Y_{lM_l} can only have a minimum value for different p_1. $D_2Y_{lM_l}$ in (64) is plotted as a function of p_1 for given p_2 values and of p_2 for given p_1 values respectively. Zero $D_2Y_{lM_l}$ can be observed in the plots, where zeros of $D_2Y_{lM_l}$ occur in quite a narrow region of p_2 for different p_1.

The curve of p_1 vs p_2 for maximized Y_{lQ_l} is shown in Fig. 14. The maximized Y_{lQ_l} is a function of p_2 for given p_1. If plotted, it can be seen that the maximized Y_{lQ_l} is a monotonically increasing function of p_2 for specified p_1.

Fig. 15 shows 3 curves of p_1 vs. p_2. Curve 1 corresponds to the minimized Y_{lM_l} as a function of p_1 for given p_2. The minimized Y_{lM_l} is a monotonically decreasing (increasing in magnitude) function of p_2. Each point of (p_1, p_2) on curve 2 is obtained by letting $D_1Y_{lM_l} = 0$. This point corresponds to a maximized Y_{lM_l} for given p_2 as a function of p_1. The maximized Y_{lM_l} is, if plotted, a monotonically increasing function of p_2. On curve 3, zero Y_{lM_l} can be obtained for each pair of (p_1, p_2).

Based on the above analysis, once the side loads from the disturbance source are correctly identified, the system parameters p_1 and p_2 can be adjusted in the allowable range to minimize the effect on the lateral web behavior.

Discussion

Using beam theory, the effect of disturbances due to lateral loads has been investigated in some detail for a single web span under restricted conditions. In a web process line, some devices have to be introduced to perform some kinds of special tasks. As a result, the disturbances can thus be brought to the web span. A web handling system designer needs the information on how those disturbances might affect the web behavior. And if possible, how one can design a system to minimize the effect of those disturbances. The information supplied here, though limited, can be helpful in answering these questions.

A system designer often has the freedom to choose some system parameters in a specified range, such as the parameters used here, p_1, p_2, etc. The length of a web span can often be adjusted, for example, which changes p_1. Often the location of a processing device is not necessarily fixed. As a disturbance source, it can be located in such a way that its effect is as small as possible. If more information on the disturbance can be identified, then the parameters as identified above, p_3, p_4, p_5, etc., can also be used in trying to reduce the unwanted disturbance effect.

Through the analysis, it is seen that a stiff or relatively short web span has a better resistance capability to disturbances than a less stiff or relatively long one. The effect of lateral force on a web span is one sided and thus independent of the location of the disturbance regarding the direction of the effect. The effect of moment is, however, two sided depending on the location of the disturbance source. This characteristic makes it possible to totally eliminate its effect at a desired location. This, of course, first requires identification of the disturbance type as a lateral moment.

More work needs to be done in identifying disturbance types. Less restricted conditions should be included, such as the slack edge case, the span interaction, and the shear deflection effect.

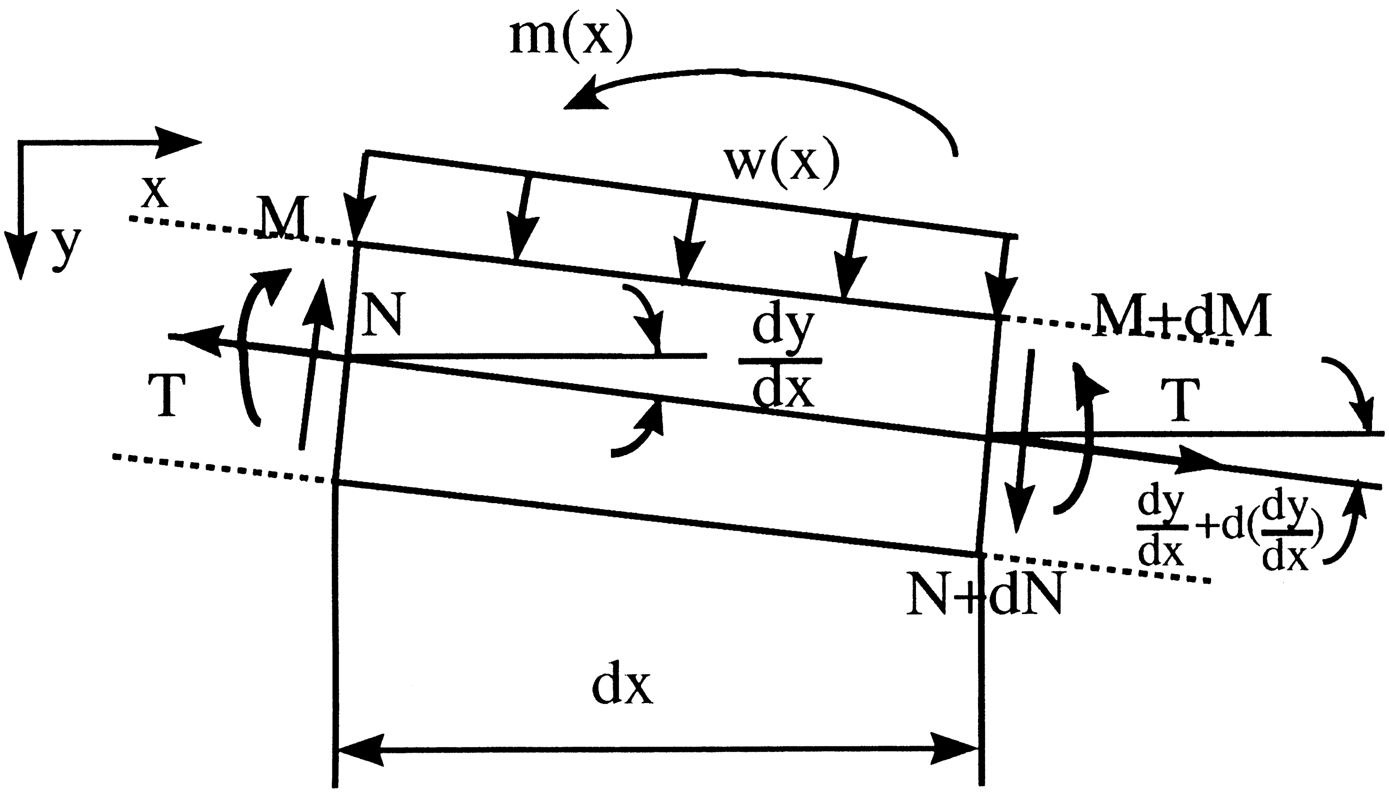

Figure 4. A Web Element With Lateral Loads

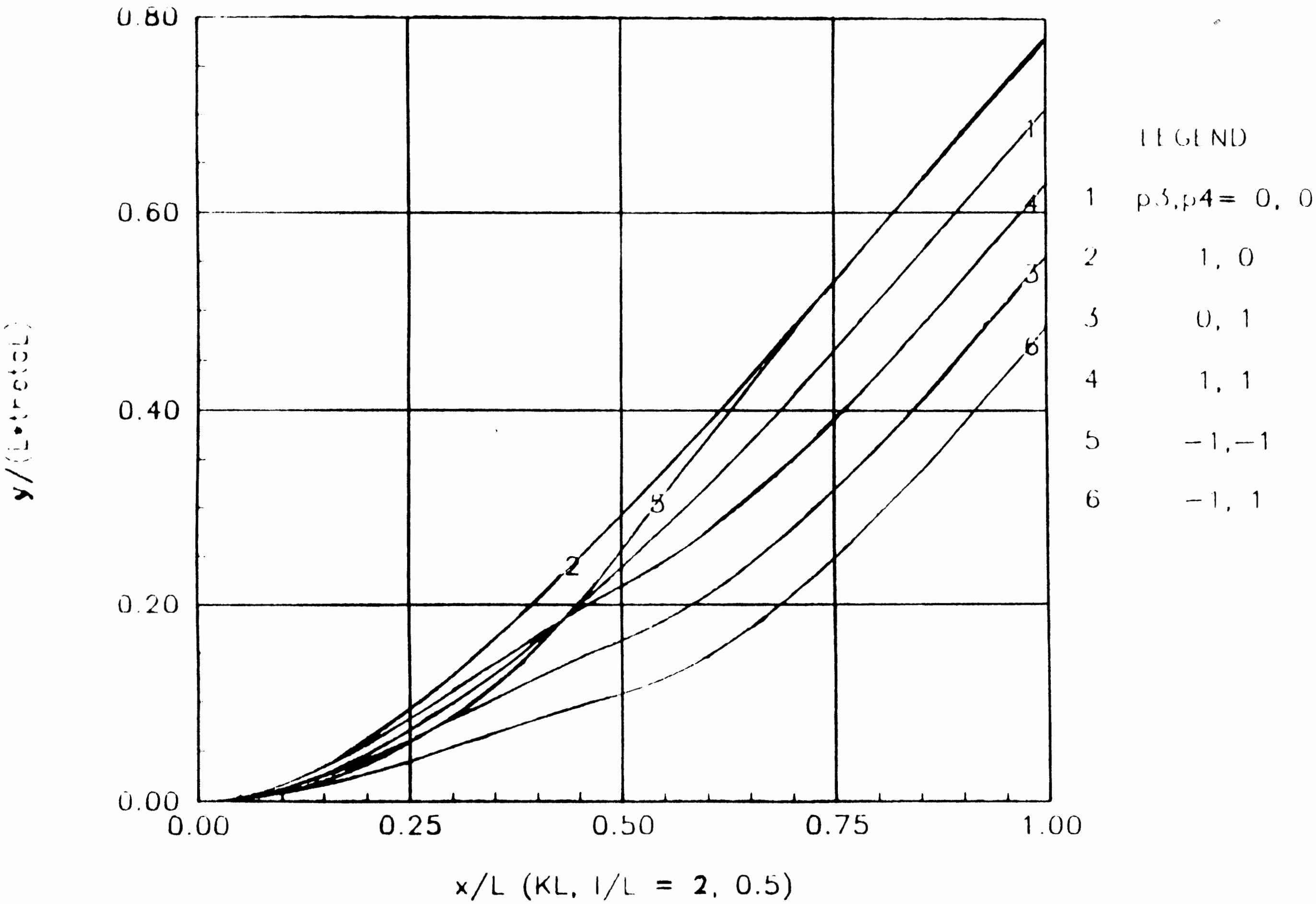

Figure 5. Normalized Elastic Curves of Webs Using Steering
With Lateral Load Effects

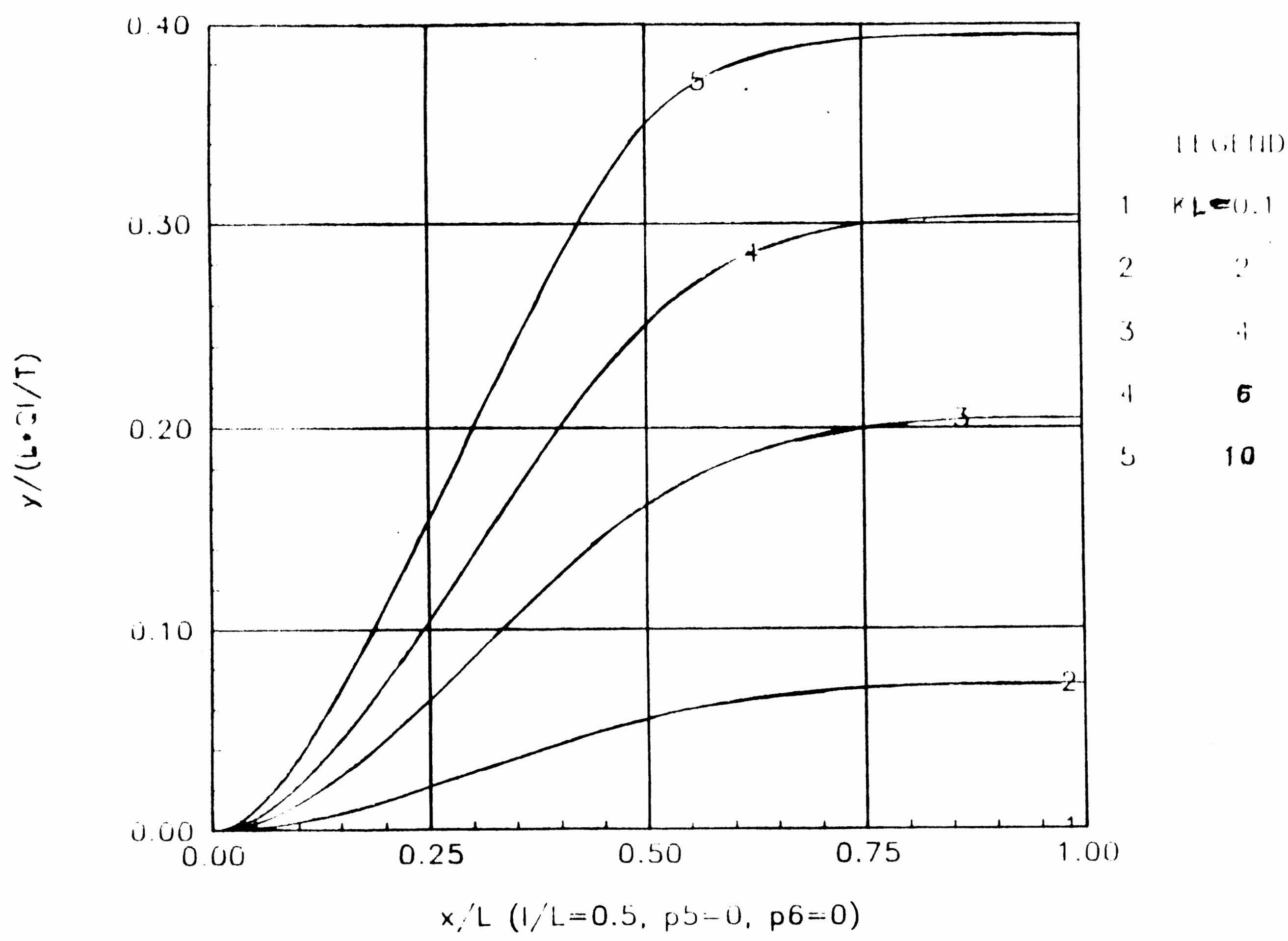

Figure 6. Elastic Curves of Webs Due to Lateral Force

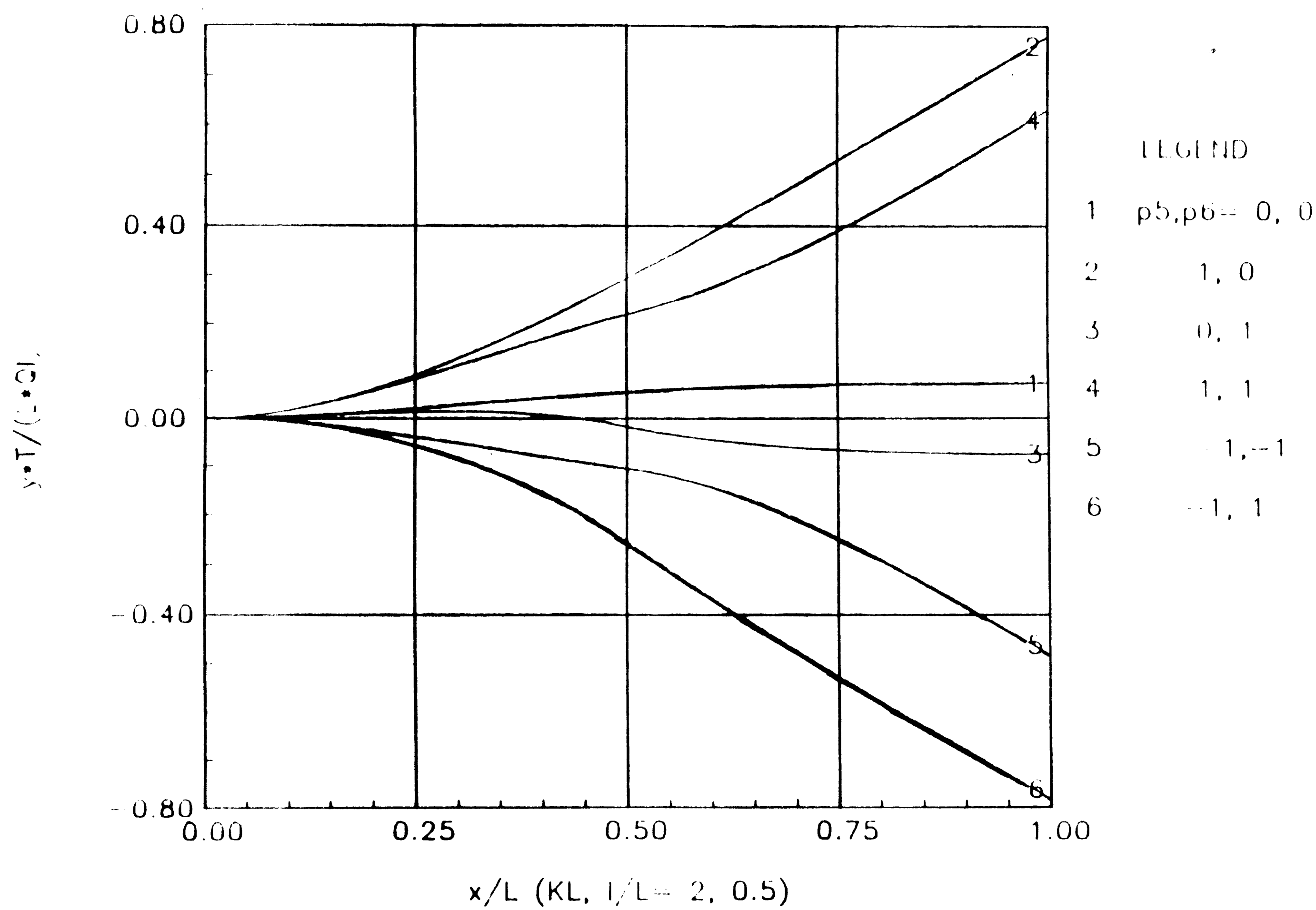

Figure 7. Normalized Elastic Curves of Webs Using Lateral Force With Steering and Lateral Moment Effects

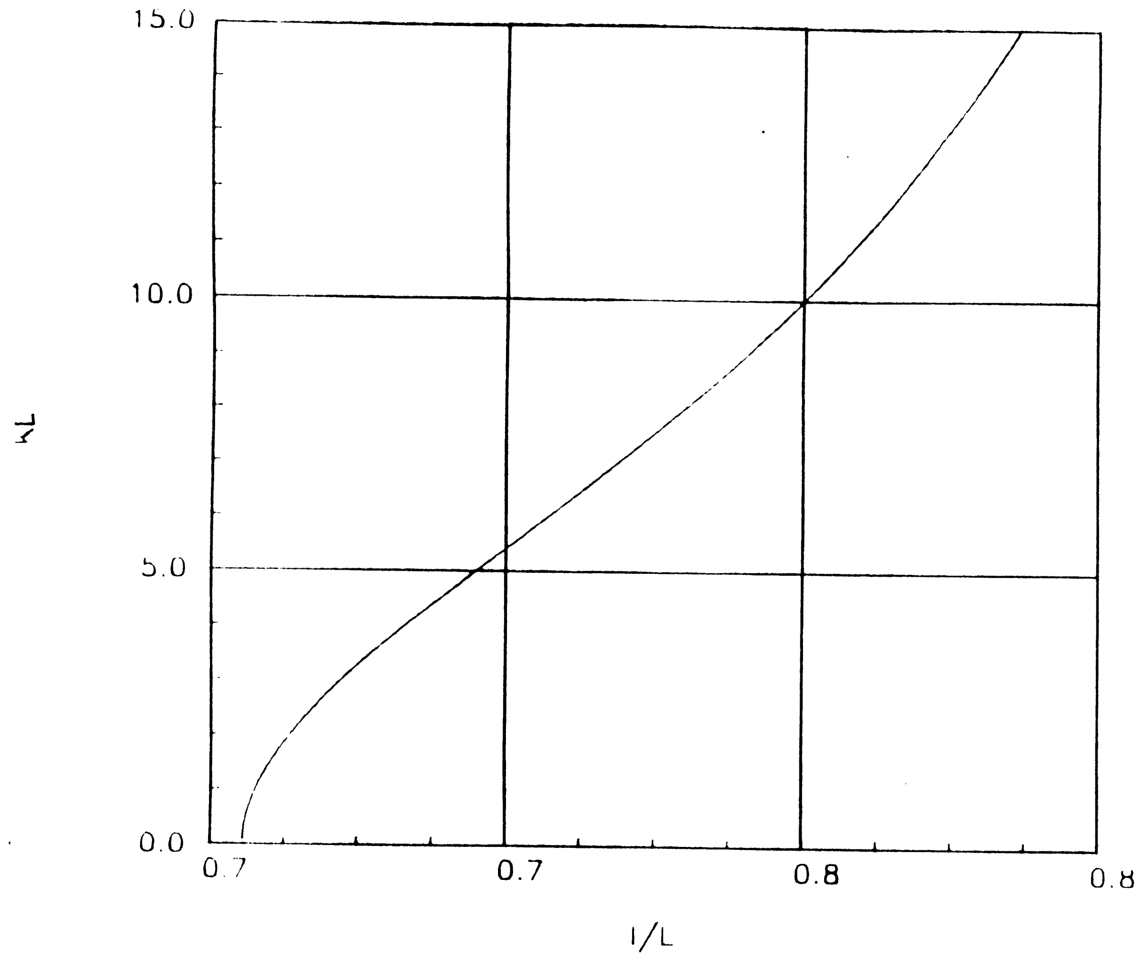

Figure 8. The Curve of KL vs l/L for Maximum Curvature Factor Due to Lateral Force

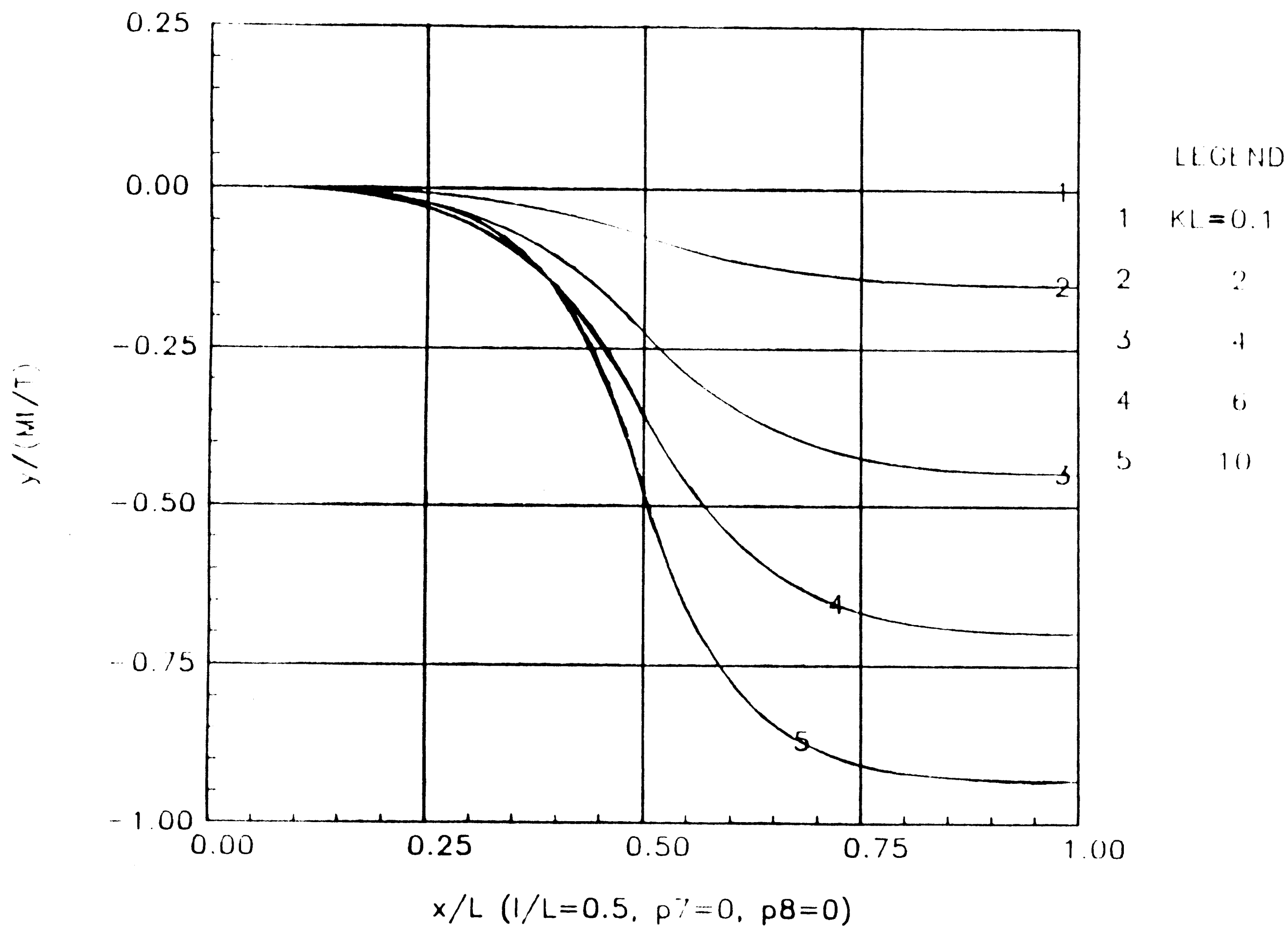

Figure 9. Elastic Curves of Webs Due to Lateral Moment

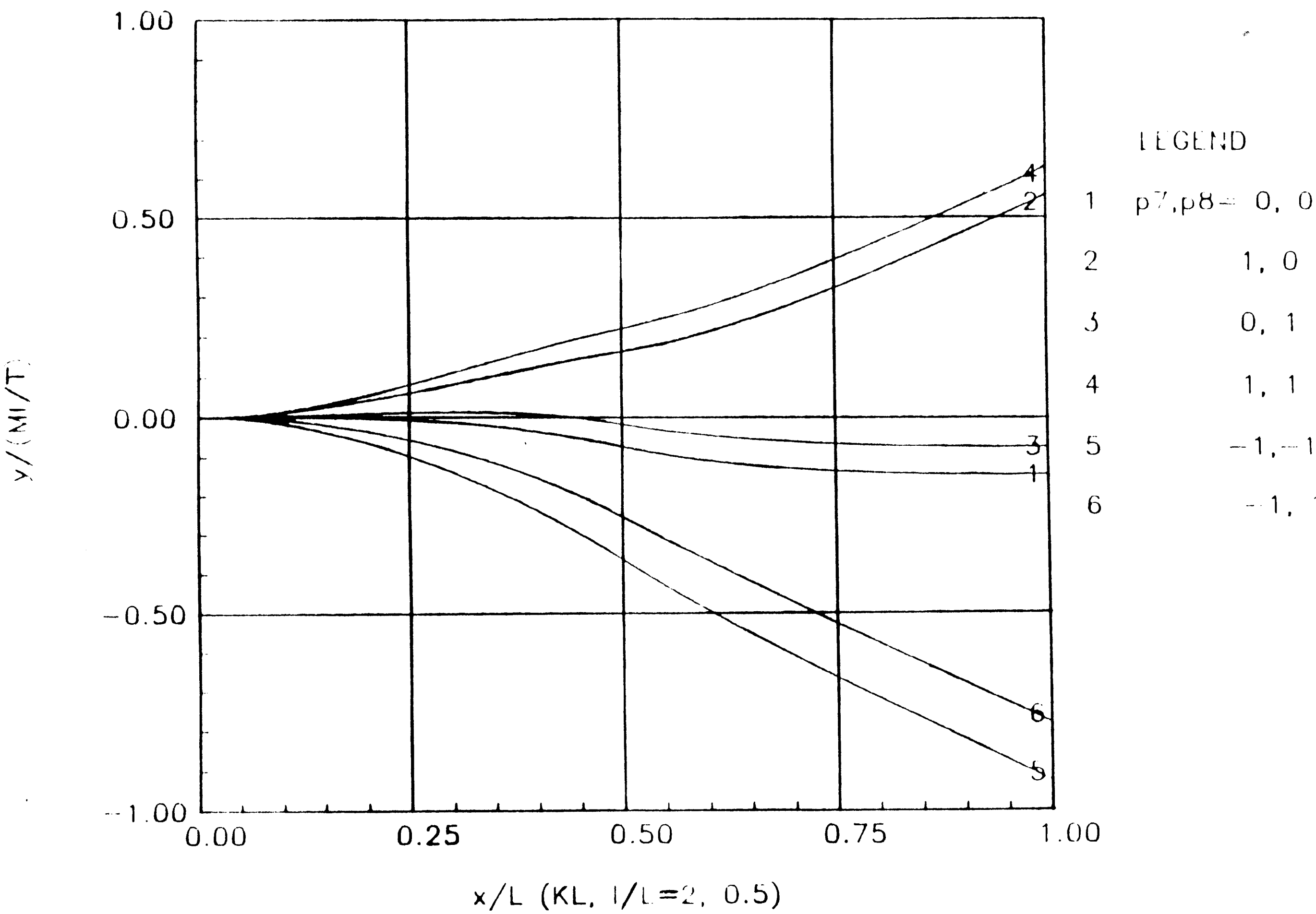

Figure 10. Normalized Elastic Curves of Webs Using Lateral Moment With Steering and Lateral Force Effects

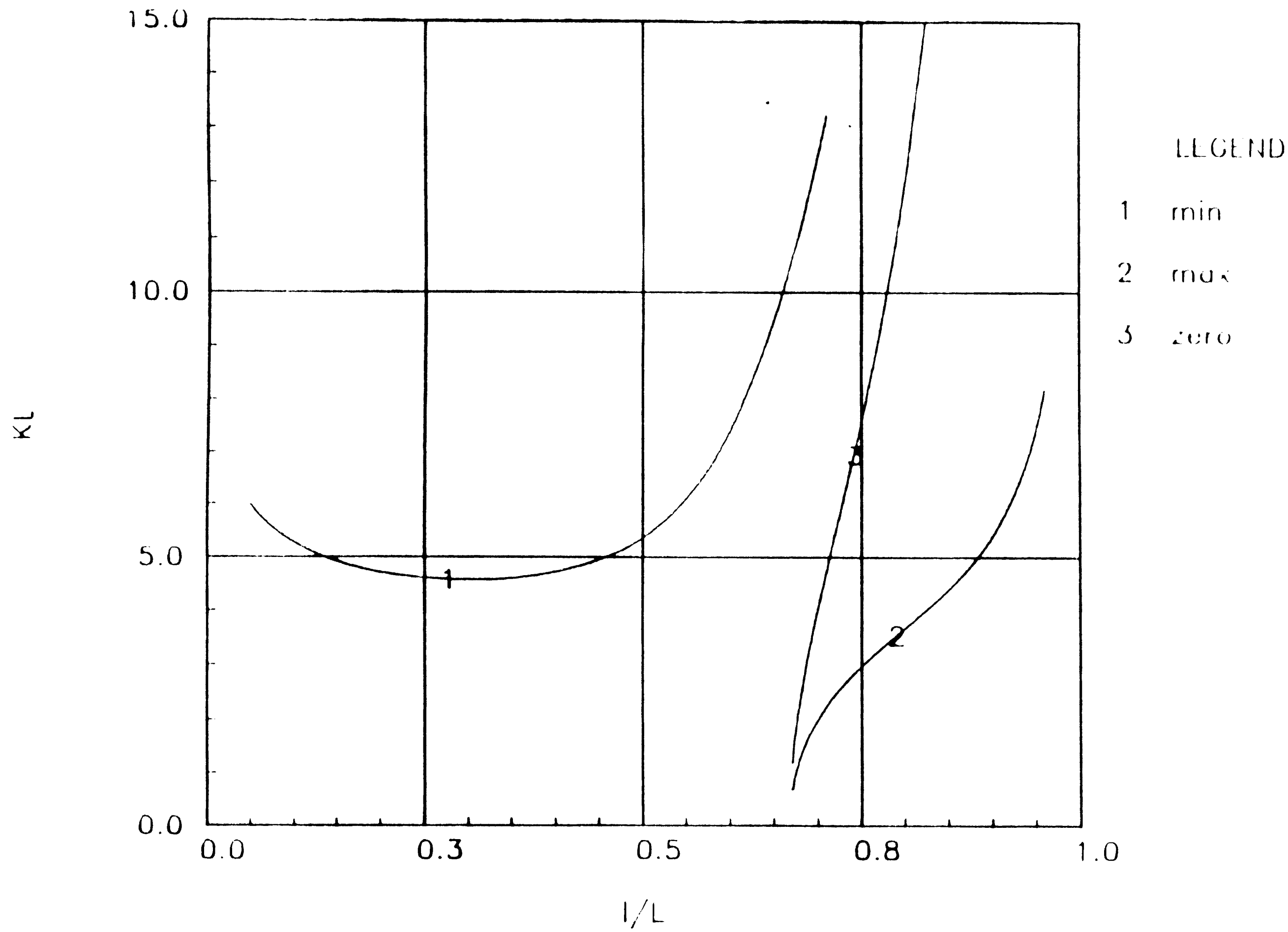

Figure 11. Curves of KL vs l/L for Extreme and Zero Curvature Factors Due to Lateral Moment

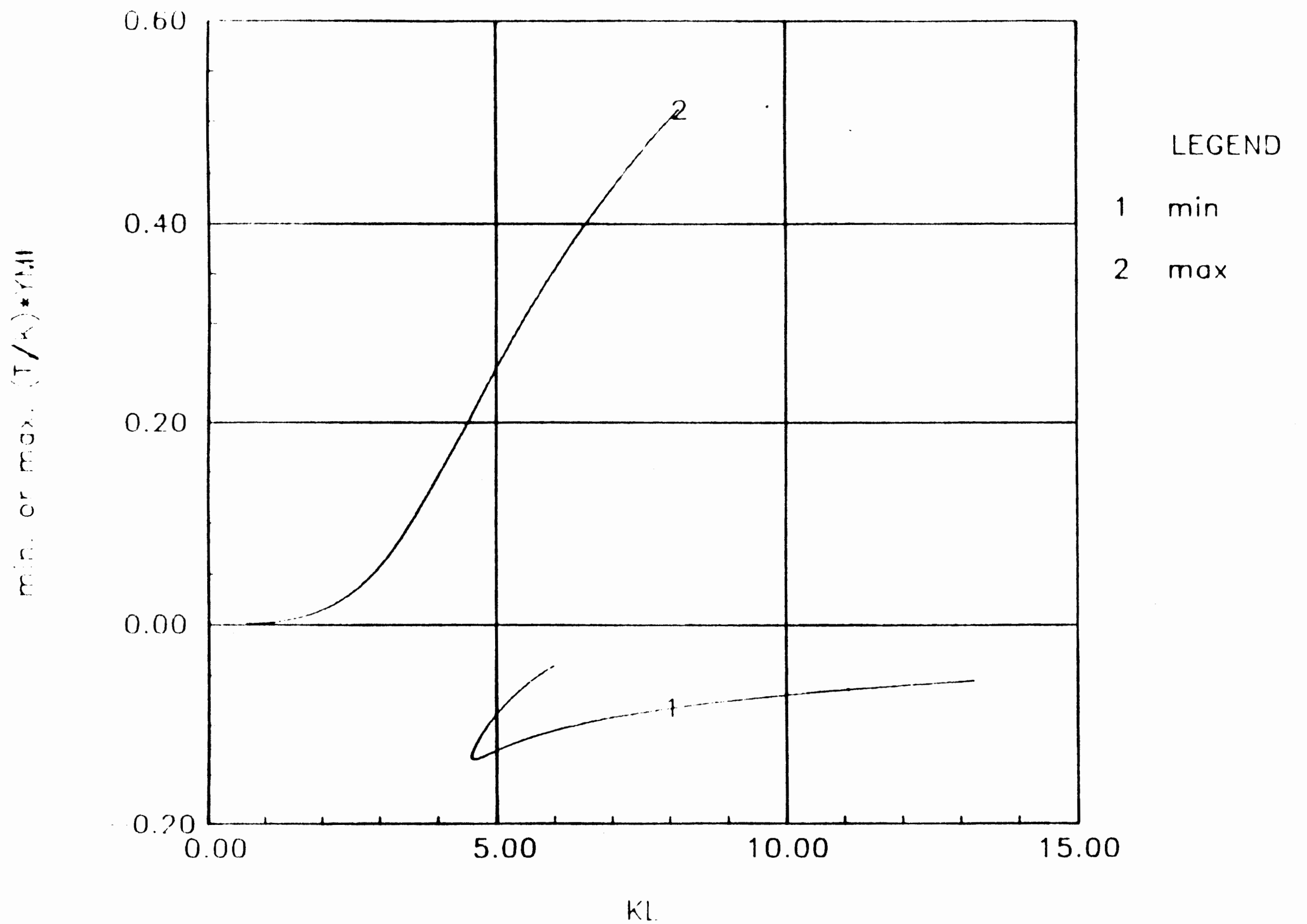

Figure 12. Minimized and Maximized Curvature Factors Due to Lateral Moment vs KL as Functions of KL for Given l/L

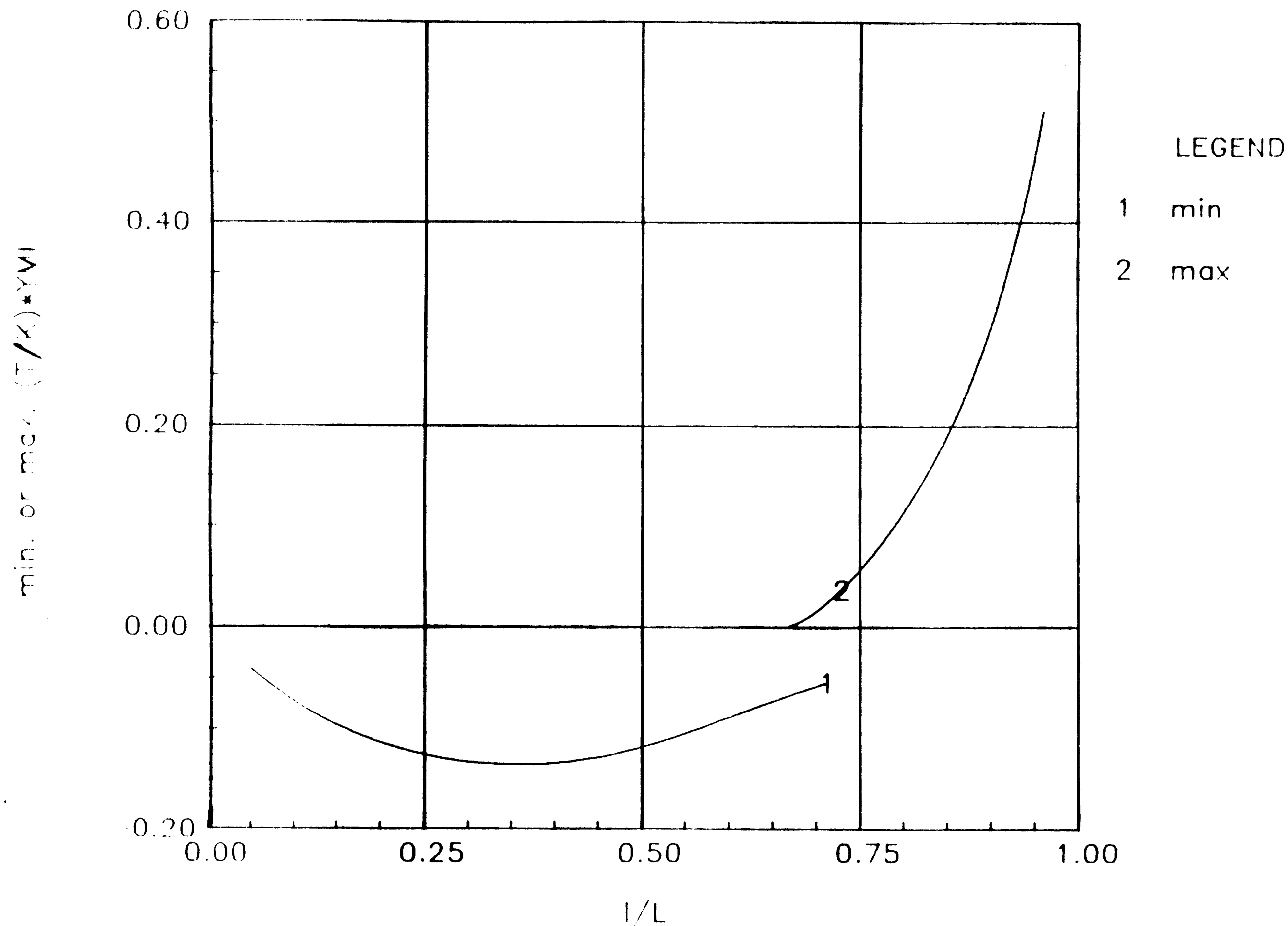

Figure 13. Minimized and Maximized Curvature Factors Due to Lateral Moment vs l/L as Functions of KL for Given l/L

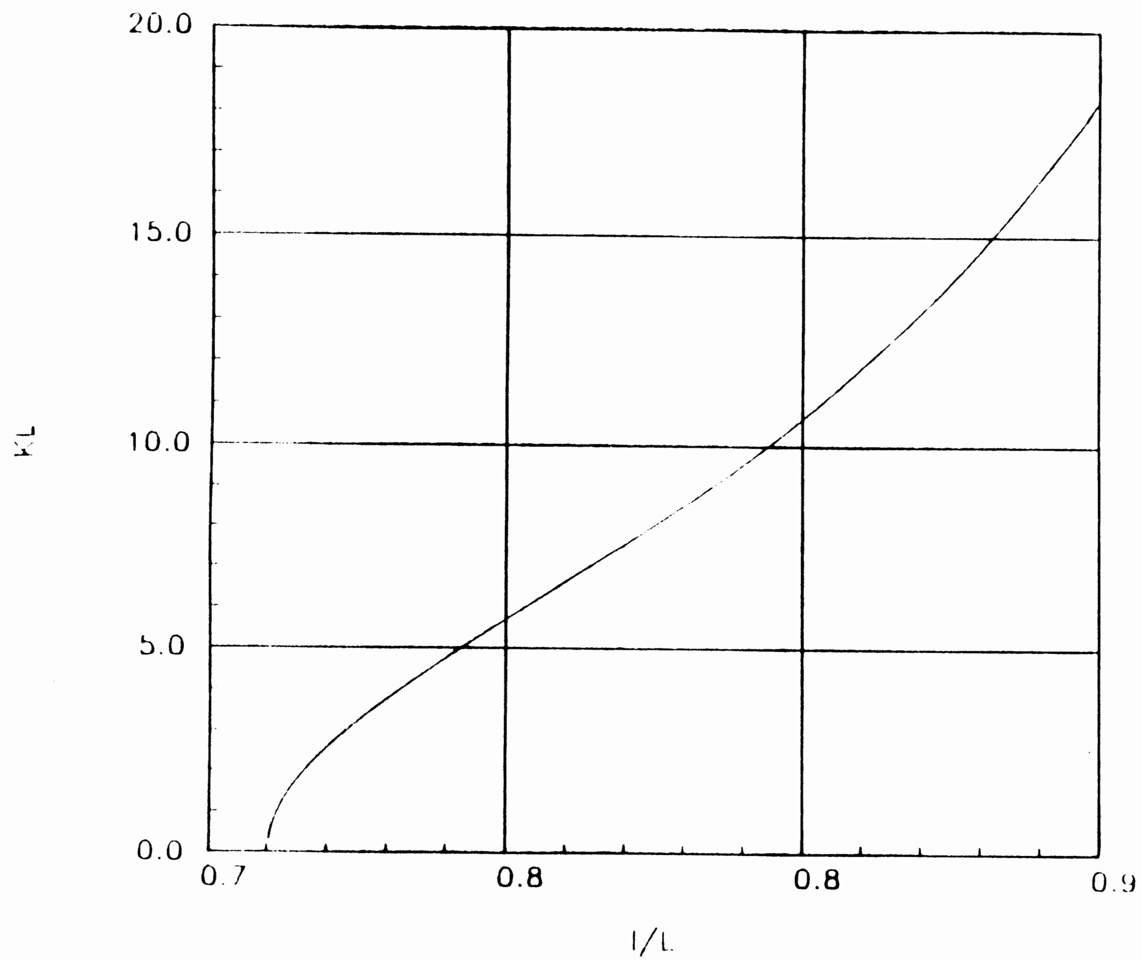

Figure 14. The Curve of KL vs l/L for Maximum Curvature Factor
at the Disturbance Location Due to Lateral Force

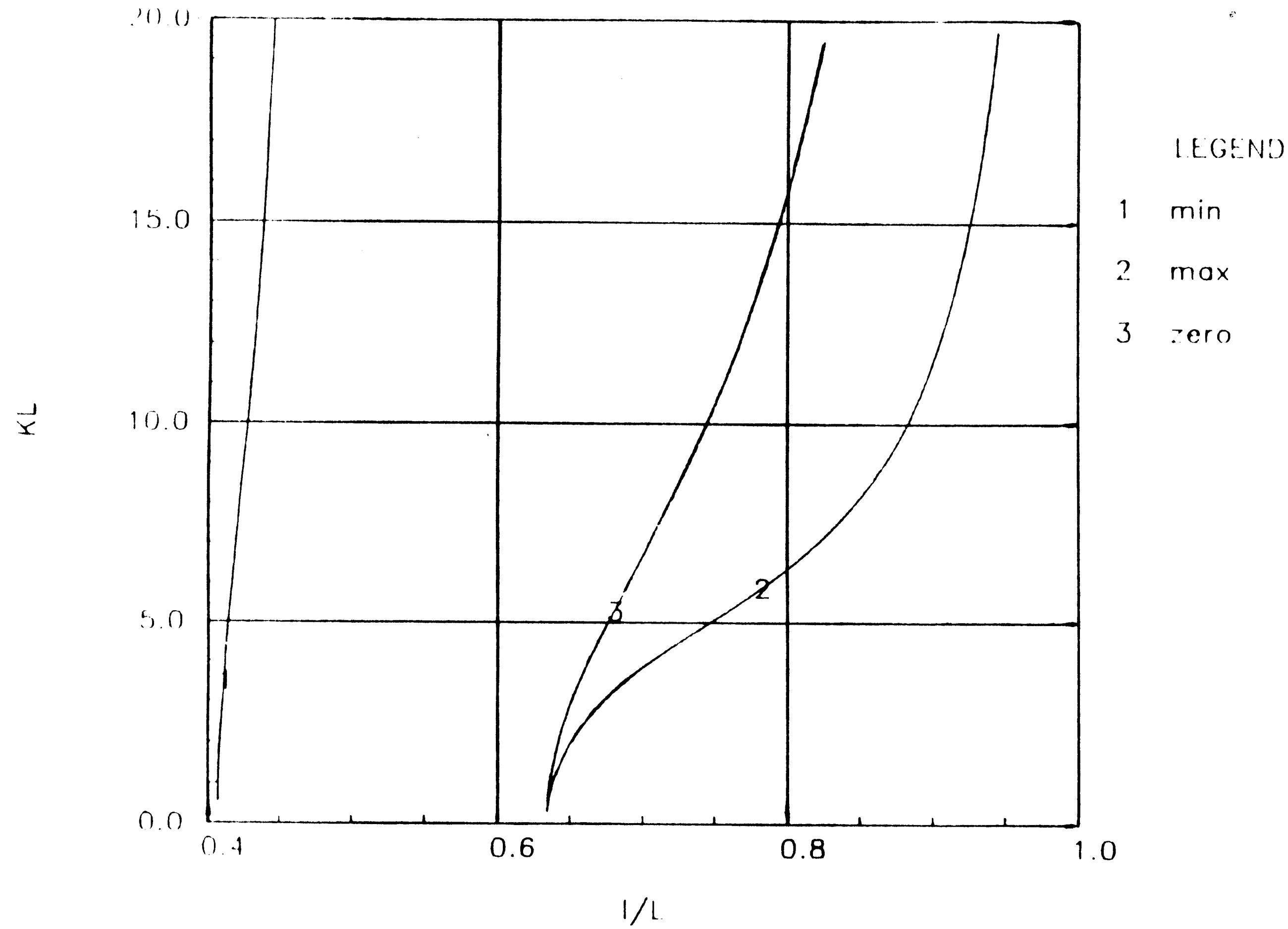

Figure 15. Curves of KL vs l/L for Extreme and Zero Curvature Factors at Disturbance Location Due to Lateral Moment

CHAPTER III

DYNAMICS WITH SIDE LOADS ON A MOVING WEB SPAN

The theory of the second-order dynamics of a massless web, developed by Shelton [1], is applied to the case with considerable side loads on a moving web span. The analysis of web mechanics follows the same procedure as used in Chapter II with more generalized BC's applied.

Considering the lateral displacement of the web span at a certain location as the only system output, a single moving web span can be described as a multiple-input-single-output (MISO) system. The inputs include the lateral web displacement at the upstream roller, the guide roller motion, and the lateral load disturbances. To make the analysis of dynamics for a type II interactive system complete, one should construct models to characterize the lateral load disturbances through the lateral web motion and the disturbance causing devices. Model building is beyond the scope of this research. No such work will be reported in this chapter. The following is an analysis of web lateral dynamics including the side load effect.

Basic Equations

If web mass is negligible, the governing equation of the elastic web lateral displacement is applicable to the web span in both steady and unsteady states. The BC's, however, have to be changed accordingly. This governing equation is given by

$$\frac{\partial^4 y}{\partial x^4} - K^2 \frac{\partial^2 y}{\partial x^2} = 0 \tag{65}$$

The time factor is not involved in (65) due to the consideration of negligible web mass.

Equations for dynamic steering have been established by Shelton [1], which are applicable in the cases considered here

$$\frac{\partial y_L}{\partial t} = V(\theta_r - \frac{\partial y_L}{\partial x}) + \frac{dz}{dt} \tag{66}$$

$$\frac{\partial^2 y_L}{\partial t^2} = V^2 \frac{\partial^2 y_L}{\partial x^2} + \frac{d^2 z}{dt^2} \tag{67}$$

where q_r is the downstream roller angle, and z the lateral position of the downstream roller.

(66) indicates that the lateral velocity of the web edge at the line of entering contact is equal to the velocity of steering plus the velocity of lateral transport. In (67) only the accelerations due to the curvature and the steering are included.

Web Mechanics Analysis

From statics analysis for a moving web with considerable side force and moment loaded as given in Chapter II, the general solution for (65) is given by

$$y = C_1 shKx + C_2 chKx + C_3 x + C_4 \qquad 0 \le x < l \tag{68}$$

$$y = C_5 shKx + C_6 chKx + C_7 x + C_8 \qquad l < x \le L \tag{69}$$

The following set of BC's are used to determine the coefficients involved in (68) and (69)

1) $y(0) = y_0$ 2) $y'(0) = 0$ 3) $y(L) = y_L$

4) $y'(L) = \theta_L$ 5) $y(l^+) = y(l^-)$ 6) $y'(l^+) = y'(l^-)$

7) $M_{l^+} - M_{l^-} = -M_l$ 8) $N_{l^+} - N_{l^-} = -Q_l$

In this set of BC's, one restriction is BC 2) which specifies that the web span is always perpendicular to the upstream roller. This is possible if the upstream roller is part of the displacement guide. A more generalized set of BC's may have an arbitrary y'(0), the angular displacement at the upstream roller. In this case the relation defined by (66) will be applied at the upstream roller to express y'(0) as a function of y(0), the lateral web displacement at the upstream roller. Kardamilas [6] has used this approach to construct a model which describes the lateral web motion for a single web span passing two rollers with arbitrary angular displacements at both up- and down-stream rollers. To avoid complexity in the coefficients, this restricted set of BC's instead of the most general one is used to illustrate the dynamics analysis for the type II interactive system.

After applying those BC's, (68) and (69) can be expressed as

$$y = C_1(shKx - Kx) + C_2(chKx - 1) \qquad (70)$$

$$0 \le x < l$$

$$y = -(Q_3 - \frac{C_7}{K})shK(L-x) + (y_L - y_0 - C_7L - C_8)chK(L-x) + C_7x + C_8 \qquad (71)$$

$$l < x \le L$$

The coefficients involved in (70) and (71) are given by

$$C_1 = (C_{11}\ C_{12}\ C_{13}\ C_{14})\begin{bmatrix} y_L - y_0 \\ Q_3 \\ Q_4 \\ Q_5 \end{bmatrix} \qquad (72)$$

$$C_2 = (C_{21}\ C_{22}\ C_{23}\ C_{24})\begin{bmatrix} y_L - y_0 \\ Q_3 \\ Q_4 \\ Q_5 \end{bmatrix} \qquad (73)$$

$$\frac{C_7}{K} = (C_{71}\ C_{72}\ C_{73}\ C_{74})\begin{bmatrix} y_L - y_0 \\ Q_3 \\ Q_4 \\ Q_5 \end{bmatrix} \qquad (74)$$

$$C_8 = (C_{81}\ C_{82}\ C_{83}\ C_{84})\begin{bmatrix} y_L - y_0 \\ Q_3 \\ Q_4 \\ Q_5 \end{bmatrix} \qquad (75)$$

Defining D = KLshKL - 2(chKL-1), one has

$C_{11} = -shKL/D;$ $\qquad$ $C_{12} = (chKL - 1)/D;$

$C_{13} = \frac{1}{D}(chKL\text{-}1\text{-}(KL\text{-}Kl)shKL+chKl(2chKL\text{-}1)\text{-}chK(L+l));$

$C_{14} = \frac{1}{D}(\text{-}shKl(2chKL\text{-}1)+shK(L+l)\text{-}shKL);$

$C_{21} = (chKL-1)/D;$ $\qquad$ $C_{22} = (KL-shKL)/D;$

$C_{23} = \frac{1}{D}(\text{-}Kl(chKL\text{-}1)+KL(chKL\text{-}chK(L\text{-}l))\text{-}shKl(2chKL\text{-}1)+shK(L+l)\text{-}shKL);$

$C_{24} = \frac{1}{D}(\text{-}KLshK(L\text{-}l)\text{-}chK(L+l)+chKl+(chKL\text{-}1)(2chKl+l));$

$C_{71} = shKL/D;$ $\qquad$ $C_{72} = -(chKL - 1)/D;$

$C_{73} = \frac{1}{D}(\text{-}chK(L\text{-}l)+chKl+chKL\text{-}1\text{-}KlshKL);$

$C_{74} = \frac{1}{D}(\text{-}shK(L\text{-}l)+shKL\text{-}shKl);$

$C_{81} = -(chKL-1)/D;$ $\qquad$ $C_{82} = -(KL-shKL)/D;$

$C_{83} = \frac{1}{D}(\text{-}shK(L\text{-}l)+KL(shK(L\text{-}l)\text{-}chKL+KlshKL)+shKL\text{-}shKl\text{-}Kl(chKL\text{-}1));$

$C_{84} = \frac{1}{D}(\text{-}chK(L\text{-}l)+KL(shK(L\text{-}l)\text{-}shKL)+chKl+chKL\text{-}1).$

In the coefficients, Q_3 is the parameter related to guiding and is defined as θ_L/K, which has been introduced in the analysis for type I interactive systems [12]. The parameters Q_4 and Q_5 are related to lateral load disturbances, which are defined as $Q_4 = Q_l/TK$ and $Q_5 = M_l/T$, i.e., they are related to the lateral force and moment respectively.

The above results are applied in dynamic response analysis below.

Response at the Downstream Roller

The response at the downstream roller for the given set of system inputs, i.e., y_0, z, Q_4, and Q_5, can be derived using (66), (67), and the results given in the section above.

The curvatures of the web span can be obtained by taking the second derivatives of (70) and (71) with respect to x respectively. The results are

$$y'' = K^2(C_1 shKx + C_2 chKx) \tag{76}$$

$$0 \leq x < l$$

$$y'' = K^2(-(Q_3 - \frac{C_7}{K})shK(L-x) + (y_L - y_0 - C_7L - C_8)\, chK(L-x)) \tag{77}$$

$$l < x \leq L$$

At the downstream roller by setting x = L, (77) gives

$$y_L'' = K^2 (C_{L1}\ C_{L2}\ C_{L3}\ C_{L4}) \begin{bmatrix} y_L - y_0 \\ Q_3 \\ Q_4 \\ Q_5 \end{bmatrix} \tag{78}$$

where

$C_{L1} = -(chKL-1)/D; \qquad C_{L2} = -(KLchKL-shKL)/D;$

$C_{L3} = \frac{1}{D}(-KL(chKl-1)+(shK(L-l)-shKL+shKl+Kl(chKL-1));$

$C_{L4} = \frac{1}{D}(KL(shKl+chK(L-l)-chKl-chKL+1).$

Combining (67) and (78) yields

$$\frac{\partial^2 y_L}{\partial t^2} = (VK)^2 (C_{L1}\ C_{L2}\ C_{L3}\ C_{L4}) \begin{bmatrix} y_L - y_0 \\ Q_3 \\ Q_4 \\ Q_5 \end{bmatrix} + \frac{d^2 z}{dt^2} \tag{79}$$

Applying the Laplace transform to (79) by assuming zero initial conditions for $y_L(t)$, $z(t)$, $\frac{\partial y_L}{\partial t}$ and $\frac{dz}{dt}$ gives

$$s^2 y_L(s) = (VK)^2 (C_{L1}\ C_{L2}\ C_{L3}\ C_{L4}) \begin{bmatrix} y_L(s) - y_0(s) \\ Q_3(s) \\ Q_4(s) \\ Q_5(s) \end{bmatrix} + s^2 z(s) \tag{80}$$

By definition, $Q_3 = y'_L/K$, and using (66) one has

$$y_L' = \frac{-1}{V}\frac{\partial y_L}{\partial t} + \frac{z}{x_g} + \frac{1}{V}\frac{dz}{dt} \tag{81}$$

where x_g is the distance upstream from the guiding roller to the instant steering center.

Thus the following relationship can be derived

$$\begin{bmatrix} y_L(s)\text{-}y_0(s) \\ Q_3(s) \end{bmatrix} = \begin{bmatrix} -1, & 1, & 0 \\ 0, & \frac{-s}{KV}, & \frac{s}{KV} + \frac{1}{Kx_g} \end{bmatrix} \begin{bmatrix} y_0(s) \\ y_L(s) \\ z(s) \end{bmatrix} \tag{82}$$

Substituting (82) into (80), rearranging, and letting $T_1 = L/V$, one has

$$y_L(s) = \frac{1}{D(s)}\left(-C_{L1}, \left(\frac{T_1 s}{KL}\right)^2 + \frac{C_{L2}}{KL}(T_1 s + \frac{L}{x_g}), C_{L3}, C_{L4}\right) \begin{bmatrix} y_0(s) \\ z(s) \\ Q_4(s) \\ Q_5(s) \end{bmatrix} \tag{83}$$

where $D(s) = (T_1 s/KL)^2 + (C_{L2}/KL)T_1 s - C_{L1}$.

(83) indicates that 4 system inputs, y_0, z, Q_4, and Q_5, affect the single system output, y_L. If one intends to examine the individual input effect on the output, setting other inputs identically equal to zero in (83), then the transfer function to that input is obtained. One can investigate the effect of Q_4 on y_L, for example, by setting $y_0 = 0$, $z = 0$, and $Q_5 = 0$, the transfer function for the response of y_L to the input Q_4 is given by

$$y_L(s)/Q_4(s) = C_{L3}/D(s) \tag{84}$$

Thus (83) actually corresponds to 4 different transfer functions.

The transfer functions of $y_L(s)/y_0(s)$ and $y_L(s)/z(s)$ have been derived by Shelton [1] as special cases of response at a fixed roller to an input at a previous roller and steering guide response. Two more transfer functions are $y_L(s)/Q_4(s)$ and $y_L(s)/Q_5(s)$, which are also given in (83). The magnitude ratio and phase angle for $y_L(s)/Q_4(s)$ have been obtained using two plots, on which KL is specified as 0.1 and l/L assumes 4 different values, 0.25, 0.5, 0.68, and 0.86. The phase plot indicates that the phase angle is not a function of l/L. In two other plots, the magnitude ratio and phase angle for $y_L(s)/Q_5(s)$ are obtained. The same set of KL and l/L values are used as for $y_L(s)/Q_4(s)$. Two sets of phase angles are possible for different l/L as seen in the phase plot. Due to the similarity to the previous plots and a space limitation, these plots are not shown in this thesis. The magnitude ratio and phase angle for $y_L(s)/Q_4(s)$ are shown in Figs. 16 and 17 for specified l/L = 0.25, and the set of KL = 0.5, 2, 6, and 10. It clearly shows that both the magnitude ratio and the phase angle are functions of KL. Similarly, Figs. 18 and 19 are the plots for $y_L(s)/Q_5(s)$ for the same specified l/L and KL values as in Figs. 16 and 17. From this set of figures, one can see that there is no resonance possible at the downstream roller due to each individual side load effect.

Response at a Point Between Two Rollers

The response at the disturbance source is often of interest to a system designer. In practice it is often impossible to put a sensor right at the roller location. Thus the response at a point between two rollers should be investigated.

For given locations x_1 and x_2 such that $0 < x_1 < l$ and $l < x_2 < L$, from (78) and (79), one has

$$y_1 = \left(shKx_1 - Kx_1\ ,\ chKx_1 - 1\right)\begin{bmatrix} C_{11} & C_{12} & C_{13} & C_{14} \\ C_{21} & C_{22} & C_{23} & C_{24} \end{bmatrix}\begin{bmatrix} y_L - y_0 \\ Q_3 \\ Q_4 \\ Q_5 \end{bmatrix} \tag{85}$$

$$y_1 = \left\{\left(-shK(L-x_2), chK(L-x_2)\right)\begin{bmatrix} C_{k1} & C_{k2} & C_{k3} & C_{k4} \\ C_{L1} & C_{L2} & C_{L3} & C_{L4} \end{bmatrix} + \left(Kx_2, 1\right)\begin{bmatrix} C_{71} & C_{72} & C_{73} & C_{74} \\ C_{81} & C_{82} & C_{83} & C_{84} \end{bmatrix}\right\}\begin{bmatrix} y_L - y_0 \\ Q_3 \\ Q_4 \\ Q_5 \end{bmatrix} \tag{86}$$

The definition of C_{ki} is given below. Taking the Laplace transform to both (85) and (86) by assuming zero initial conditions again, and simplifying, the results can be expressed as

$$y_1(s) = X_1 A \begin{bmatrix} y_0(s) \\ z(s) \\ Q_4(s) \\ Q_5(s) \end{bmatrix} \tag{87}$$

$$y_2(s) = X_2 B \begin{bmatrix} y_0(s) \\ z(s) \\ Q_4(s) \\ Q_5(s) \end{bmatrix} \tag{88}$$

where $X_1 = [shKx_1\text{-}Kx_1,\ chKx_1\text{-}1]$;

$$A = \begin{bmatrix} -C_{11}-\frac{C_{L1}}{D(s)}(C_{11}-\frac{C_{12}}{KL}T_1s),\ a_{12},\ C_{13}+\frac{C_{L3}}{D(s)}(C_{11}-\frac{C_{12}}{KL}T_1s),\ C_{14}+\frac{C_{L4}}{D(s)}(C_{11}-\frac{C_{12}}{KL}T_1s) \\ -C_{21}-\frac{C_{L1}}{D(s)}(C_{21}-\frac{C_{22}}{KL}T_1s),\ a_{22},\ C_{23}+\frac{C_{L3}}{D(s)}(C_{21}-\frac{C_{22}}{KL}T_1s),\ C_{24}+\frac{C_{L4}}{D(s)}(C_{21}-\frac{C_{22}}{KL}T_1s) \end{bmatrix};$$

$$a_{12} = \frac{C_{12}}{KL}(T_1s + \frac{L}{x_g}) + \frac{1}{D(s)}(C_{11}-\frac{C_{12}}{KL}T_1s)\left(\left(\frac{T_1s}{KL}\right)^2 + \frac{C_{L2}}{KL}(T_1s + \frac{L}{x_g})\right);$$

$$a_{22} = \frac{C_{22}}{KL}(T_1s + \frac{L}{x_g}) + \frac{1}{D(s)}(C_{21}-\frac{C_{22}}{KL}T_1s)\left(\left(\frac{T_1s}{KL}\right)^2 + \frac{C_{L2}}{KL}(T_1s + \frac{L}{x_g})\right);$$

$$X_2 = (-shK(L\text{-}x_2),\ chK(L\text{-}x_2))\begin{bmatrix} C_{k1} & C_{k2} & C_{k3} & C_{k4} \\ C_{L1} & C_{L2} & C_{L3} & C_{L4} \end{bmatrix} + (Kx_2,\ 1)\begin{bmatrix} C_{71} & C_{72} & C_{73} & C_{74} \\ C_{81} & C_{82} & C_{83} & C_{84} \end{bmatrix};$$

$$B = \begin{bmatrix} -1-\frac{C_{L1}}{D(s)}, & b_{12}, & \frac{C_{L3}}{D(s)}, & \frac{C_{L4}}{D(s)} \\ \frac{C_{L1}}{KLD(s)}T_1s, & b_{22}, & \frac{-C_{L3}}{KLD(s)}T_1s, & \frac{-C_{L4}}{KLD(s)}T_1s \\ 0, & 0, & 1, & 0 \\ 0, & 0, & 0, & 1 \end{bmatrix};$$

with $b_{12} = \frac{1}{D(s)}\left(\left(\frac{T_1s}{KL}\right)^2 + \frac{C_{L2}}{KL}(T_1s + \frac{L}{x_g})\right)$;

$$b_{22} = \frac{1}{KL}(T_1s + \frac{L}{x_g}) - \frac{T_1s}{KLD(s)}\left(\left(\frac{T_1s}{KL}\right)^2 + \frac{C_{L2}}{KL}(T_1s + \frac{L}{x_g})\right);$$

The definition for C_{ki}, (i = 1, 4) is given by

$$Q_3 - \frac{C_7}{K} = (C_{k1}\ C_{k2}\ C_{k3}\ C_{k4})\begin{bmatrix} y_L - y_0 \\ Q_3 \\ Q_4 \\ Q_5 \end{bmatrix}$$

where

$C_{k1} = -shKL/D;$ $\qquad C_{k2} = (KLshKL\text{-}\ chKL+1)/D;$

$$C_{k3} = \frac{1}{D}(chK(L\text{-}l)\text{-}chKl\text{-}chKL+1+KlshKL);$$

$$C_{k4} = \frac{1}{D}(shK(L\text{-}l)\text{-}shKL+shKl)\ .$$

Setting $x_1 = l$ or $x_2 = l$ in (87) and (88) respectively yields the response at the location of lateral loads disturbance.

Only the results for transfer functions corresponding to the side loads are shown in

Figs. 20 to 23. The transfer functions to $y_0(s)$ and $z(s)$ are also included in (87) and (88), but the results are not presented. Figs. 20 and 21 are for $y(s)/Q_4(s)$ for given set of $x/L = 0.25, 0.35, 0.5, 0.65, 0.75$, and 0.85 with specified $KL = 0.5$ and $l/L = 0.5$. With the same specification, Figs. 22 and 23 are for $y(s)/Q_5(s)$. Note in Fig. 23, $y(s)$ can be in or out of phase with $Q_5(s)$ due to different x/L. Other results were also obtained but not graphically shown here due to the space limitation. There were two plots obtained similar to Figs. 20 and 21, and another two to Figs. 22 and 23, but with $KL = 2$, to see the parameter KL effect. Again two plots obtained were similar to Figs. 20 and 21, and the other two to Figs. 22 and 23, but with $l/L = 0.75$ to see the effect of disturbance source location. As shown in the plots, no resonance exists due to the effect of each individual side load. In general y has a larger magnitude in a low frequency range than in a high frequency range. For small x/L values, y can have a smaller magnitude in a low frequency range than in a high frequency range as observed in some of the plots.

Discussion

The dynamics for web lateral motion has been extended to the case with side loads disturbance. For a single span, the general dynamic equations for the responses at both the downstream roller and a point between two rollers are derived in 4 system inputs, y_0, z, Q_4, and Q_5. The effect of the side loads on the lateral web behavior can thus be analyzed.

No resonance exists at either the downstream roller or a point between two rollers due to each individual side load effect. The lateral displacement always has a larger magnitude in a low frequency range than in a high one at the downstream roller for a given set of system parameters. The same trend holds for the displacement at a point between two rollers except for the locations quite near the upstream roller, where a smaller magnitude is possible in a low frequency range.

The analysis so far assumes that the system inputs are independent of each other. The side loads in fact not only depend on the disturbance source type, but also the displacement at the upstream roller and the steering at the downstream roller. More work needs to be done to identify the model for the given disturbance device in the process line so that the functional relationship between side loads and other system inputs can be established. An experimental study has been done using the parameter identification technique to see if a type II interactive system, which has an air-bar providing lateral load disturbances, can be modeled as an ARMA process between the lateral web displacements at up- and down-stream rollers. The details are presented in Chapter V. The basic finding in the investigation is that when there is no amplification in lateral web displacement at the downstream end compared to that at the upstream end, the ARMA process is applicable. On the other hand when the amplification occurs, large lateral load disturbances are involved and the ARMA process is not appropriate to describe the lateral web behavior of the system. This fact has motivated a unified approach through experimental study to investigate the lateral web behavior in a web system with an air-bar unit providing lateral load disturbances. The details of this study are also included in the following chapter.

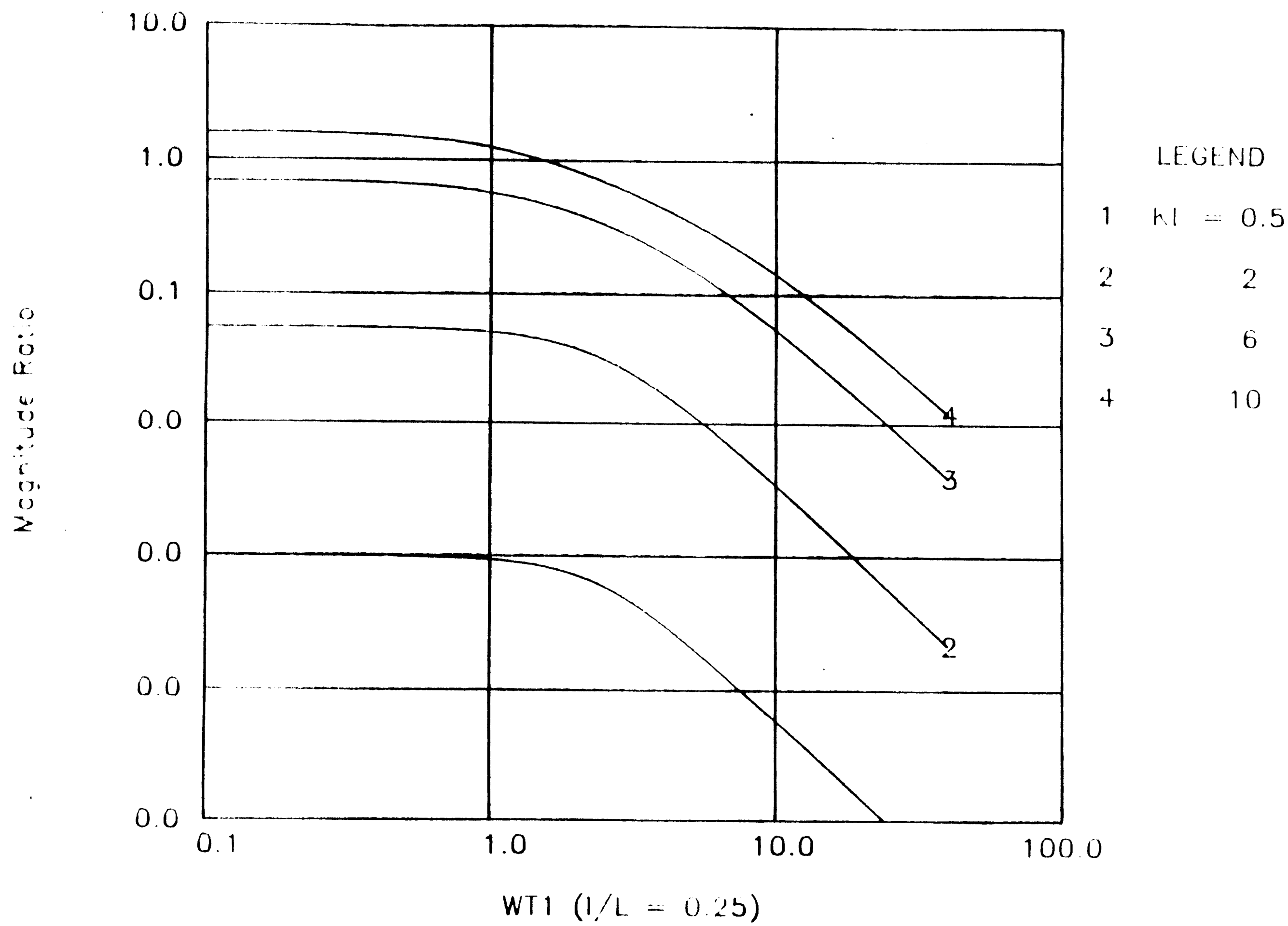

Figure 16. Magnitude Ratio in the Frequency Response of Web at the Downstream Roller Due to Q_4

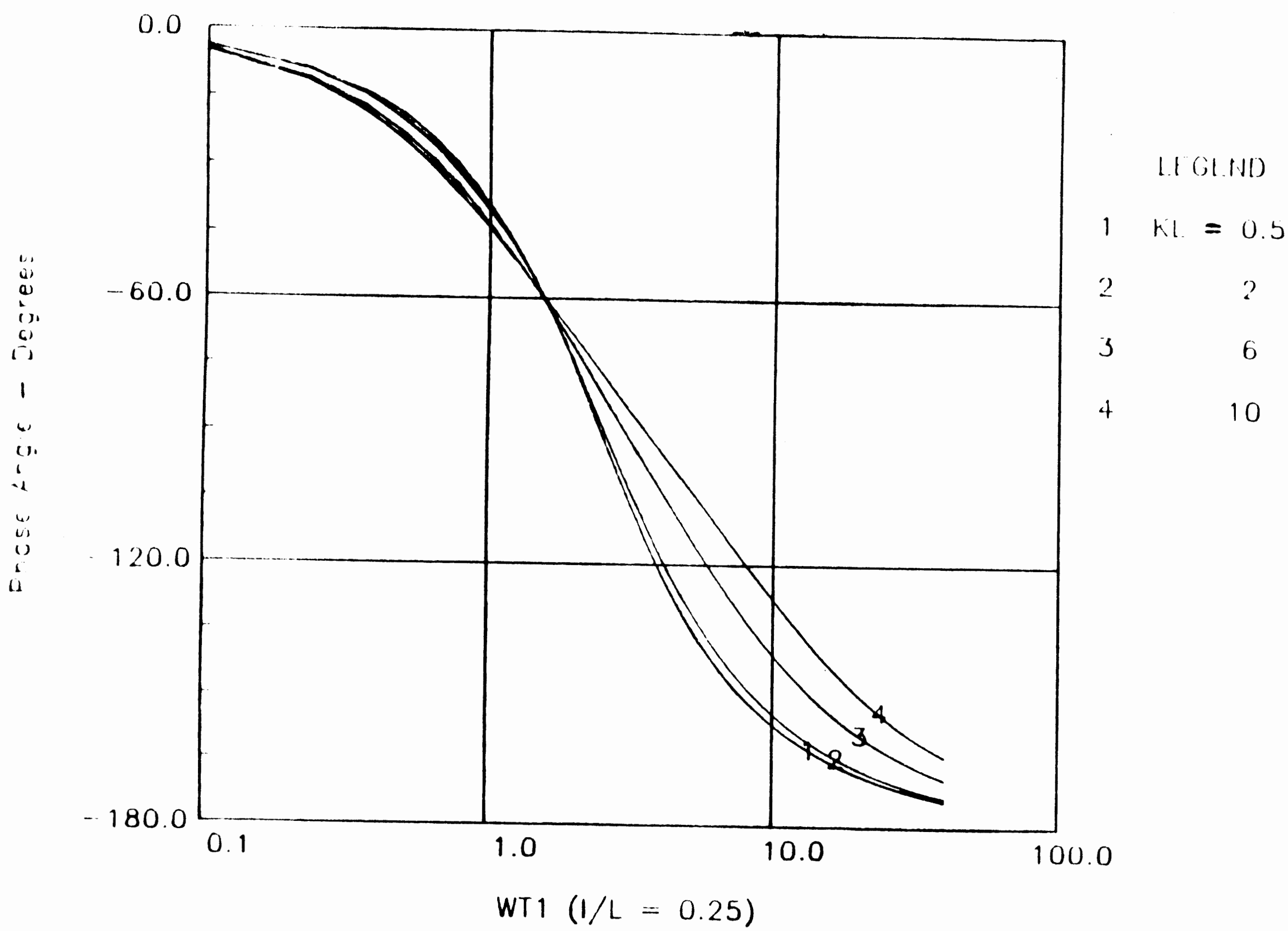

Figure 17. Phase Angle in the Frequency Response of Web at the Downstream Roller Due to Q_4

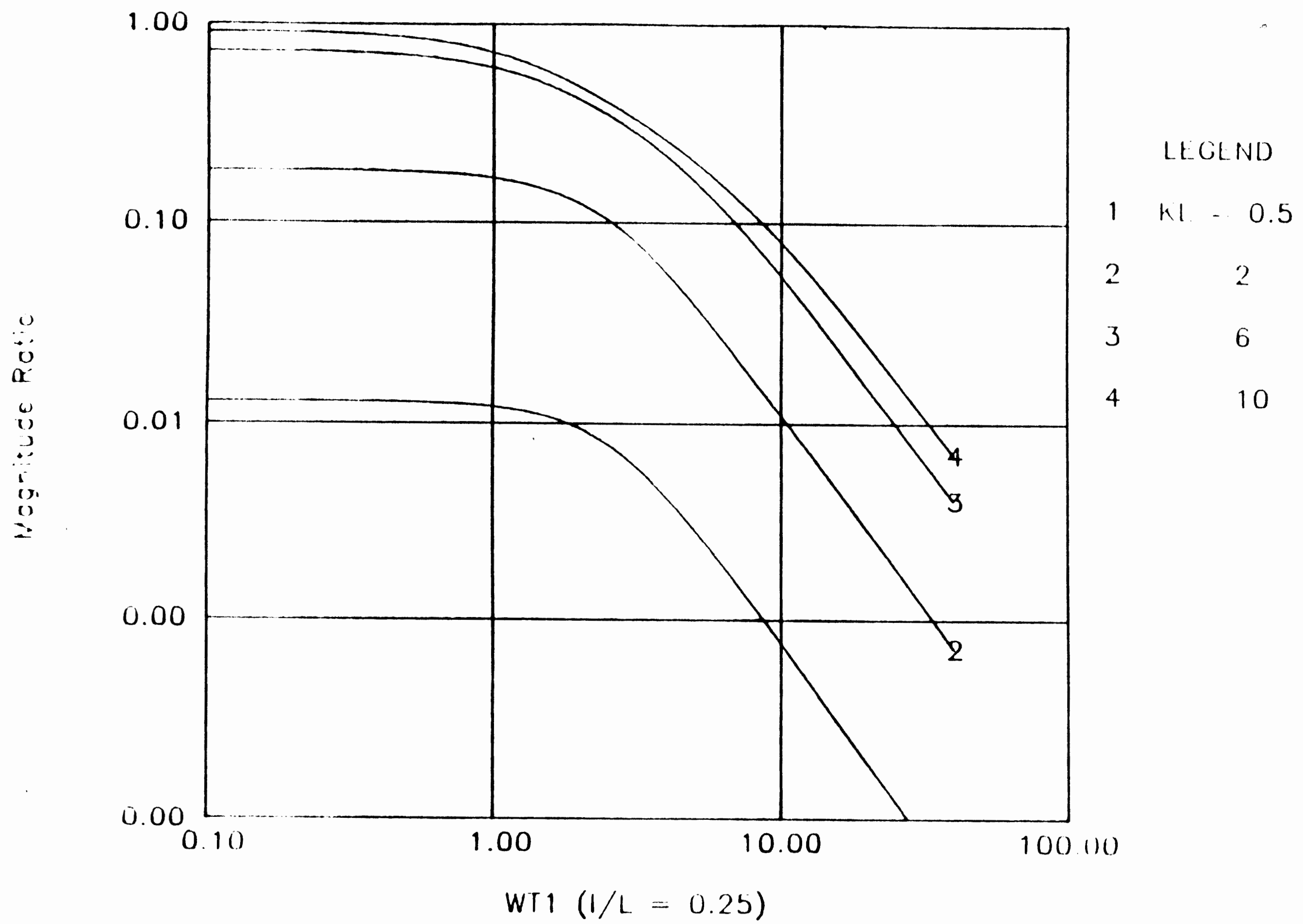

Figure 18. Magnitude Ratio in the Frequency Response of Web at the Downstream Roller Due to Q_5

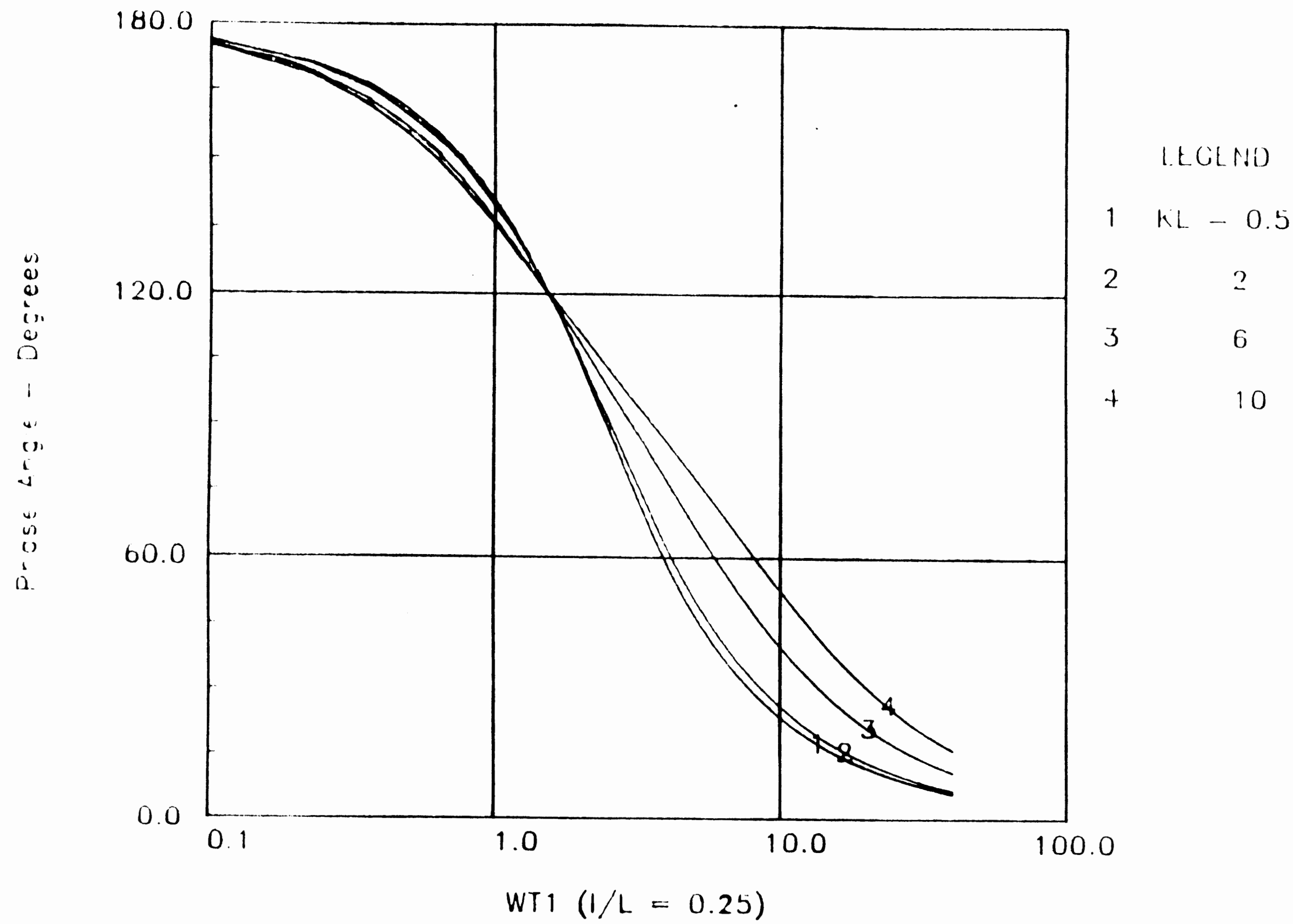

Figure 19. Phase Angle in the Frequency Response of Web at the Downstream Roller Due to Q_5

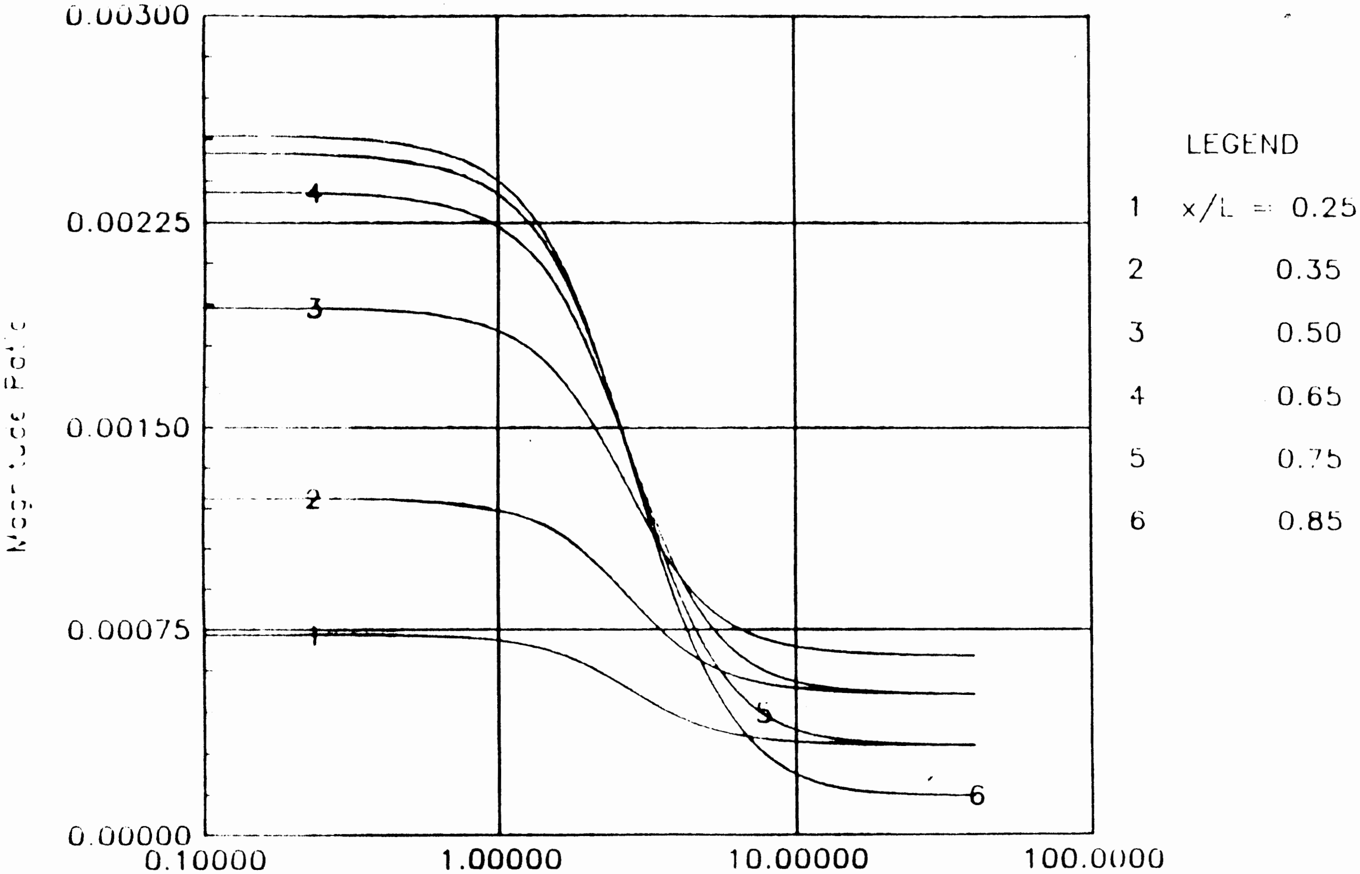

Figure 20. Magnitude Ratio in the Frequency Response of Web at a Point Between Two Rollers Due to Q_4

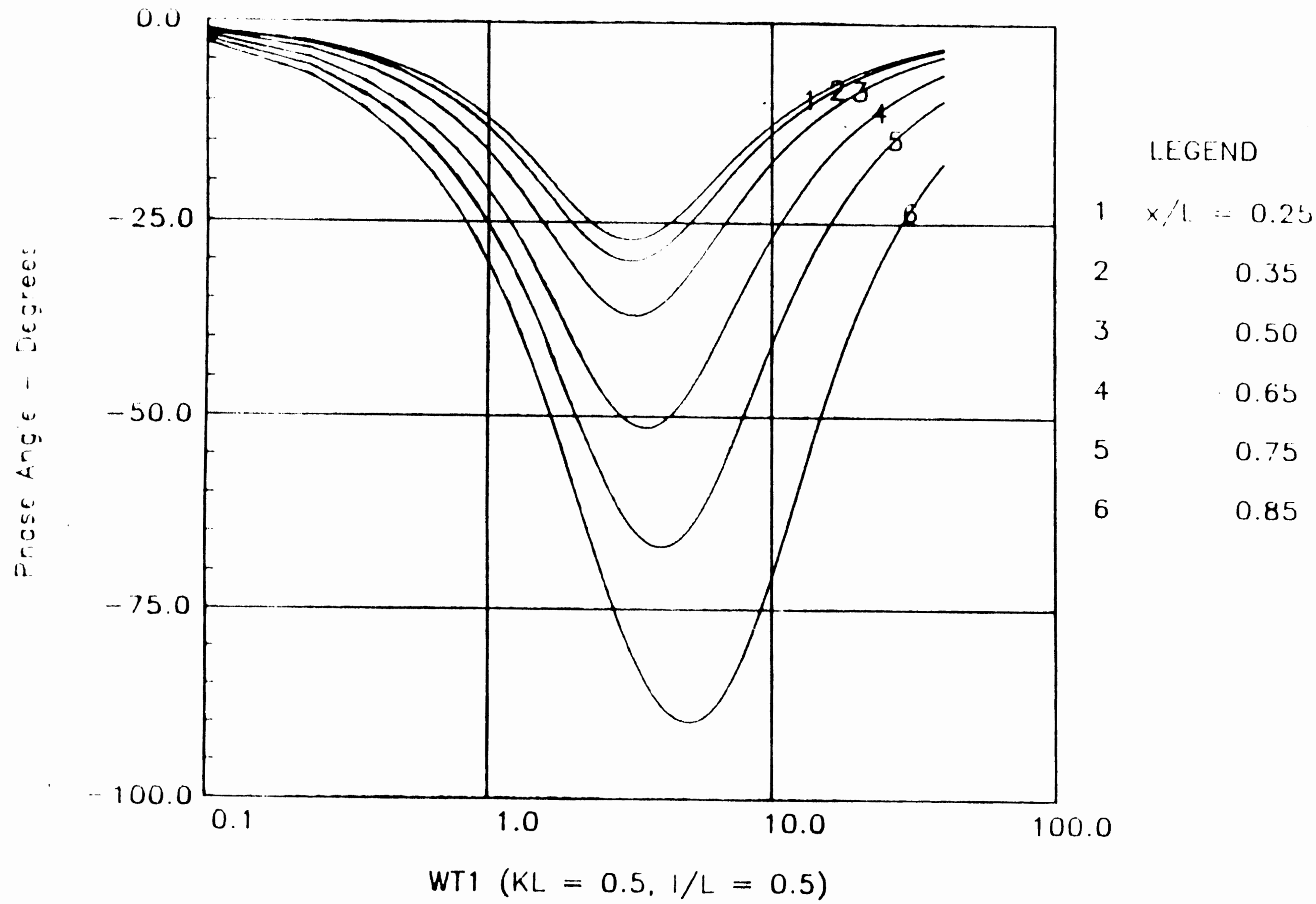

Figure 21. Phase Angle in the Frequency Response of Web at a Point Between Two Rollers Due to Q_4

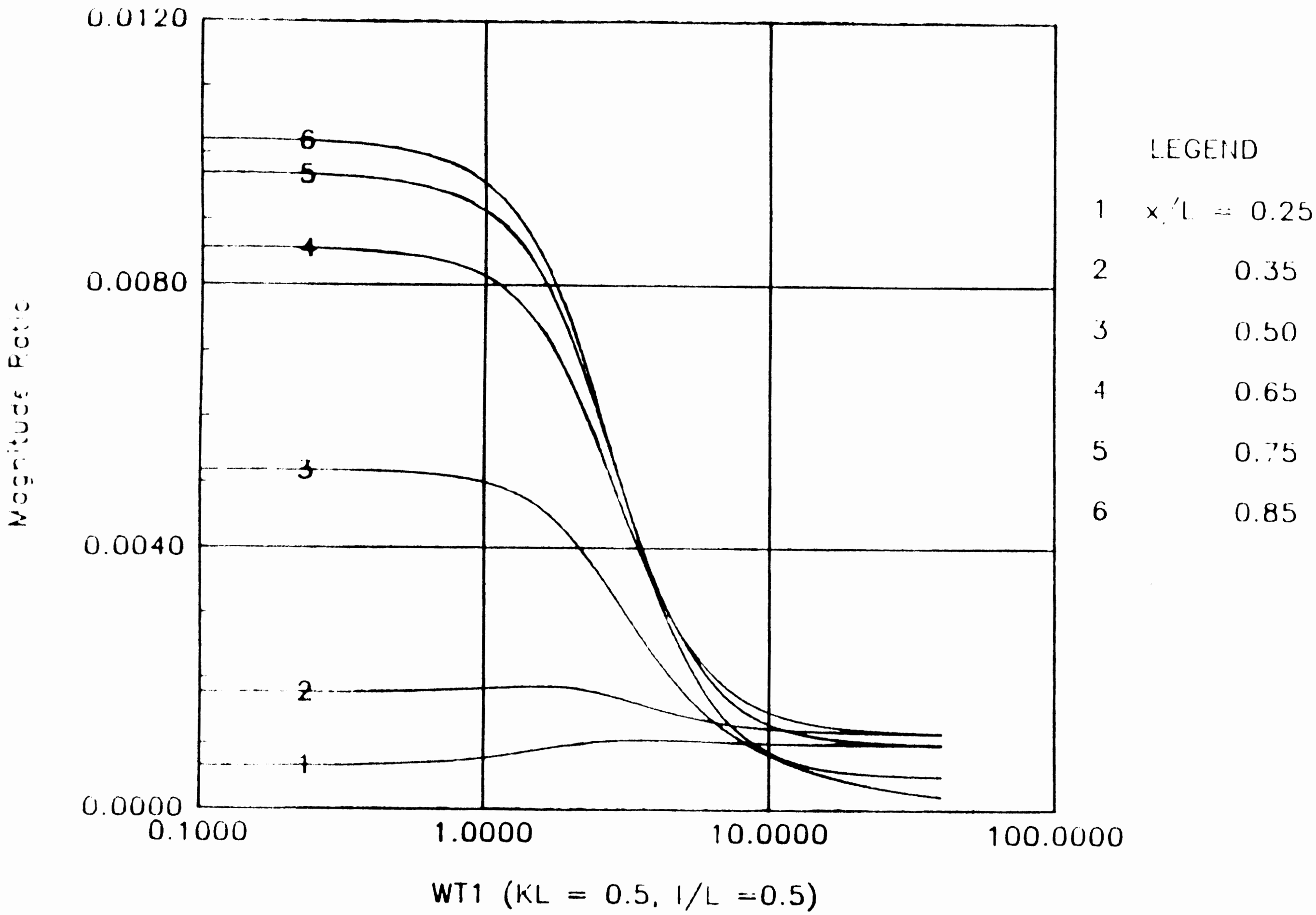

Figure 22. Magnitude Ratio in the Frequency Response of Web at a Point Between Two Rollers Due to Q_5

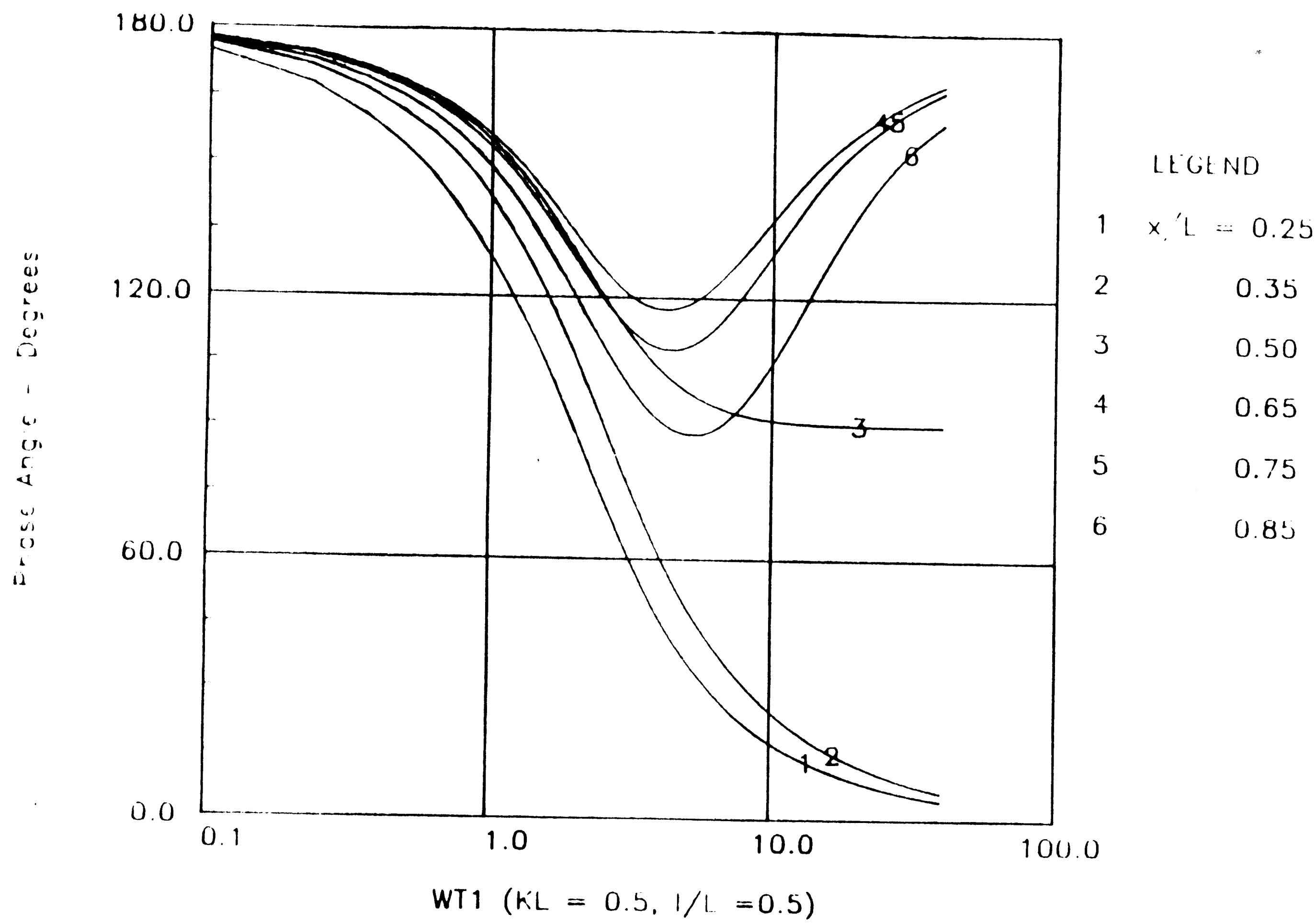

Figure 23. Phase Angle in the Frequency Response of Web at a Point Between Two Rollers Due to Q_5

CHAPTER IV

INTERACTION WITH SIDE LOADS ON PRE-ENTERING SPAN

The statics of type III interactive systems, which are the combination of interactive systems of type I and type II, are investigated in this chapter. The system in consideration is schematically shown in Fig. 3. This is one of the many configurations of the type III interactive system. The procedure developed for this special configuration will establish the main principles in analyzing type III interactive systems. For those configurations with more complexity, some more details may need to be worked out but the basic principles hold in the analysis.

For such a system, four interaction modes are possible. Due to the complexity of the interaction as a function of, besides system parameters, the steering and the side loads, the conditions for mode determination must be determined. One restriction of the analysis is the taut edges for web spans. To establish the domain for current analysis, and also for the slack edge analysis of the future work, the conditions for maintaining taut edges also have to be determined. Those conditions can be established only after all possible interaction mode analyses have been accomplished.

Three equations are adequate to describe the lateral web motion for the system in consideration. These equations are

$$y_A = C_{A1} shKx_A + C_{A2} chKx_A + C_{A3}x_A + C_{A4} \qquad (89)$$

$$0 \leq x_A < l_A$$

$$y_A = C_{A5}shKx_A + C_{A6}chKx_A + C_{A7}x_A + C_{A8} \tag{90}$$

$$l_A < x_A \leq L_A$$

$$y_B = C_{B1}shKx_B + C_{B2}chKx_B + C_{B3}x_B + C_{B4} \tag{91}$$

$$0 \leq x_B \leq L_B$$

These equations involve 12 coefficients, which requires 12 BC's to determine the coefficients uniquely. A different interaction mode corresponds to a different set of BC's. The analysis for each interaction mode is to apply the appropriate set of BC's, and thus uniquely determine the corresponding set of coefficients.

The Mode of Interaction Free

Here the interaction free only indicates that there is sufficient friction between the web and the entering roller that no interaction exists between two spans. This definition is from the work done for type I interactive systems [12].

Due to the lack of interaction the two spans can be treated separately for the system in such a mode. For span A, the results in Chapter II above are applicable by neglecting the steering terms. Shelton's work [1] is valid for span B. By applying continuity in both displacement and slope for the web at the entering roller location, the following results are obtained.

For span A, one has

$$y_A = C_{A1}(shKx_A - Kx_A) + C_{A2}(chKx_A - 1) \tag{92}$$

$$0 \leq x_A < l_A$$

where the coefficients involved are

$$C_{A1} = \frac{1}{chKL_A - 1}\left(Q_4(chKl_A - chKL_A) - Q_5 shKl_A\right) \tag{93}$$

$$C_{A2}=\frac{1}{chKL_A-1}\left(Q_4(shKL_A-shKl_A-shK(L_A-l_A))-Q_5(chK(L_A-l_A)-chKl_A)\right) \quad (94)$$

and

$$y_A = -(C_{A1}+Q_4)(Kx_A+shK(L_A-x_A)) + C_{A8} \quad (95)$$

$$l_A < x_A \leq L_A$$

where C_{A8} is given by

$$C_{A8}=\frac{1}{chKL_A-1}\left(Q_4(Kl_A(chKL_A-1)+shKl_A-shKL_A+shK(L_A-l_A))+\right.$$
$$\left.Q_5(chK(L_A-l_A)-chKl_A-chKL_A+1)\right) \quad (96)$$

For span B

$$y_B = \frac{Q_3}{chKL_B-1}(shK(L_B-x_B) - shKL_B+ Kx_BchKL_B) + y_{AL} \quad (97)$$

$$0 \leq x_B \leq L_B$$

where

$$y_{AL} = -(C_{A1}+Q_4)KL_A + C_{A8} \quad (98)$$

The conditions for the interaction free mode can be derived using the results obtained above. The details will be given in the section for the conditions of mode determination below.

The Mode of Interaction With Moment Transfer Only

When the web system is in the moment transfer mode, the friction between the web and the entering roller (roller B) is not sufficient to prevent the lateral moment transfer from downstream to upstream. Appropriately combining the BC's from the analyses for the type II interactive system in Chapter II and for the type I interactive system [12], the 12 BC's used for determining the coefficients involved in (89) to (91) are given by

1) $y_{A0} = 0$, 2) $y'_{A0} = 0$, 3) $y'_{BL} = \theta_L$

4) $y''_{BL} = 0$, 5) $y_{AL} = y_{BL}$, 5) $y'_{AL} = 0$

7) $y'_{B0} = y'_{AL}$, 8) $y_{l_A^-} = y_{l_A^+}$, 9) $y'_{l_A^-} = y'_{l_A^+}$

10) $M_{B0} - M_{AL} = -M_r$ 11) $M_{l_A^+} - M_{l_A^-} = - M_l$ 12) $N_{l_A^+} - N_{l_A^-} = - Q_l$

Applying this set of BC's, one can derive, for span A

$$y_A = C_{A1}(shKx_A - Kx_A) + C_{A2}(chKx_A - 1) \tag{99}$$

$$0 \leq x_A < l_A$$

with

$$C_{A1} = \frac{1}{chKL_A - 1}\left(-Q_2 shKL_A + Q_3\frac{shKL_A shKL_B}{chKL_B - 1} + Q_4(chKl_A - chKL_A) - Q_5 shkl_A\right) \tag{100}$$

where $Q_2 = M_r/T$, with M_r the frictional moment at the entering roller, which has been introduced in the analysis for type I interactive systems [12], $Q_4 = Q_{l_A}/TK$, $Q_5 = M_{l_A}/T$, and

$$C_{A2} = \frac{1}{chKL_A - 1}\Big(Q_2(chKL_A - 1) - Q_3\frac{shKL_B(chKL_A - 1)}{chKL_B - 1} + Q_4(shKL_A - shKl_A - shK(L_A - l_A)) + Q_5(chkl_A - chK(L_A - l_A))\Big) \tag{101}$$

$$y_A = \frac{C_{A7}}{K}(shK(L_A - x_A) + Kx_A) + (C_{B2} - Q_2)chK(L_A - x_A) + C_{A8} \tag{102}$$

$$l_A < x_A \leq L_A$$

with

$$C_{A7} = \frac{K}{chKL_A - 1}\left(Q_2 shKL_A - Q_3\frac{shKL_A shKL_B}{chKL_B - 1} - Q_4(chKl_A - 1) + Q_5 Shkl_A\right) \tag{103}$$

$$C_{A8} = - C_{A2} - Kl_A\left(C_{A1} + \frac{C_{A7}}{K}\right) - Q_5 \tag{104}$$

$$C_{B2} = Q_3\frac{shKL_B}{chKL_B - 1} \tag{105}$$

and for span B

$$y_B = C_{B1}(shKx_B - Kx_B) + C_{B2}chKx_B + C_{B4} \tag{106}$$

$$0 \le x_B \le L_B$$

with

$$C_{B1} = - Q_3 \frac{chKL_B}{chKL_B - 1} \tag{107}$$

$$C_{B4} = - Q_2 + C_{A7}L_A + C_{A8} \tag{108}$$

The details in obtaining those coefficients involved in solving the governing equations have been given in Chapter II and the analysis for the type I interactive systems [12]. A similar procedure is followed in the derivations above without giving any step-by-step descriptions. In the following sections the same approaches are adopted in listing the results for the determination of coefficients in the solutions of governing equations for web lateral motion in different interaction modes.

Above equations determine the web displacement in the moment transfer only condition.

The Mode of Interaction With Shear Transfer Only

When lateral load disturbances are negligible, the interaction mode of shear transfer only rarely, if ever, occurs in a web handling system. With considerable disturbances, however, this mode does occur for a given web system. Therefore, it is necessary to analyze the web lateral behavior in the shear transfer only mode in order to gain a thorough understanding of an interactive web system

Among the 12 BC's in the moment transfer only mode analysis, the 10th does not hold anymore. It must be replaced by

10) $N_{B0} - N_{AL} = N_r$

Applying above BC's, one can obtain the following results

$$y_A = C_{A1}(shKx_A - Kx_A) + C_{A2}(chKx_A - 1) \tag{109}$$

$$0 \le x_A < l_A$$

$$y_A = \frac{1}{shKL_A}\left(\frac{C_{A7}}{K}(chK(L_A - x_A) - chKx_A) - (Q_4(chKl_A - 1) - Q_5 shKl_A)chK(L_A - x_A)\right) + C_{A7}x_A + C_{A8} \tag{110}$$

$$l_A < x_A \le L_A$$

$$y_B = \frac{C_{B3}}{KchKL_B}(shK(L_B - x_B) + Kx_B chKL_B) + C_{B4} \tag{111}$$

$$0 \le x_B \le L_B$$

where

$$C_{B2} = Q_3\frac{shKL_B}{chKL_B - 1} \tag{112}$$

$$C_{B3} = KQ_3\frac{chKL_B}{chKL_B - 1} \tag{113}$$

$$C_{A7} = K(-Q_1 + \frac{C_{B3}}{K}) \tag{114}$$

where $Q_1 = N_r/TK$, with N_r the frictional shear force at the entering roller, which has also been introduced in the analysis for type I interactive systems [12], and

$$C_{A1} = Q_1 - \frac{C_{B3}}{K} - Q_4 \tag{115}$$

$$C_{A2} = \frac{1}{shKL_A}\left(\frac{C_{A7}}{K}(chKL_A - 1) + Q_4(chKL_A - chK(L_A - l_A)) - Q_5 shK(L_A - l_A)\right) \tag{116}$$

$$C_{A8} = -C_{A1}Kl_A - C_{A2} - Q_5 - C_{A7}l_A \tag{117}$$

$$C_{B4} = \frac{1}{shKL_A}\left(-\frac{C_{A7}}{K}(chKL_A - 1) - Q_4(chKl_A - 1) + Q_5 shkl_A\right) + C_{A7}L_A + C_{A8} - C_{B2} \tag{118}$$

The results given above describe the lateral web displacement for the system in the shear transfer only condition.

The Mode of Interaction With Both Moment and Shear Transfer

Among the 12 BC's given in the moment transfer only mode analysis, the 6th one does not hold. It must be replaced by the shear relation on the entering roller, i.e.,

6) $N_{B0} - N_{AL} = N_r$

Applying those BC's yields

$$y_A = -Q_1(shk(L_A\text{-}x_A)+kx_AchKL_A\text{-}shkL_A)\text{-}Q_2(chk(L_A\text{-}x_A)+kx_AshKL_A\text{-}chKL_A)$$

$$-(Q_3\text{-}\frac{C_{B3}}{K})(shK(L\text{-}x_A)+Kx_AchKL\text{-}shKL)+Q_4(shK(l_A\text{-}x_A)+Kx_AchKl_A\text{-}shKl_A) \quad (119)$$

$$\text{-}Q_5(ch(l_A\text{-}x_A)+Kx_AshKl_A\text{-}chKl_A)$$

$$0 \leq x_A < l_A$$

where the total web length in two web spans $L = L_A + L_B$ and

$$C_{B3} = \frac{K}{chKL\text{-}1}(Q_1(chKL_A\text{-}1)+ Q_2shKL_A+Q_3chKL \quad (120)$$

$$\text{-}Q_4(chKl_A\text{-}1)+Q_5shKl_A)$$

$$y_A = -Q_1(shK(L_A\text{-}x_A)+Kx_A)\text{-}Q_2shK(L_A\text{-}x_A)\text{-}(Q_3\text{-}\frac{C_{B3}}{K})shK(L\text{-}x_A) \quad (121)$$

$$+C_{B3}x_A+C_{A8}$$

$$l_A < x_A \leq L_A$$

where

$$C_{A8} = Q_1(shKL_A\text{-}Kl_A(chKL_A\text{-}1))+Q_2(chKL_A\text{-}Kl_AshKL_A)+(Q_3\text{-}\frac{C_{B3}}{K})$$

$$(shKL\text{-}Kl_AchKL)+Q_4(Kl_AchKl_A\text{-}shKl_A)\text{-}Q_5(1+Kl_AshKl_A\text{-}chKl_A)\text{-}C_{B3}l_A \quad (122)$$

$$y_B = -(Q_3\text{-}\frac{C_{B3}}{K})shK(L_B\text{-}x_B)+C_{B3}x_B+C_{B4} \quad (123)$$

$$0 \leq x_B \leq L_B$$

where

$$C_{B4} = - Q_1 K L_A - Q_2 + C_{B3} L_A + C_{A8} \tag{124}$$

The web lateral displacement under both moment and shear transfer is determined using the above equations.

Conditions for Mode Determination

When lateral load disturbances are large enough, the downstream shear transfer (DS) can occur. Even when the disturbances are not large enough to cause DS, upstream shear transfer (US) may occur corresponding to a certain range of steering angle. This is different from the web systems with negligible lateral load disturbances. Thus for a given web system with considerable lateral load disturbances, possible modes are: 1) Interaction free (IF); 2) Upstream moment transfer (UM); 3) US; 4) DS; and 5) Both moment and shear transfer (MS).

For a given web system, different modes may occur corresponding to different disturbances and steering angles. The conditions have to be established in order to identify correctly the mode a system is in for specified disturbances and steering angle. Then the appropriate analysis can be applied for the known interaction mode. It has been found that DS and US modes are not easy to be separately identified except for zero steering angle, which makes US impossible. Thus in categorizing the interaction modes, only 4 of them are used, which are the following.

(1) IF;

(2) Moment transfer only (MO), which is equivalent to UM;

(3) Shear transfer only (SO), which includes US and DS; and

(4) MS.

The conditions for the above four interaction modes can be derived using the moment and shear relationships at the entering roller from different mode analysis.

Conditions for IF

The IF mode analysis alone can determine the conditions for IF to occur. In the IF mode, the moment at the downstream end of span A, M_{AL}, is identically zero. Thus at entering roller, the moment relationship can be defined using a moment ratio as

$$r_{m1} = \frac{M_{B0}}{|M_r|} \tag{125}$$

and the shear relationship using a shear ratio as

$$r_{n2} = \frac{N_{B0} - N_{AL}}{|N_r|} \tag{126}$$

In (125) and (126), M_{B0}, N_{B0}, and N_{AL} are from the IF analysis and can easily be determined as

$$M_{B0} = \frac{-\,TQ_3 shKL_B}{chKL_B - 1} \tag{127}$$

$$N_{B0} = \frac{TKQ_3 chKL_B}{chKL_B - 1} \tag{128}$$

$$N_{AL} = \frac{-\,TK}{chKL_A - 1}(Q_4(chKl_A\text{-}1) - Q_5 shKl_A) \tag{129}$$

Using (127), (128), and (129), the moment and shear ratios in (125) and (126) can be expressed as

$$r_{m1} = \frac{-\,Q_3 shKL_B}{|Q_2|(chKL_B - 1)} \tag{130}$$

$$r_{n2} = \frac{1}{|Q_1|}\left(\frac{Q_3 chKL_B}{chKL_B - 1} + \frac{1}{chKL_A - 1}(Q_4(chKl_A\text{-}1) - Q_5 shKl_A)\right) \tag{131}$$

Using the concept of moment and shear ratios, the conditions for IF to occur are

$$|r_{m1}| \leq 1 \tag{132}$$

$$|r_{n2}| \leq 1 \tag{133}$$

In this mode, the expressions for frictional moment and shear are given by

$$M_r = sign(Q_3)|M_r| \tag{134}$$

$$N_r = sign(r_{n2})|N_r| \tag{135}$$

(134) and (135) are useful in calculating other moment and shear ratios given in the following sections.

Conditions for MO

Depending on the transition process, two cases exist for MO mode. One is from IF to MO, and another from DS to MO. The conditions corresponding to different transition process are different.

One common condition for these two processes is that the shear ratio at the entering roller from MO analysis cannot exceed unity. The definition of the shear ratio has the same form as in (126) except that N_{B0} and N_{AL} are from the MO analysis, which is given by

$$r_{n3} = \frac{N_{B0} - N_{AL}}{|N_r|} \tag{136}$$

where N_{B0} is the same as in (128), and

$$N_{AL} = \frac{TK}{chKL_A - 1}(Q_2 shKL_A - Q_3\frac{shKL_A shKL_B}{chKL_B - 1} - Q_4(chKl_A - 1) + Q_5 shKl_A) \tag{137}$$

Substituting (128) and (137) into (136) then simplifying the expression, one has

$$r_{n3} = \frac{1}{|Q_1|(chKL_A - 1)}(-Q_2 shKL_A + Q_3\frac{chKL - chKL_B}{chKL_B - 1} + Q_4(chKl_A - 1) - Q_5 shKl_A) \tag{138}$$

The frictional shear is expressed as

$$N_r = sign(r_{n3})|N_r| \tag{139}$$

The condition is given by

$$|r_{n3}| \leq 1 \tag{140}$$

For the process of IF to MO, the moment ratio, r_{m1}, defined above must exceed unity. Thus in this transition process, besides the condition specified by (140), another one is given by

$$|r_{m1}| > 1 \tag{141}$$

where r_{m1} is in (130). The frictional moment can be expressed as

$$M_r = sign(Q_3)|M_r| \tag{142}$$

(142) determines the sign of Q_2 in (138).

For the process of DS to MO, the moment ratio from SO analysis is needed to specify another condition. Define this moment ratio as

$$r_{m2} = \frac{M_{B0} - M_{AL}}{|M_r|} \tag{143}$$

where M_{B0} and M_{AL} are from SO analysis and are given by (128) for M_{B0}, and

$$M_{AL} = \frac{T}{ShKL_A}(-Q_1(chKL_A\text{-}1)+Q_3\frac{chKL_B(chKL_A\text{-}1)}{chKL_B - 1} + Q_4(chKl_A\text{-}1)\text{-}Q_5 shKl_A) \tag{144}$$

After substituting (127) and (144) into (143) and simplifying, one has

$$r_{m2} = \frac{1}{|Q_2|ShKL_A}(Q_1(ChKL_A\text{-}1)\text{-}Q_3\frac{(chKL\text{-}chKL_B)}{chKL_B - 1} \text{-}Q_4(chKl_A\text{-}1)+Q_5 shKl_A) \tag{145}$$

The frictional moment is expressed as

$$M_r = -\ sign(r_{m2})|M_r| \tag{146}$$

Thus for the process of DS to MO, one condition is in (140), and another one is

$$|r_{m2}| > 1 \tag{147}$$

Note for the process of IF to MO, M_r is determined by (142), and for the DS to MO, M_r by (146). If $r_{m2}Q_3 < 0$, the M_r from (142) and (146) have different signs, which will give different r_{n3} in (138). It clearly shows that different transition processes require different conditions to determine the occurrence of the mode.

Conditions for SO

Similar to MO, two cases exist for this mode, too. It is possible to have the transition process either from IF to SO or from MO to SO. Again, the conditions are different.

The common condition for these two processes is that the moment ratio at the entering roller from the SO analysis must not exceed unity. The ratio, r_{m2}, has been defined in (143), and given by (145). The condition is thus given by

$$|r_{m2}| \leq 1 \tag{148}$$

The frictional moment is determined by

$$M_r = -\, sign(r_{m2})|M_r| \tag{149}$$

For the process of IF to SO, the shear ratio from IF analysis must exceed unity, i.e.

$$|r_{n2}| > 1 \tag{150}$$

The frictional shear is given by

$$N_r = sign(r_{n2})|N_r| \tag{151}$$

For the process of MO to SO, the shear ratio from MO analysis must exceed unity, i.e.

$$|r_{n3}| > 1 \tag{152}$$

The frictional shear is given by

$$N_r = sign(r_{n3})|N_r| \tag{153}$$

Different conditions also correspond to different transition processes in the SO mode as derived above

Conditions for MS

There are also two cases in this mode from MO to MS, and from SO to MS

The conditions for MO to MS are that both the moment ratio, r_{m1}, which is from the IF analysis, and the shear ratio, r_{n3}, which is from the MO analysis, exceed unity, i e

$$|r_{m1}| > 1 \tag{154}$$

$$|r_{n3}| > 1 \tag{155}$$

The frictional moment and shear are given by

$$M_r = sign(Q_3)|M_r| \tag{156}$$

$$N_r = sign(r_{n3})|N_r| \tag{157}$$

The conditions for SO to MS are that both the moment ratio, r_{m2}, which is from the SO analysis, and the shear ratio, r_{n2}, which is from the IF analysis, exceed unity, i e

$$|r_{m2}| > 1 \tag{158}$$

$$|r_{n2}| > 1 \tag{159}$$

The frictional moment and shear are given by

TABLE I

INPUT DATA FOR MODE DETERMINATION

$KL_B = 0.75$	$L_A/L_B = 1.4$	$l_A/L_A = 0.5$
$L_B = 100$ in	$T = 30$ lbf	$\lvert Q_1 \rvert = 0.5$ in
$\lvert Q_2 \rvert = 0.25$ in	$Q_4 = 1.5$ in	$\lvert Q_5 \rvert = 0.85$ in
$\lvert Q_{3i} \rvert = -0.2$ in	$\lvert Q_{3f} \rvert = 0.2$ in	

$$M_r = - sign(r_{m2})|M_r| \tag{160}$$

$$N_r = sign(r_{n2})|N_r| \tag{161}$$

Unlike the modes of MO and SO, no common condition exists for different transition processes in the MS mode.

In order to see if the DS mode occurs, a shear ratio can be defined as

$$r_{n1} = \frac{- N_{AL}}{|N_r|} \tag{162}$$

where N_{AL} is obtained from the IF analysis as in (129). Thus it has the expression

$$r_{n1} = \frac{1}{|Q_1(chKL_A - 1)}(Q_4(chKl_A\text{-}1) - Q_5 shKl_A)) \tag{163}$$

The US mode, if possible, is caused by the steering of the guide roller. For $Q_3 = 0$, i.e., no steering, the US mode is impossible. Under such a condition, the DS mode occurs if r_{n1} exceeds unity. The condition is thus given by

$$|r_{n1}| > 1 \tag{164}$$

with $Q_3 = 0$.

A computer program in FORTRAN has been developed and implemented using the definitions and conditions described above. The computer code is listed in Appendix A.

The mode distribution can be identified as a function of Q_3 for a given set of system parameters and the specified range for Q_3. Table I shows the input data specifying the system parameters for the program, and Table II gives the result for mode distribution of the given system.

TABLE II

OUTPUT RESULTS FOR MODE DETERMINATION

$-0.2000 < Q_3 < -0.05849$	mode = MS
$-0.05849 < Q_3 < -0.1748$	mode = SO
$-0.1748 < Q_3 < 0.08959$	mode = IF
$0.08959 < Q_3 < 0.1416$	mode = MO
$0.1416 < Q_3 < 0.2000$	mode = MS

Note: Q_3 is in inches.

Taut Edge Conditions for Interactive Web Spans

One of the limitations in current analysis for web span lateral behavior is the requirement of taut edges of web spans in consideration. Further analysis will try to remove this restriction by including slack edge analysis. In doing so, the taut edge conditions have to be identified so that the current analysis can be applied in the regions where the taut edge conditions are satisfied, and the slack edge analysis applied in the regions where the taut edge conditions are violated.

For the cases of negligible lateral load disturbances, it is relatively easy to establish the taut edge conditions. For a given web system, the taut edge conditions depend only on the steering angle of the guide roller. The possible slack edge starting location is at the upstream end of each web span. In cases with considerable lateral load disturbances, however, the situation is more complicated. For a given web system the taut edge conditions depend not only on the steering angle, but also on the disturbances. For example, the pre-entering span can be slack even without any steering from the guide roller if the disturbances are large enough. The number of possible slack edge starting locations also increases. In the entering span, with the assumption of negligible lateral load disturbances the number of locations is still only one and it is at the upstream end of the span. For the pre-entering span, however, the number of locations increases to 4, which are at both ends of the span, and both sides of the disturbance location.

Due to the complexity involved, no effort has been made to derive analytically what the taut edge conditions are. Instead, the moments for all interaction modes at all possible locations are derived, which are the functions of system parameters, disturbances, and the steering angle of the guide roller. A computer program is developed to find the regions of steering angle corresponding to taut edge conditions for a given web system and specified disturbances. In the program, the mode distribution is first identified by assuming taut web spans. The other relationships used are given as follows.

Interaction Free

According to the fundamental theory, the moment in a web span is given by

$$M = -EIy'' \qquad (165)$$

From IF mode analysis, one can derive the moments at $x_A = 0$, l_{A^-}, l_{A^+}, L_A, and $x_B = 0$

$$M_{A0} = \frac{-T}{chKL_A-1}(Q_4(shKL_A-shKl_A-shK(L_A-l_A))-Q_5(chK(L_A-l_A)-chKl_A)) \qquad (166)$$

$$M_{Al^-} = \frac{-T}{chKL_A-1}\,(-Q_4shK(L_A-l_A)(chKl_A-1)-Q_5(chK(L_A-l_A)chKl_A-1)) \qquad (167)$$

$$M_{Al^+} = \frac{TshK(L_A-l_A)}{chKL_A-1}(Q_4(chKl_A-1)-Q_5shKl_A) \qquad (168)$$

$$M_{AL} = 0 \qquad (169)$$

$$M_{B0} = \frac{-\,TQ_3shKL_B}{chKL_B - 1} \qquad (170)$$

In IF mode, the steering has no effect on the pre-entering span, which can be seen from (166) to (169). Thus the taut edge conditions in this mode are determined by, besides system parameters, disturbances represented by Q_4 and Q_5.

From (170), one has

$$Q_3 = \frac{-\,(chKL_B - 1)}{TshKL_B}M_{B0} \qquad (171)$$

Letting $M_{B0} = \pm\,|M_{cr}|$, the range of Q_3 is obtained, in which the taut edge conditions are satisfied. If this range is in IF mode range, then the taut edge conditions are established in span B. Otherwise other mode conditions must be examined. Also the taut edge conditions include both spans. Thus span A needs to be examined using (166) to (168). Any one of $|M_{A0}|$, $|M_{Al^-}|$, and $|M_{Al^+}|$ greater than unity causes a slack edge in span A.

Moment Transfer Only

The MO analysis is used to obtain the moments, which are given by

$$M_{A0} = \frac{-T}{chKL_A-1}(Q_2(chKL_A-1)-\,Q_3\frac{shKL_B(chKL_A-1)}{chKL_B-1} + Q_4(shKL_A-shKl_A-shK(L_A-l_A))-Q_5(chK(L_A-l_A)-chKl_A)) \qquad (172)$$

$$M_{Al^-} = \frac{-T}{chKL_A\text{-}1}(Q_2(chK(L_A\text{-}l_A)\text{-}chKl_A)\text{-}\ Q_3\frac{shKL_B}{chKL_B\text{-}1}\ (chK(L_A\text{-}l_A)\text{-}chKl_A)$$
$$-\ Q_4shK(L_A\text{-}l_A)(chKl_A\text{-}1)\text{-}Q_5(chK(L_A\text{-}l_A)chKl_A\text{-}1)) \tag{173}$$

$$M_{Al^+} = \frac{-T}{chKL_A\text{-}1}(Q_2(chK(L_A\text{-}l_A)\text{-}chKl_A)\text{-}\ Q_3\frac{shKL_B}{chKL_B\text{-}1}\ (chK(L_A\text{-}l_A)\text{-}chKl_A)$$
$$+\ shK(L_A\text{-}l_A)(-\ Q_4(chKl_A\text{-}1)+Q_5shKl_A)) \tag{174}$$

$$M_{AL} = T(Q_2 - \frac{Q_3shKL_B}{chKL_B - 1}) \tag{175}$$

$$M_{B0} = \frac{-\ TQ_3shKL_B}{chKL_B - 1} \tag{176}$$

Expressing Q_3 as a function of other parameters, (172) to (176) become

$$Q_3 = \frac{(chKL_B\text{-}1)}{shKL_B(chKL_A\text{-}1)}(\frac{(chKL_A\text{-}1)\ M_{A0}}{T} + Q_2(chKL_A\text{-}1) + Q_4(shKL_A\text{-}shKl_A$$
$$-\ shK(L_A\text{-}l_A)\ ) + Q_5(chKl_A\ \text{-}chK(L_A\text{-}l_A))) \tag{177}$$

$$Q_3 = \frac{(chKL_B\text{-}1)}{shKL_B(chK(L_A\text{-}l_A)\text{-}chKl_A)}(\frac{(chKL_A\text{-}1)\ M_{Al^-}}{T} + Q_2(chK(L_A\text{-}l_A)\text{-}chKl_A)\text{-}$$
$$Q_4shK(L_A\text{-}l_A)(chKl_A\text{-}1)\text{-}Q_5(chK(L_A\text{-}l_A)chKl_A\ \text{-}1))$$
$$l_A \neq L_A/2 \tag{178}$$

$$Q_3 = \frac{(chKL_B\text{-}1)}{shKL_B(chK(L_A\text{-}l_A)\text{-}chKl_A)}(\frac{(chKL_A\text{-}1)\ M_{Al^+}}{T} + Q_2(chK(L_A\text{-}l_A)\text{-}chKl_A)$$
$$+shK(L_A\text{-}l_A)(\text{-}Q_4(chKl_A\text{-}1)+Q_5ShKl_A\ ))$$
$$l_A \neq L_A/2 \tag{179}$$

$$Q_3 = \frac{(chKL_B\text{-}1)}{shKL_B}(\frac{-\ M_{AL}}{T} + Q_2) \tag{180}$$

$$Q_3 = \frac{-\ (chKL_B\ \text{-}\ 1)}{TshKL_B}M_{B0} \tag{181}$$

Setting M_{A0}, M_{Al^-} , M_{Al^+} , M_{AL}, and M_{B0} equal to $\pm\ |M_{cr}|$ and selecting the minimum range obtained from (177) to (181) to establish the taut edge conditions.

Shear Transfer Only

The SO analysis is used here. The moments are given by

$$M_{A0} = \frac{-T}{shKL_A}\Big(-Q_1(chKL_A\text{-}1)+ Q_3\frac{chKL_B(chKL_A\text{-}1)}{chKL_B\text{-}1} + Q_4(chKL_A\text{-}chK(L_A\text{-}l_A))\text{-}Q_5 shK(L_A\text{-}l_A)\Big) \tag{182}$$

$$M_{Al^-} = \frac{-T}{shKL_A}\Big(-Q_1(chK(L_A\text{-}l_A)\text{-}chKl_A)+ Q_3\frac{chKL_B(chK(L_A\text{-}l_A)\text{-}chKl_A)}{chKL_B\text{-}1} - Q_4 chK(L_A\text{-}l_A)(chKl_A\text{-}1)\text{-}Q_5 shK(L_A\text{-}l_A)chKl_A\Big) \tag{183}$$

$$M_{Al^+} = \frac{-T}{shKL_A}\Big(-Q_1(chK(L_A\text{-}l_A)\text{-}chKl_A)+ Q_3\frac{chKL_B(chK(L_A\text{-}l_A)\text{-}chKl_A)}{chKL_B\text{-}1} - Q_4 chK(L_A\text{-}l_A)(chKl_A\text{-}1)+Q_5 shK(L_A\text{-}l_A)chKl_A\Big) \tag{184}$$

$$M_{AL} = \frac{-T}{shKL_A}\Big(Q_1(chKL_A\text{-}1)\text{-} Q_3\frac{chKL_B(chKL_A\text{-}1)}{chKL_B\text{-}1} - Q_4(chKl_A\text{-}1)+Q_5 shKl_A\Big) \tag{185}$$

$$M_{B0} = \frac{-TQ_3 shKL_B}{chKL_B - 1} \tag{186}$$

Expressing Q_3 as a function of other parameters, (182) to (186) become

$$Q_3 = \frac{(chKL_B\text{-}1)}{chKL_B(chKL_A\text{-}1)}\Big(\frac{-shKL_A\, M_{A0}}{T} + Q_1(chKL_A\text{-}1) - Q_4(chKL_A\text{-}chK(L_A\text{-}l_A))+Q_5\, shK(L_A\text{-}l_A)\Big) \tag{187}$$

$$Q_3 = \frac{(chKL_B\text{-}1)}{chKL_B(chK(L_A\text{-}l_A)\text{-}chKl_A)}\Big(\frac{-shKL_A\, M_{Al^-}}{T} + Q_1(chK(L_A\text{-}l_A)\text{-}chKl_A) + Q_4 chK(L_A\text{-}l_A)(chKl_A\text{-}1)+Q_5\, shK(L_A\text{-}l_A)chKl_A\Big) \tag{188}$$

$$l_A \neq L_A/2$$

$$Q_3 = \frac{(chKL_B\text{-}1)}{chKL_B(chK(L_A\text{-}l_A)\text{-}chKl_A)}\Big(\frac{-\,shKL_A\,M_{Al^+}}{T} + Q_1(chK(L_A\text{-}l_A)\text{-}chKl_A) + chK(L_A\text{-}l_A)(Q_4(chKl_A\text{-}1)\text{-}Q_5\,shKl_A)\Big) \tag{189}$$

$$l_A \neq L_A/2$$

$$Q_3 = \frac{(chKL_B\text{-}1)}{chKL_B(chKL_A\text{-}1)}\Big(\frac{shKL_A\,M_{AL}}{T} + Q_1(chKL_A\text{-}1)\,\text{-}Q_4(chKl_A\text{-}1) + Q_5\,shKl_A\Big) \tag{190}$$

$$Q_3 = \frac{-\,(chKL_B - 1)}{TshKL_B}M_{B0} \tag{191}$$

By setting M_{A0}, M_{Al^-}, M_{Al^+}, M_{AL}, and M_{B0} equal to $\pm\,|M_{cr}|$, the minimum range for Q_3 obtained from (187) to (191) is the one for the taut edge conditions in SO mode.

Both Moment and Shear Transfer

The moments are obtained using the MS analysis and are given by

$$M_{A0} = \frac{T}{chKL\text{-}1}\big(Q_1(shKL\text{-}shKL_A\text{-}shKL_B) + Q_2(chKL_B\text{-}chKL_A)\text{-}Q_3shKL + Q_4(shK(L\text{-}l_A)+shKl_A\text{-}shKL)+Q_5(chK(L\text{-}l_A)\text{-}chKl_A)\big) \tag{192}$$

$$M_{Al^-} = \frac{T}{chKL\text{-}1}\big(Q_1(shK(L_A\text{-}l_A)(chKL\text{-}1)\text{-}shK(L\text{-}l_A)(chKL_A\text{-}1)) + Q_2(chK(L_A\text{-}l_A)(chKL\text{-}1)\text{-}shK(L\text{-}l_A)shKL_A)\text{-}Q_3shK(L\text{-}l_A) + Q_4shK(L\text{-}l_A)(chKl_A\text{-}1)+Q_5(chKL\text{-}1\text{-}shK(L\text{-}l_A)shKl_A)\big) \tag{193}$$

$$M_{Al^+} = \frac{T}{chKL\text{-}1}\big(Q_1(shK(L_A\text{-}l_A)(chKL\text{-}1)\text{-}shK(L\text{-}l_A)(chKL_A\text{-}1)) + Q_2(chK(L_A\text{-}l_A)(chKL\text{-}1)\text{-}shK(L\text{-}l_A)shKL_A)\text{-}Q_3shK(L\text{-}l_A) + Q_4shK(L\text{-}l_A)(chKl_A\text{-}1)\text{-}Q_5shK(L\text{-}l_A)shKl_A)\big) \tag{194}$$

$$M_{AL} = \frac{T}{chKL\text{-}1}\big(\text{-}Q_1(chKL_A\text{-}1)shKL_B + Q_2(chKL\text{-}1\text{-}shKL_AshKL_B) \text{-}Q_3shKL_B + Q_4(chKl_A\text{-}1)shKL_B\ \text{-}Q_5shKl_AshKL_B\big) \tag{195}$$

$$M_{B0} = \frac{-\,TshKL_B}{chKL\text{-}1}\big(Q_1(chKL_A\text{-}1) + Q_2shKL_A+Q_3\text{-}\,Q_4(chKl_A\text{-}1)+Q_5shKl_A\big) \tag{196}$$

As a function of other parameters, Q_3 can be derived from (192) to (196) as

$$Q_3 = \frac{1}{shKL}\left(\frac{-M_{A0}}{T}\ (chKL-1)+Q_1(shKL-shKL_B-shKL_A)+ Q_2(chKL_B-chKL_A)\right.$$
$$\left. + Q_4(shK(L-l_A)+shKl_A-shKL) +Q_5(chK(L-l_A)-chKl_A)\right) \qquad (197)$$

$$Q_3 = \frac{1}{shK(L-l_A)}\left(\frac{-M_{Al^-}}{T}(chKL-1)+Q_1(shK(L_A-l_A)(chKL-1)-shK(L-l_A)(chKL_A-1))\right.$$
$$+ Q_2(chK(L_A-l_A)(chKL-1)-shK(L-l_A)shKL_A)$$
$$\left. + Q_4shK(L-l_A)(chKl_A-1)+Q_5(chKL-1-shK(L-l_A)shKl_A)\right)$$
$$(198)$$

$$Q_3 = \frac{1}{shK(L-l_A)}\left(\frac{-M_{Al^+}}{T}(chKL-1)+Q_1(shK(L_A-l_A)(chKL-1)-shK(L-l_A)(chKL_A-1))\right.$$
$$+ Q_2(chK(L_A-l_A)(chKL-1)-shK(L-l_A)shKL_A)$$
$$\left. + Q_4shK(L-l_A)(chKl_A-1)-Q_5shK(L-l_A)shKl_A\right)$$
$$(199)$$

$$Q_3 = \frac{1}{shKL_B}\left(\frac{-M_{AL}}{T}(chKL-1)-Q_1(chKL_A-1)shKL_B+ Q_2(chKL-1-shKL_AshKL_B)\right.$$
$$\left. + Q_4(chKl_A-1)shKL_B -Q_5shKL_BshKl_A\right)$$
$$(200)$$

$$Q_3 = \frac{-M_{B0}}{TshKL_B} -Q_1(chKL_A-1) - Q_2shKL_A+ Q_4(chKl_A-1)-Q_5shKl_A \qquad (201)$$

Again by setting M_{A0}, M_{Al^-}, M_{Al^+}, M_{AL}, and M_{B0} equal to $\pm\,|M_{cr}|$, the minimum range for Q_3 from (197) to (201) is the one for the taut edge conditions in MS mode.

As mentioned in the interaction free analysis for the taut edge conditions, span A does not depend on the steering angle, i.e., Q_3. If Q_4 or Q_5 is pre–specified, the taut edge conditions can be expressed in terms of Q_4 or Q_5.

If Q_4 is undetermined, from (166), (167), and (168), one has

$$Q_4 = \frac{1}{(shKL_A-shKl_A-shK(L_A-l_A))}\left(\frac{-M_{A0}}{T}(chKL_A-1)+Q_5(chK(L_A-l_A)-chKl_A)\right) \quad (202)$$

$$Q_4 = \frac{1}{shK(L_A-l_A)(chKl_A-1)}\left(\frac{M_{Al^-}}{T}(chKL_A-1)-Q_5(chK(L_A-l_A)chKl_A-1)\right) \quad (203)$$

$$Q_4 = \frac{1}{(chKl_A-1)}\left(\frac{M_{Al^+}}{T}\frac{(chKL_A-1)}{shK(L_A-l_A)} +Q_5shKl_A\right) \quad (204)$$

Similarly if Q_5 is undetermined, one has

$$Q_5 = \frac{1}{(chK(L_A\text{-}l_A)\text{-}chKl_A)}(\frac{M_{A0}}{T}(chKL_A\text{-}1)+Q_4(shKL_A\text{-}shKl_A\text{-}shK(L_A\text{-}l_A))) \quad (205)$$

$$Q_5 = \frac{1}{(chK(L_A\text{-}l_A)chKl_A\text{-}1)}(\frac{M_{Al^-}}{T}(chKL_A\text{-}1)\text{-}Q_4 shK(L_A\text{-}l_A)(chKl_A\text{-}1)) \quad (206)$$

$$Q_5 = \frac{1}{shKl_A}(\frac{-M_{Al^+}}{T}\frac{(chKL_A\text{-}1)}{shK(L_A\text{-}l_A)}+Q_4(chKl_A\text{-}1)) \quad (207)$$

The signs of Q_1 and Q_2 are not known in the above equations. The mode determination analysis must be used to determine their signs correctly. The program has combined the mode determination analysis and the above equations to determine the taut edge conditions for a given web system and specified disturbances.

TABLE III

INPUT DATA FOR TAUT EDGE CONDITIONS

KL_B = 0.75	L_A/L_B = 1.4	l_A/L_A = 0.5
L_B = 100 in	T = 30 lbf	W = 5.0 in
$\|Q_1\|$ = 0.5 in	$\|Q_2\|$ = 0.25 in	Q_4 = 2.5 in
$\|Q_5\|$ = 0.85 in	$\|Q_{3i}\|$ = -0.8 in	$\|Q_{3f}\|$ = 0.8 in

As an illustrative example, the analyses presented above are used to work on a problem with the system shown in Fig. 3. Table III shows the input data for the system parameter and disturbance specifications. Also the range for Q_3 is given. Table IV gives the results for mode distribution by assuming taut edges in all given Q_3 region, and the actual regions for the taut edge web spans. The ratios of the moment and shear, which determine the mode of the web system are shown in Fig. 24. Figs. 25 and 26 are the plots for the moments and shears respectively at $x_A = 0, l_A^-, l_A^+,$ and $x_B = 0$ in the taut edge region. In Fig. 27, the web lateral displacements at $x_A = l_A, L_A,$ and $x_B = L_B$ are shown. Finally the web slopes at $x_A = l_A,$ and L_A are shown in Fig. 28.

TABLE IV

OUTPUT RESULTS FOR TAUT EDGE CONDITIONS

Mode Distribution By Assuming Taut Edges In All Regions:	
$-0.80000 < Q_3 < -0.08142$	mode = MS
$-0.08142 < Q_3 < -0.07064$	mode = SO
$-0.07064 < Q_3 < 0.089590$	mode = IF
$0.089590 < Q_3 < 0.118600$	mode = MO
$0.118600 < Q_3 < 0.800000$	mode = MS
Mode Distribution Corresponding To Actual Taut Edge Regions:	
$-0.19330 < Q_3 < -0.08142$	mode = MS
$-0.08142 < Q_3 < -0.07064$	mode = SO
$-0.07064 < Q_3 < 0.089590$	mode = IF
$0.089590 < Q_3 < 0.118600$	mode = MO
$0.118600 < Q_3 < 0.314100$	mode = MS

Note: Q_3 is in inches.

Discussion

The statics of a special interactive web system with the combination of systems of type I and type II have been analysed. An illustrative example is given in the last section combining all the analyses done so far. It has been clearly seen that the effect due to the side loads makes the analysis in determining mode distribution and taut edge conditions much more complicated. A similar analysis can be done using the same approach for the interactive system with side loads on the entering span or other type III interactive systems. The lateral behavior of the web under each interaction mode can be analyzed for the system in consideration using the results given above. It is complicated because more system parameters are involved. If one is capable of identifying the functional relationship among the side loads and the web displacements at rollers, a more meaningful analysis can be done to investigate the effect of the side loads on the lateral web behavior in interactive systems. Another consideration is that in order to make the analysis applicable to more widely distributed system parameters, the slack edge analysis must be established. The taut edge conditions obtained above are helpful to define the boundary for the slack edge analysis.

The dynamics analysis can be performed combining the approaches used in type I [13] and type II interactive systems presented in Chapter III. Numerical techniques or the Fourier expansion must be used in doing this analysis. Thus one could expect more complicated and non-closed form descriptions of the type III interactive system if its dynamics analysis were performed.

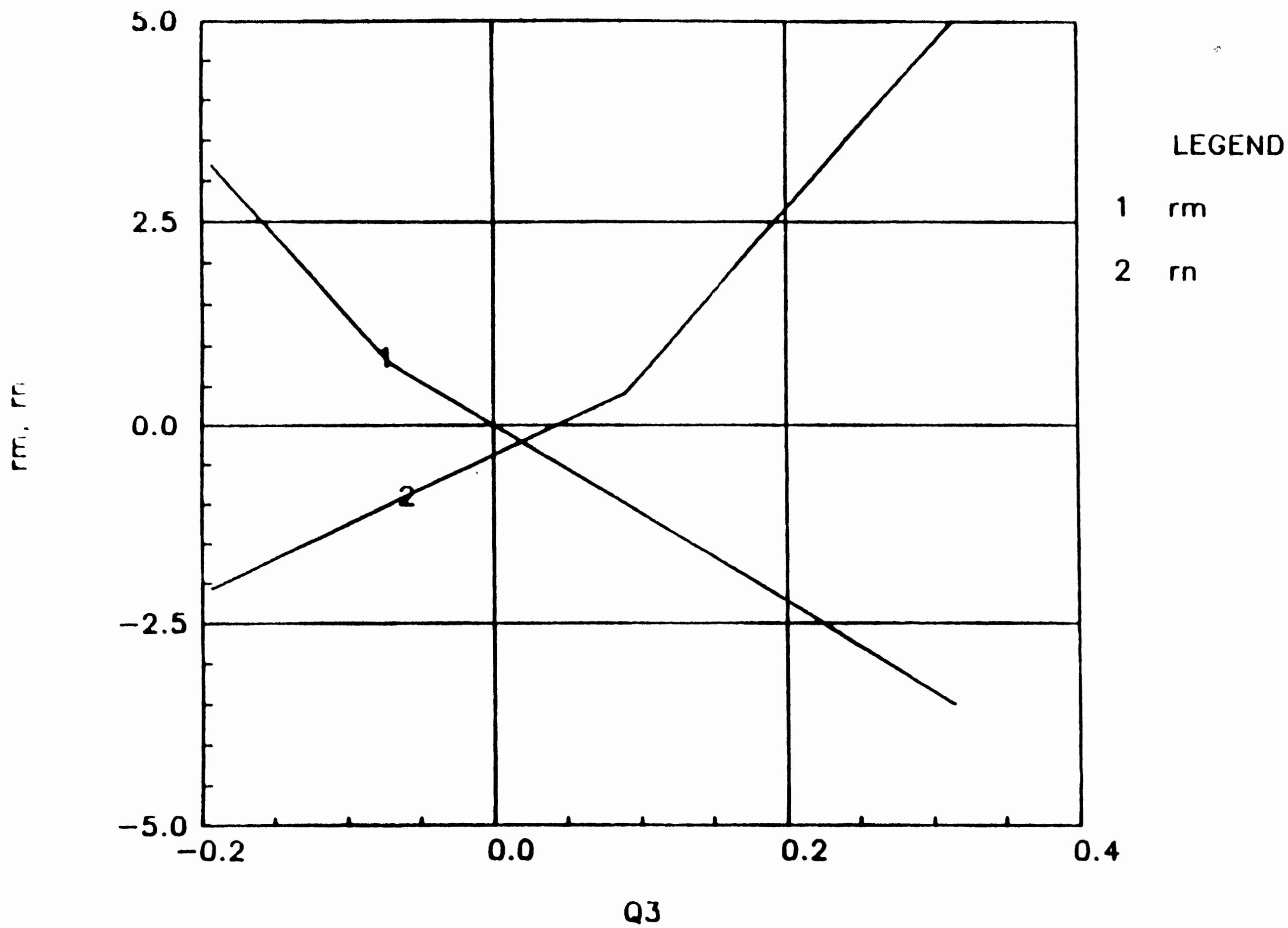

Figure 24. Active Moment and Shear Ratios for an Interactive Web System

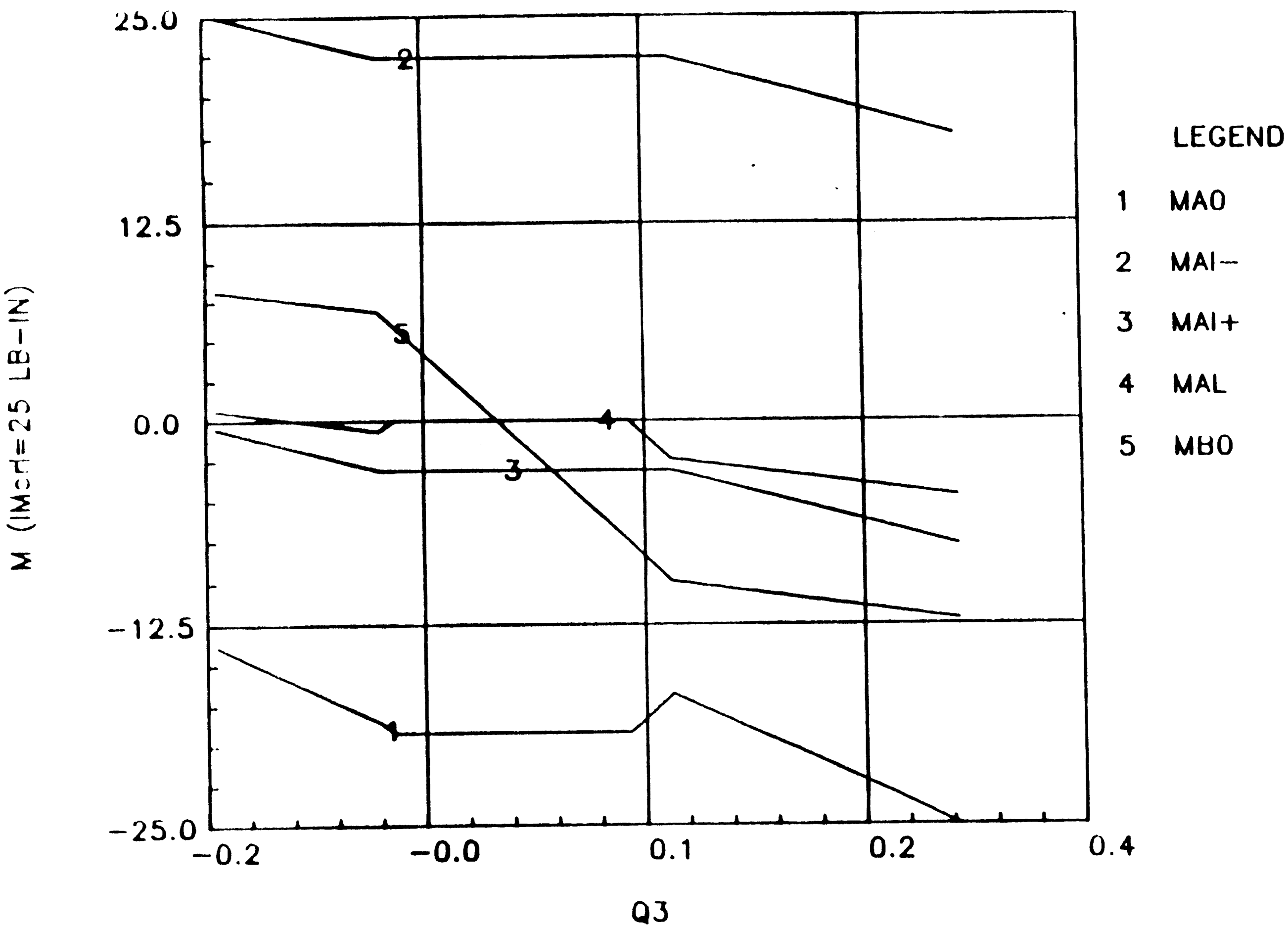

Figure 25. Moments at $x_A = 0$, l_{A^-}, l_{A^+}, L_A, and $x_B = 0$ for the Web in Taut Edge Conditions

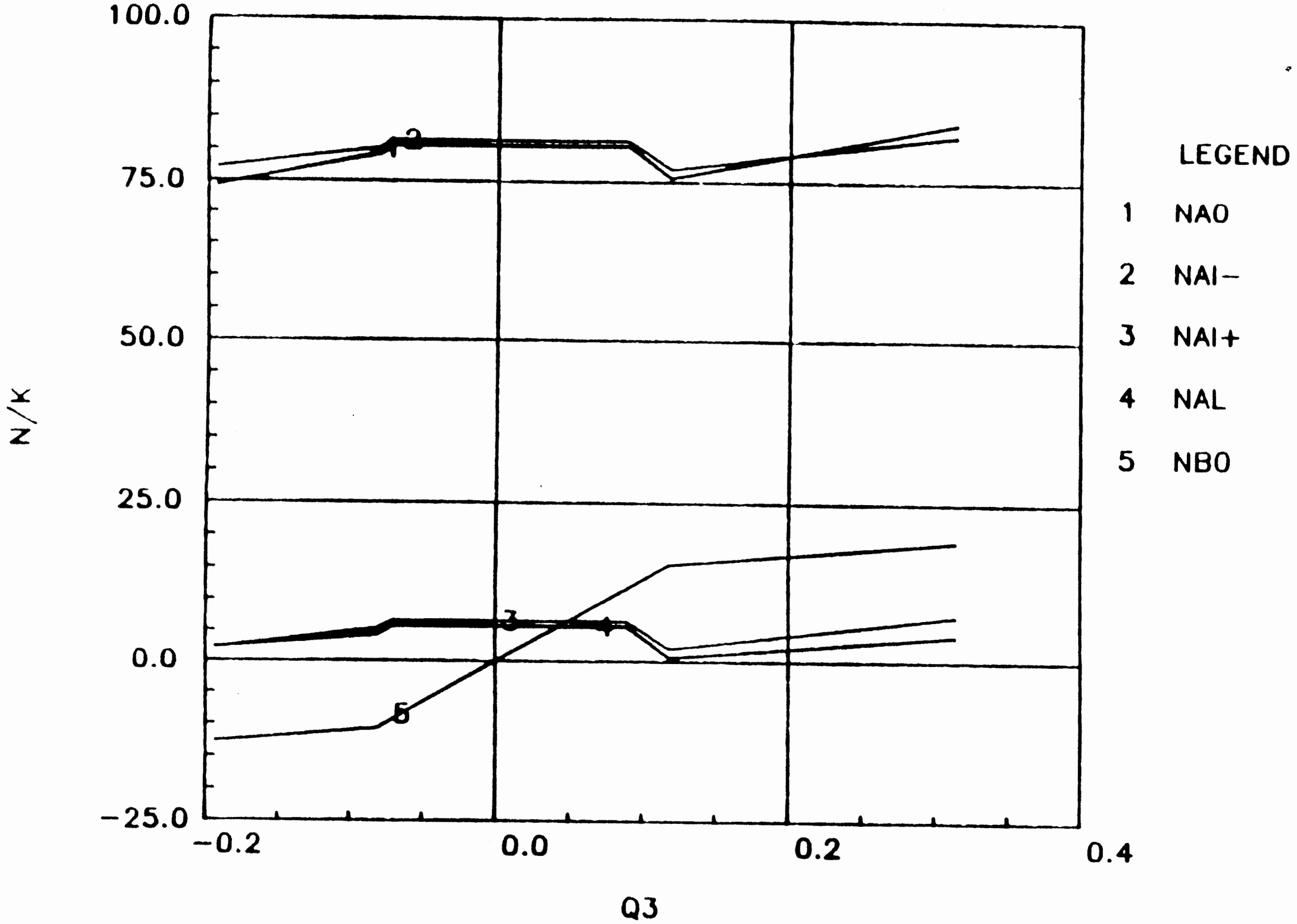

Figure 26. Shear Forces Normalized by K at $x_A = 0$, l_{A^-}, l_{A^+}, L_A, and $x_B = 0$ for the Web in Taut Edge Conditions

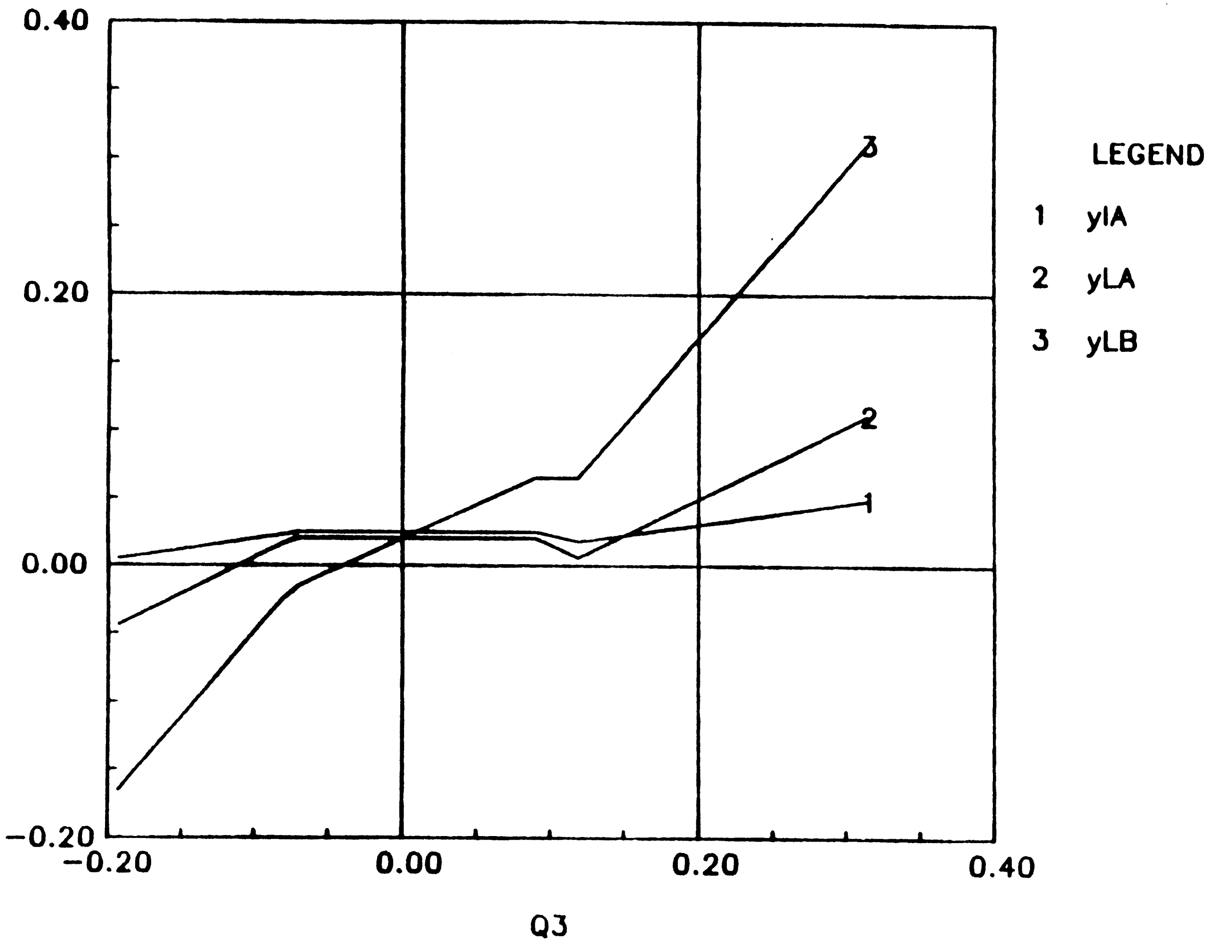

Figure 27. Web Lateral Displacements at $x_A = l_A$, L_A, and $x_B = L_B$ for the Web in Taut Edge Conditions

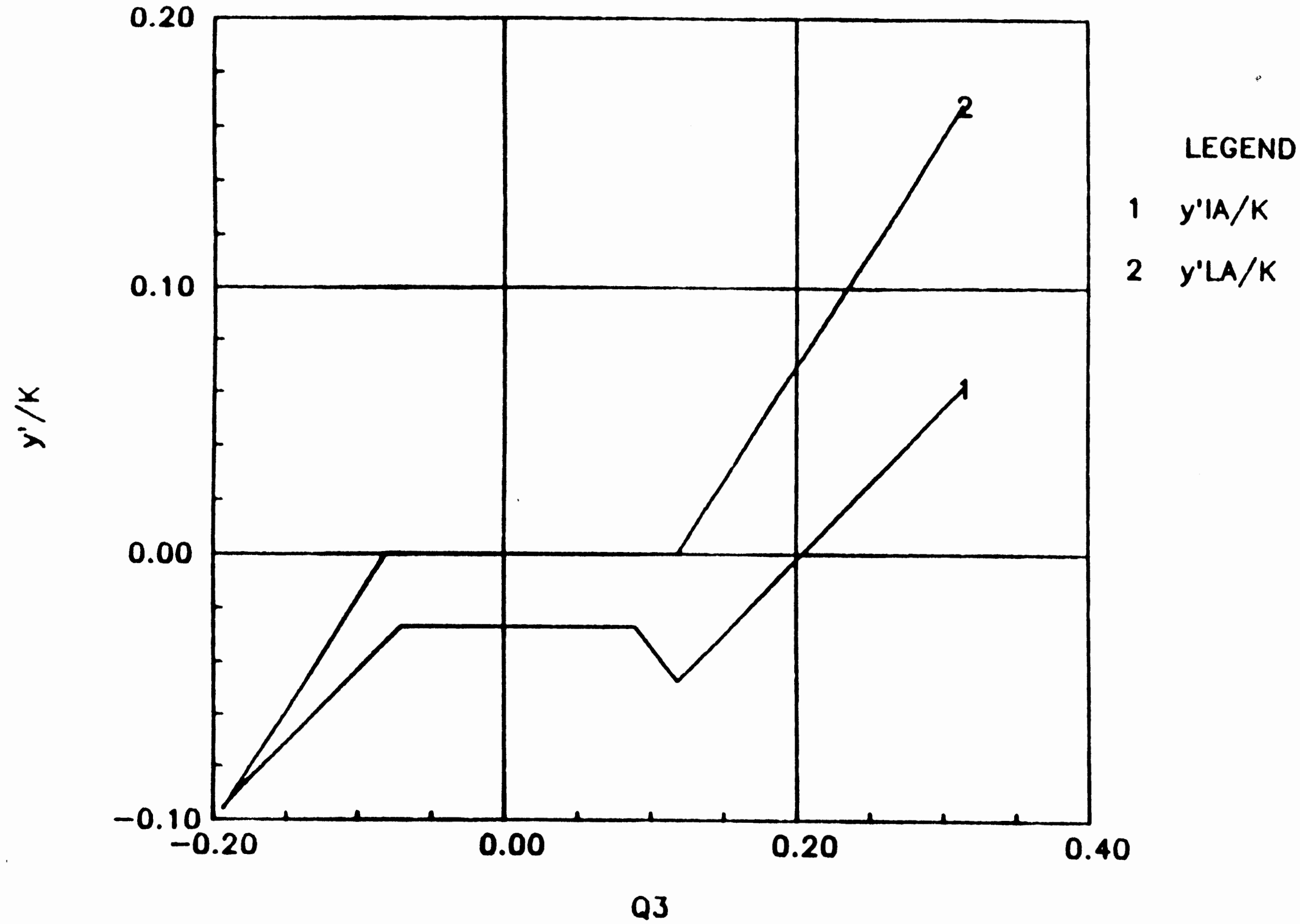

Figure 28. Web Slopes Normalized by K at $x_A = l_A$ and L_A for the Web in Taut Edge Conditions

CHAPTER V

EXPERIMENTAL STUDY OF A WEB SYSTEM WITH AN AIR-BAR UNIT

With an air-bar unit as a lateral load disturbance source in a web system, the analyses of lateral web motion of both statics and dynamics of the type II interactive system are applicable. In applying the theory, however, the disturbance related terms involved in the theory must be adequately modeled. Unfortunately modeling those disturbance related terms is almost always difficult, if not impossible, to accomplish. For the problem at hand, it is required to model the lateral loads on the web span containing the air-bar. This modeling task has been accomplished only for very restricted conditions. The work done in this aspect is mostly on so called "foil bearing" problems, which involves only the creep flow. The air flow field at an air-bar in web handling can range from laminar to turbulent flow. The complicated flow field combined with the elastic behavior of a web makes the modeling of lateral loads on a web span with an air-bar a challenging task in web handling research. So far no known adequate analysis has been available.

The experimental study is to investigate the lateral web motion without the knowledge of modeling the lateral loads provided by an air-bar. With a wide web (W = 6.0 in.), the parameter identification scheme has been used to establish the conditions under which the lateral web motion between up- and down-stream rollers can be described using linear differential equations. The amplification of lateral web displacement at the upstream end can be observed at the downstream end under certain conditions. It is important to maintain the web system in the running state without amplification. The amplification free condition has been established through the experimental study in terms of experimental parameters.

To verify the discoveries and conclusions from the wide web experimentation, a further experimental study with a narrow web (W = 1.0 in.) has been carried out. With a variety of tests performed, a better understanding on the web system involving air flotation has been gained. The jumping effect has been found, for example, in the static test. The misalignment in the rollers and air-bar units has a more confounding effect on the lateral web motion. With both the narrow web and gap, the limit cycle in lateral web oscillation may exist if there are some misalignment in the system, the moment transfer at the upstream roller, and the appropriate range for the web speed. The details on those issues along with the moving dam test and the frequency test will be discussed later.

Experimental Set-Up

The Shelton machine has been used to perform the experimental study on the web system with an air-bar unit. The machine was built by J. J. Shelton while he was doing his research on the lateral dynamics of a moving web for his doctoral degree at OSU. For the interest of this research, an air-bar unit was added to the machine. Fig. 29 schematically shows the Shelton machine with the added air-bar unit.

There are two types of web guiding devices on the machine: displacement guide and steering guide. An HP3300A function generator is used to change the guide point of the displacement guide, and as a result to provide the lateral web motion disturbances to the air-bar unit. The web is made of polypropylene with the width of 6.0 in. and the thickness of 0.0013 in. The air drum size and pattern are shown in Fig. 30. The original length of the slots on the air drum is shown in the figure. In doing experiments, this length can be shortened by taping both sides symmetrically. The slots on the air drum are in the radial direction. A Chicago blower is used to provide the pressurized air to the air drum. A valve is used on the blower to control the air flow rate. The full opening of the valve corresponds to 90.0^{o}. The pipes with a diameter of 6.0 in. are used to connect the blower and air drum.

A tension adjustment device with two springs can be used to control the total tension in the web. The transmitted-light sensors are used to measure the lateral web positions. This position measurement can later be changed to the lateral web displacement measurement. A data acquisition system developed by Kardamilas on the Motorola System V/68 computer is used to collect experimental data. Because extensive experimental tests have been done through the study, this data acquisition system has helped a lot as far as the data gathering is concerned.

Experimentation Incorporating Parameter Identification

In performing theoretical analysis, the lateral load disturbances are assumed to be known. In fact, those disturbances from various non-contact handling devices are different. Many research projects can be carried out to accomplish the task of modeling those disturbances. The lateral load disturbances from an air-bar is complicated due to the complex flow field and the elastic web property. Over-simplified two dimensional models involving creeping flow field, which is termed as foil bearing problems, have been reported, for example, by Wildmann [9]. A working model adequately describing the laminar or turbulent flow field at an air-bar and combining the elastic web property is not available. In order to gain more understanding of the effect of an air-bar on the lateral web motion, an experimental study is necessary.

The experimentation incorporating parameter identification of the lateral web motion in a web system with an air-bar unit is a preliminary experimental study. Based on the previous studies and the theoretical work involving significant lateral load disturbances, some guidelines for the system model structure have been deducted. The industrial practice has shown that there are two totally different running states for the web system with an air-bar unit: states with and without amplification in lateral web displacement. This study tries to ascertain if the system model structures for the two running states are the same. Also it tries to determine if the model structure for the two-parallel-roller system is applicable to the web system involving an air-bar unit.

As suggested by the previous studies and the theoretical work the web system involving an air-bar unit is assumed to be describable using an autoregressive and moving average (ARMA) model. Through experimentation the parameter estimation technique is used to identify the unknown parameters in the model. An ARMA model of order (n_a, n_b, n_c, n_d) can be described, in discretized form, by

$$y(z) = \frac{B(z)}{A(z)}\ u(z) + \frac{C(z)}{D(z)}\ e(z) \qquad (208)$$

where

$$A(z) = 1 + a_1 z^{-1} + \ldots + a_{n_a} z^{-n_a}$$
$$B(z) = b_0 + b_1 z^{-1} + \ldots + b_{n_b} z^{-n_b}$$
$$C(z) = 1 + c_1 z^{-1} + \ldots + c_{n_b} z^{-n_c}$$
$$D(z) = 1 + d_1 z^{-1} + \ldots + d_{n_d} z^{-n_d}$$

with n_a, n_b, n_c, and n_d integers greater than or equal to zero, and y(z), u(z), and e(z) the z–transforms of the response, excitation, and noise respectively.

For the problem in consideration, the excitation, u(z), corresponds to the lateral displacement at the upstream end, the response, y(z), to that at the downstream end, and the noise, e(z), to all errors such as the measurement error, the non-perfect web edge, and nonlinearity error etc.

The recursive maximum likelihood (RML) algorithm [14, 15] is used to perform the task of parameter estimation. Such an algorithm is capable of estimating all the coefficients in (208) if the data are rich enough in frequency and the parameters involved in the algorithm are properly selected. The RML is an on-line parameter identification algorithm; therefore, the initial guess of the parameters in the model and the covariance matrix in the algorithm affects the accuracy of the identified results during the start-up period of the algorithm. Since the main concern using the identification scheme in this study is not on the convergence but on the accuracy of identified system parameters, the initial guess required by the algorithm should be as accurate as possible. The repetition in applying the algorithm to the same experimental data has been used to accomplish this task. The initial guess is arbitrarily made only on the first time in applying the algorithm. The identified results are then used as the initial guess in the next application of the algorithm. The identified results will be improved in terms of accuracy of the system parameters. The repetition goes on until there is little improvement in identified results between two contiguous algorithm applications.

Three cases have been investigated on the test results using this parameter identification scheme. Case 1 verifies that the lateral web motion between two parallel rollers can be described using an ARMA model as established by Shelton [1]. Case 2 works on the web system involving small lateral load disturbances provided by an air-bar. Under such a condition, no amplification exists and the web system is also describable using an ARMA model. Case 3 investigates the web system with considerable lateral load disturbances from an air-bar. The lateral web displacement at the upstream roller is amplified when passing an air-bar as observed at the downstream roller. The linearity of the model for the web system is no longer applicable. The web system cannot be described using an ARMA model as it can be in the previous cases.

Test and Identification of Lateral Web Displacement With Parallel Rollers

According to the theory of the second-order dynamics of lateral web motion established by Shelton [1], the transfer function for the response at the fixed parallel roller to the input at the previous roller including the angular displacement effect is given by

$$\frac{y_L(s)}{y_0(s)} = \frac{-\dfrac{f_3(KL)}{T_1}s + \dfrac{f_1(KL)}{T_1{}^2}}{s^2 + \dfrac{f_2(KL)}{T_1}s + \dfrac{f_1(KL)}{T_1{}^2}} \tag{209}$$

which is an ARMA model with the order (2, 1, 0, 0). It is assumed that whenever both the orders of C(s) and D(s) are zero, the noise effect is treated to be negligible as in the case above.

As a verification of this theory, a test has been done to see if the ARMA model with an order (2,1,0,0) can be indeed used to describe the web system with the conditions assumed in (209).

A schematic description is shown in Fig. 31 for the layout of the test. In this figure roller A is a displacement guide; roller C an air-bar; and rollers B, D, and E normal rollers. Sensor 1 is used to measure the input $y_0(k)$, and sensor 2 the output $y_L(k)$. The excitation is controlled at the displacement guide, i.e., roller A. In the test, a sine wave excitation is used with the frequency of 0.1 Hz. Other test conditions are given in Table V.

When plotted it can be seen that the measured lateral web displacements from sensors 1 and 2 involve heavy high frequency noise. In order to make the identification algorithm work properly, it is desirable to remove that high frequency noise. A moving average technique has been used to remove some amount of noise in the measured data. The procedure to remove the high frequency noise is called smoothing. After smoothing the RML algorithm is used to identify the system parameters by assuming the degree of ARMA model as (2, 1, 0, 0), which is suggested by (209). The parameters identified in A(z) and B(z) are shown in Figs. 32 and 33 respectively. With this set of parameters in the (2, 1, 0, 0) ARMA model and the smoothed $y_0(k)$ as the input, the estimated $\hat{y}_L(k)$ can be obtained. Fig. 34 shows the estimated response $\hat{y}_L(k)$, the smoothed response $y_L(k)$ and the residual e(k) , which is defined as $y_L(k) - \hat{y}_L(k)$.

To verify the identified system parameters in A(z) and B(z) used for obtaining Fig. 34, another set of data was taken. The test conditions are the same as those of the previous case except the excitation is changed to a triangular wave instead of a sine wave. The measured lateral web displacements from sensors 1 and 2 are again processed using the smoothing to remove some high frequency noise. The previously obtained parameters, i.e., shown in Figs. 32. and 33, are used for the ARMA model with an order (2, 1, 0, 0) working on the smoothed $y_0(k)$ as the input. The estimated response $\hat{y}_L(k)$ can then be obtained, which along with the smoothed $y_L(k)$ and the residual e(k) is shown in Fig. 35.

TABLE V

WEB SYSTEM PARAMETERS FOR CASE I

Web span length: 38.0 in	Web velocity: 64.6 in/sec
Total tension in web: 4.6 lbf	Air flow rate: 3.446 ft^3/sec
Sampling time: 0.01 sec	Data points: 1,000

No effort has been made to see if through discretization the coefficients in (209) can be correctly related to the identified parameters in this test. The test results do quite convincingly verify that the structure in (209) is correct under the assumed conditions.

Test and Identification of Lateral Web Displacement

With an Air-Bar Providing Small Disturbances

Based on the theory of the second-order dynamics of lateral web motion and introducing the lateral load disturbances, the response at the fixed parallel roller to the input at the previous roller including the angular displacement effect is given by

$$y_L(s) = \frac{(KV)^2}{s^2 + KLc_{L1}s + (KV)^2 c_{L6}} \left(c_{L4} - \frac{s}{V} c_{L5},\ c_{L2},\ c_{L4} \right) \begin{bmatrix} y_0(s) \\ Q_4(s) \\ Q_5(s) \end{bmatrix} \qquad (210)$$

where c_{Li}, i = 1, 2, 4, 5, and 6, are functions of KL and l; $Q_4(s)$ and $Q_5(s)$ are the Laplace transforms of the terms related to the lateral disturbance force and moment respectively.

When the disturbances are small enough that their effect on the response $y_L(s)$ is negligible or their related terms can be expressed proportional to or linear in s with the lateral web displacement at the upstream roller, then according to (210) the lateral web displacement at the downstream roller can be described using an ARMA model of an order (2, 1, 0, 0) with the lateral displacement at the upstream roller as the input.

An air-bar is such a device which provides the web system with lateral load disturbances. With $l = L/2$, i.e., an air-bar located at the mid point of a web span between two parallel rollers, the amplification occurs if the lateral web displacement at the downstream roller is greater than that at upstream roller. It has been observed through experiments that when no amplification occurs the thickness of the air cushion between the web and the air-bar is quite uniform in the direction of both across the web and around the wrap angle. Under such a condition, the air-bar causes little lateral load disturbances. Thus the ARMA model of an order (2, 1, 0, 0) can be used to describe the lateral web behavior for this case.

As a verification of this theory, a test has been taken to see if the ARMA model with an order (2, 1, 0, 0) can be indeed used to describe the web system with the conditions when no amplification occurs.

A schematic description is shown in Fig. 36 for the layout of the test. It is basically the same configuration as in Fig. 31 except the location of two sensors. Sensor 1 is used to measure the input $y_0(k)$, and sensor 2 the output $y_L(k)$, which are at the upstream and downstream ends with respect to the air-bar respectively. The excitation is again controlled at the displacement guide, i.e., roller A. In the test, a sine wave excitation is used with a frequency of 0.1 Hz. Other test conditions are given in Table VI.

In Fig. 37 the measured lateral web displacements from sensors 1 and 2, indicated as y_{0m} and y_{Lm} respectively, are plotted. Again one can see clearly the data from the test involve heavy high frequency noise. Before performing the identification on the measured data, the moving average has been used to remove some amount of noise in the measured data. After smoothing, the RML algorithm is used to identify the system parameters by assuming the degree of the ARMA model as (2, 1, 0, 0). The parameters identified in A(z) and B(z) are shown in Figs. 38 and 39 respectively. Using this set of parameters in the (2, 1, 0, 0) ARMA model and the smoothed $y_0(k)$ as the input results in the estimated $\hat{y}_L(k)$. Fig. 40 shows the estimated response $\hat{y}_L(k)$, the smoothed response $y_L(k)$ and the residual e(k).

TABLE VI

WEB SYSTEM PARAMETERS FOR CASE II

Web span length: 104.0 in	Web velocity: 82.0 in/sec
Total tension in web: 4.6 lbf	Air flow rate: 3.446 ft^3/sec
Sampling time: 0.05 sec	Data points: 1,000

To verify the identified system parameters in A(z) and B(z) as shown in Figs. 38 and 39, another set of data has been taken. The test conditions are the same as those of the previous case except the excitation frequency is changed to 0.05 Hz instead of 0.10 Hz. Again the smoothing is used on the measured lateral web displacements from sensors 1 and 2 to remove some high frequency noise. The parameters in Figs. 38 and 39 are used for the ARMA model with an order (2, 1, 0, 0) working on the smoothed $y_0(k)$ as the input. The estimated response $\hat{y}_L(k)$ can then be obtained, which along with the smoothed $y_L(k)$ and the residual e(k) is shown in Fig. 41.

In the above two tests there is no amplification in the measured data for the lateral web displacements. This fact can be seen in the plot shown in Fig. 37. The identified results verify that the web system under such a condition is describable using a (2, 1, 0, 0) ARMA model with time-invariant coefficients.

Test and Identification of Lateral Web Displacement With an Air-Bar Providing Considerable Disturbances

As pointed out in the investigation of the cases corresponding to small disturbances, the response of lateral web displacement at the downstream roller to input at the upstream roller including the angular displacement and considerable lateral load disturbance effects is given by (210).

When no amplification occurs, the lateral load disturbances are quite small. As a result, their effect on the lateral web motion is also small. The relationship between the lateral web displacements at the upstream roller and the downstream roller can be described using an ARMA model of an order (2, 1, 0, 0). With considerable disturbances, however, the amplification occurs, i.e., the lateral web displacement is greater at the downstream roller than at the upstream roller. Under such a condition, a relatively large oscillation of the web span can be observed. Partial web will ride on the shoulder of the air-bar when the oscillation is near its maximum magnitude. Consequently the uniformity of the air cushion does not hold anymore comparing with the case when the entire web width is riding within the range of the slot length of the air-bar.

When the amplification occurs, i.e., the web system involves considerable lateral load disturbances, some questions need to be answered.

1. If the web system can still be describable using an ARMA model between the lateral web displacements at the upstream roller and the downstream roller.

2. If the answer is "yes" to the above question, then the disturbance related terms $Q_4(s)$, and $Q_5(s)$ can be described using ARMA models relating to the lateral web displacement $y_0(s)$ at the upstream roller. The order for the ARMA model then needs to be determined.

3. If the answer is "no" to question 1, then the disturbance related terms $Q_4(s)$, and $Q_5(s)$ have non-rational polynomial relationships to $y_0(s)$. To gain more insight on the problem, more research work on modeling the air-bar involving complex flow field

combined with the elastic web property should be undertaken.

TABLE VII

WEB SYSTEM PARAMETERS FOR CASE III

Web span length: 104.0 in	Web velocity: 100.7 in/sec
Total tension in web: 4.6 lbf	Air flow rate: 3.446 ft^3/sec
Sampling time: 0.025 sec	Data points: 1,000

As an endeavor in trying to find the answers to the above questions, a test has been run. A schematic description is the same as shown in Fig. 36 for the layout of the test. In the test, the slot width has been narrowed by taping so that partial web can easily ride on the shoulder of the air-bar. As a result the air-bar yields considerable lateral load disturbances on the web span at its location. A triangular wave excitation is used with the frequency of 0.07 Hz. Other test conditions are given in Table VII

In Fig. 42, the measured lateral displacements from sensors 1 and 2, indicated as y_{0m} and y_{Lm} respectively, are plotted. The moving average technique has been used to remove some amount of high frequency noise in the measured data. After smoothing, the RML algorithm is used to identify the system parameters.

First, to see if the case is similar to the one corresponding to small disturbances, the degree of the ARMA model is assumed to be (2, 1, 0, 0). The parameters identified in A(z) and B(z) do not converge to constant values as shown in the results from the RML algorithm. Using this set of parameters in the (2, 1, 0, 0) ARMA model with the smoothed $y_0(k)$ as the input results in the estimated $\hat{y}_L(k)$. Fig. 43 shows the estimated response

$\hat{y}_L(k)$, the smoothed response $y_L(k)$, and the residual e(k). The plot clearly indicates that the assumed model fails to reveal the functional relationship between the two lateral web displacements.

Secondly, by increasing the order in B(z) by 1, i.e., assuming the ARMA model of an order (2, 2, 0, 0), the RML algorithm is applied again to perform the parameter identification on the measured data. The estimated parameters associated with A(z) and B(z) have not been improved as compared with the results obtained before. In obtaining the estimated response $\hat{y}_L(k)$ using this set of parameters with the smoothed input $y_0(k)$, the result is again not satisfactory.

Thirdly, by increasing both the orders in A(z) and B(z) by 2 based on the second case, i.e., with the (4, 4, 0, 0) ARMA model, the identification procedure is again repeated. The parameters in A(z) and B(z) are consequently obtained, which have been shown to converge quite well. In obtaining the estimated response using this set of estimated parameters, the result is little different as far as the residual e(k) is concerned, which can be observed in Fig. 44 where the estimated response $\hat{y}_L(k)$, the smoothed response $y_L(k)$, and the corresponding residual e(k) are plotted.

The above cases have one thing in common as far as the identification scheme is concerned. The forgetting factor λ is taken to be unity in the RML algorithm, which is equivalent to assuming the parameters involved in A(z) and B(z) are time-invariant. In order to estimate the time-varying or nonlinear parameters in the system, the forgetting parameter l must be set to less than unity. The fourth case investigated uses a (2, 2, 0, 0) ARMA model to describe the web system. The forgetting parameter l is set to 0.995 to accommodate the nonlinearity or the time-varying parameters in the model when the RML is used to perform the identification task. The parameters in A(z) and B(z) thus obtained are shown in Figs. 45 and 46. The estimated parameters themselves look like the random signals as observed from the plots. When this set of parameters are used to obtain the estimated response $\hat{y}_L(k)$, however, the result matches with the smoothed response $y_L(k)$ reasonably well as plotted in Fig. 47 along with the residual e(k).

It is clear that an ARMA model with time-invariant parameters are not sufficient to represent the web system involving considerable lateral load disturbances. By allowing the time-varying or nonlinear parameters in the ARMA model, as in the last case, the parameters estimated are too irregular to find a reasonable mathematical description to relate the disturbance terms to the lateral web displacement at the upstream roller. A different approach must be used as mentioned in question 3, i.e., to do more research work on modeling the air–bar in the complex flow field combining the elastic web property. Until the functional relationship between the disturbance terms and the lateral web displacement at the upstream roller is established, the dynamics of the lateral web motion involving considerable lateral load disturbances from an air-bar cannot be adequately analyzed.

Discussion and Conclusion

The study shows that the model structures of the web system with an air-bar unit are totally different for two different running states. Similar to a two parallel roller system the system with an air-bar unit is describable using an ARMA model of an order (2, 1, 0, 0) if it is in the running state without amplification. The highly nonlinear effect involved in the running state with amplification makes the ARMA model invalid in describing the web system with an air-bar unit. The change in model structure indicates that considerable lateral load disturbances may have significant influence on the lateral web dynamics.

The theoretical analysis of the web system involving considerable lateral load disturbances established in the previous chapters requires the understanding of physical insight on those disturbances. Much work needs to be done in accomplishing the modeling task on the lateral load disturbances provided by the non-contact web handling devices. The particular problem encountered in this investigation is to model the lateral load disturbances from an air-bar, which involves the combination of a complex flow field and the elastic web property.

Before an adequate model for the air-bar is constructed, more understanding of the lateral web dynamics involving an air-bar unit can be gained only through more experimental study. The results from this preliminary experimental study have motivated a unified approach to investigate the web system with an air-bar unit including both running states. The amplitude factor study has subsequently been done experimentally through a set of experimental parameters. Through this study the effects of experimental parameters on the system running states and the amplification free condition have been empirically established. The details of this part of the experimental study will be reported and discussed in the following sections.

The confirmation of the model structure for the web system with an air-bar unit being the same as the one in a two parallel roller system is important. In the application of a series of air-bar units with the same characteristics the lateral web motion is controllable only if the system is operated in the running state without amplification. Under such a condition the lateral web position control can be done by directly applying the work of Kardamilas, etc [6]. i.e., the unknown parameters in the known model structure can be estimated using the parameter estimation scheme and the control task is performed based on the identified results. The further experimental study of the unified approach including both running states is, however, necessary because in making a system design the knowledge of amplification free condition for the web system with an air-bar unit is essential.

Experimentation for Amplitude Factor Study

The experimental study incorporating parameter identification of the web system with an air-bar unit has been carried out, as discussed in the last section. It has been found that when the disturbances are small there is no amplification; the relationship between the lateral web displacements at the down- and up-stream ends can be described using an ARMA model. On the other hand with large disturbances the amplification does occur; an ARMA model is not applicable. The results of this study have motivated the experimental study of the amplitude factor of a web system with an air-bar unit, which is the unified approach to the lateral web motion in such a system including both running states. The definition of amplitude factor is the ratio of the magnitudes of lateral web oscillation at the downstream end to that at the upstream end. The running state without amplification corresponds to an amplitude factor less than unity. For an amplitude factor greater than unity, the web system is operated in the running state with amplification. This section deals with experimentation in the amplitude factor study. It includes the experimental set up, the selection of experimental parameters, obtaining experimental data, the regression analysis on the data obtained, and the synthesis of experimental data.

Selection of Experimental Parameters

Depending on the scale of lateral load disturbances from the air-bar, the lateral web displacement at the downstream end may or may not be larger than that at the upstream end of the air-bar. The parameter identification study indicates that when the disturbances are small there is no amplification. On the other hand the amplification does occur when the disturbances become large. In industrial applications, a series of air-bar units with the same characteristics may be used for non-contact web handling. If one of the air-bar units involves large lateral load disturbances, the amplification of lateral web displacement will occur. This amplified response will then be further amplified by the following air-bar units. Eventually excessive lateral web oscillation will be reached and as a result the web will be broken or damaged, an event which a web system designer is trying his best to prevent.

Whether the scale of lateral load disturbances is small or large depends on many factors if one defines the small scale corresponding to the state without amplification and the large scale to that with amplification of lateral web displacements. These factors include the web system and lateral web displacement at the upstream roller, which is the system input. The web system factors include the web tension, the air-bar pattern, the type of web, the web process speed, the air flow rate of the air-bar, the gap length defined as the difference of lengths of the slots in the air-bar and the width of the web, the length of web span, etc. The system input factors are the excitation function type, oscillation magnitude and frequency. The theoretical analysis of the amplification is currently unavailable due to the difficulty in modeling lateral load disturbances. An experimental approach has thus been adopted to do the investigation of the amplification effect. To quantify this effect, the amplitude factor concept is introduced, which as mentioned above is defined as the ratio of the oscillation magnitude at the downstream end to that at the upstream end. Such a definition enables one to study the effects involving both the running states with and without amplification. It has been observed through experiments that the amplification effect is closely related to the input ratio, which is defined as the ratio of the oscillation magnitude from the system input to the half gap length. The basic experimental data are the input ratio as the input and the amplitude factor as the response for the given set of other factors and system parameters, which are identified as the experimental parameters. Besides the input ratio the other experimental parameters investigated are the system input oscillation frequency, the air flow rate of the air-bar, the web span length to width ratio, and the web tension.

The effect of the input oscillation magnitude is represented by the input ratio, which is one experimental parameter of an input factor, i.e., the input oscillation magnitude, normalized by a system parameter, i.e., the half gap length. The oscillation frequency effect is reflected using the experimental parameter called the normalized frequency, which is one of an input factor, i.e., the input oscillation frequency, normalized by a system parameter, i.e., the time constant of the web span. One important web parameter identified by Shelton [1] is KL. Two experimental parameters related to this parameter have been selected, the web span length, which is normalized by the web span width called the length to width ratio, and the web tension. The volume air flow rate of the air-bar has also been chosen as one of the experimental parameters. This is based on the consideration that the lateral load disturbances from the air-bar are closely related to the air flow between the air–bar and the web.

When the web tension changes, so does the air flow rate of the air-bar. In order to make comparisons among cases with different tension, the air flow rate of the air-bar should be the same. To do so the valve opening of the blower must be adjusted according to the web tension. The air flow rate of the air-bar can be calculated using the orifice formula $Q = C_d\sqrt{2gh}$, where h is the pressure head depending on the pressure difference $p_s - p_0$, with p_s the source pressure inside the air-bar, which has been found through experiment to be little affected by web motion, and p_0 the pressure in the air cushion under the web, which can be approximated by T/rW. By neglecting the difference in the air flow rate at the uncovered part of the air-bar slot, the air flow rate of the air-bar was determined by the pressure difference. A reference tension was chosen to be 4.60 lbf. The three different valve openings used ware 12.5^o, 15.0^o, and 17.5^o. After p_s values were measured, the pressure differences $p_s - p_0$ were calculated as 0.1609, 0.2633, and 0.3258 psi respectively. When the web tension changed, a different pressure difference was obtained. In the experiment, the same set of valve openings were used. The measured pressure differences were then used to adjust the valve openings to match the reference pressure differences through interpolation or extrapolation if necessary. For the configuration used in the experiment, the air flow rates, web tensions and corresponding valve openings are listed in Table VIII. In calculating air flow rate, the discharge coefficient C_d is set to 0.94.

The total web tension is a very important parameter in web handling. In the application involving air-bars a very low tension might be required. In the experimentation the lowest total web tension was set to 1.15 lbf, which makes the average line tension in the web of 0.1917 pli. While doing experiments it was found that at low tensions, the friction between the web and the driving roller was not large enough to keep the web at the speed used for other tension levels. The lower speed was used instead. To keep the normalized frequency unchanged, the oscillation frequency of the input was changed accordingly.

Obtaining Experimental Data

The first step in the experimental study is to obtain the experimental data. As in the parameter identification study the tests were done on the modified Shelton machine as shown in Fig. 29. A schematic description shown in Fig. 48 is for the layout of all the tests. Again sensor 1 was used to measure the system input oscillation $y_0(k)$, and sensor 2 the output oscillation $y_L(k)$. Sensor 3 was newly added to measure the air pressure inside the air-bar. The excitation is controlled at the displacement guide, i.e., roller A, using an HP3300A function generator, which is capable of changing the oscillation function type, magnitude, and frequency. The sinusoidal excitation was used in the experiments. The steps in collecting the experimental data were as follows:

1. At one running condition of the Shelton machine with an air-bar, obtain 3 sets of data of $y_0(k)$ and $y_L(k)$ using the Kardamilas data acquisition system on Motorola. The time duration in each data set is at least one time period of the oscillation.

2. Above data sets are signals with the electrical unit in volts. The data sets are then transformed into signals with displacement unit in inches with the bias removed.

3. The data sets contain high frequency noise due to the noise signals in the measurement system and the imperfect web edge condition. The smoothing technique is used to remove part of the high frequency noise. After smoothing, the searching technique is used on the data sets, which contain both the smoothed and original measured $y_0(k)$ and $y_L(k)$, to find the minimum and maximum y_0 and y_L (smoothed), and y_{0m} and y_{Lm} (measured). Through visual inspection on those extremum values, the abnormal measured signals can be detected and consequently deleted to gain better accuracy.

4. By averaging the 3 sets of extremum values a better set of magnitudes in accuracy for y_0, y_L, y_{0m} and y_{Lm} is obtained. These oscillation magnitudes are designated as M_{y_0}, M_{y_L}, $M_{y_{0m}}$, and $M_{y_{Lm}}$.

5. Steps 1 to 4 are repeated for a number of system input magnitudes using the function generator. A set of oscillation magnitudes M_{y_0}, M_{y_L}, $M_{y_{0m}}$, and $M_{y_{Lm}}$ for a set of

TABLE VIII

VALVE OPENING ADJUSTMENT FOR DIFFERENT WEB TENSION

Q (ft^3/sec)	T (lbf)	V_o (deg)
	1.15	10.3
2.694	2.30	10.9
	4.60	12.5
	6.90	13.5
	1.15	12.8
3.446	2.30	13.7
	4.60	15.0
	6.90	17.0
	1.15	14.2
3.833.	2.30	15.5
	4.60	17.5
	6.90	19.3

different input ratios is then obtained.

6. The desired experimental data set is obtained by taking the ratio forms as

The input ratio (IR): M_{y_0}/H_{gl}, where M_{y_0} is the smoothed input oscillation magnitude, and H_{gl} the half gap length.

The amplitude factor (AF): M_{y_L}/M_{y_0}, where M_{y_L} is the smoothed response oscillation magnitude.

The measured to smoothed input ratio: M_{y0m}/M_{y0}, where M_{y0m} is the original measured input oscillation magnitude.

The measured amplitude factor: M_{yLm}/M_{y0}, where M_{yLm} is the original measured response oscillation magnitude.

Through the tests five experimental parameters have been investigated, the input ratio, the oscillation frequency, the air flow rate of the air-bar, the web span length to width ratio, and the total web tension.

There were three air flow rates, two web span length to width ratios, and four web tensions used in the tests. For most of the tests the number of oscillation frequencies used was four; in a few tests five or more were used with an intention to see the trend of amplitude factor at high frequency. The number of input ratios was also unequally used. It was in the range of eight to twelve for most of the tests. The ratios M_{yL}/M_{y0}, M_{y0m}/M_{y0}, and M_{yLm}/M_{y0} were obtained corresponding to a set of input ratio, M_{y0}/H_{g1}, values for each quadruple of the oscillation frequency, ω^*, air flow rate, Q, length to width ratio, L/W, and web tension, T. The oscillation frequency was normalized using the web span time constant T_1 defined as L/V, i.e., $\omega^* = T_1\omega$ in radians. The units for the air flow rate and web tension are shown in Table VIII.

The web system parameters common to all tests were the slot length on the air-bar of 6.25 in. and the width of web, which made the gap length constant. Fig. 49 shows the amplitude factor and other two ratios as a function of input ratio for the other four fixed experimental parameters. This set of data was one of the data sets obtained using the procedure described above. The normalized oscillation frequency, ω^*, was 0.6065 rad, the air flow rate, Q, 3.446 ft^3/sec, the length to width ratio, L/W, 17.0, and the web tension, T, 4.60 lbf. If the noise to signal ratio is small the amplitude factor M_{yL}/M_{y0} and the ratio M_{yLm}/M_{y0} will be close or equal to each other and the ratio M_{y0m}/M_{y0} close or equal to unity. From Fig. 49. one can see that the effect of noise is relatively large at the low level of input ratio. Thus in order to gain better accuracy in the experimental data, a relatively high level of input ratio should be used if possible.

Regression Analysis

One is more interested in finding under what condition the amplification in the web system can be avoided. To specify such a condition, the concept of critical input ratio, which corresponds to unity amplitude factor, is useful. For a given set of other experimental parameters, the amplification can be avoided if the input ratio is controlled not exceeding the critical input ratio. It is not easy to find the critical input ratio directly through experiments though. If the input ratio and the amplitude factor can be curve-fitted fairly well through regression analysis, the critical input ratio can be found by definition through the regression found functional relationship.

Many sets of data for the amplitude factor have been obtained through experiments as a function of the input ratio for other fixed experimental parameters. In performing regression analysis, it has been found that the functional relationship between the amplitude factor and the input ratio can be described using a third order polynomial function. Some sets of data are appropriately described for the input ratio to be a third order polynomial in the amplitude factor, which can be expressed as in (211)

$$M_{y_0}/H_{gl} = a_0 + a_1 M_{y_L}/M_{y_0} + a_2(M_{y_L}/M_{y_0})^2 + a_3(M_{y_L}/M_{y_0})^3 \qquad (211)$$

One such an example is illustrated in Fig. 50. Both the experimental data and the curve fitting from regression analysis are plotted in the figure. The experimental parameters for this set of data are the normalized oscillation frequency of 0.9576 rad, the air flow rate of 3.446 ft^3/sec, the length to width ratio of 17.0, and the web tension of 4.60 lbf. As indicated on the plot, the coefficient of determination for the regression is 0.988, which confirms the appropriateness of the regression function used in the analysis.

The other data sets have been found, however, to be appropriate to express the amplitude factor as a third order polynomial in the input ratio, i.e., using (212)

$$M_{y_L}/M_{y_0} = b_0 + b_1 M_{y_0}/H_{gl} + b_2(M_{y_0}/H_{gl})^2 + b_3(M_{y_0}/H_{gl})^3 \qquad (212)$$

Fig. 51 shows both the experimental data and the results from the regression analysis for such a case. In obtaining this set of data, the experimental parameters used are the normalized oscillation frequency of 0.9576 rad, the air flow rate of 2.694 ft^3/sec, the length to width ratio of 12.3, and the web tension of 4.60 lbf. Again the coefficient of determination for regression analysis proves that the functional relationship in (212) is appropriate.

Through trial-and-error in doing regression analysis, it has been found that the functional relationship between the amplitude factor and the input ratio can be adequately described using either (211) or (212). Due to the inaccuracy in measured data at low levels of input ratio, most of tests have been done in the range of relatively high levels of input ratio. This is justified by the interest of this experimentation. Since the goal of the experimental study is to establish the amplification free condition, the experimental parameter values should be chosen in such a way that the corresponding amplitude factor has a value near unity. In a few tests at high oscillation frequencies, the range for relatively low level of input ratio has been used, which is caused by the low-pass filtering effect on lateral web displacement at the pre-entering span. For those data sets one has to use extrapolation through the regression results to obtain the critical input ratios.

Experimental Data Synthesis

The purpose of the experimental study of the amplitude factor is to empirically find the effects of other experimental parameters. The regression analysis discussed above is between the amplitude factor and the input ratio only with other experimental parameters specified. This analysis has also been tried between the amplitude factor and the two other experimental parameters, i.e., the normalized oscillation frequency and web tension, without a success. It has not been tried in air flow rate or length to width ratio because only few discrete values have been used. To see the effects of experimental parameters on the amplitude factor the synthesis of experimental data based on the regression analysis between the amplitude factor and the input ratio is required. The procedure is as follows:

1. The curve fitting is performed using (211) or (212), whichever is appropriate for all data sets corresponding to other discrete experimental parameter values.

2. Discretize the input ratio, M_{y_0}/H_{gl}, as a set of values in a proper range. The set of (1.0, 1.5, 2.0, 2.5, 3.0, 3.5) has been used in this investigation. Using (211) or (212) as appropriate to find the corresponding set of amplitude factors, M_{y_L}/M_{y_0}, for each data set.

3. Group above sets of M_{y_L}/M_{y_0} into proper data sets depending on which experimental parameter effect one wants to investigate. For instance one may look at the frequency response of amplitude factor by grouping the amplitude factor and frequency data corresponding to other fixed experimental parameters.

In general, with the other specified system parameters, the amplitude factor can be expressed as a function of experimental parameters used in the tests, which has a form as

$$M_{y_L}/M_{y_0} = f(M_{y_0}/H_{gl}\,,\ \omega^*,\ Q,\ L/W,\ T) \tag{213}$$

Applying the above procedure the amplitude factor has been obtained corresponding to the set of discrete experimental parameters. The interpolation can be used to approximate the continuous function of amplitude factor as other experimental parameters.

One frequency response of the amplitude factor is shown in Fig. 52. The responses for different levels of input ratio have been grouped in one plot. The other three experimental parameters for this plot are the air flow rate of 3.446 ft^3/sec, the length to width ratio of 17.0, and the web tension of 4.60 lbf. In a similar manner, the amplitude factor as a function of air flow rate, input ratio, length to width ratio, or web tension can be obtained following the same procedure.

Setting the amplitude factor to unity (213) implies that another functional relationship exists in the critical input ratio in terms of the other four experimental parameters. Similar to (213) this functional relationship can be specified as

$$(M_{y_0}/H_{gl})_{cr} = g(\omega^*,\ Q,\ L/W,\ T) \tag{214}$$

It is crucial in establishing the amplification free condition through (214). In order to accomplish this task the effect of experimental parameters on the critical input ratio needs to be investigated. In Fig. 53 the frequency response of critical input ratio is shown for different air flow rates. The other two experimental parameters for this data set are the web length to width ratio of 17.0 and the total web tension of 1.15 lbf. This frequency response indicates that the high frequency in the system input increases the level of critical input ratio.

Since the amplitude factor and the experimental parameters are in discrete form, many combinations exist in (213) and 214). To investigate the effect of each experimental parameter on the amplitude factor and the critical input ratio, every possible combination should be inspected carefully. The results from the synthesis on experimental data do, however, provide necessary information in analyzing the effect on the amplitude factor and the critical input ratio due to those experimental parameters.

Discussion and Conclusion

An experimental study involves many experimental parameters and requires a lot of time to accomplish. In this experimental study on the amplitude factor of a web system with an air-bar, only a limited set of experimental parameters has been chosen. The part dealing with experimentation has been described above. Through the regression analysis it has been found that the functional relationship between the amplitude factor and the input ratio can be described using a third order polynomial. The synthesis of experimental data based on the regression analysis has been accomplished.

In such a way the amplitude factor can be investigated experimentally through five experimental parameters : the input ratio, oscillation frequency, air flow rate, length to width ratio, and web tension. Through regression analysis the functional relationship between the amplitude factor and the input ratio has been well defined in the range of experimentation. However this functional relationship between the amplitude factor and the other experimental parameters has not been found. Through regression analysis, for the given other experimental parameters, the critical input ratio has been found as specified by (214), which describes the amplification free condition for the given system parameters. The ideal result for establishing the amplification free condition is to find well defined regression functional relationships between the amplitude factor and all other experimental parameters such as the input ratio, oscillation frequency, air flow rate, length to width ratio, and web tension, etc. Then the critical input ratio can be well defined as a function of those parameters. As a result the amplification free condition can be readily established. If this functional relationship cannot be well defined through regression analysis, the interpolation among experimental data has to be used. Such an approach gives a rough approximation for the critical input ratio and thus for the amplification free condition.

The effect of experimental parameters on the amplitude factor and the critical input ratio will be investigated using the results from the experimental data synthesis. The amplification free condition can then be established empirically using the concept of critical input ratio in terms of experimental parameters. The details are described in the following section.

Effect of Experimental Parameters on Amplitude Factor

The lateral web motion is complicated due to the lateral load disturbances from an air-bar. With small disturbances, the web span has a lateral motion similar to the one passing two parallel rollers, i.e., it is describable using an ARMA model as seen from the parameter identification study. When the disturbances are large, the behavior of the lateral web motion changes. An ARMA model is not applicable. The amplitude factor is used as a unified approach for describing lateral web motion in both small and large disturbances. In practical application, a series of air-bar units with the same characteristics are often used. It is important to maintain the system stable in the lateral web motion. The amplitude factor study is helpful in establishing the amplification free condition, which is the necessary condition for stability in the lateral web motion.

In the description of the experimentation on the amplitude factor, the procedure for obtaining the experimental data of amplitude factor, the choice of experimental parameters, the synthesis on the amplitude factor, and critical input ratio in terms of experimental parameters have been discussed. Using the results from the experimental data synthesis, the effects due to the experimental parameters on the amplitude factor are investigated in the following. Also the discussion for the critical input ratio, its prediction, and the web system design considerations related to the amplification is included.

Input Ratio Effect

By definition the input ratio is a measure of partial web riding on the shoulder of an air-bar at the maximum oscillation magnitude of the web span. For an input ratio less than or equal to unity, no partial web across its width will be riding on the shoulder of an air-bar if the web is initially properly centered on the air-bar. Under such a condition, the entire web is always within the slot opening range of an air-bar. The air-cushion between the web and the air-bar is quite uniform in thickness and so is the air pressure. As a result little lateral force and moment on a web span are provided by the air-bar. The lateral web behavior does not change much as indicated through parameter identification investigation.

For an input ratio greater than unity, it is inevitable for partial web to ride on the shoulder of an air-bar. The time for the partial web riding on the shoulder in one oscillation period depends on both the magnitude of the input ratio and the oscillation frequency. For a fixed oscillation frequency, in addition to a larger riding area this time will be longer corresponding to a larger input ratio. In the shoulder riding region, the air pressure is lower than that in the slot opening region. As a result the uniformity of the air-cushion is destroyed. A slope in the shoulder riding region will be formed and thus yield a lateral force on the web span. Due to the oscillation, the amount of partial web riding on the air-bar shoulder in the direction of wrapping angle is not uniform either. A lateral moment can thus be generated on the web span. The momentum change due to the different air flow rates at different sides of web span also contributes to the generation of lateral force and moment on web. In order to adequately model the lateral force and moment on the web span from an air-bar at the partial web shoulder riding condition, the complex air flow field at the air-bar has to be analyzed in detail. So far no such an analysis has been available.

With a large input ratio, the amplitude factor can exceed unity, which means the air–bar behaves like, among other things, an amplifier for the lateral web motion. The critical input ratio corresponds to the unity amplitude factor. It depends on the web system parameters and the oscillation frequency of the disturbance at the upstream roller. It is critical in the sense that if a series of air-bar units with the same characteristics are used the web system will go unstable laterally for an input ratio larger than its corresponding critical value. Naturally one wants to know quantitatively more about the effect of the input ratio on the amplitude factor. Such a knowledge is helpful in establishing the amplification free condition for a web system involving an air-bar application.

For relatively large input ratios the experimental results show that the amplitude factor is a monotonically increasing function of the input ratio for all experiments but one. The only exception corresponds to the experimental parameters $\omega^* = 0.5094$ rad, $Q = 3.833$ ft^3/sec, $L/W = 12.3$, and $T = 4.60$ lbf. In this case when the input ratio was very large, the amplitude factor decreased, which means the rate of increase in the magnitude of lateral displacement at the downstream end is less than that at the upstream end. The reason for this to occur is because of the contact of web with the air-bar. When the shoulder riding region becomes large, it is more likely to have a contact between the web and the air-bar. This contact prevents a further amplification in lateral web displacement at the downstream end. In practice the air-bar is used for non-contact handling applications. Thus the contact between the web and air-bar should be avoided. The effect due to contact is not considered further in this investigation.

There are cases when the input ratio is relatively small in which the amplitude factor decreases with increasing input ratio. Fig. 51 shows one set of experimental data along with the regression curve. The functional relationship used in the regression analysis is that the amplitude factor is a third order polynomial in the input ratio. This decrease can be understood if one relates the web system with an air-bar unit to the one with two parallel rollers as investigated by Shelton [1]. His analysis of the second-order frequency response of a web at a fixed roller to the input at the previous roller shows that for relatively low normalized frequencies the amplitude factor is less than but near unity. The actual value for the amplitude factor depends on the web parameter KL and the normalized frequency ω^*. As the disturbances from the upstream roller become small, the lateral force and moment on the web span from an air-bar decrease. In the limit the effect of lateral load disturbances from an air-bar is totally negligible as far as the lateral web motion is concerned. Under such a condition the air-bar merely deflects the longitudinal web direction. The behavior in lateral web motion of the two web systems are equivalent. As the disturbance from the upstream roller increases, the effect due to lateral load disturbances becomes significant. The decrease in the amplitude factor indicates that the air-bar has actually provided a damping effect on the lateral web motion. The amplitude factor reaches its minimum at the input ratio near unity, which corresponds to the optimum damping effect. It is conceivable that this input ratio, which corresponds to the optimum damping effect, depends on the normalized frequency, web parameter KL, air flow rate for the air-bar, and other system parameters.

The experimental results show that the lateral web motion disturbances are quite small for an input ratio less than its value corresponding to the optimum damping effect. In order to investigate the amplification effect due to an air-bar, a much larger input ratio must be considered. From now on one concentrates on the input ratio effect only in the region corresponding to the monotonically increasing functional relationship between the input ratio and amplitude factor. The experimental data show that this region is also the most common one encountered in practice, which justifies the interest.

The monotonically increasing amplitude factor with increasing input ratio indicates that the increase in the response is always larger than that of the input. The regression analysis is used to find this functional relationship between the amplitude factor and the input ratio. It has been found that a third-order polynomial between the input ratio and the amplitude factor is the most appropriate function form. One example is presented in Fig. 50. From this functional relationship, it is easy to obtain the critical input ratio, which corresponds to the unity amplitude factor.

The critical input ratio is an important concept. It is a function of the oscillation frequency, air flow rate, length to width ratio, and total web tension if other system parameters are fixed. In establishing the amplification free condition, the critical input ratio plays an important role. In the experiments performed, it has been found that the critical input ratio is greater than 2.0. As a rule of thumb, one may consider the amplification free condition corresponds to $M_{y0}/H_{gl} < 2.0$ for a large web width to gap length ratio.

Oscillation Frequency Effect

As one knows, a web span between two parallel rollers behaves like a low pass filter to lateral web motion. A low frequency disturbance in lateral web displacement at the upstream end is able to pass the web span and appear at the downstream end with little change in its magnitude. But a disturbance at a high frequency will show only a small fraction of its original magnitude in the response. For a web span with an air-bar, a similar situation occurs to the input ratio as an input and the amplitude factor as a response.

For those input ratios such that the amplitude factors are less than unity in all frequency ranges, i.e., the web system is under the condition of amplification free, there are only small lateral load disturbances involved from the air-bar. In this case, the web span is similar in terms of lateral motion to one between two parallel rollers. When the amplification does occur at some level of input ratio, the amplitude factor can be reduced by increasing the oscillation frequency while holding the level of input ratio unchanged. If the oscillation frequency is increased enough, the amplitude factor will be reduced lower than unity, which is defined as the amplification free condition. In other words the critical input ratio has a high magnitude at high frequencies if other system parameters are specified. Fig. 54 shows the frequency response of amplitude factor corresponding to different levels of input ratio. The experimental parameters in obtaining this set of experimental data are $Q = 3.833$ ft^3/sec, L/W = 12.3, and T = 4.60 lbf. Note at relatively low frequencies the amplitude factor does not necessarily decrease when the frequency increases, while at relatively high frequencies the amplitude factor does decrease as the frequency increases. On the plot all amplitude factors obtained from the experiments are reduced to less than unity at high frequency.

The time factor in the oscillation frequency effect on the amplitude factor plays a crucial role. As mentioned earlier the time for partial web riding on the air-bar shoulder in one oscillation period depends on both the level of input ratio and the oscillation frequency. While holding the level of input ratio constant, this time solely depends on the oscillation frequency. The geometric shape of the web across its width and the air flow field at the air-bar change with time, as does the momentum of the air flow. Roughly speaking with the more shoulder riding time of the web at a given oscillation frequency, the more changes in the web shape and the air flow momentum can be expected. As a result larger lateral load disturbances are generated by the air-bar, causing the amplification at the downstream end. With a high frequency, the shoulder riding time is reduced therefore with less amplification being observed. The effect can be seen clearly through the plot with different input ratios as shown in Fig. 54.

<u>Air Flow Rate Effect</u>

An adequate supply of pressurized air to the air-bar is essential in supporting the web and realizing the non-contact handling. In the experiments a blower is used for the air supply. The air flow rate is controlled by both the valve opening of the blower and the web tension.

With the other system parameters specified the air flow rate effect on the amplitude factor is complicated, depending on the oscillation frequency, input ratio, length to width ratio, and total tension in the web. Intuitively for a large air flow rate, the thickness of the air-cushion between the web and the air-bar is large in magnitude. Also the momentum change in the air flow is large with more air flow rate. Thus there is more room for the web span to move around, which combined with the air flow momentum change means the amplitude factor should be large accordingly. Examination of the results from experiments shown in plots of the amplitude factor as a function of air flow rate at fixed oscillation frequency, length to width ratio, and web tension, and for different levels of input ratio reveals that this intuition is not always true. Fig. 55 shows such a plot. It clearly indicates that the amplitude factor is not necessarily small for a low air flow rate especially at low levels of input ratio. The data in the plot correspond to the experimental parameters $\omega^* = 1.5959$ rad, L/W = 17.0, and T = 4.60 lbf as indicated on the plot. The complex air flow field and the web geometric shape change together cause a complicated lateral load disturbance. This dynamic interaction in terms of air flow rate cannot be intuitively explained. From the above plot, one can see that the curves corresponding to different input ratios do not intersect each other. One with a high level of input ratio is always above the one with a lower level of input ratio, which is a further proof of the monotonic nature of the amplitude factor in terms of the input ratio.

If the experimental results are shown in the plot of the amplitude factor as a function of air flow rate at fixed input ratio, length to width ratio, and web tension, and for different oscillation frequencies, this non-intersection of curves does not exist. For the air flow rate effect on the amplitude factor in terms of different oscillation frequencies, no general rule can be summarized at this time from the experimental observations.

Web Span Length to Width Ratio Effect

In practical applications, such as in a drying process, the web span length is expected to be long. But often due to the space limitation, the span length is limited to be relatively short. Thus it is important to investigate the web span length effect on the lateral web displacement amplification. In order to remove the factor of the length dimension, the length is normalized using the web width, i.e., the length to width ratio, L/W.

Only two length to width ratios have been used in the experiments on the investigation of lateral displacement amplification. Thus the results obtained are just indicative rather than thorough. First one may look at the effect with only the input ratio changing, i.e., holding other system parameters constant. The experimental results show that for small input ratios the corresponding amplitude factors are lower in magnitude for the case with a large length to width ratio than for that with a small one. The actual difference between two cases depends on other system parameters, such as the oscillation frequency and air flow rate. The plot in Fig. 56 shows the amplitude factor as a function of input ratio for two length to width ratios of 12.3 and 17.0. The other parameters in obtaining experimental data are $\omega^* = 0.9576$ rad, $Q = 2.694$ ft^3/sec, and $T = 4.60$ lbf. As one knows, small input ratios correspond to low lateral load disturbances from the air-bar. Under such a condition, the web span behaves similar to the one passing two parallel rollers, which has been investigated by Shelton [1]. The analysis shows for ω^* less than a certain moderately large value, which is larger than those used in the experiments, the magnitude ratio of lateral web displacements decreases as the web parameter KL increases. The experimental results agree with this conclusion for small input ratios as observed from Fig. 56. When the input ratio becomes large, i.e., near or greater than its critical value, the difference in the amplitude factors for different length to width ratios reverses as can be seen in Fig. 56. This fact indicates that the large lateral load disturbances from the air-bar act more effectively on a long or less stiff web span than on a relatively short or stiff one.

Secondly one wants to look at the oscillation frequency effect. At the low level of input ratio, the web span lateral motion is affected very little by the lateral load disturbances from the air-bar. This conclusion is also true in the oscillation frequency aspect. At a high level of input ratio, the frequency change can alter the direction of the difference in amplitude factors for different length to width ratios. In other words, the oscillation frequency changes the critical input ratio if other system parameters are constant.

With regard to the effect related to the air flow rate, again no generalized conclusion can be formed at this time. Before any more insight can be gained in this aspect a model adequately describing both the web elasticity and air flow field at the air-bar must be constructed.

Web Tension Effect

The total tension in the web is a very important parameter for a given web system. To improve the tracking capability a high tension is always helpful. In some applications, the tension must be kept low. Nip rollers have to be introduced to avoid slippage between the web and rollers.

In the previous study for the case involving contact between the web and rollers [1], the web tension is included in the web parameter KL. If other parameters are constant, KL is a monotonically increasing function of web tension. The amplitude factor is, however, a monotonically decreasing function of KL for the normalized frequency less than a moderately large value (≈ 6.0 rad) [1]. The lateral web behavior should be similar to that of the web system with contact handling if the lateral load disturbances from an air-bar are small. The experimental data shows this is not true of the effect of web tension for low levels of input ratio. The amplitude factor is not necessarily small for a high web tension with the other conditions constant. There are reasons for this. In the contact handling problem only the lateral effect due to the web tension is considered. With the problem using air flotation devices for non-contact handling, the web tension also affects the normal web behavior. The air-bar causes lateral load disturbances, which are dependent upon the normal web condition. For example the geometric shape of the web across its width affects the air flow momentum change. The curvature of the web determines the air pressure distribution. Also the restoring force for the web span to return to its equilibrium position is closely related to the web tension. Those factors are not reflected in the web parameter KL. Thus the tension effects for small lateral load disturbances are not necessarily the same as predicted by the case of contact handling.

Inspecting the results from data for the web tension, one can see that the effect due to the web tension is interrelated with other experimental parameters. In general the monotonic property of web tension for other fixed experimental parameters does not exist. For some intermediate input ratio values, however, the monotonic decrease in the amplitude factor has been observed. Fig. 57 shows the frequency response of the amplitude factor for different web tensions. The other experimental parameters are the input ratio, $M_{y0}/H_{gl} = 2.0$, the air flow rate, $Q = 3.833$ ft^3/sec, and the web length to width ratio, $L/W = 17.0$. The figure clearly indicates that the amplitude factor increases when the web tension decreases in the range of experimental frequency. By further inspecting the effect of web tension corresponding to the amplitude factor near unity, the monotonic decrease in the amplitude factor does exist with increasing web tension. This indicates that a high tension in the web is helpful in preventing amplification in the web system.

Critical Input Ratio and Its Prediction

For a web system with an air-bar unit there are two totally different running states of the lateral web motion: without and with amplification in lateral web displacement. The amplitude factor is a quantitative description for this two states. The critical input ratio corresponds to unity amplitude factor, which is the transition of the two states. Due to the monotonic functional relationship between the input ratio and the amplitude factor, the critical input ratio is a perfect indicator for specifying the state change in web system running conditions. As investigated above, other parameters used in the experiments do not have a definite monotonic functional relationship with the amplitude factor. They thus are not eligible in specifying the transition of the system running conditions. The critical input ratio, which is a function of other experimental parameters, can be used to specify the amplification free condition for a web system. Another use of the concept of critical input ratio is to quantitatively categorize the lateral load disturbances from an air-bar. It has been loosely mentioned that when the disturbances are "small" the lateral motion of the web span is describable using an ARMA model. This "smallness" or "largeness" on the other hand has been used without a reference. With the introduction of the critical input ratio, this reference has been established. When the input ratio is less than its critical value, the disturbances from the air-bar are small. Otherwise they are large.

When the web system is in the state with amplification, the lateral web displacement at the upstream end is amplified at the downstream end. For only one or few air-bar units being used, a relatively large web displacement causes difficulty in controlling the web span at its desired position. For a system with a series of air-bar units with the same characteristics, the state with amplification can drive the web unstable in the lateral motion, which means the system would totally lose its control of the web position and the entire process line would be broken down. This is the event a system designer must avoid in the process of design.

For the system in its amplification free state the magnitude of response at the downstream end is by definition less than that of the disturbance at the upstream end. The reduction in magnitude is helpful in controlling the lateral position at the downstream end. With more air-bar units being used, this reduction becomes more significant.

The critical input ratio is difficult or impossible to obtain directly through experiments. For those fixed parameters used in the experiments, the critical input ratio is predicted through regression analysis on the input ratio with respect to the amplitude factor, which has been found to be a third order polynomial functional relationship between the input ratio and the amplitude factor. For other parameters not coincident with the ones used in the experiments, the interpolation technique has to be used.

One plot for the critical input ratio as a function of air flow rate is shown in Fig. 58. As a comparison the curves for different oscillation frequencies are plotted together. The experimental parameters for this set of data are L/W = 17.0 and T = 1.15 lbf. It clearly shows that intersections exist between curves, which indicates the critical input ratio is not a monotonic function of oscillation frequency. A general trend reflected from this plot and similar data sets is that at a very high frequency the level of the critical input ratio is high.

System Design Consideration

There are many applications for web systems with air-bar units. The system design is often application oriented. Furthermore a web system involves a variety of parameters such as web length, width, thickness, tension, material, air-bar pattern, the number of air-bar units, web guiding devices, spreading devices, non-contact consideration, drying process, etc. It is out of the scope of this investigation to consider the entire web system design problem. The interest of this investigation is in the effect of an air-bar on the lateral web motion. Thus only the system design considerations related to the effect on lateral web motion caused by air-bar units are discussed.

One of the main considerations is to keep the web system in the amplification free condition. As pointed out earlier, if a web system is in the running state with amplification, the lateral web position at the downstream end is either hard to control when using only one or very few air-bar units, or totally out of control when a series of air-bar units with the same characteristics are used. To avoid the running state with amplification, the amplification free condition has to be established first. In this investigation, the amplification free condition is specified by the critical input ratio, which is a function of other system parameters including the disturbance parameters at the upstream end.

The basic rule to prevent the state with amplification is to keep the actual level of input ratio less than its critical value. If the range of the magnitude and frequency of the disturbance in lateral web displacement at the upstream end can be identified, increasing the slot width of the air-bar with a fixed web width can always reduce the actual level of input ratio. One drawback to this approach is that the excess in slot width may cause a lot of waste of pressurized air. To solve this problem, in air-bar design the slot width should be made adjustable in a certain range so that the web system can be tuned to the amplification free state without much wasting of pressurized air.

The level of the critical input ratio is high at high frequencies. It is possible to keep the web system in the running state without amplification by effectively increasing the level of the critical input ratio while keeping the actual input ratio unchanged. A control device may be mounted at the upstream end, which has a characteristic of a high pass filter. The low frequency disturbances are blocked or significantly reduced and those disturbances with high frequencies are passed to the air-bar units.

Changing air flow rate alone has little effect in altering the level of critical input ratio. Thus it is not recommended to adjust only the air flow rate in order to keep the web system in the state without amplification. It is vital however to have such an air flow rate that non-contact handling be maintained. In combining both the air flow rate and the web span length, the change in the level of critical input ratio can be large. In Fig. 59, the critical input ratios for different oscillation frequencies are shown. The data were obtained with the air flow rate of 2.694 ft^3/sec and the web tension of 4.60 lbf. It shows that the level of critical input ratio decreases as the web span becomes relatively long or less stiff. An opposite effect is observed in the similar plot for the air flow rate of 3.446 ft^3/sec and the same tension level at the frequency $\omega^* = 0.9576$ rad as shown in Fig. 60. The level of critical input ratio increases for a relatively long or less stiff web span. Thus it is important to combine properly the air flow rate and the web span length in order to raise the level of critical input ratio. Another example is on the combined effect of web tension. The curves shown in Fig. 58 clearly indicate that the magnitude level of critical input ratio is high for a lower air flow rate at a given oscillation frequency. The tension in this case is 1.15 lbf. The similar curves shown in Fig. 61 do not have this trend, in which case only the web tension is increased to 4.60 lbf. No definite guidelines can be given at present though. More thorough experimental study is required to identify this relationship.

The web tension has a definite effect on the critical input ratio. The data show that the critical input ratio is a monotonically increasing function of web tension in the range of experimental parameters. Fig. 62 shows one set of curves of critical input ratio as a function of web tension for different air flow rates. The data correspond to the oscillation frequency of 0.9576 rad and the web length to width ratio of 17.0. The monotonic nature of the functional relationship is confirmed in this figure. It is held true in similar data sets with different parameter values.

In the control of lateral web position in the state without amplification, the disturbances in lateral web displacement are always damped by the air-bar units. The more such units used, the smaller the disturbances at the downstream end. As a result the controlling task is made easier at the downstream end. The only potential danger with a series of air-bar units is the instability in lateral web motion if the disturbance at the upstream end is large enough to make the actual input ratio exceed its corresponding critical value.

Discussion and Conclusion

The amplitude factor in web systems with an air-bar unit has been investigated through five experimental parameters: the input ratio, the oscillation frequency, the web length to width ratio, the air flow rate, and the web tension. For a given set of oscillation frequency, air flow rate, web length to width ratio, and web tension and specifying other system parameters, it has been found that the functional relationship between the input ratio and the amplitude factor are describable using a third order polynomial. Accordingly the critical input ratio can be readilv obtained from this functional relationship, which is applicable for specifying the amplification free condition in the web systems involving air-bars.

The effects on the amplitude factor for a web system with air-bar units have been investigated for the above parameters. The amplification free condition is established through the concept of critical input ratio, which is a function of experimental parameters if other system parameters have been pre-specified. The design considerations involving the system stability in lateral web motion have been discussed. The categorization of a lateral load disturbance from an air-bar being small or large depends on the critical input ratio of the web system. Depending on the magnitude of disturbances two running states are possible for a web system: the state without amplification and the state with amplification. The running state with amplification should always be avoided if possible. It makes either the control of lateral web position difficult if few air-bar units are used or causes instability in the lateral web motion if a series of air-bar units are used. In the amplification free condition, the use of a series of air-bar units can significantly reduce the disturbances from the upstream end, which is helpful in keeping the web span at its desired lateral position.

A Further Experimental Study With a Narrow Web Span

It is desirable to have a more extensive variation in the experimental parameters in an experimental study so that the system characteristics under investigation can be more thoroughly explored. The above experimental study has used a wide web, which, due to the limited span lengths on the test machine, results in relatively small length to width ratios. To extend the parameter variation, a narrow web has been used in this newly performed experimental study to carry out a series of tests. The test results have further confirmed the discoveries and conclusions from the previous experimental study. Furthermore new phenomena have been found through the static test, moving dam test, and frequency test.

This experimental study includes five types of tests: the static, dynamic, oscillation frequency, moving dam, and limit cycle in lateral web motion. The detailed description for and the results from those tests will be given and presented in the following sub-sections. In regarding to the web span used, it is made of polyester, a width of 1.0 in., and a thickness of 0.00325 in. The experimental parameters considered are the input ratio, lateral web displacement at the upstream end, excitation frequency, web tension, length ratio (l/L), and half gap length. In the length ratio, l is the location of the air drum measured from the upstream roller (see Fig. 63 (a)). The air flow rate has a complex effect on the system behavior as found through the previous experimental study. Furthermore with a narrow web the accurate air flow rate is hard to control. Instead of keeping the air flow rate a constant within the given system parameter variation, the valve opening of the blower has been set to a constant value (20.0 degrees). This has been proven to be capable of providing enough pressurized air to support the passing web with the given system parameter variation.

The Static Test on Lateral Web Displacement

The static test is to obtain the functional relationship of lateral web displacement at the downstream end in steady state for a given step input at the upstream end. The effect of the transient air flow on the lateral web motion cannot be explored through this test. One hopes that it may provide more information in establishing a model for the air-bar therefore to gain more physical insight of the air flotation problem in web handling.

The experimental parameters involved are the web tension (T), gap length (H_{gl}), and location of air-drum (l/L). Two gap lengths have been used, which are referred to as a wide gap (H_{gl} = 0.5 in.) and a narrow gap (H_{gl} = 0.125 in.). When the air-drum sits at the mid-point (l/L = 0.5), the system has a symmetric configuration in terms of the air-bar units (see Fig. 63 (b)). Changing the location of the air-drum causes non-symmetry in the system configuration (see Fig. 63 (c) and (d)).

In doing the tests, a step input in lateral web displacement was introduced at roller A, which caused displacements at both rollers B and D (see Fig. 63 (a)). These are the input and output of the air-drum respectively. Due to the limitation of the range in the light-emitting sensors, a Vernier caliper was used to measure these displacements instead. After a step input was introduced, the test machine was run for a while to let the system reach its steady state. The test machine was then stopped and the measurements on the lateral web displacement were taken. Fig. 64 shows the relationship of lateral web displacements between the upstream end (y_0) and the downstream end (y_L) at one test condition. The system in this case has a symmetric configuration and a wide gap. Three observations can be made from this plot: (1) two distinct operation regions in y_0 separated by a jumping effect and an overlap between the two regions; (2) the region with the web supported by air cushion, which has a nonlinear effect in the response and the air-drum having a centering effect; and (3) the region with the web slide over the shoulder of the air-drum, which is the abnormal operation region. It shows that the jump occurs around $y_0 = 1.0$ in., which corresponds to half of the web span riding on the air-drum shoulder at the entry region given the web width of 1.0 in. and the half gap length of 0.5 in.

The basic characteristics were maintained when different experimental parameters were used. Fig. 65 shows the comparison between two responses in lateral web motion with different web tensions. With a higher tension, the jump points corresponding to the lateral web displacement at the upstream end are shifted away from the air supporting region, i.e., the air supporting region is extended when a high tension is involved. But the centering effect in this region is weakened, which causes a relatively large response in lateral web displacement comparing with the effect of a lower tension given the same amount of disturbance at the upstream end.

In industrial applications, the multiple air-bar units are often used. The configuration for each air-bar unit is most probably symmetric, which has been assumed throughout the above tests. Some people may also be interested in the effect of different lengths of the upstream and downstream spans, i.e., with a non-symmetric configuration. Some tests have been done with this consideration in mind. Instead of changing the location of the air-drum (roller C), the position of roller B or roller D has been changed (see Fig. 63 (a)). The test procedures are the same as the previous ones. Fig. 66 shows the comparison between two static responses in the response of lateral web displacement with the length ratio pair of (0.433, 0.567). Again for each test result, the basic characteristics are maintained as that in the symmetric configuration. From this comparison one sees that under the same test conditions the one with a larger downstream span length has a better centering effect when the system is in the air supporting region. This region is, however, slightly narrowed as can be observed in this figure. A further comparison between Figs. 65 and 66 indicates that increasing the ratio l/L has a similar effect in the lateral web displacement response to reducing the web tension.

The static test involves only the steady state conditions, which excludes the transient air flow effect. The previous wide web span experimental study indicates that two different running states exist. It is obvious that the web was in the air supporting region for all the wide span tests. The static test results show that no amplification in lateral web displacement in this region exists. This conflict indicates that the transient air flow plays a vital role in driving the web system into the running state with amplification. In trying to establish a model to describe the effect of an air-drum on the lateral web motion, the static test alone cannot be adequate when the amplification in lateral web displacement is involved.

The static test with a narrow gap (H_{gl} = 0.125 in.) has also been done. The non–symmetric responses in lateral web displacement have been obtained. The non-symmetry was caused either by the misalignment of the air-drum, the taping of the air-drum slot opening, or both. The limit cycle in lateral web displacement has been observed. The details on the static test of a narrow gap along with the limit cycle effect will be reported and discussed in the section of limit cycle investigation.

The Dynamic Test on Lateral Web Displacement

Contrary to the static test, the measurement in the dynamic test was carried out with web span oscillating laterally. Instead of the lateral displacements in the static test, the amplitude factor and input ratio are used to present the test results. The procedure for the dynamic test is the same as that for the amplitude factor study done for the wide web span.

It has been shown through the experimental study with the wide web span that the web system is always in the running state without amplification when the entire web is oscillating within the slot opening region of the air-drum. In terms of the input ratio, this condition means $M_{y_0}/H_{gl} < 1.0$. One might suspect that this fact is still true for the web system with a drastically different parameter combination. The dynamic test with a narrow web and a large gap is partially intended to remove this doubt. As a result the conclusions from the experimental study with a wide web can be further confirmed. Furthermore the tests on the non-symmetric configurations has also been done as in the static test case. The other experimental parameters used are the web tension and oscillation frequency.

With the limitation in the light-emitting sensors, only a small range in the input ratio could be covered. In all the tests done with different experimental parameter combinations, no amplification has ever occurred. This result provides a further experimental proof for the fact that a web system cannot be in the running state with amplification unless a part of the web is riding on the air-drum shoulder. A comparison of the amplitude factor with different oscillation frequencies is illustrated in Fig. 67. The experimental parameters are listed in the figure. As can be seen, the amplitude factors are all less than unity. Under this test condition, the amplitude factors increase with frequencies. It is known from the wide web experimental study that the amplitude factor has a low magnitude when the oscillation frequency gets very high.

It is interesting to look at the difference between the oscillation magnitude from the dynamic test and the lateral web displacement from the static test. Fig. 68 shows such a comparison. The input ratio and amplitude factor for the dynamic test have been converted into the lateral web displacements at the upstream and downstream ends first. Since the magnitude is used, only the positive half of the comparison is plotted. Again the small region in the dynamic test is due to the limitation in the light-emitting sensors. It clearly indicates that within the test region the oscillation in the lateral web displacement has a lower magnitude than its corresponding static displacement.

The dynamic test has also been carried out for different system configurations. The comparison of the amplitude factor with the length ratio pair of (0.433, 0.567) is shown in Fig. 69. Under this test condition, the amplitude factor has a lower magnitude for a large l/L value than that of a small l/L value, which is consistent with the results from the static test (see Fig. 66). When the frequency, or the tension, or both are increased, however, the consistency between the dynamic and static tests disappeared. Again this phenomenon indicates that the transient air flow affects the lateral web motion quite significantly. The consistency holds in the tension effect between the dynamic and static tests. Fig. 70 shows the comparison of the amplitude factor with the tension pair of (0.575 lbf, 1.150 lbf). The amplitude factor is higher in magnitude with the high tension than that with the low tension. The observation is the same from the static test results (see Fig. 65). Furthermore this phenomenon holds true for all the experimental parameter combinations used in the tests. One has to notice, however, that the region for the input ratio is relatively small in this set of dynamic tests. The experimental study with the wide web span has indicated that the critical input ratio increases with the web tension. This fact indicates when the web system is in the transition from the running state without amplification to that with amplification, the tension has an opposite effect on the amplitude factor comparing to the static test results. This is again due to the significant effect from the transient air flow on the web span.

The Limit Cycle in Lateral Web Oscillation

In performing the narrow gap test (H_{gl} = 0.125 in.), the limit cycle in lateral web oscillation was found when the web longitudinal speed was low. The limit cycle was caused by the combination of the misalignment of the rollers and the air-drum in the air-bar unit, the taping of the exceeding slot opening on the air-drum, the moment transfer at the upstream roller, and the low web speed.

The misalignment of the air-bar unit and the unparallel taping of the slot opening may cause the non-symmetric response in the lateral web displacement of the static test. With a large gap (H_{gl} = 0.5 in.) this effect is relatively insignificant. The response in Fig. 64, for example, maintains a quite nice symmetry though the misalignment effect can be detected. With a narrow gap (H_{gl} = 0.125 in.), however, the symmetry can be totally destroyed by the misalignment and the unparallel taping. In Fig. 71 the results for the response in lateral web displacement of the static test with a narrow web are shown. The non-symmetry in the response is obvious. In order to verify the correctness in the measurement, two test results obtained at different times under the same test condition have been plotted together. The repeatability in the measurement is quite satisfactory. Only one jump point exists in the response curve. Similarly another two test results are shown in Fig. 72 . Again there is no problem in the repeatability of the measurement. Only the tension was increased comparing with the previous case. The non-symmetry exists in the response curve with a drastic change in the shape of the curve and the position of the jumping point, though the number of jumping points is still only one.

It was during the dynamic test when the limit cycle in lateral web displacement was encountered. Before starting the dynamic test, the guide point is adjusted so that the web span is located at its nominal position at the steady state. The nominal position corresponds to the equal amount of gap opening on both sides of the passing web span at the air-drum. When setting the web tension of 0.575 lbf and the web longitudinal velocity of 295.5 ft./min., instead of adjusting the web span to its nominal position the limit cycle occurred. Fig. 73 shows one measurement for the lateral web displacements at both upstream and downstream ends in one limit cycle. It is clearly seen from this plot that the amplification in the lateral web displacement also occurred in the limit cycle.

Both the limit cycle and the amplification are undesirable in the application. If such a situation does occur in a web system, one should be able to modify the system configuration or adjust the system parameters so that the limit cycle be eliminated and the amplification be avoided. With a long pre-entering span between rollers A and B (see

Fig. 63 (e)), one suspects the moment transfer at roller B may contribute to the limit cycle. The study on the type I interactive web system has shown that the negative steering due to the moment transfer can be reduced or eliminated by either reducing the pre-entering span length, increasing the web tension, increasing the friction between the web and the entering roller, or doing some of or all of them at the same time. With this guideline in mind, a roller E was introduced between rollers A and B but near roller B (see Fig. 63 (f)), which drastically reduced the length of pre-entering web span. While keeping the other conditions unchanged, the limit cycle was found to be eliminated. Keeping the configuration in Fig. 63 (e) unchanged but increasing the web tension to 1.150 lbf, the limit cycle also disappeared. One way to increase the friction is to use nip rollers. After adjusting the web system running with a limit cycle, a nip roller was added at the entering roller (roller B in Fig. 63 (e)). While keeping the other conditions unchanged, the limit cycle was found to have disappeared. Through the experimentation, it was found that increasing the web longitudinal speed to 393.5 ft./min. also kept the web system out of the limit cycle. Thus four parameters have been found useful in eliminating the limit cycle in the lateral web displacement when it does occur. Three of them are based on the study of the type I interactive systems.

Both the tension and speed of the web affect the characteristics of a limit cycle if it does occur. As mentioned above, if an adequate adjustment has been made, either the tension or the speed can completely remove the limit cycle. Through more experimentation by slightly changing the tension or the speed, it has been found that each of them has a different way of affecting the behavior of a limit cycle. Keeping the tension a constant ($T = 0.431$ lbf), a comparison for the lateral web displacement at the downstream end during the limit cycle is shown for two slightly different web speeds in Fig. 74. With the speed increased, the oscillation frequency was reduced but the oscillation magnitude increased. As has been known when the speed is high enough, the frequency is reduced to zero, thus the limit cycle is eliminated. A similar comparison in tension is shown in

Fig. 75, where the web speed used was 218.5 ft./min. There is a slightly decrease in magnitude for increasing web tension. The frequency change is undetectable from this comparison.

Eliminating the limit cycle through increasing the web speed, the dynamic test on this narrow gap system has been done. A comparison of the amplitude factor with the tension pair of (0.575 lbf, 1.150 lbf) is shown in Fig. 76 . Similar to the wide gap test, the effect of tension on the amplitude factor is consistent with the static test for the wide gap system. This consistency holds for different oscillation frequencies. The comparison in different oscillation frequencies shows a similar effect to the dynamic test with the wide gap. Without a limit cycle, the amplification was avoided in all test results.

It is not necessarily true that the limit cycle is always accompanied by the amplification in lateral web oscillation. Like the limit cycle itself, whether there is an amplification during a limit cycle also depends on the tension and speed combination as found through the limit cycle tests with different web tension and speed combinations.

The Frequency Test

From the results of pioneer web handling researchers, it is well known that the web mass is negligible in lateral web dynamics unless the web tension is extremely low or the web velocity extremely high. Some people have suggested that one may want to model the web system as a lumped spring-mass system. By finding the transfer function of the system through experimentation, the equivalent spring can then be characterized. This way the web system can be subsequently modeled without considering the air flow effect.

A premise for this approach is to assume that the web mass plays a significant role in the lateral web dynamics when the air flotation is involved. Before actually taking this approach, the significance of web mass in the lateral web dynamics in air flotation systems has been explored through the frequency test. Since the previous study has not covered the air flotation system, this test on the web mass effect is necessary.

The basic idea of this frequency test is to find the frequency of the free oscillation of the web span involving the air-drum. The time period of the oscillation can then be known. Let the time constant of the web span be equal to this period, the critical velocity of web span can be obtained based on the test system configuration. This velocity is critical since with a disturbance at the upstream end, the system can be excited at its resonance frequency. Under such a condition the web mass needs to be considered in analysing the lateral web dynamics. If this critical velocity is much higher than the maximum limit in the industrial application, however, the web mass effect on the lateral web dynamics is negligible.

The system configuration is shown in Fig. 63 (g). The web was stationary but supported at the air-drum (roller C) with pressurized air during the frequency test. The web was plucked away from its nominal position, which is equivalent to giving an initial displacement for the lateral web oscillation. The light-emitting sensor E was used to measure its oscillation after the web was released. Since the high tension prevented the free web oscillation due to the contact at the air-drum, relatively low tensions were used during the tests instead. One measurement from the frequency test with the tension of 0.1438 lbf is displayed in Fig. 77 . It is seen that the nonlinear effect does exist with a large oscillation magnitude. With less than four cycles, the oscillation was settled down to its linear oscillation region. The damping effect is present since the oscillation magnitude decreases as the time lapses. The rising curve at the end of oscillation is due to another attempt on doing a similar test. The time period for this test has been calculated to be 0.02413 sec., which corresponds to a frequency of 41.45 Hz. Using the web span length of the system, the critical web speed is turned out to be 21139.9 ft./min. For this test the sampling time step was set to 0.0005 sec. With too large a time step, the aliasing in sampled data may cause a much lower frequency than the actual one. Trying to detect if there was an aliasing problem in the above test, one more test was done with a sampling time step of 0.0006 sec. while keeping the other test conditions the same. A similar measurement was obtained, which had nonlinear oscillation at a large magnitude and settled down into its linear oscillation after a few cycles. The estimated time period turns out to be 0.02452 sec., which corresponds to the oscillation frequency of 40.79 Hz and the critical speed of 20800.9 ft./min. Comparing to the previous test results, one concludes that no aliasing exists in the sampled data with a time step of 0.0005 sec. in the process of data acquisition. Another test was repeated with the web tension doubled (T = 0.2875 lbf). Similar characteristics in measured data were observed. The time period from the test data is estimated to be 0.02357 sec., which gives the oscillation frequency of 42.43 Hz, and the critical velocity of 21639.6 ft./min.

The test results show a slight increase in oscillation frequency for a high tension over a low tension. In industrial practice, the velocity limit for plastic webs is about 3000.0 ft./min. The above estimated critical velocities from the frequency test are far greater than this limit, which indicates that web mass effect on the lateral web dynamics involving air flotation is negligible under the normal operation conditions. The decrease in oscillation frequency at a low tension verifies again that correctness of the conclusion that the web mass effect on the lateral web dynamics may be significant when the web tension is extremely low or the web velocity extremely high. Under non-extreme operation conditions of the web system, however, the modeling of the web system with air flotation including the web mass is impractical.

The Moving Dam Test

From the amplitude factor study, i.e., through the dynamic test, it has been known that with the input ratio less than its critical value the web system is in the running state without amplification. This means the air-drum has a centering effect on the passing web, since the disturbance in the lateral web displacement at the upstream end is reduced in magnitude at the downstream end after passing the air-drum. In application, attempts have been made using a moving dam to guide the passing web on the air-drum. No detailed information in this aspect has been available to this researcher at present. Trying to gain understanding on how the centering effect has been achieved through an air-drum, the moving dam test has been carried out.

The original intention with this test was quite innocent. By bringing the dam close to the web span, the air pressure and flow between the web edge and the dam would be built up. As a result the action causing the centering effect would be exaggerated. With such a drastic action, it would be possible to visualize through observation. Consequently the physical insight of the centering effect could be gained. When actually doing the test, it was quite frustrating. The test configuration is shown in Fig. 63 (h) with the moving dam E. The actual test procedure is illustrated by Fig. 78 . The moving dam test is similar to the static test described above. The web span is first placed at its nominal position, i.e., centered on the air-drum, without introducing the moving dam. Then the moving dam is mounted on one end of the air-drum as seen in Fig. 78 . In carrying out the test, the dam E was moved close to the passing web F. To one's dismay, no obvious change could be observed in the web motion and condition as originally expected. The same test had been repeated with other web tensions and valve openings, the drastic action brought by the moving dam on the passing web failed to be realized. This is also a failure in terms of realizing the original goal for this test.

The failure in observing the drastic action on the web span due to the presence of the dam does not necessarily mean the dam has no effect on the lateral web motion. The static test with a moving dam was then carried out to see the effect of the dam on the lateral web motion. After the web is positioned, the dam is mounted. The parameter H_{md} is used to describe the distance between the dam and the nominal position of the near side web edge, which has been taken less than or equal to the half gap length H_{gl} in the test (see Fig. 78). The web position with $H_{md} = H_{gl}$ is taken as the reference position. With the dam moving towards the passing web, i.e., reducing the parameter H_{md}, the lateral web positions at both upstream and downstream ends are measured using the Vernier caliper. The displacement in lateral web direction caused by the moving dam can then be obtained with respect to the reference position. A comparison of the moving dam effect with tension pair of (0.575 lbf, 1.150 lbf) is given in Fig. 79 . Both the lateral web displacements at the upstream and downstream ends are plotted. Due to the fixed guide point, the displacement at the upstream end (y_0) is virtually zero. The slight offsets shown in the plot for y_0 was due to the uncertainties in the measurement, non-perfect web and its edge, and the system errors. The positive sign in the lateral web displacement y_L means the web span moves in the same direction as the dam does. With the dam mounted, the symmetry of the air-drum in the direction of the slot opening has been destroyed. When the dam moves towards the passing web, the slot opening length has also been shortened. The results shown in Fig. 79 indicate the air-drum tries to recenter the passing web at the downstream end even though the position at the upstream end has been kept unchanged.

If the dams are introduced on both sides of the passing web, the test results obtained here indicate a better centering effect can be expected. Before this configuration can be used to guide the web, more questions should be answered first. For example, with a large disturbance at the upstream end, the web may touch the dam, thus causing damage to the web. The dynamic action due to the transient air flow can have a significant effect on the lateral web motion as seen through the above experimental study. Further experimentations are needed to gain more understanding of the moving dam effect on the lateral web motion.

Discussion and Conclusion

The experimental study with a drastic difference in experimental parameters from the previous study has been carried out. Not only the same test procedure on the amplitude factor has been done, but also new procedures for testing the web system have been implemented. Through this study, the findings and conclusions from the previous study have been further confirmed and verified. By exploring the static test, the limit cycle in lateral web displacement, the frequency test, and the moving dam test, further understanding of the air flotation system has been gained.

As indicated through the static test, the web is always centered through the air-drum in the air supporting region. Without the transient air flow action on the web span, the running state with amplification cannot be realized. The tension and different system configuration on the lateral web displacement have also been explored through both the static and dynamic tests.

The limit cycle in lateral web motion has been found when doing tests with a narrow gap. It was caused by the combination of the narrow gap, uneven slot taping, misalignment in air-bar unit, and moment transfer at the entering roller. With some web tension and speed combinations, the amplification in lateral web oscillation accompanied the limit cycle. It has been found that four parameters can be adjusted to eliminate the limit cycle, which are increasing the web tension, reducing the length of pre-entering web span, increasing the friction between the web and the entering roller, and increasing the web longitudinal speed. When the limit cycle is eliminated, the dynamic test shows no amplification involved in the specified parameter variation.

The frequency test has further confirmed that the web mass is negligible in lateral web dynamics when the web system is in the normal operation condition. Thus it proves that it is impractical in trying to model the web system as a lumped spring-mass system. Observing the centering effect of the air-drum on the web span has been failed through the moving dam test. However the static test with a moving dam does indicate that the recentering of the web takes place when the dam is present, i.e., the web at the downstream end moves in the same direction as the dam does. The centering effect is more effective with a low tension than a high tension.

It is apparent that trying to construct an adequate model to describe the air-bar through simple static tests is impractical. The experimental study indicates that it is the transient air flow action on the web span that causes the amplification in the lateral web oscillation. Relatively speaking, the transient air flow action is insignificant when the system is in the running state without amplification. Under such a condition, the results from the static test are consistent with those from the dynamic test. The conflict occurs when the running state is the one with amplification. An adequate model for the air-bar has to be established before a thorough understanding can be gained of the air flotation involved web systems. The interaction of the air dynamics at the air drum with the passing web span has to be an essential part of this model. For over three decades, the air flotation analyses have been limited to the lubrication theory of the air flow. Even with a laminar flow field and two dimensional model, the boundary conditions have not been established. The air flow at the air-drum in web handling problems involves much more complicated flow field and boundary conditions. In order to conquer this combined air dynamics and elasticity problem, efforts should be put on both the theoretical and experimental studies. Only after this mission is accomplished then the lateral web dynamics in the air flotation web systems can be thoroughly and systematically investigated.

Summary of Experimental Study

The experimental study of the web system with a wide web and involving an air-bar includes two aspects: the parameter identification and the amplitude factor investigation. The former concentrates on the system model structure in lateral web motion. The investigation establishes the conditions under which the model structure of a system without an air-bar is applicable. The latter uses the concept of amplitude factor to unify the study for the web system running states of both with and without the amplification of lateral web displacement.

In the study for parameter identification, extensive tests on the web system with an air-bar have been done. The investigation starts with the web span lateral motion between two parallel rollers. Both the small and considerable lateral load disturbances to the web span from the air-bar, which correspond to without and with the amplification in lateral web displacement at the downstream roller respectively, have been investigated through the system parameter identification approach. Similar to the case with parallel rollers, the web span lateral motion with small lateral load disturbances can be described using an ARMA model. Highly nonlinear effects caused by considerable lateral load disturbances to the web system makes the ARMA model inadequate in describing the system.behavior in lateral web motion.

The experimentation is carried out for the unified approach on the web system with an air-bar unit. A set of five experimental parameters has been chosen to see the effect on the amplitude factor. The procedure for gathering experimental data, the regression analysis on the data obtained, and the synthesis on the experimental data based on the results from the regression analysis have been described. The regression analysis indicates that the functional relationship between the amplitude factor and the input ratio can be adequately described using a third order polynomial for the given set of other experimental parameters. Based on the results from experimental data synthesis, the effect on the amplitude factor due to experimental parameters has been analyzed. The critical input ratio is used for establishing the amplification free condition for the web system with air-bar units. Some guidelines for keeping such a web system from the running state with amplification can be derived based on the consideration of either increasing the critical input ratio or reducing the actual input ratio of the web system.

The running state with amplification should always be avoided. If the amplification does occur, several simple approaches can be used to bring the web system under the amplification free condition: 1) Increasing the opening slot width of the air-bar; 2) Reducing the web width; 3) Increasing the web tension; 4) Blocking the low-frequency disturbances in the lateral web displacement at the upstream end; 5) Shortening the web span length; and 6) Reducing the magnitude of lateral web oscillation at the upstream end. These approaches effectively either reduce the actual input ratio or increase the critical input ratio of the web system. As a result, the web system can be made to operate in the running state without amplification.

While the web system is kept to operate in the running state without amplification, the lateral web motion can be described using an ARMA model. In maintaining the web span at its desired lateral position the control strategies similar to the one suggested by

Kardamilas [6] may be used. The parameters in the model are dependent upon the web system and lateral load disturbances. Therefore the parameter estimation must be an essential part in performing the control task. Applying adaptive control on such a web system is necessary. More work in this aspect needs to be done in the future.

As a confirmation, the experimental study of the web system with a narrow web has also been done. The results from the dynamic test agree with those from the previous study. The static test has identified two operation regions, which are separated by the lateral web displacement at the upstream end with a jump phenomenon. In both the air supporting and shoulder riding regions, no amplification in lateral web displacement exists. This fact indicates that the transient air flow action plays an important role on the lateral web oscillation when the web system is in the running state with amplification.

With a narrow gap, the misalignment of rollers and air-bar units has a significant effect on the characteristics of the web system. The static test has shown that the symmetry of the static response can be destroyed. Also the responses are quite different when the web tension changes. With the right combination of the misalignment, moment transfer at the upstream roller, tension, and longitudinal speed, the limit cycle in lateral web oscillation may occur. Either running state may accompany the limit cycle. To eliminate the limit cycle, one may want to use some or all of following approaches: (1) removing misalignment; (2) reducing the pre-entering span length; (3) increasing the friction between the web and entering roller; (4) increasing web tension; (5) increasing web longitudinal speed; (6) increasing the slot width of the air-drum; and (7) reducing the web width.

With a dam covering a part of the slot on the air-drum, the passing web moves away from the dam at the downstream end, which is a recentering effect. The moving dam test has shown that the recentering effect is strong with either a high tension or the dam being close to the passing web. The frequency test has confirmed again that the web mass effect is negligible for the lateral web dynamics unless the web system is in extremely unusual operating conditions such as an extremely high speed or with an extremely low tension. The approach using an equivalent mass-spring system to model the air flotation problem is impractical since the web mass effect is insignificant to the lateral web dynamics under most of the operating conditions.

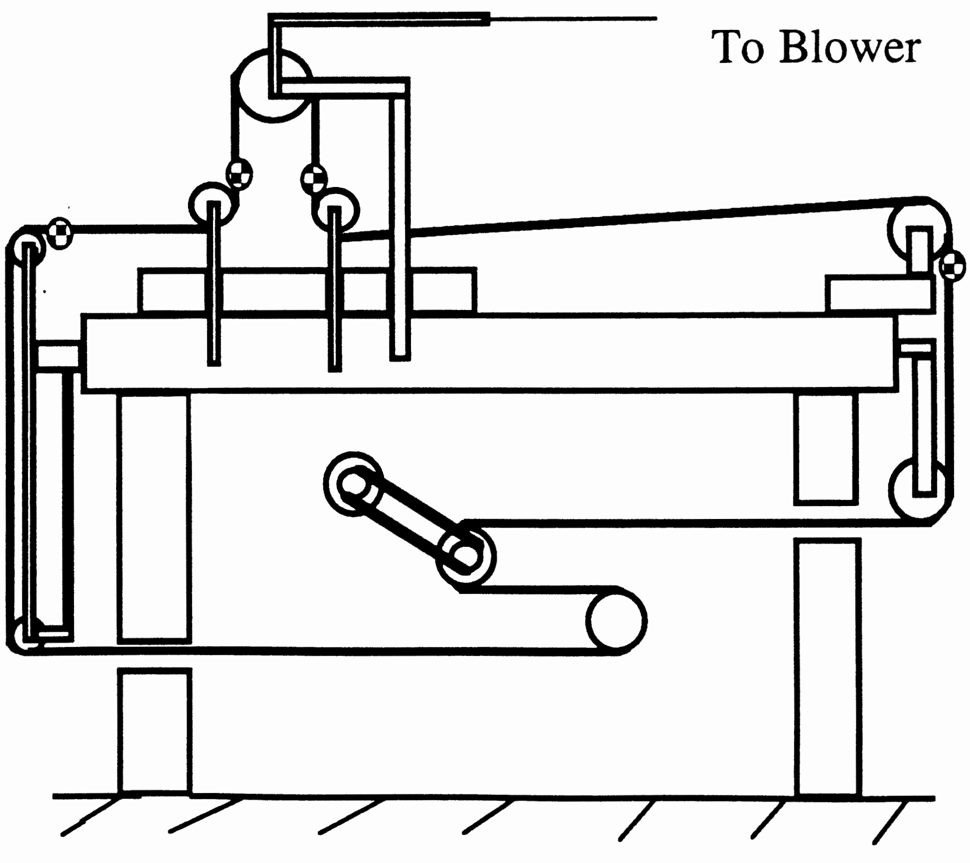

Figure 29. Shelton Machine With an Air-Bar Unit

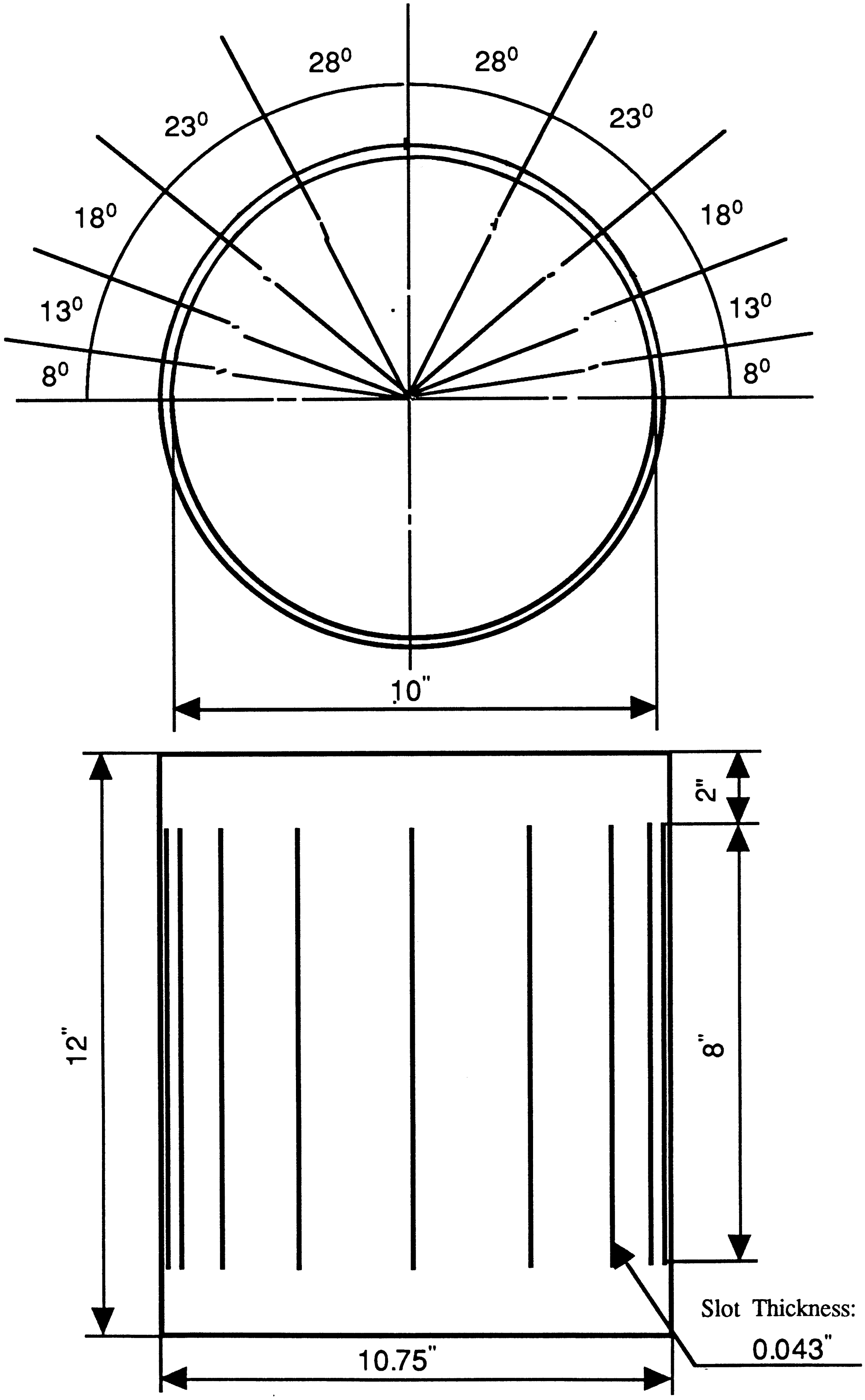

Figure 30. The Air Drum Size and Slot Pattern

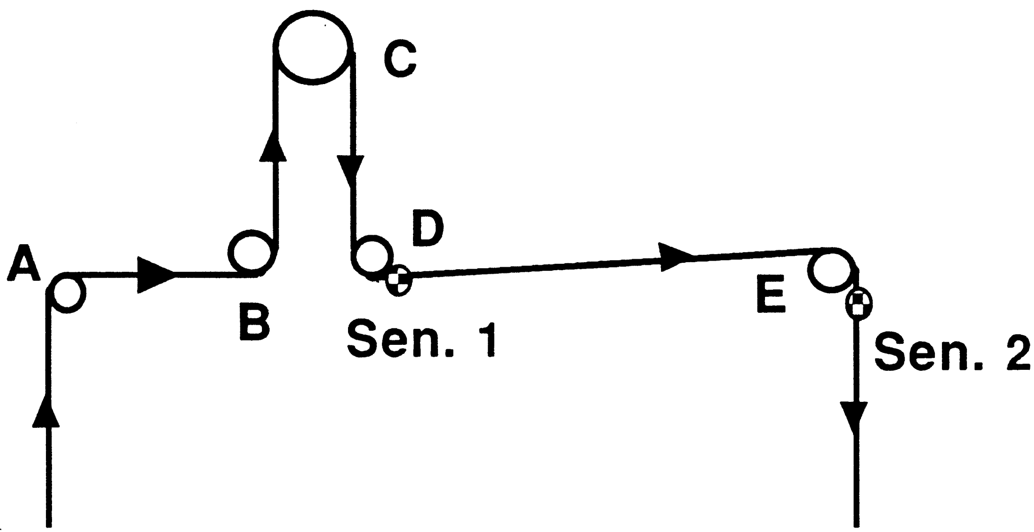

Figure 31. Test of ARMA Model for the Response Between Parallel Rollers

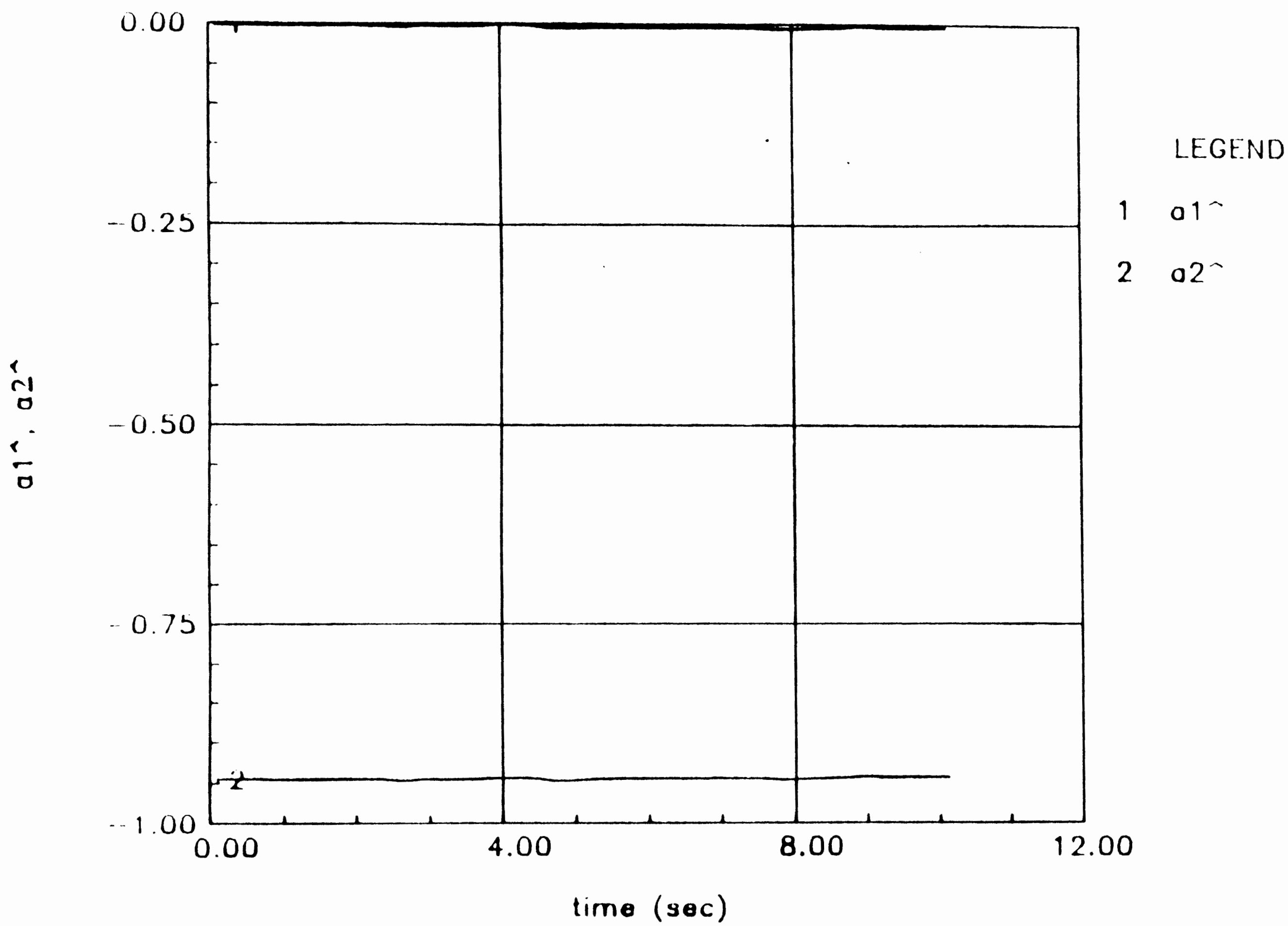

Figure 32 Estimated Parameters in A(z) for Case I

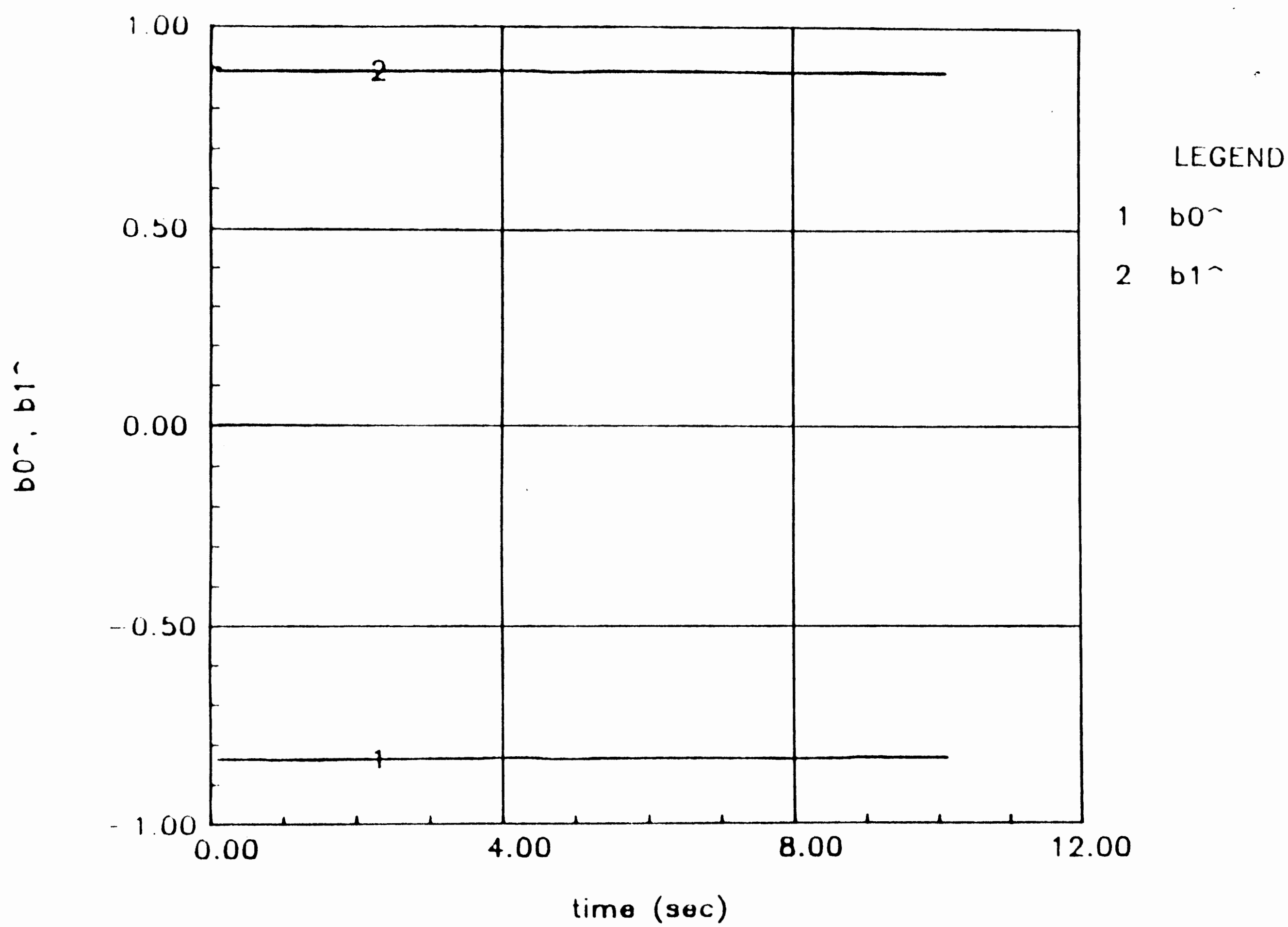

Figure 33 Estimated Parameters in B(z) for Case I

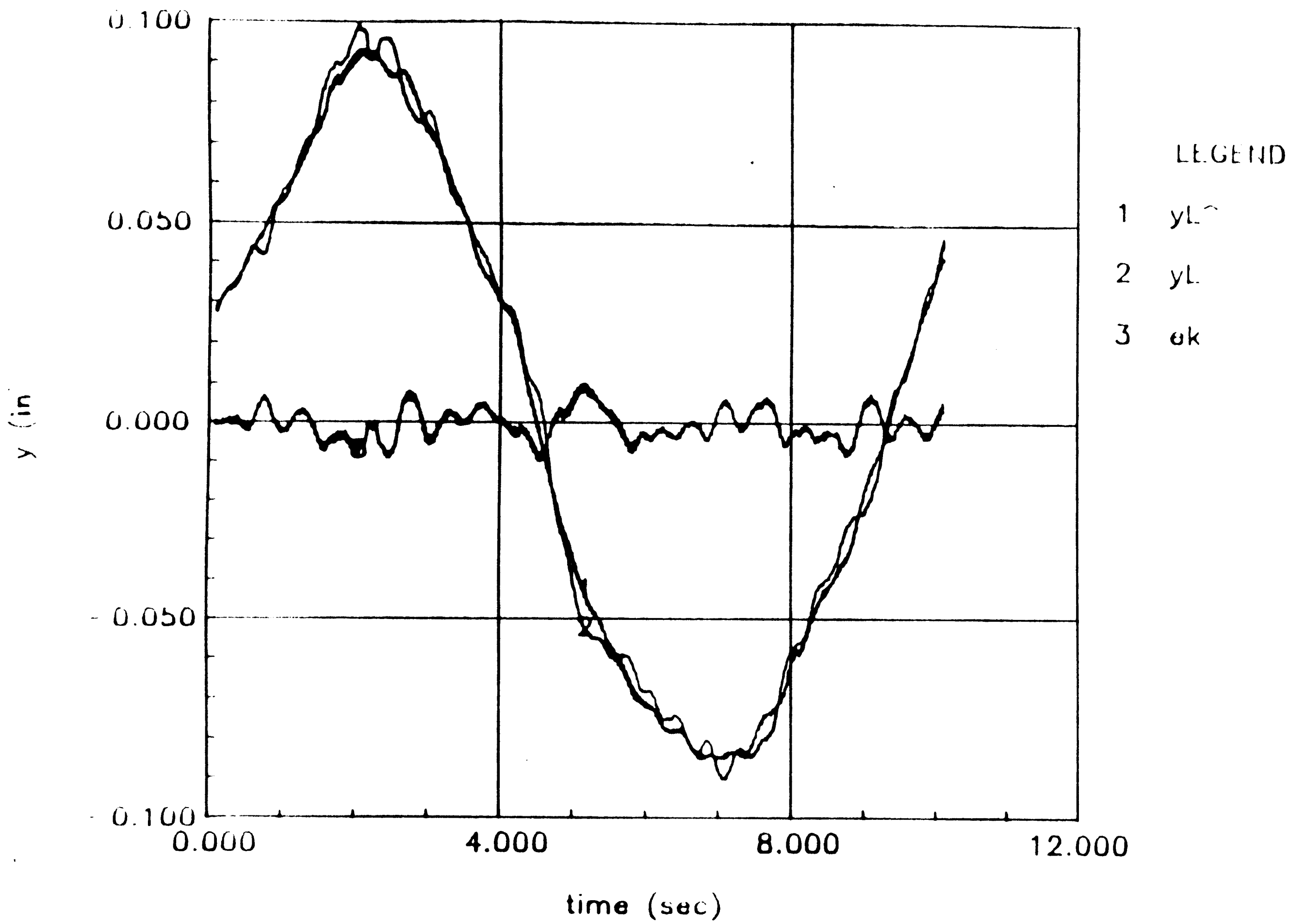

Figure 34. Estimated (yL^), Smoothed (yL) Responses and
Residual (ek) for Case I With a Sine Wave Disturbance

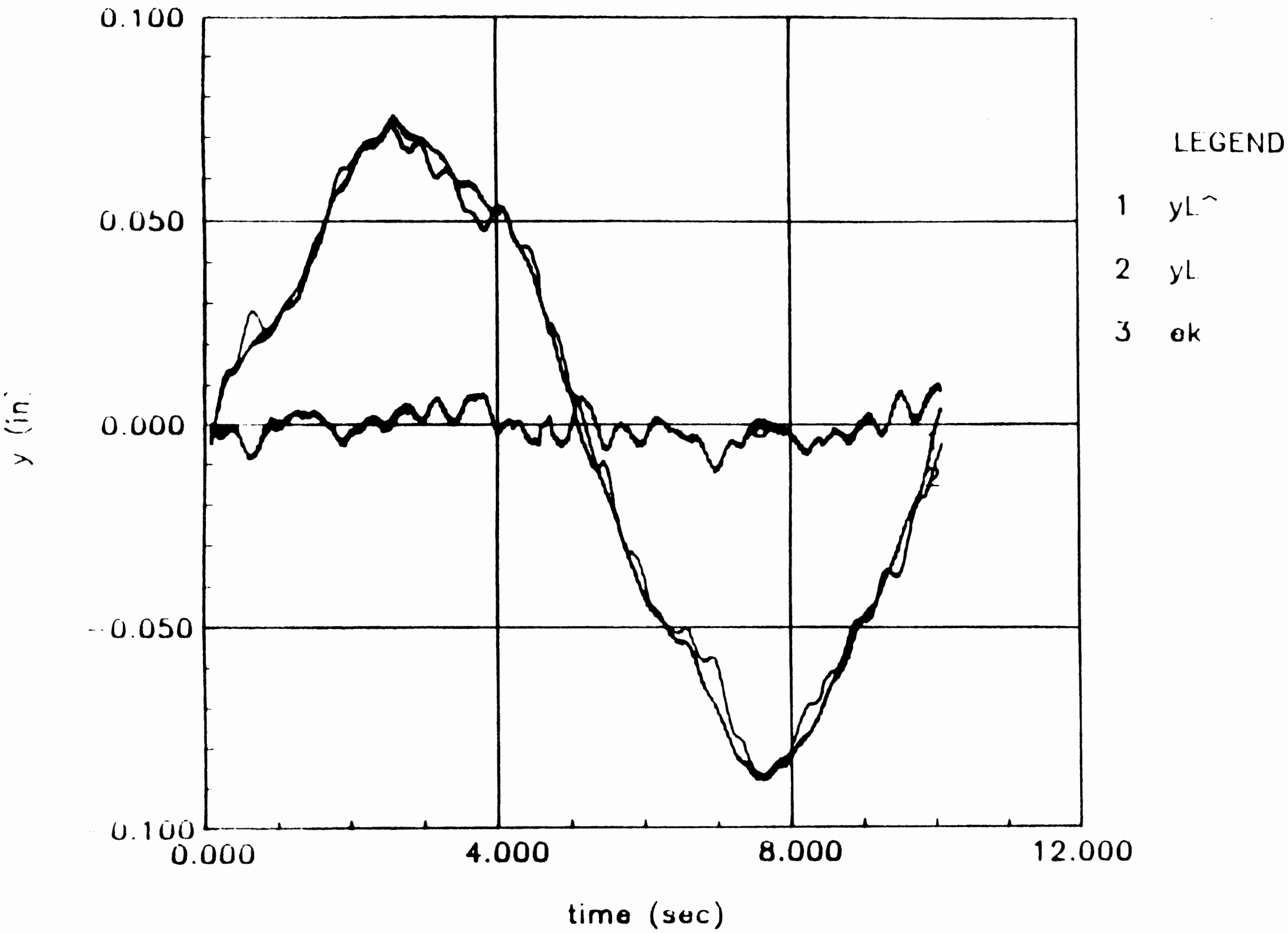

Figure 35. Estimated (yL^), Smoothed (yL) Responses and Residual (ek) for Case I With a Triangular Wave Disturbance

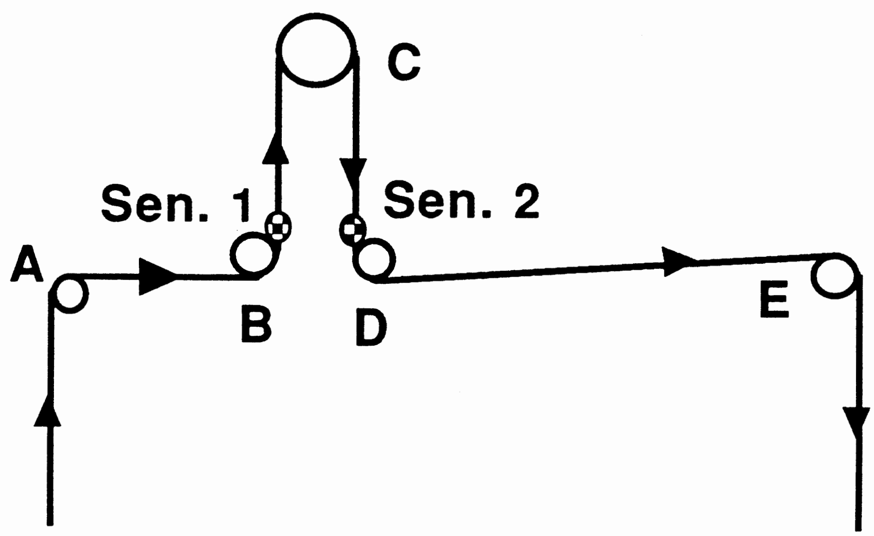

Figure 36. Test of ARMA Models for the Response of a Web System With an Air-Bar Unit

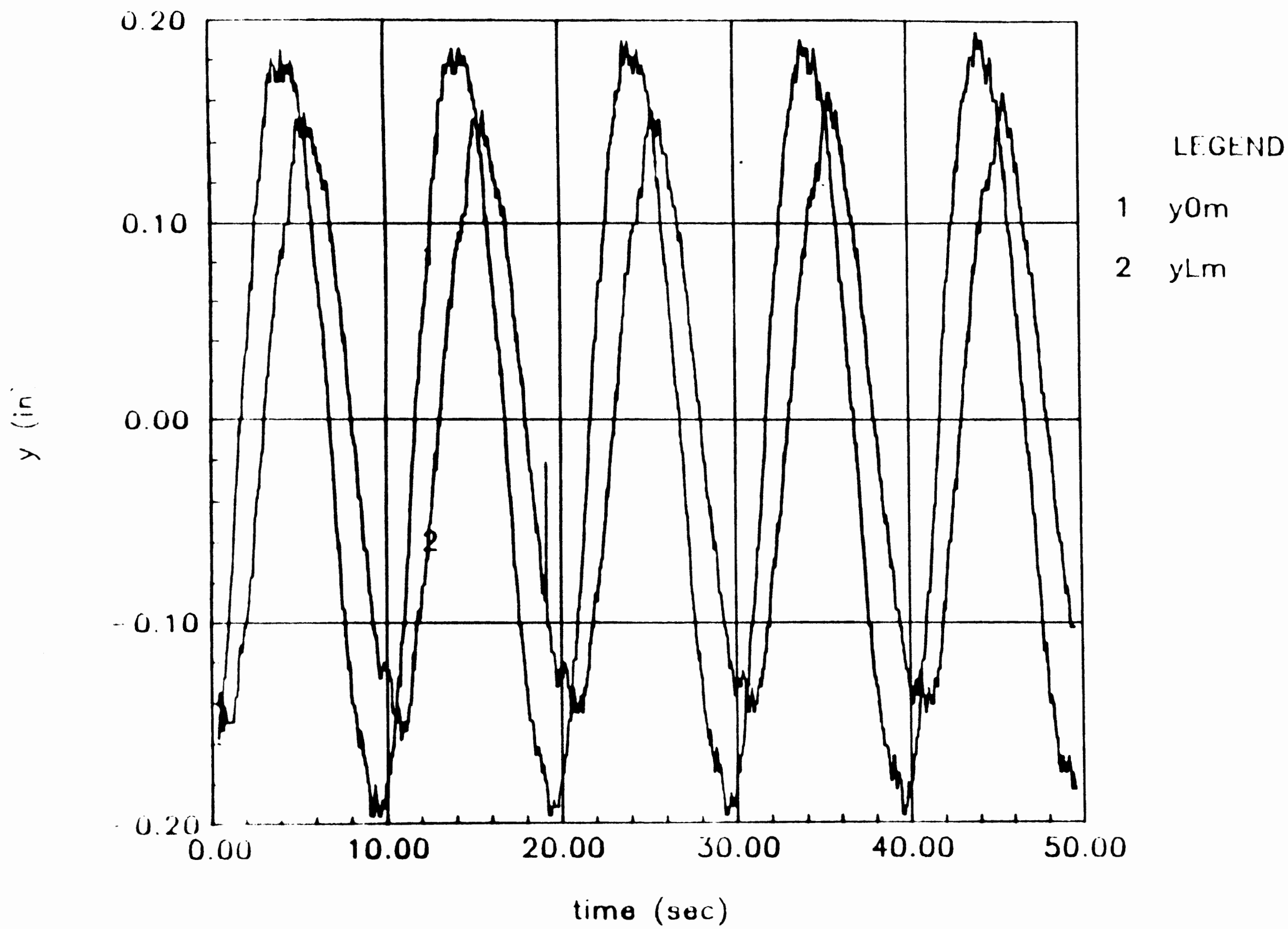

Figure 37. Measured Web Displacements at Upstream (y0m) and Downstream (yLm) Ends for Case II With a Disturbance Frequency of 0.1 Hz

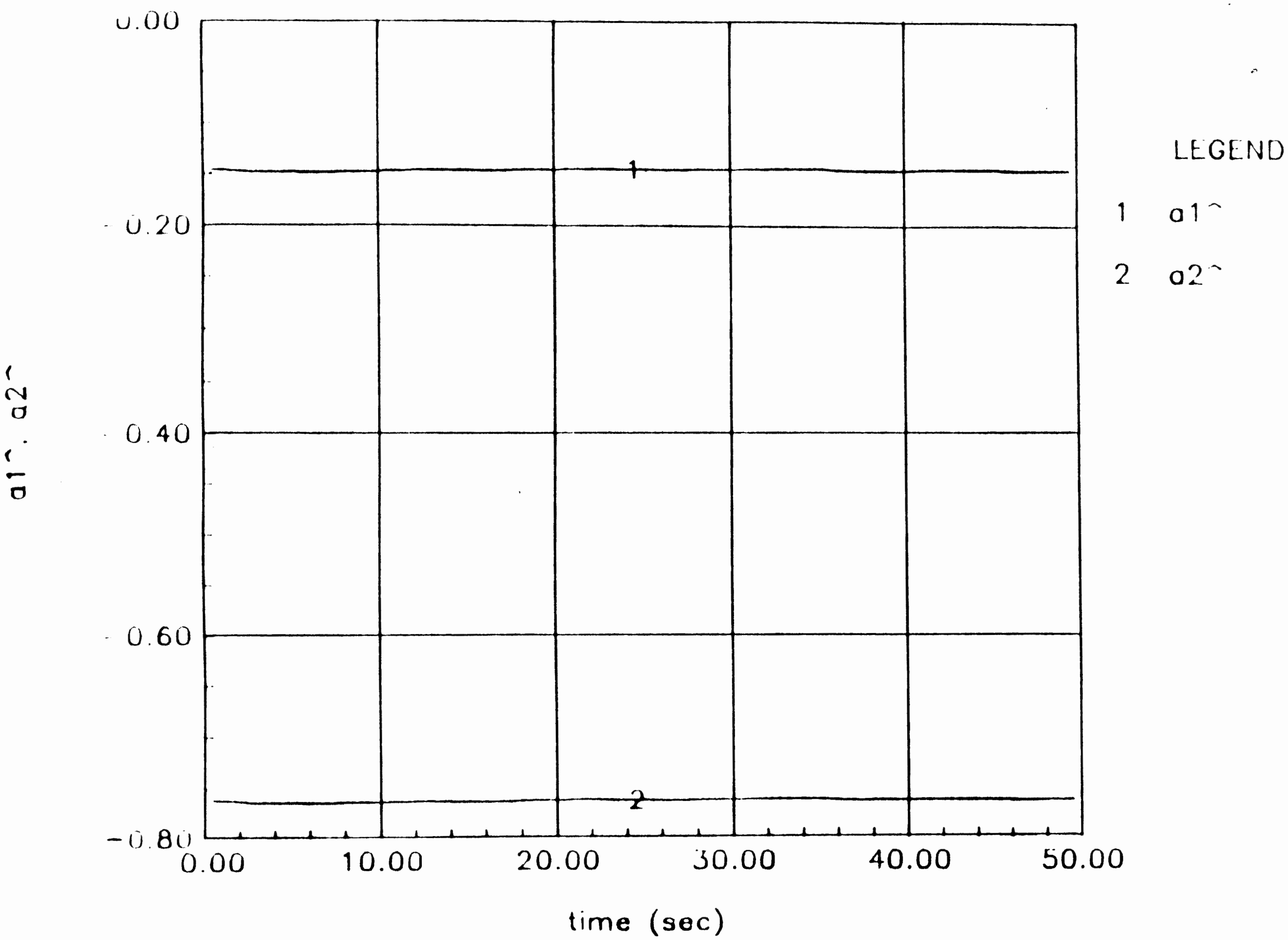

Figure 38. Estimated Parameters in A(z) for Case II

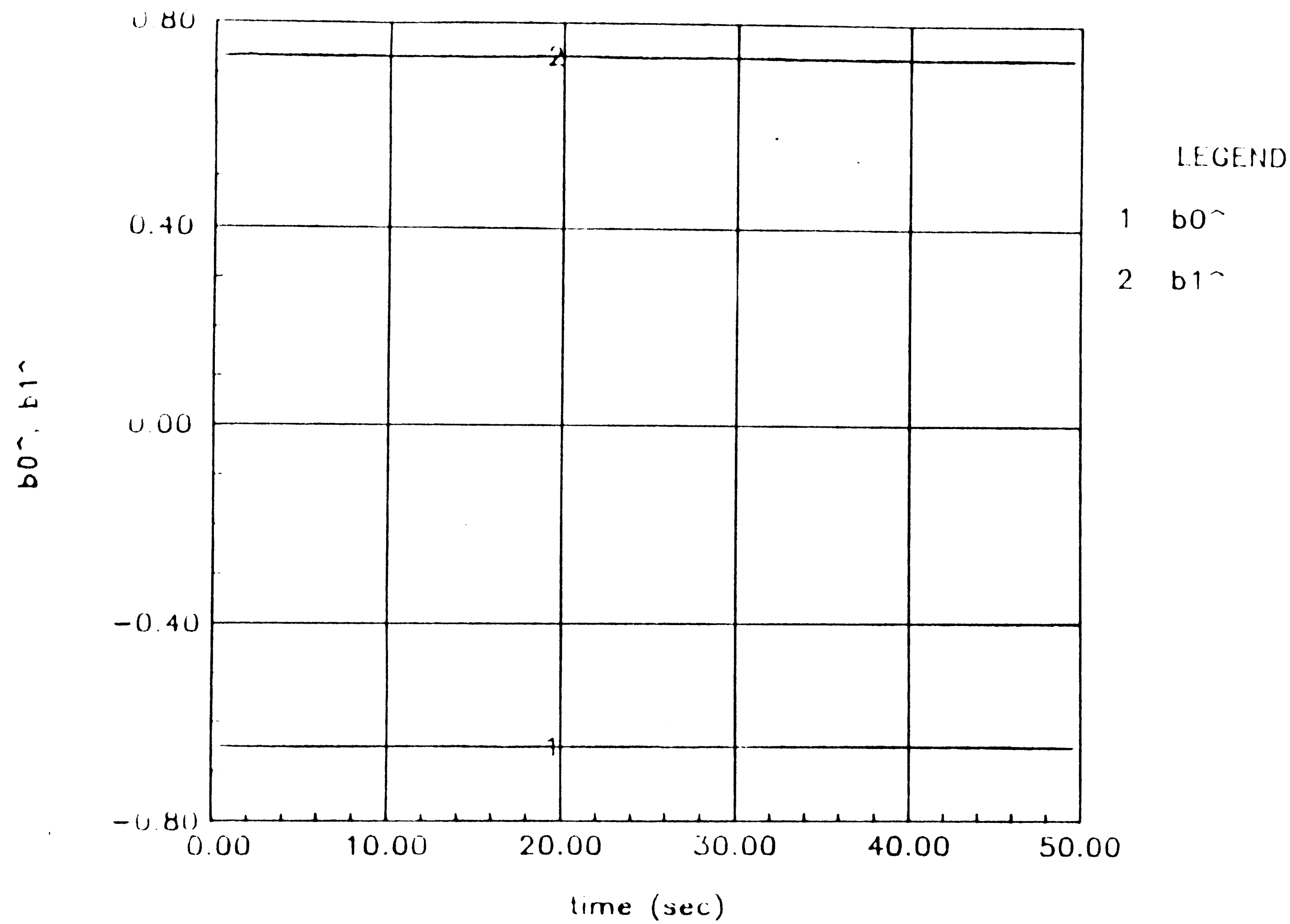

Figure 39. Estimated Parameters in B(z) for Case II

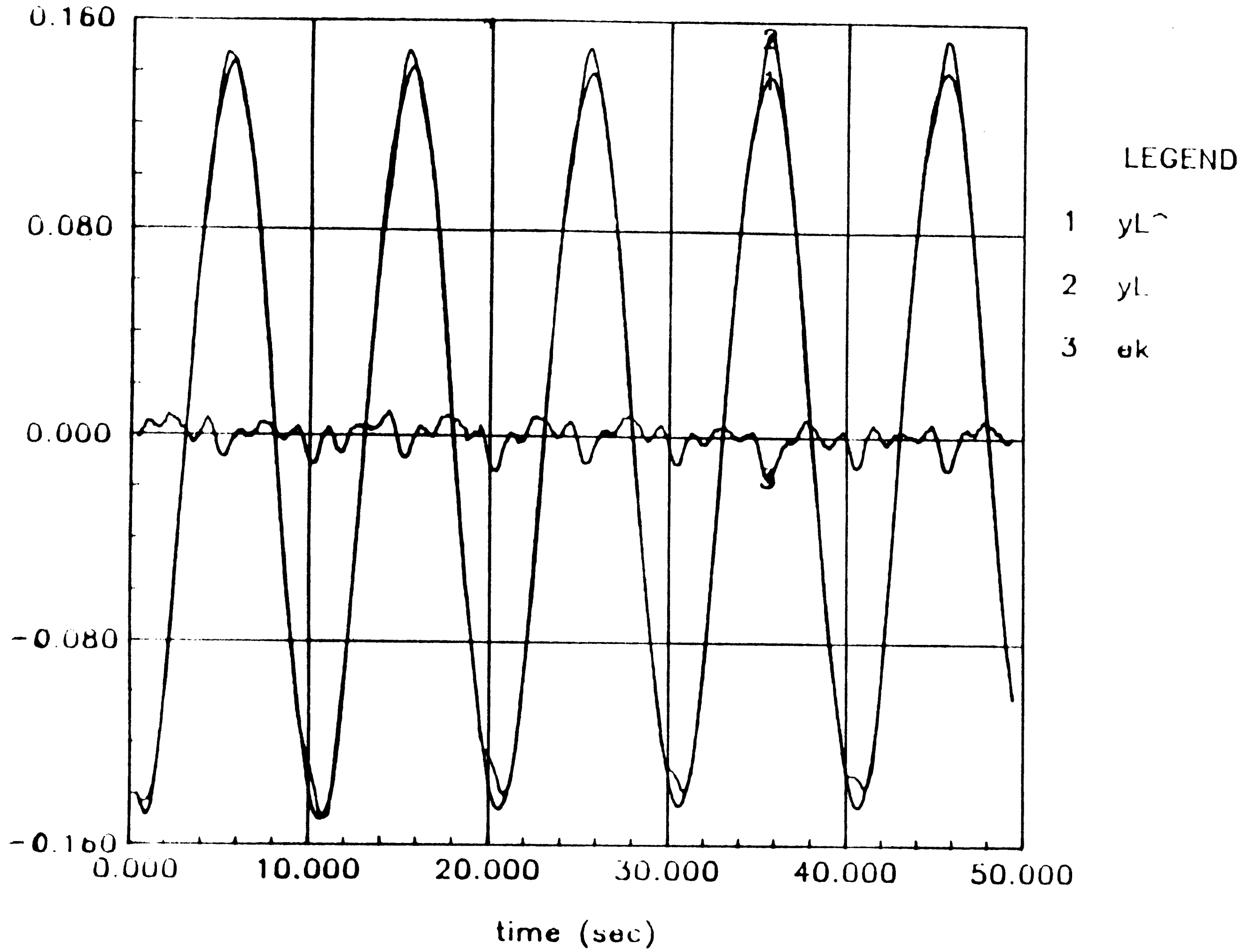

Figure 40. Estimated (yL^), Smoothed (yL) Responses and Residual (ek) for Case II With a Disturbance Frequency of 0.1 Hz

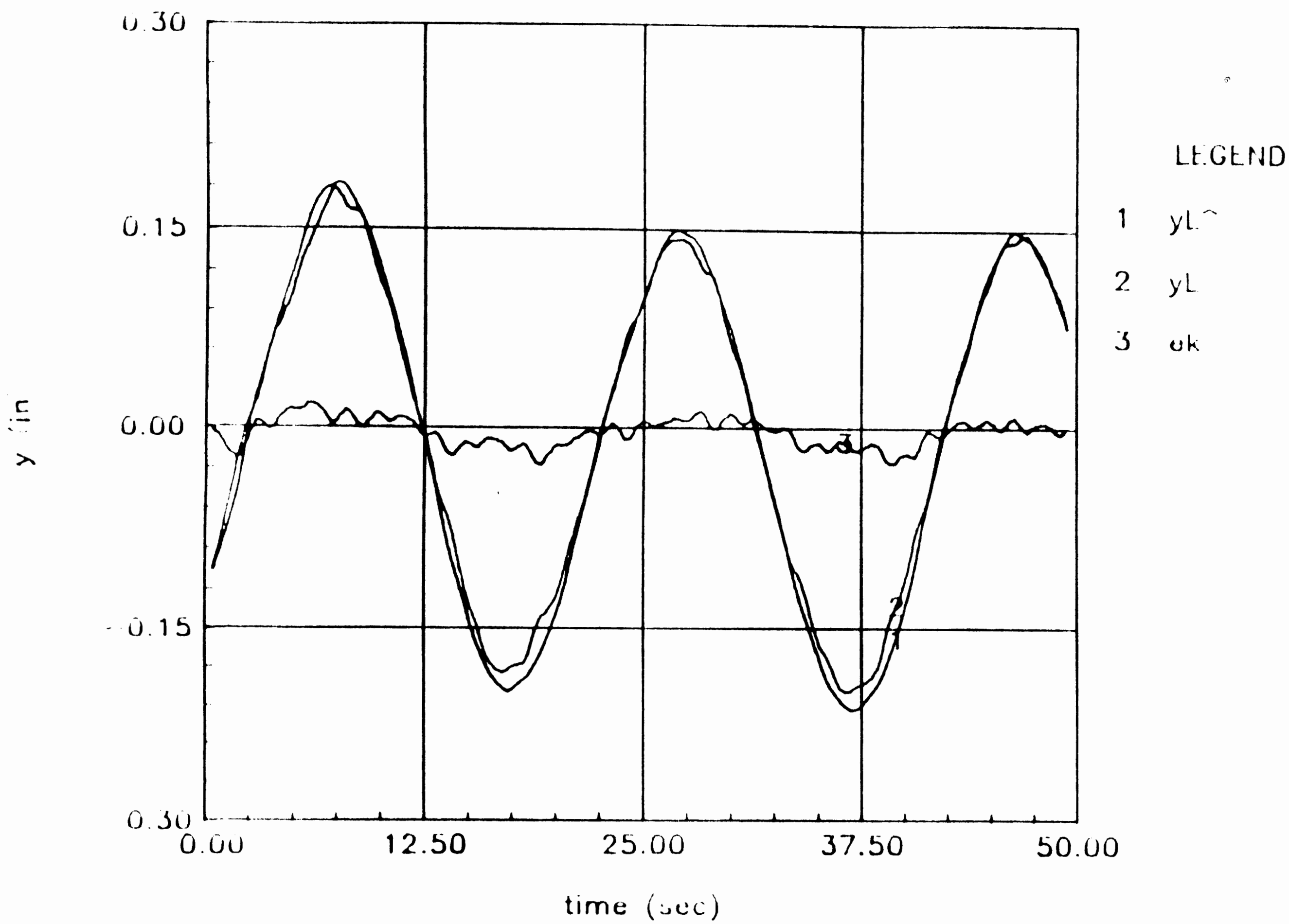

Figure 41. Estimated (yL^), Smoothed (yL) Responses and Residual (ek) for Case II With a Disturbance Frequency of 0.05 Hz

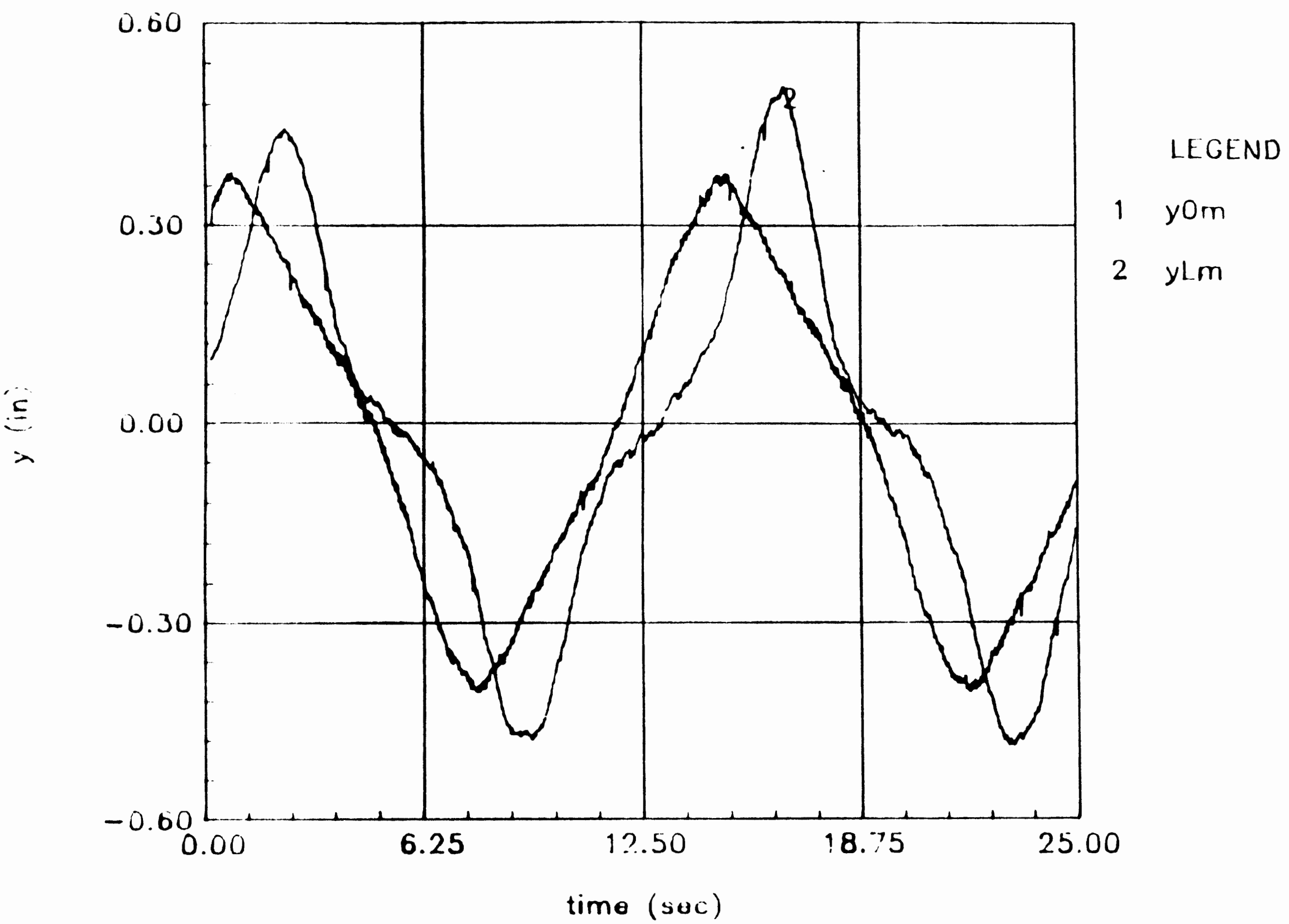

Figure 42. Measured Web Displacements at Upstream (y0m) and Downstream (yLm) Ends for Case III

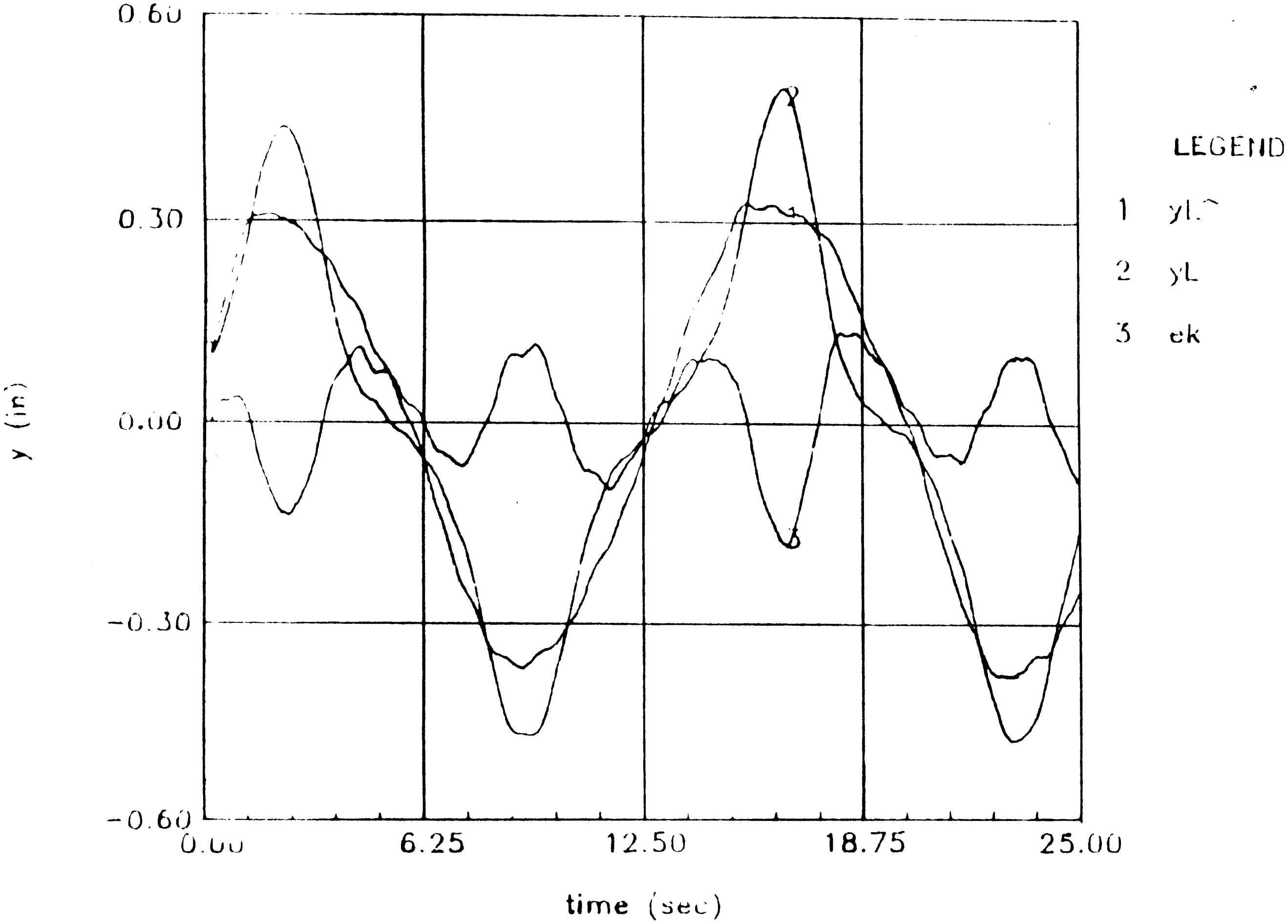

Figure 43. Estimated (yL^), Smoothed (yL) Responses and Residual (ek) for Case III Using (2, 1, 0, 0) ARMA Model With λ = 1.0

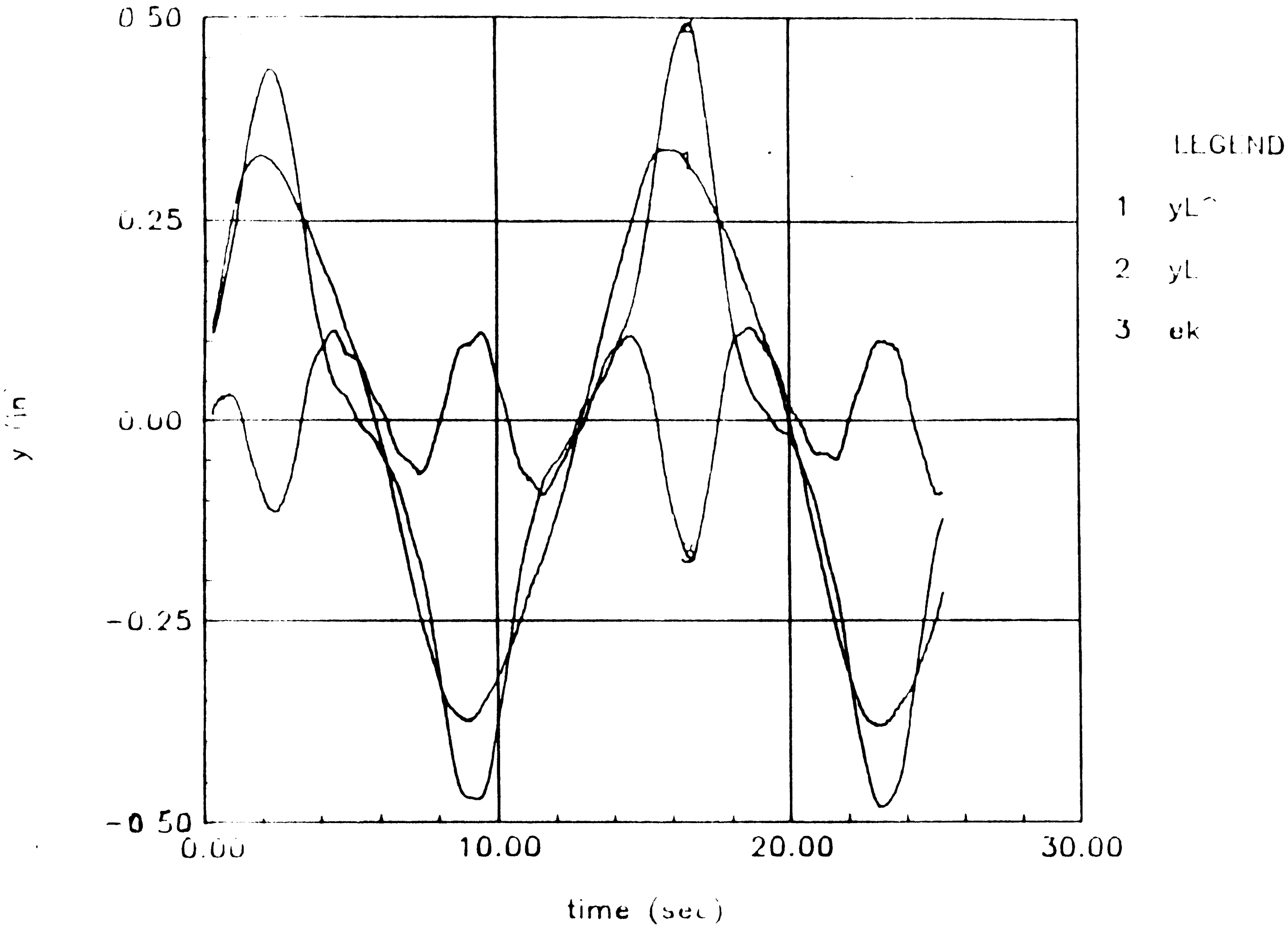

Figure 44. Estimated (yL^), Smoothed (yL) Responses and Residual (ek) for Case III Using (4, 4, 0, 0) ARMA Model With $\lambda = 1.0$

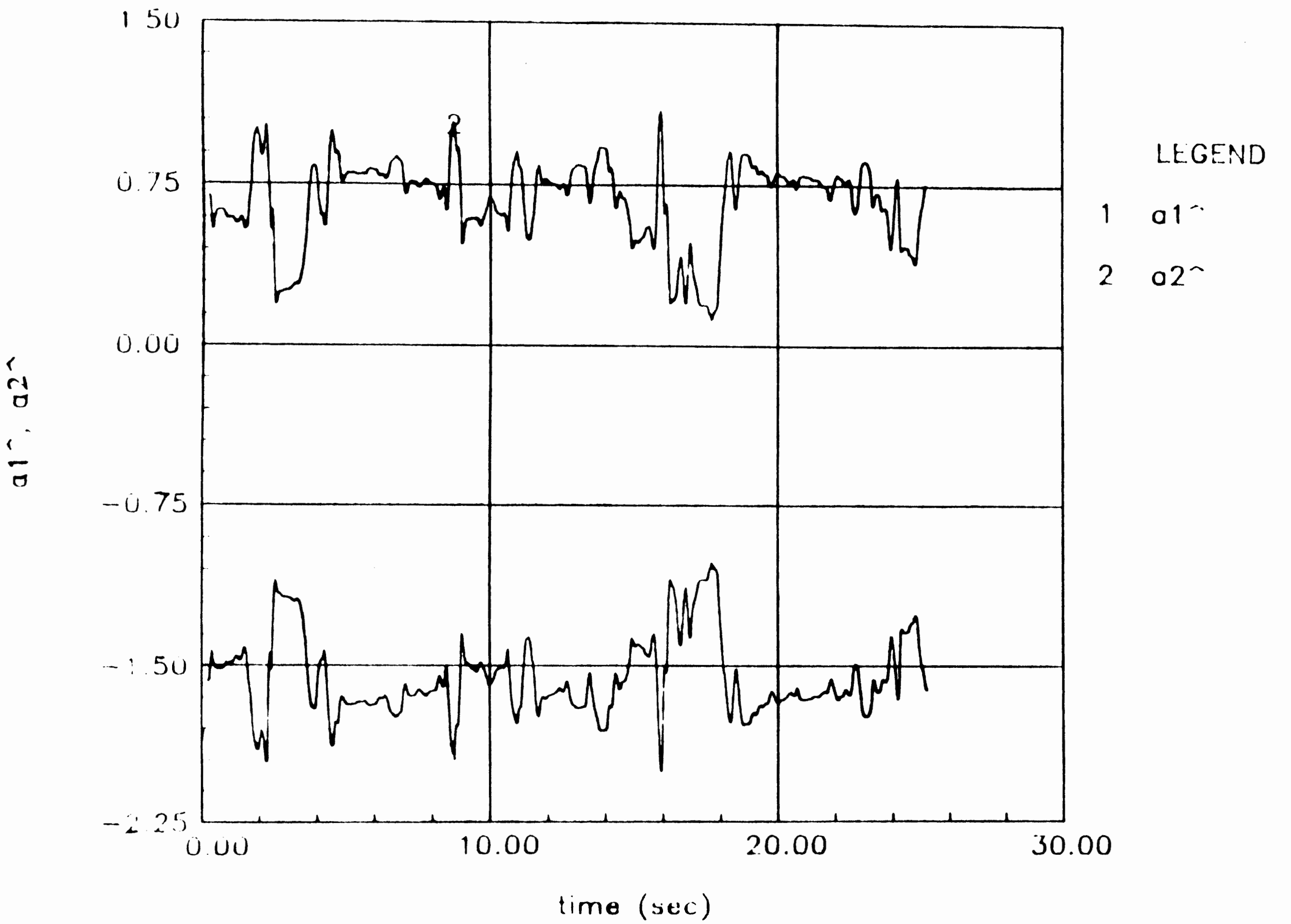

Figure 45. Estimated Parameters in A(z) for Case III Using
(2, 2, 0, 0) ARMA Model With $\lambda = 0.995$

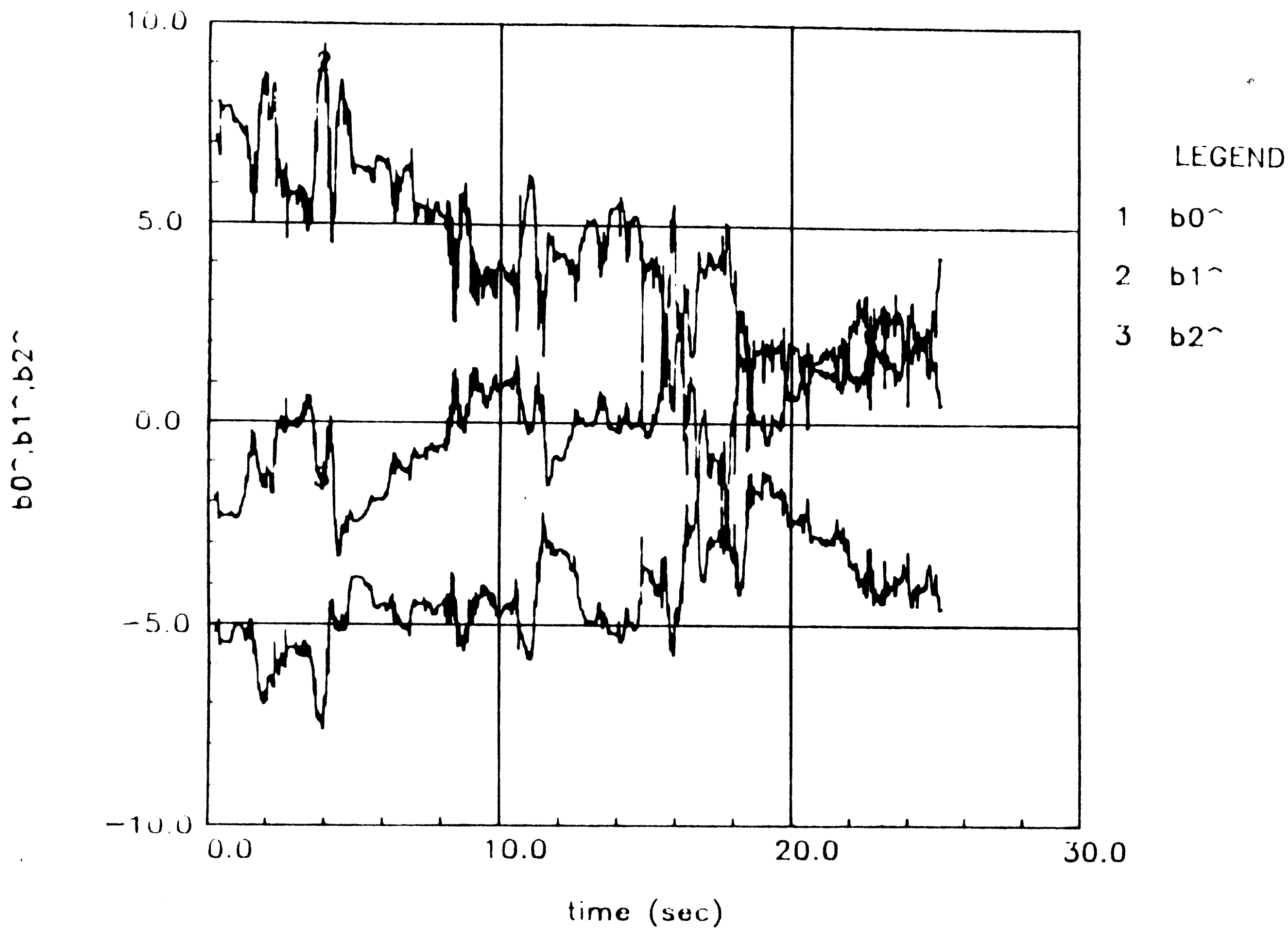

Figure 46. Estimated Parameters in B(z) for Case III Using (2, 2, 0, 0) ARMA Model With $\lambda = 0.995$

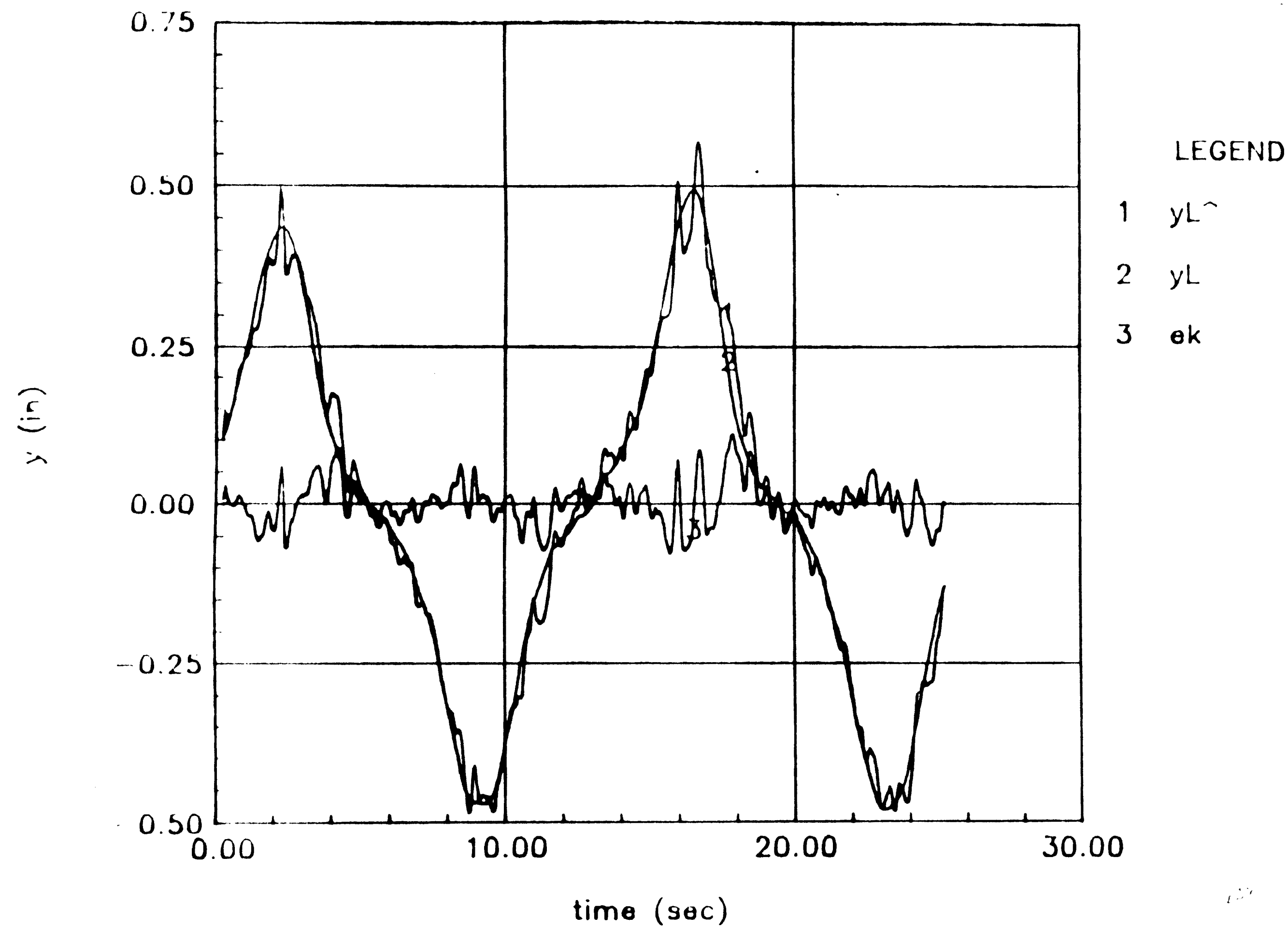

Figure 47. Estimated (yL^), Smoothed (yL) Responses and Residual (ek) for Case III Using (2, 2, 0, 0) ARMA Model With $\lambda = 0.995$

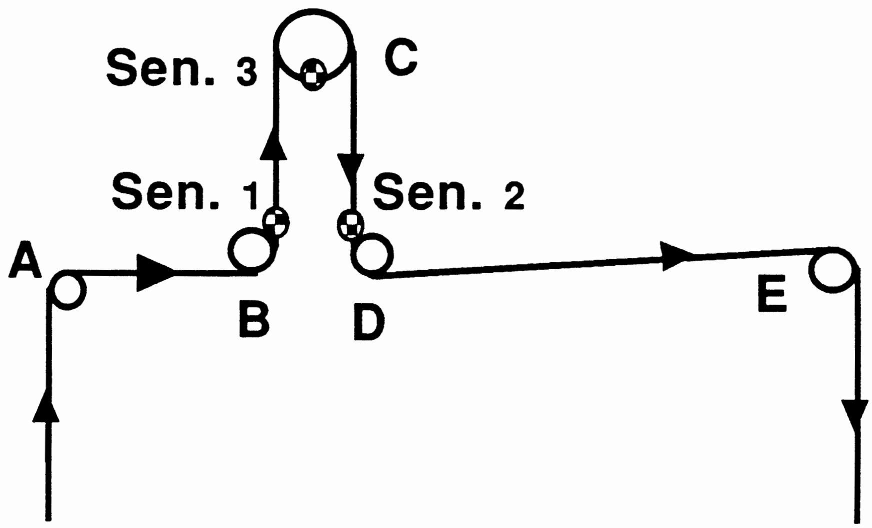

Figure 48. Schematic of Test Layout for the Amplitude Factor Study

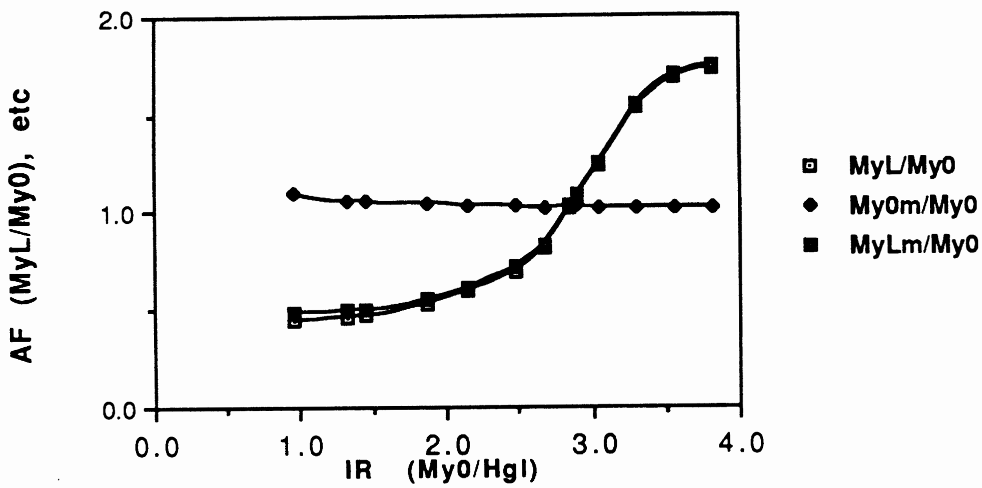

Figure 49. 3 Ratios as a Function of Input Ratio ($\omega^* = 0.6065$ rad, $Q = 3.446$ ft^3/s, L/W = 17.0, T = 4.60 lbf)

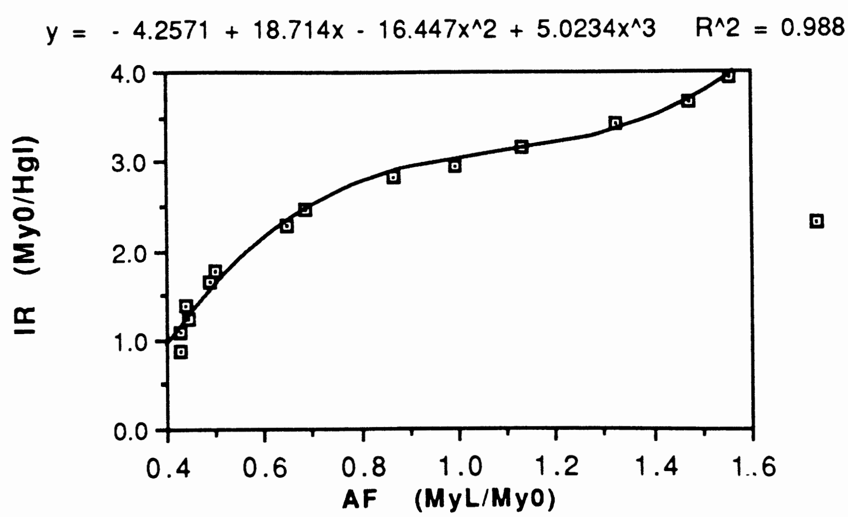

Figure 50. Input Ratio as a Function of AF ($\omega^* = 0.9576$ rad, $Q = 3.446$ ft^3/s, L/W = 17.0, T = 4.60 lbf)

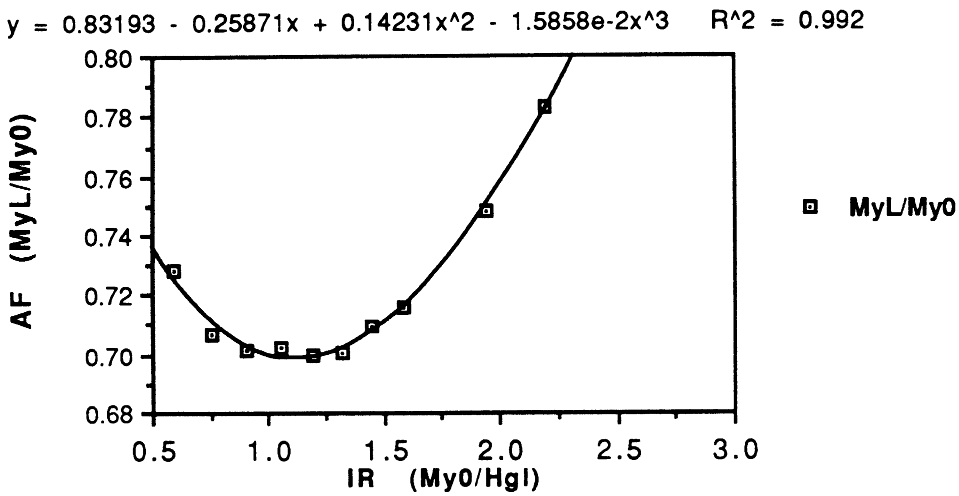

Figure 51. AF as a Function of Input Ratio ($\omega^* = 0.9576$ rad, $Q = 2.694$ ft^3/s, L/W = 12.3, T = 4.60 lbf)

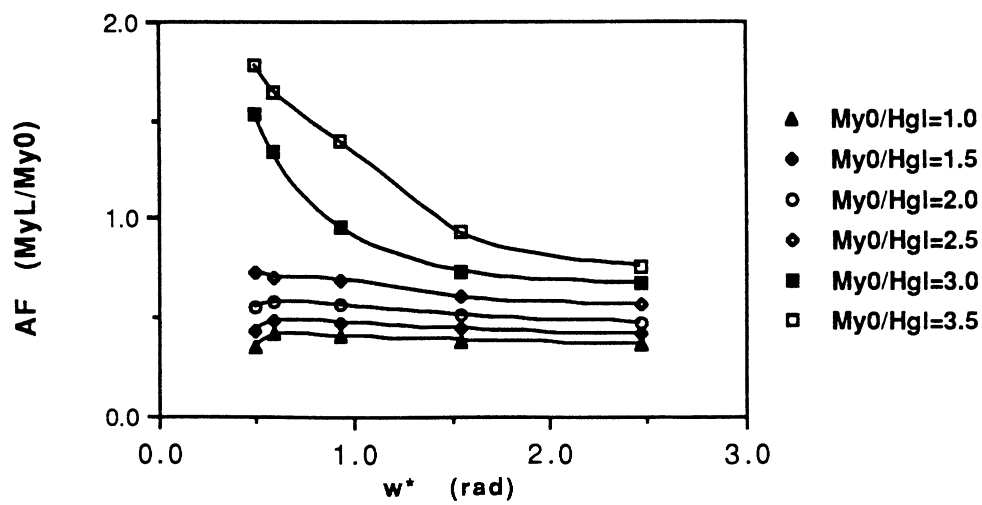

Figure 52. Frequency Response of AF ($Q = 3.446$ ft^3/s, L/W = 17.0, T = 4.60 lbf)

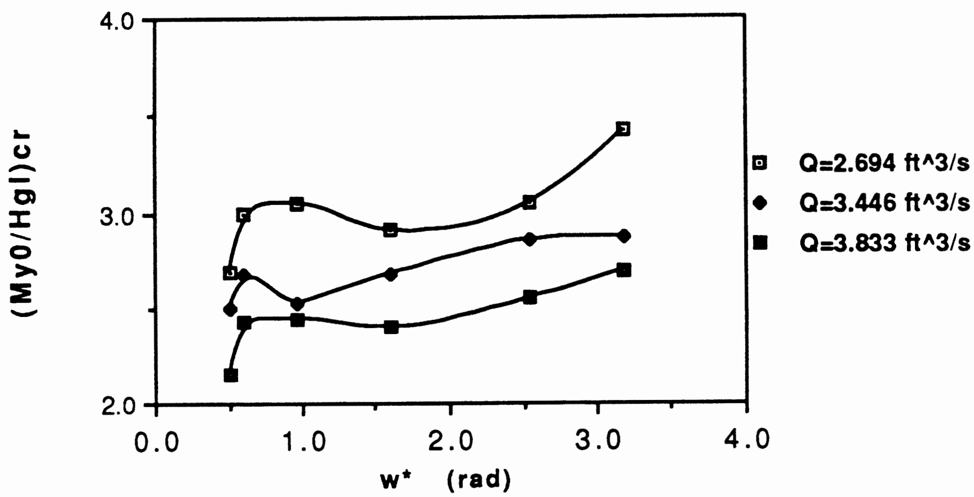

Figure 53. Frequency Response of Critical Input Ratio
(L/W = 17.0, T = 1.15 lbf)

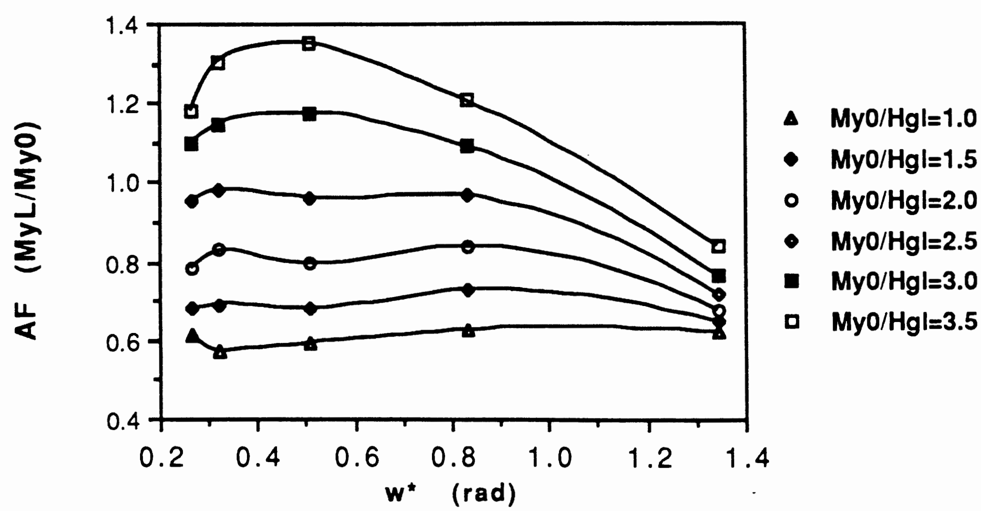

Figure 54. Frequency Response of Amplitude Factor
(Q = 3.833 ft^3/s, L/W = 12.3, T = 4.60 lbf)

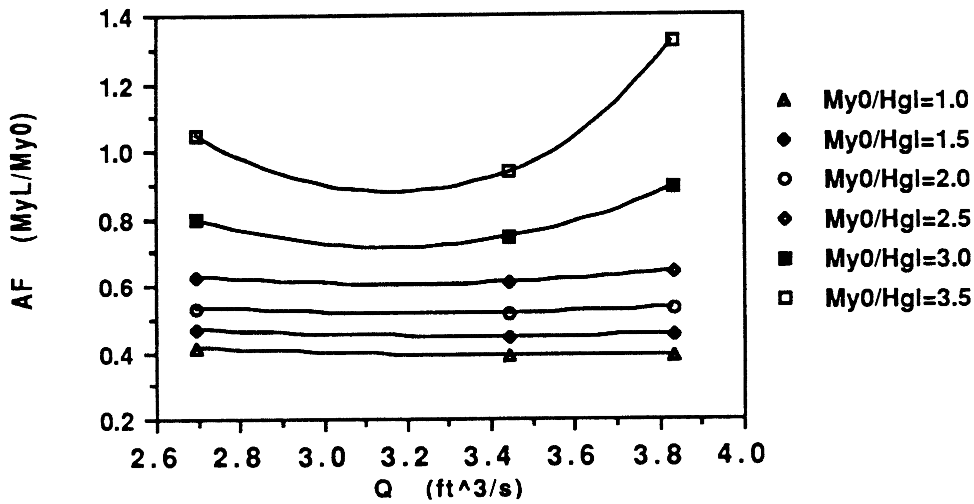

Figure 55. Amplitude Factor as a Function of Air Flow Rate
(ω^* = 1.5959 rad, L/W = 17.0, T = 4.60 lbf)

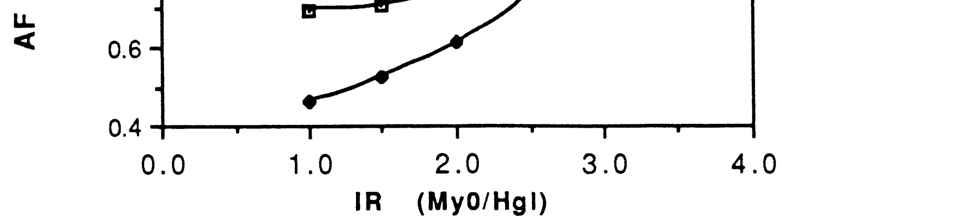

Figure 56. Amplitude Factor as a Function of Input Ratio
(ω^* = 0.9576 rad, Q = 2.694 ft^3/s, T = 4.60 lbf)

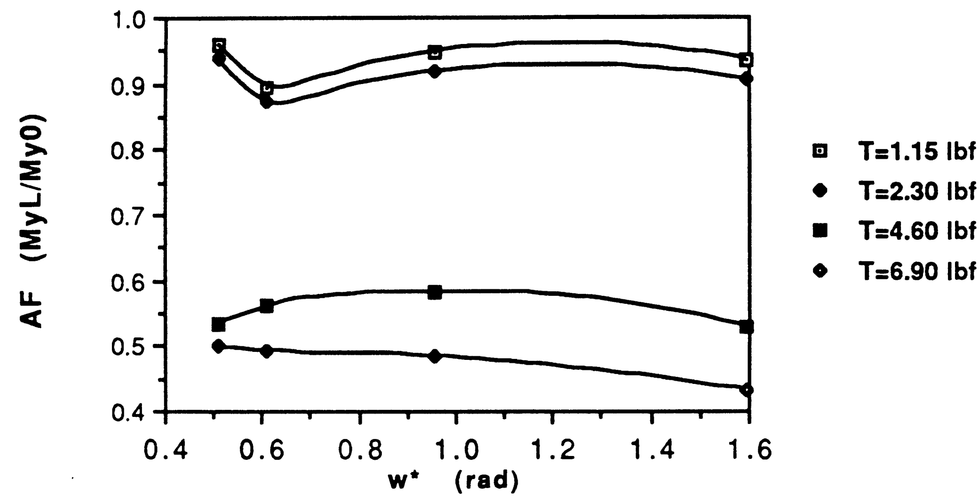

Figure 57. Frequency Response of Amplitude Factor
(M_{y_0}/H_{gl} = 2.0, Q = 3.833 ft^3/s, L/W = 17.0)

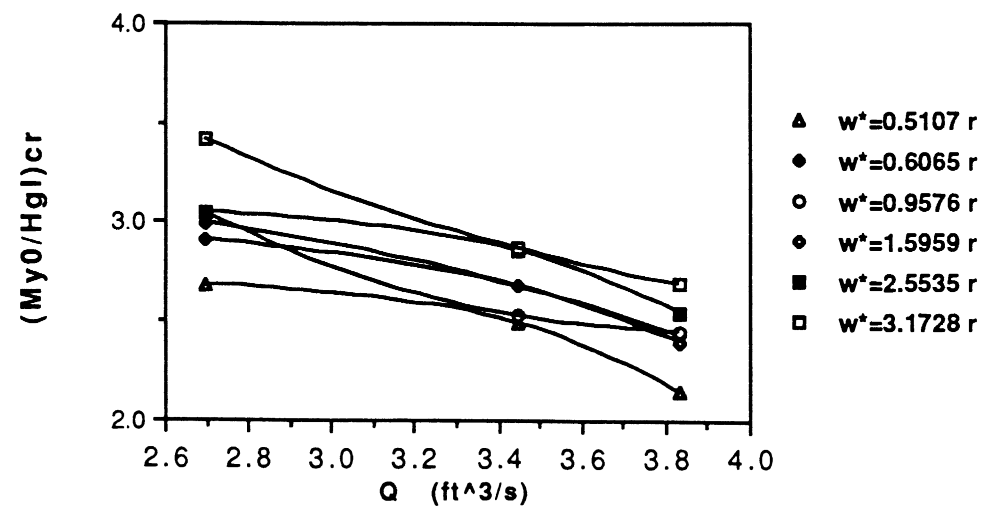

Figure 58. Critical Input Ratio as a Function of Air Flow Rate
(L/W =17.0, T = 1.15 lbf)

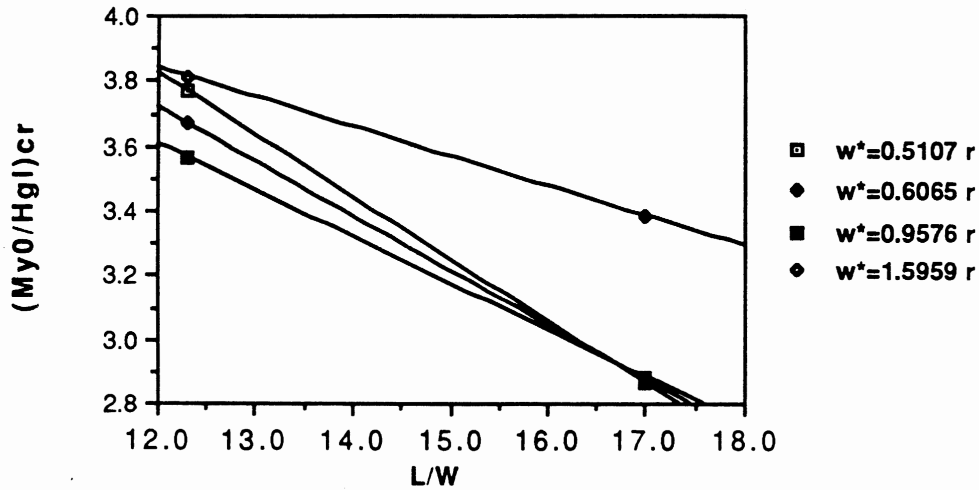

Figure 59. Critical Input Ratio as a Function of Length to Width Ratio
($Q = 2.694\ ft^3/s$, $T = 4.60$ lbf)

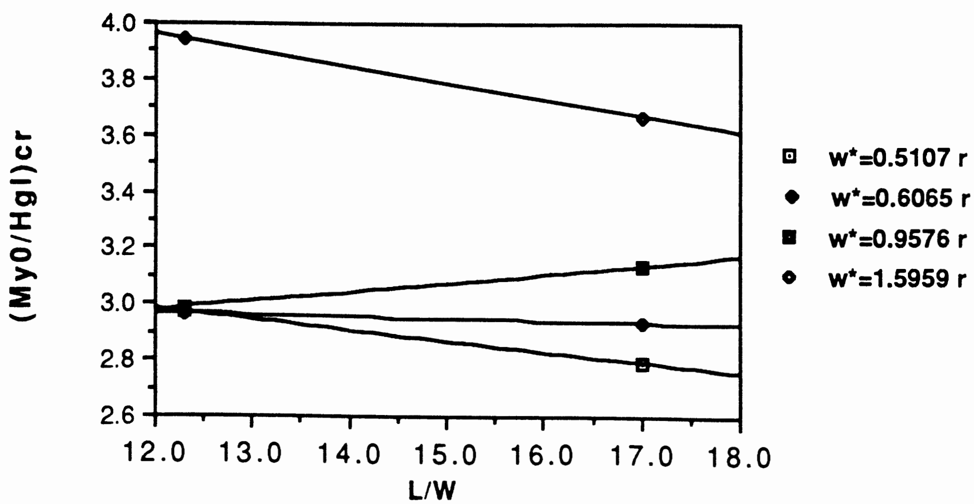

Figure 60. Critical Input Ratio as a Function of Length to Width Ratio
($Q = 3.446\ ft^3/s$, $T = 4.60$ lbf)

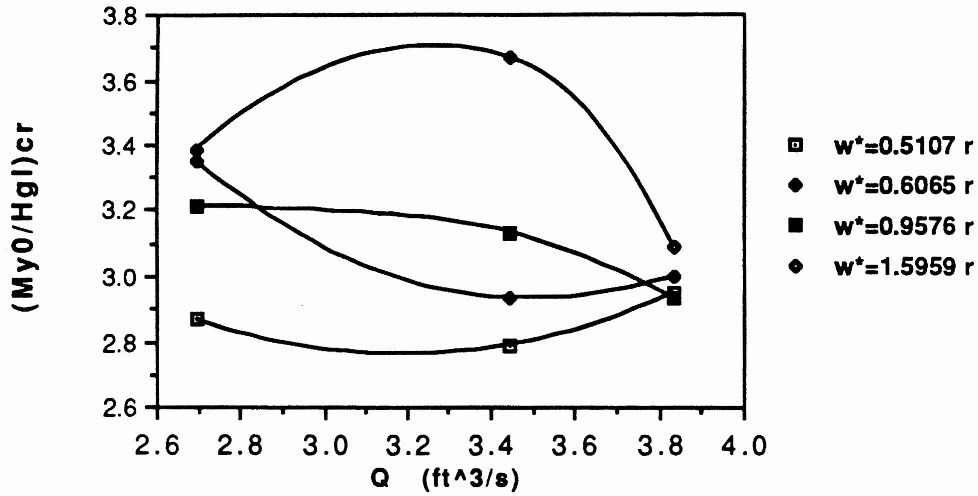

Figure 61. Critical Input Ratio as a Function of Air Flow Rate
(L/W = 17.0, T = 4.60 lbf)

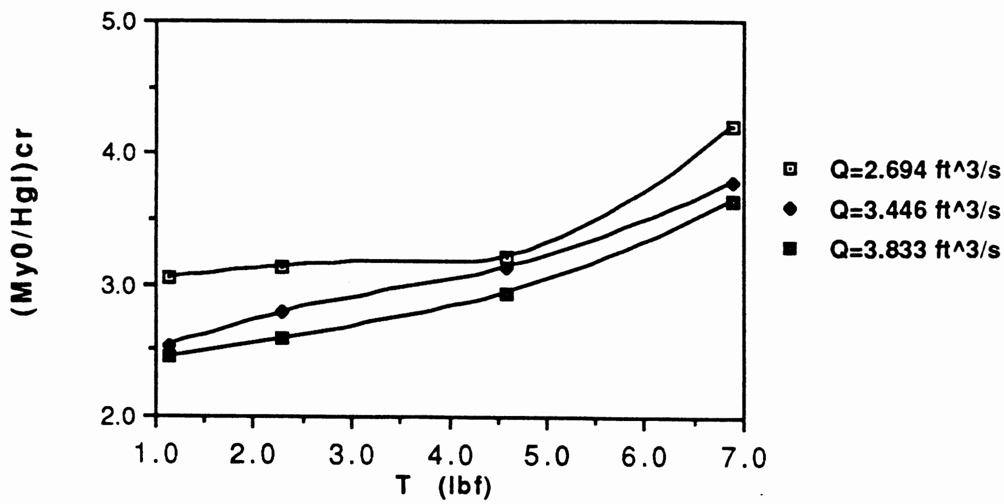

Figure 62. Critical Input Ratio as a Function of Air Flow Rate
(ω* = 0.9576 rad, L/W = 17.0)

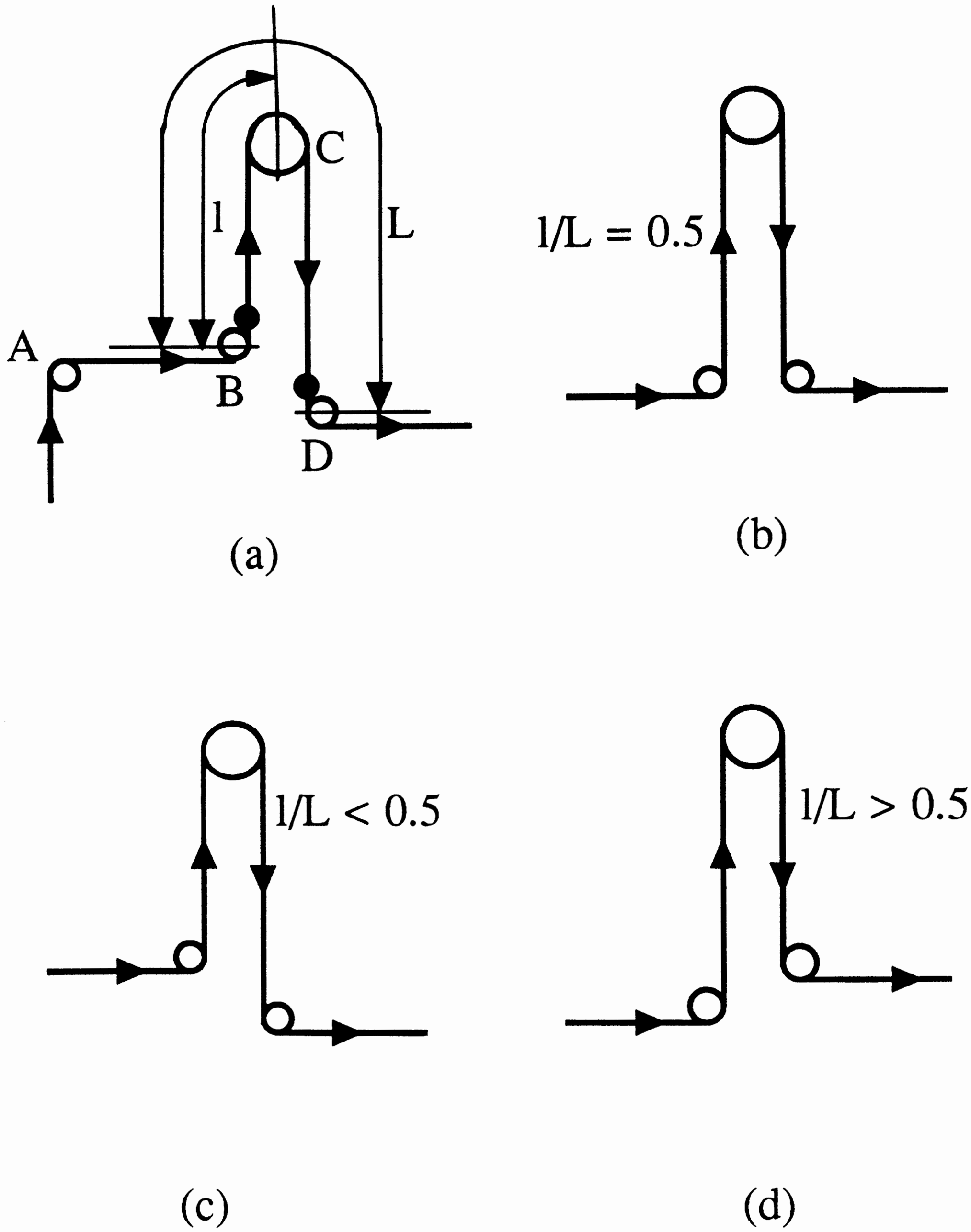

Figure 63 (a, b, c, d). System Configurations for Different Tests

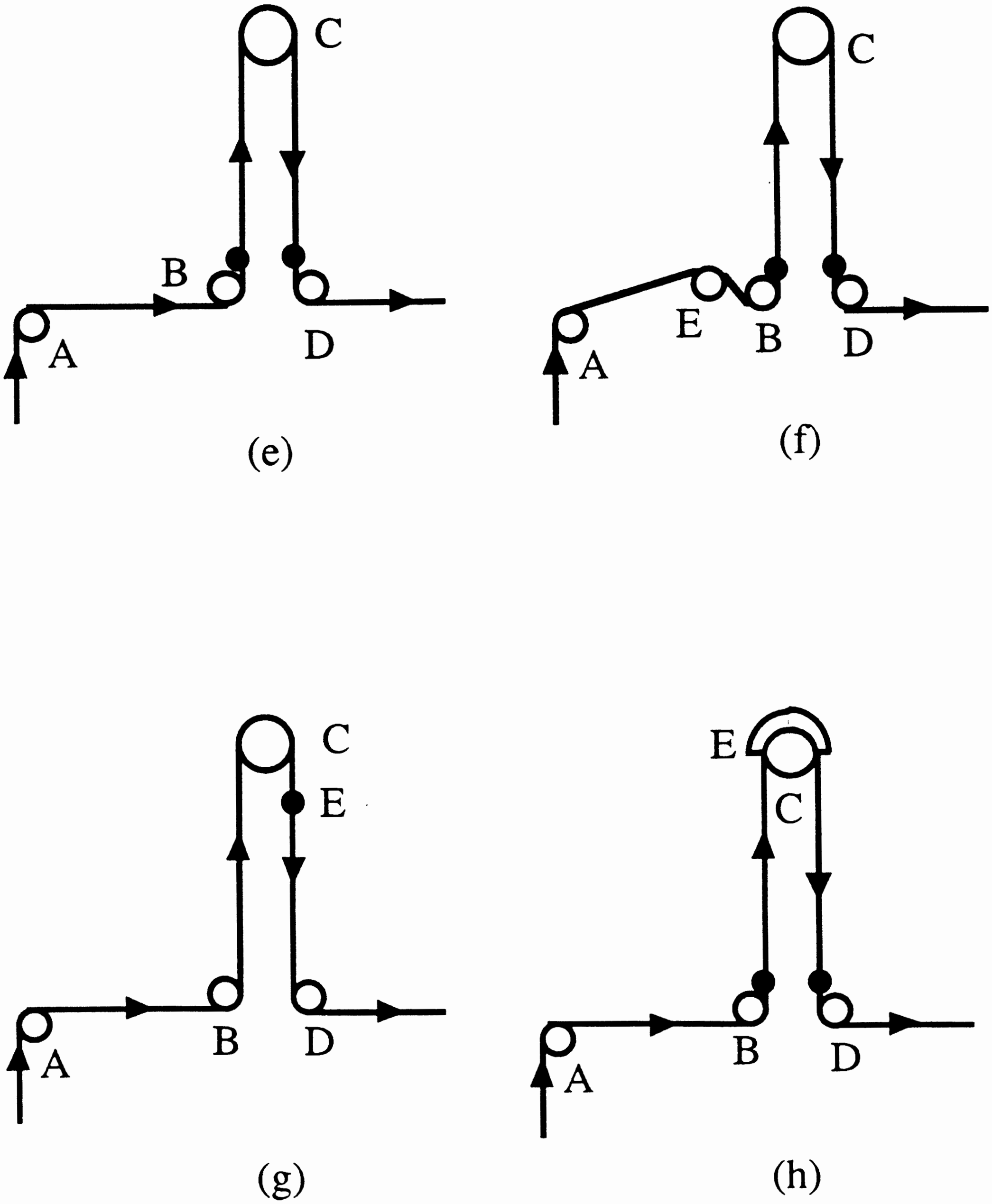

Figure 63 (e, f, g, h). System Configurations for Different Tests

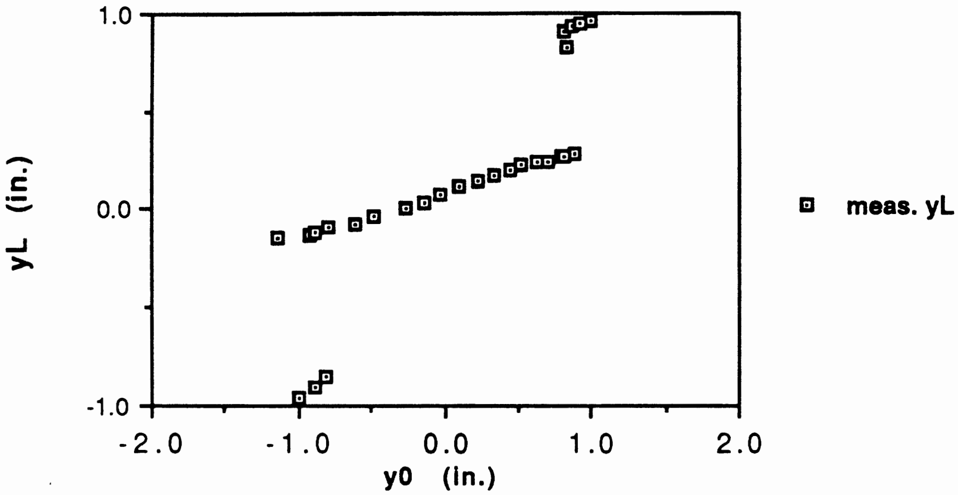

Figure 64. Static Test for the Response at the Downstream End
(L/W=102.0, T = 0.575 lbf, H_{gl}=0.5 in., l/L=0.5)

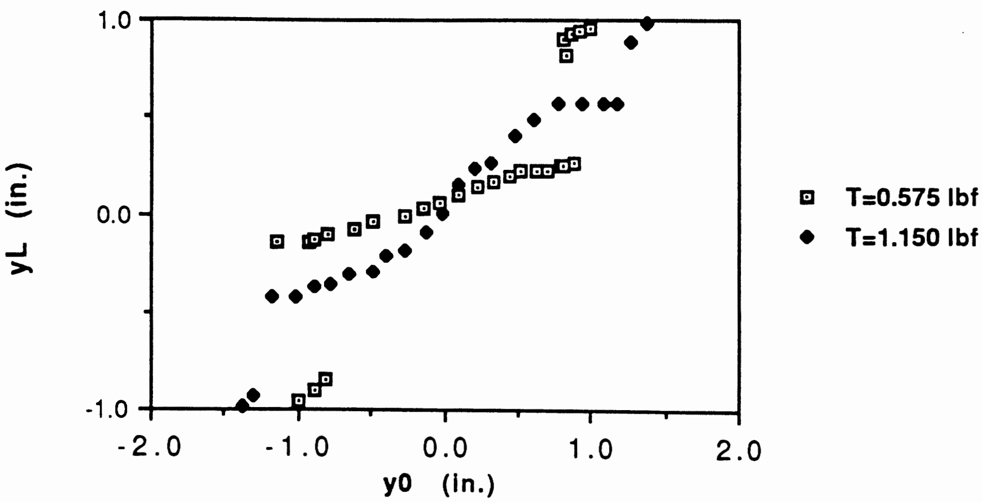

Figure 65. Comparison Between Two Static Responses in y_L
(L/W = 102.0, H_{gl}=0.5 in., l/L=0.5)

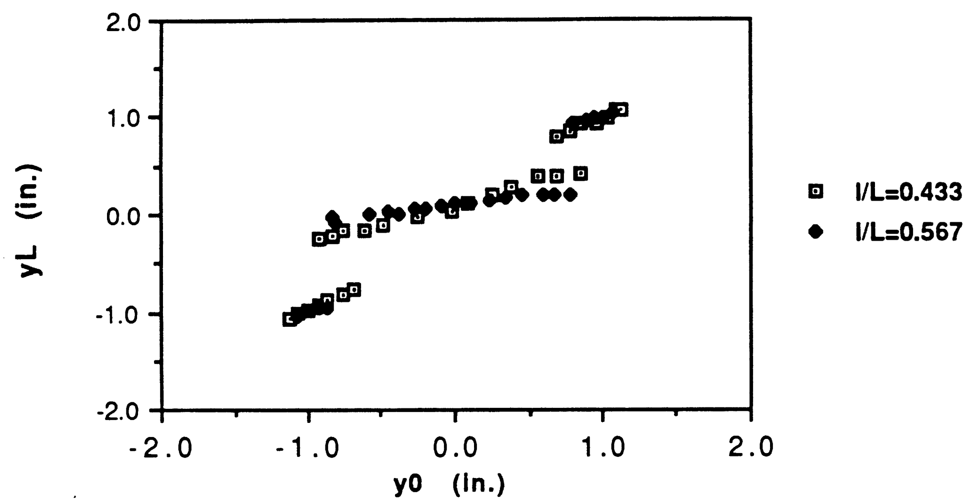

Figure 66. Comparison Between Two Static Responses in y_L With Different l/L (L/W=90.0, T = 0.575 lbf, H_{gl}=0.5)

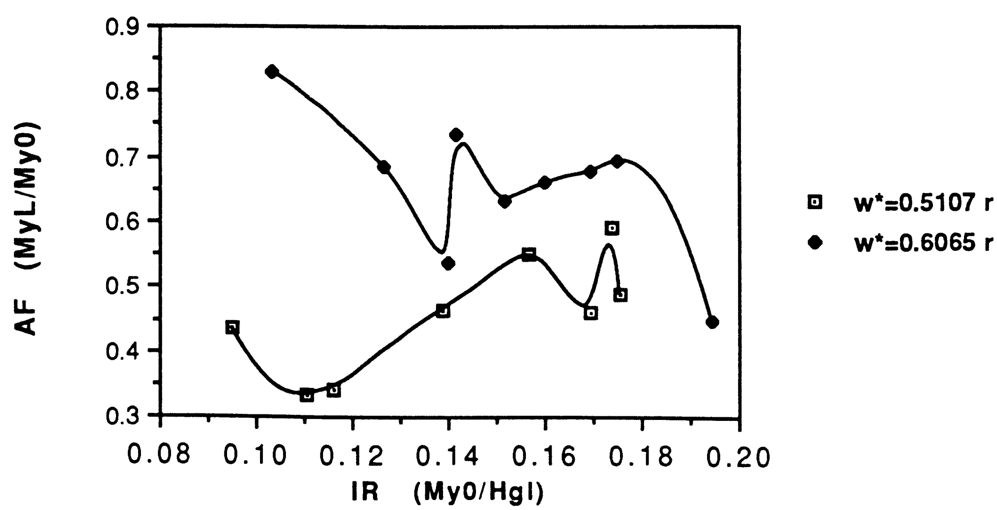

Figure 67. Comparison of AF With Different Frequencies (L/W = 102.0, T=1.150 lbf, H_{gl}=0.5 in., l/L=0.5)

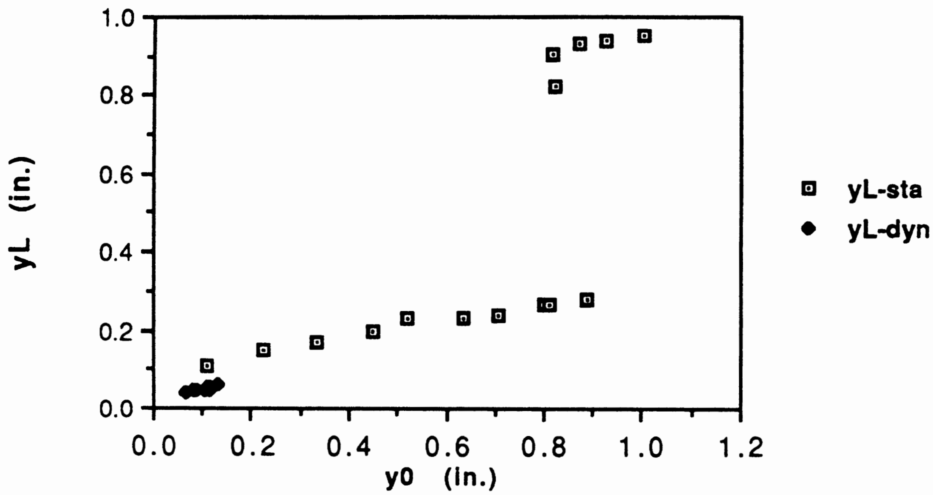

Figure 68. Comparison Between Static and Dynamic Responses in y_L (L/W=102.0, T = 0.575 lbf, ω*=0.5107 rad, H_{gl}=0.5, l/L=0.5)

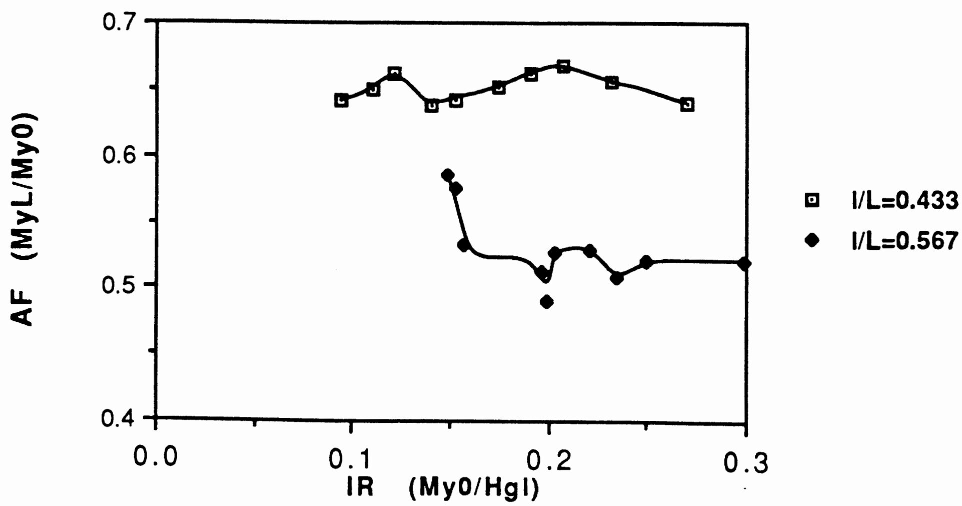

Figure 69. Comparison of AF With Different l/L (ω*=0.5107 rad, L/W=90.0, T=0.575 lbf, H_{gl}=0.5 in.)

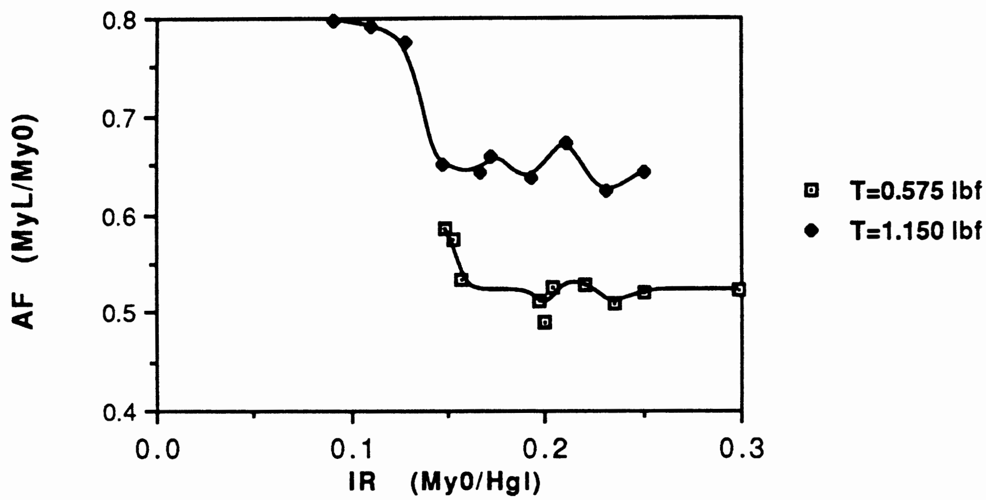

Figure 70. Comparison of AF With Different Tensions (ω^*=0.5107 rad, L/W=90.0, H_{gl}=0.5, l/L=0.567)

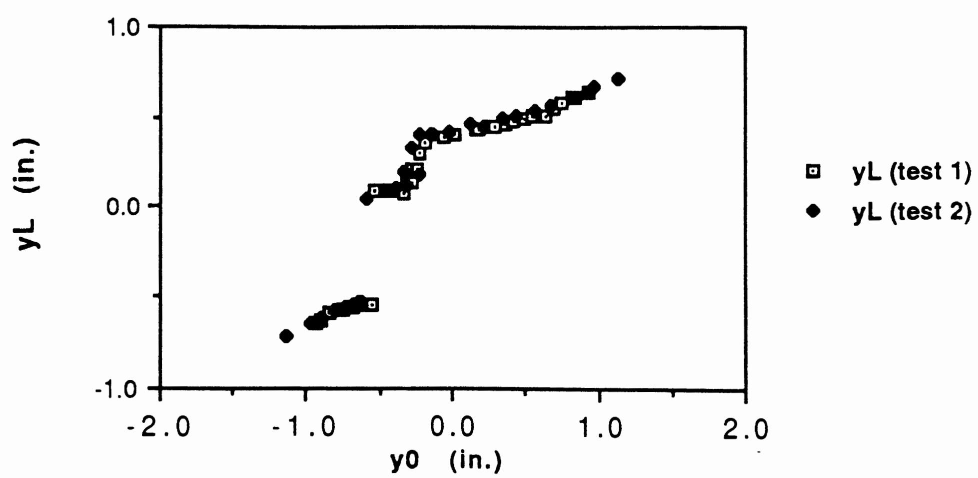

Figure 71. Comparison for 2 Measurements in Lateral Web Displacement at the Downstream End Under the Same Condition (L/W=102.0, T=0.575 lbf, H_{gl}=0.125 in., l/L=0.5)

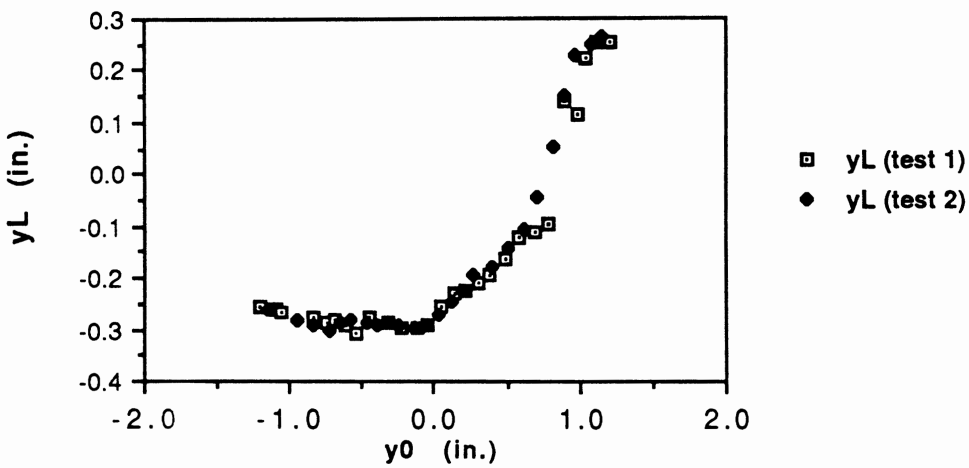

Figure 72. Comparison for 2 Measurements in Lateral Web Displacement at the Downstream End Under the Same Condition (L/W=102.0, T=1.150 lbf, H_{gl}=0.125 in., l/L=0.5)

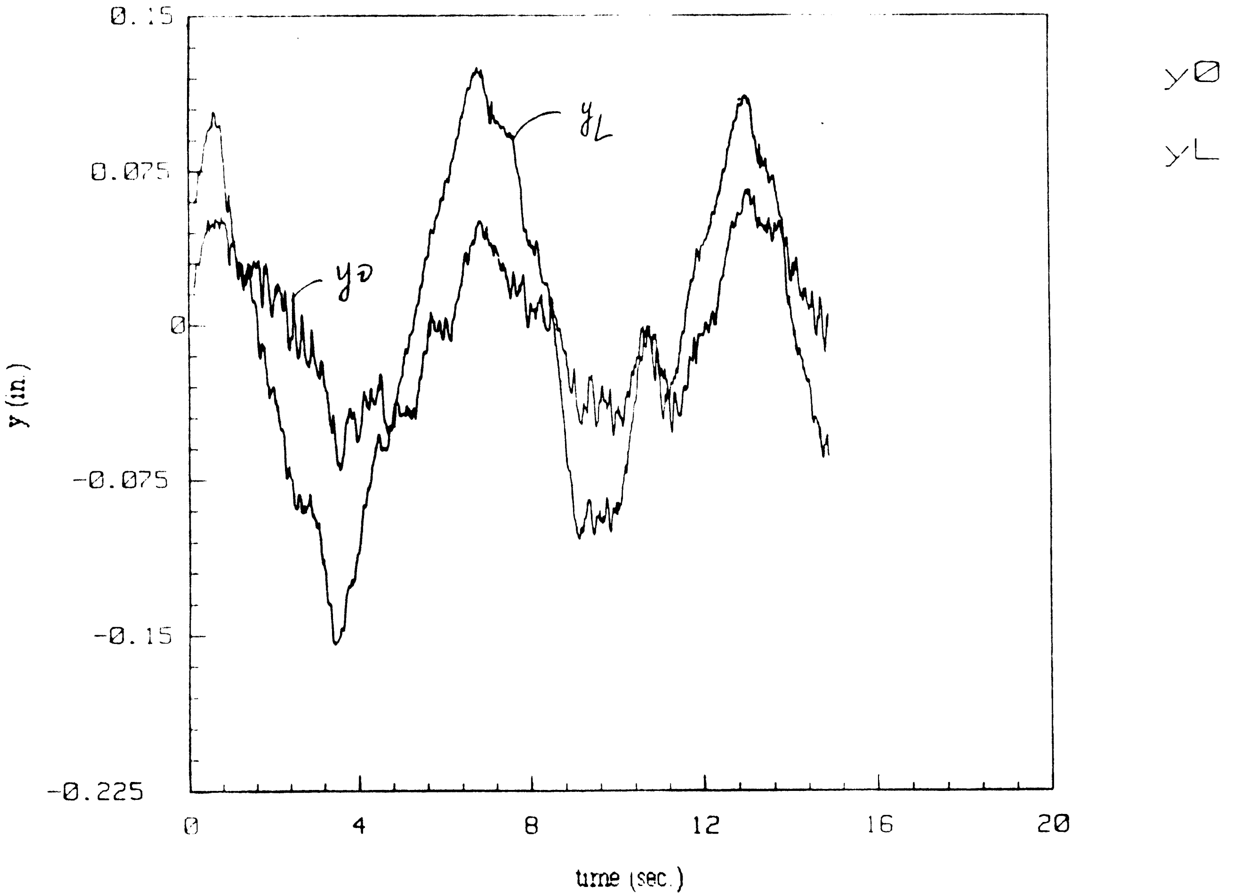

Figure 73. Lateral Web Displacements at Up- and Downstream Ends in a Limit Cycle (L/W=102.0, T=0.575 lbf, V=295.5 ft./min., H_{gl}=0.125 in., l/L=0.5)

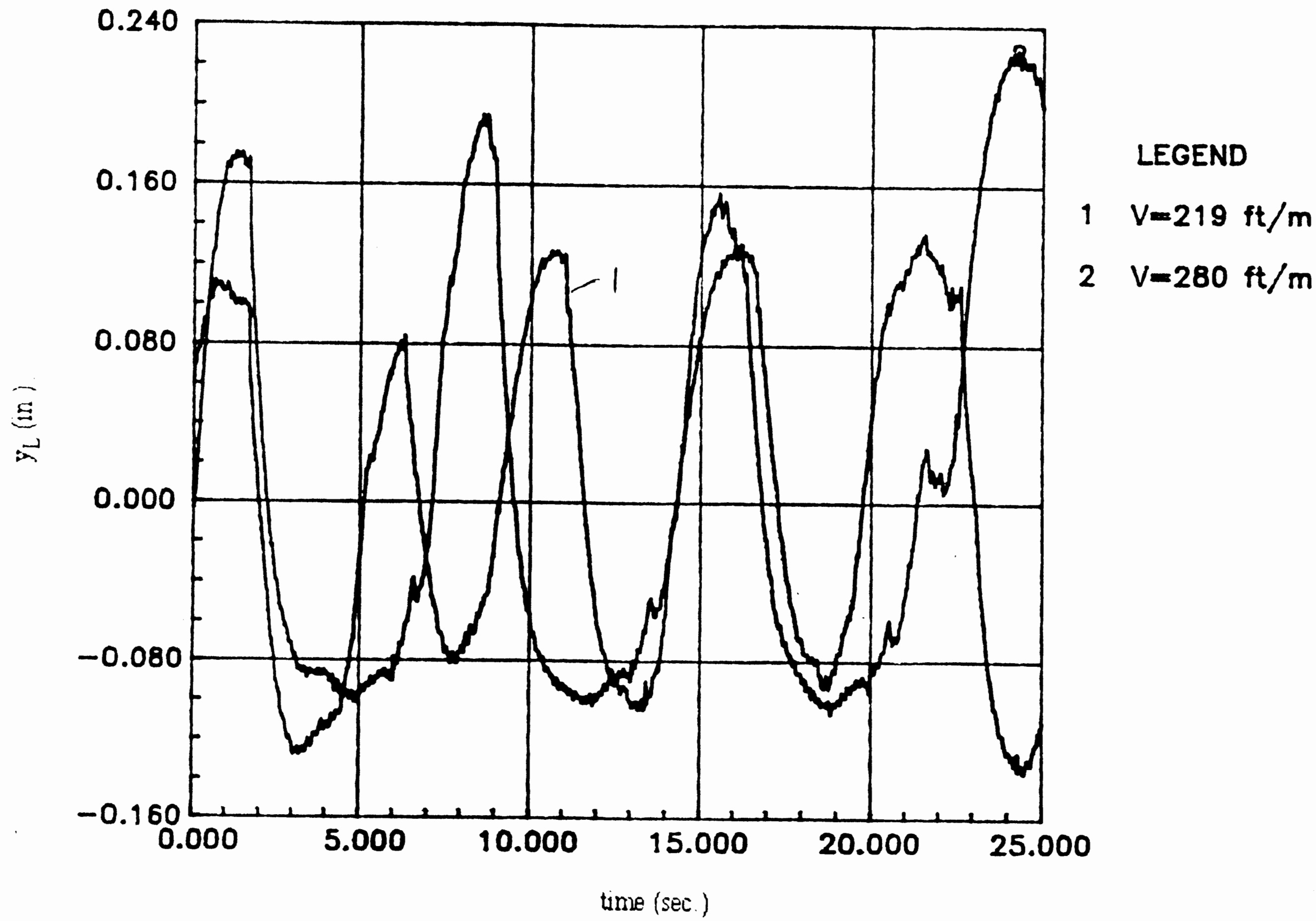

Figure 74. Comparison in y_L of Limit Cycles With Different Web Speeds
(L/W=96.0, T=0.431 lbf, V_o=30.0 deg., H_{gl}=0.125 in., l/L=0.469)

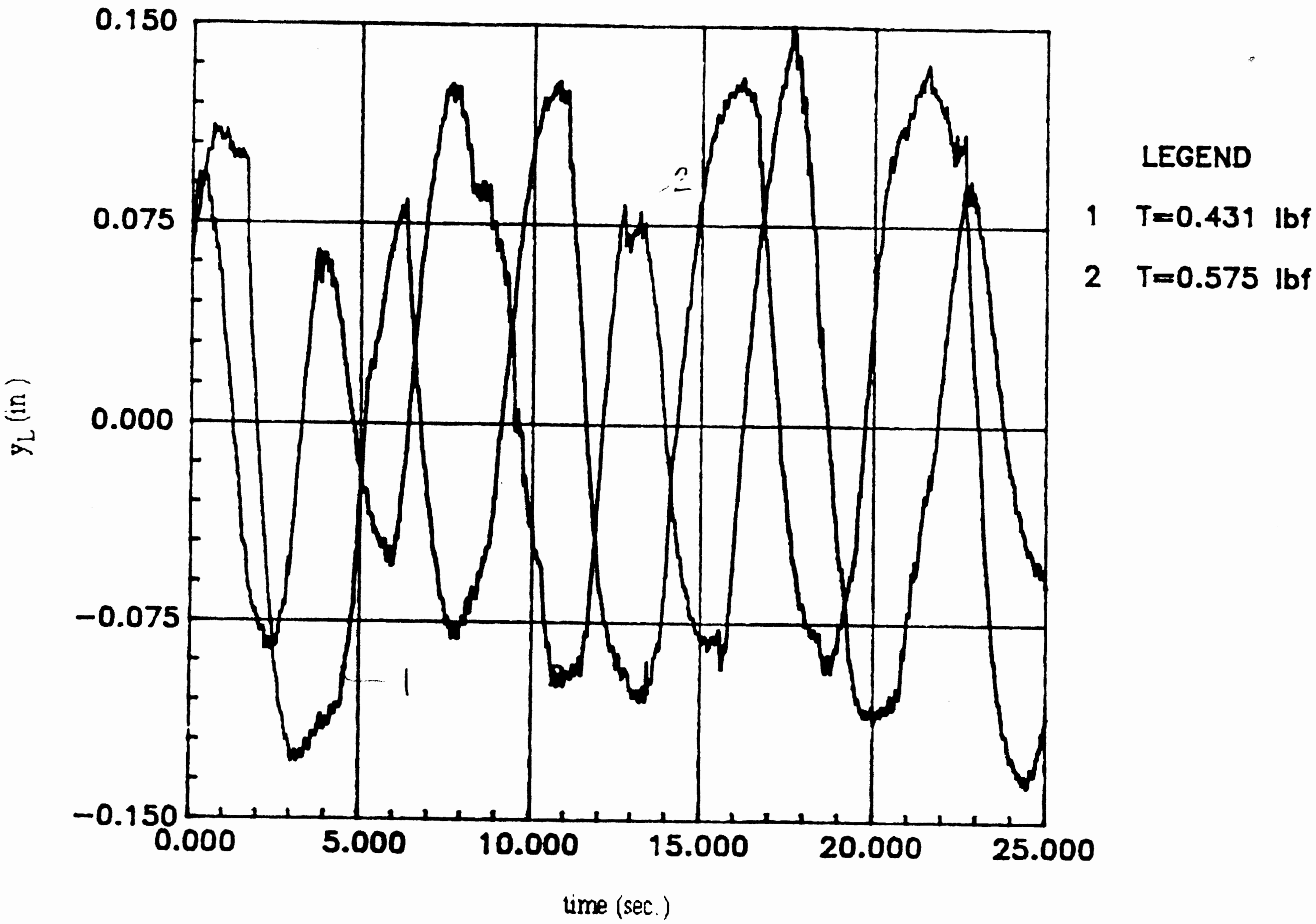

Figure 75. Comparison in y_L of Limit Cycles With Different Web Tensions (L/W=96.0, V=218.5 ft./min., V_0=30.0 deg., H_{gl}=0.125 in., l/L=0.469)

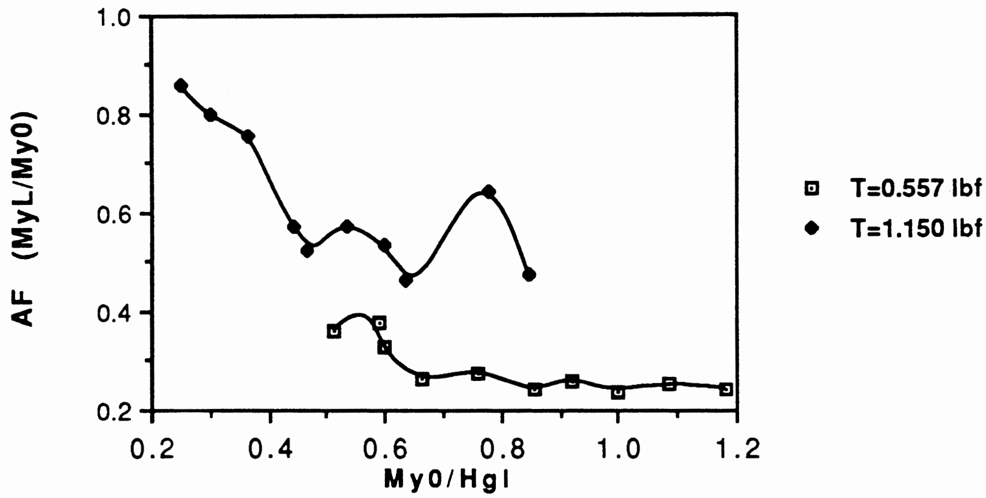

Figure 76. Comparison of AF With Different Web Tensions
(ω^*=0.5107 rad, L/W=102.0, H_{gl}=0.125 in., l/L=0.5)

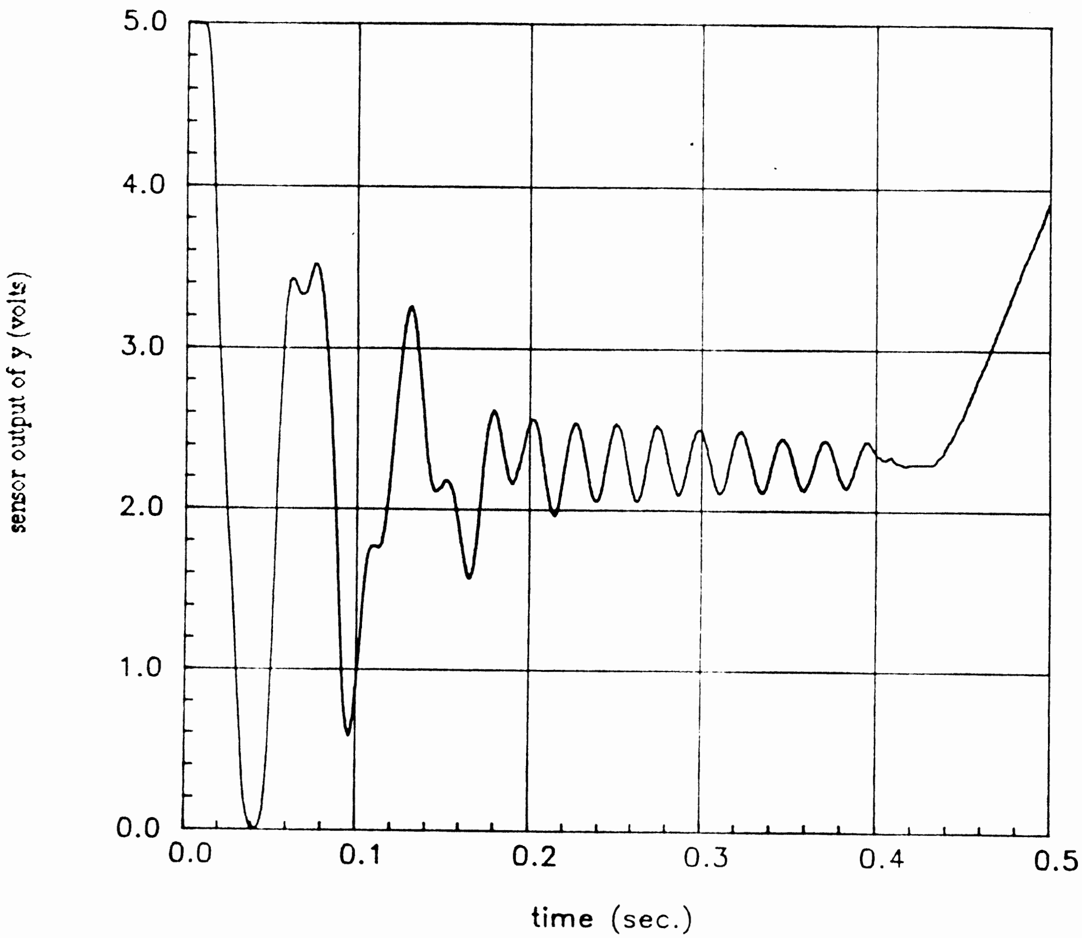

Figure 77. Sensor Output of Lateral Web Oscillation From Frequency Test (L/W=102.0, T=0.1438 lbf, H_{gl}=0.5 in., l/L=0.5)

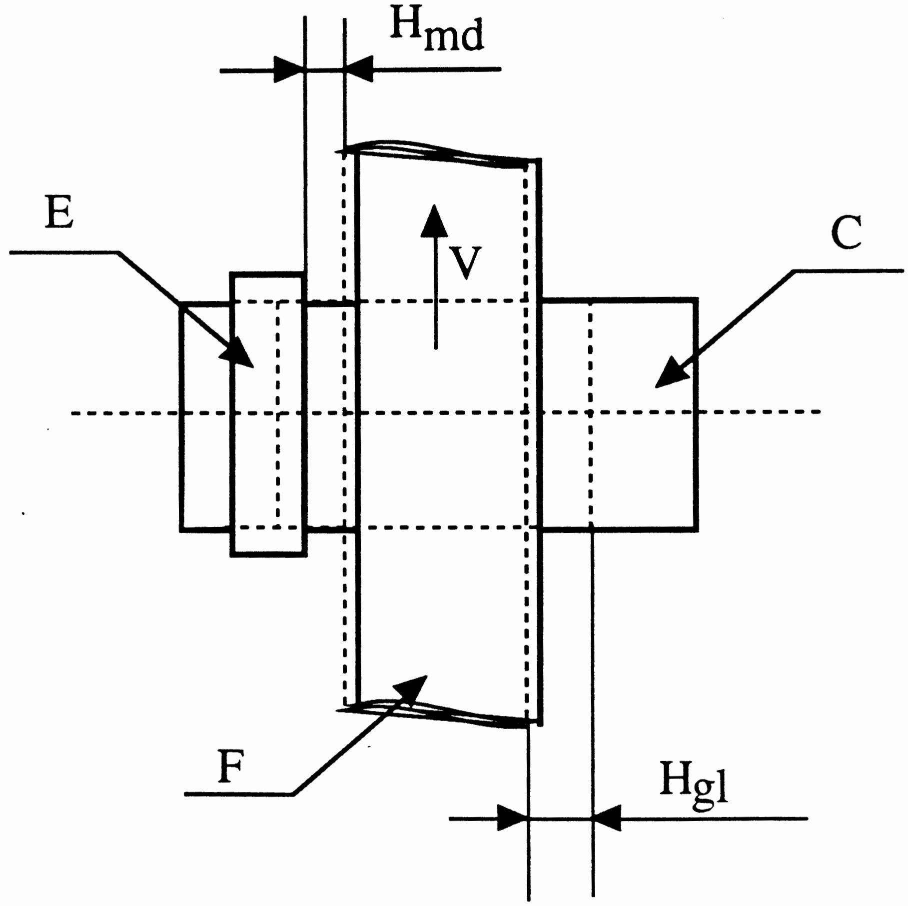

Figure 78. Schematic of Moving Dam Test

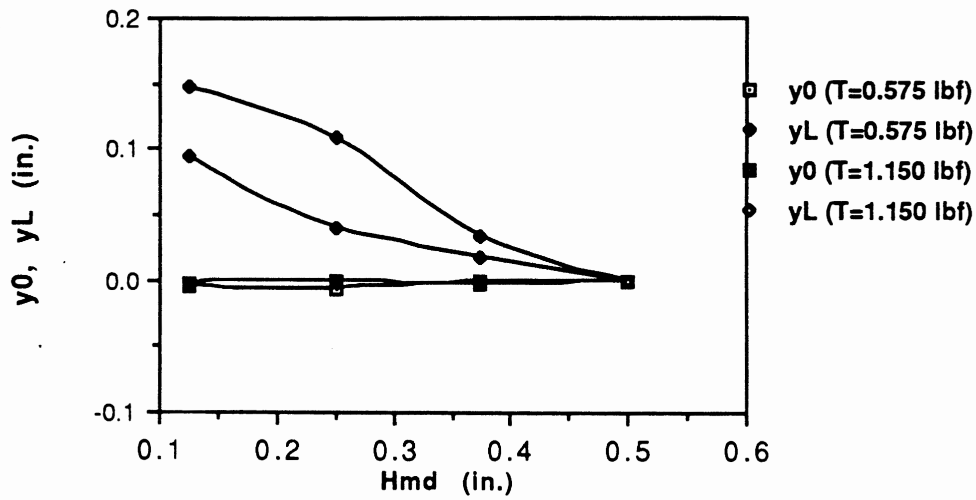

Figure 79. Comparison of Moving Dam Effect With Two Different Tensions
(L/W=102.0, H_{gl}=0.5 in., l/L=0.5)

CHAPTER VI

SUMMARY AND CONCLUSIONS

The subject of this investigation is the lateral web behavior in interactive web systems. Three types of interactive web systems have been categorized in carrying out this research project. The type I interactive system involves insufficient friction at the entering roller corresponding to a large steering effect from a guide roller. The analyses of both statics and dynamics of this type of interactive systems and the experimental verification have been reported earlier [12, 13]. No detailed description of this problem has been given in this thesis.

The analysis of the statics of the type II interactive system is the topic in Chapter II. The web systems of such a type involve considerable side loads on a moving web span causing the interaction in lateral shear and moment between adjacent portions of web span. The fundamental theory of lateral web motion for a single web span established by Shelton [1] has been extended to include the side load effect. A detailed procedure has been given in constructing the governing equations and deriving the coefficients involved in those equations in terms of the boundary conditions and the side loads on the web span.

The concept of the curvature factor has been extended to include the side load effect. There are three curvature factors due to the steering, the lateral force, and the lateral moment. By using these curvature factors, the effect on lateral web displacement due to the steering, the lateral force, and the lateral moment have been investigated separately as a function of the web parameter KL and the disturbance location l. The attention has been focused on the lateral web displacement at the locations of both the downstream end and the disturbance source.

The web mass is negligible in most web handling problems as far as the lateral web dynamics is concerned, which is the topic in Chapter III. The analysis on statics provides the fundamental web mechanics required in the dynamic analysis due to the negligible web mass effect. Considering the lateral web displacement as the only system response, a multiple-input-single-output system has been formed. There are four transfer functions considering the effect of each individual input. The frequency responses have been obtained using those transfer functions. There are two side load disturbance related inputs. Before the analysis on the response from the effect of combined inputs can be done, the modeling task on those terms must be carried out first, which is often difficult to accomplish.

The combination of both type I and type II interactive systems yields a type III interactive system. The statics on lateral web displacement of this complicated system is investigated in Chapter IV. The starting point on the analysis is to combine the statics for both the type I and type II interactive systems. Each interaction mode has been identified, its boundary conditions established, and subsequently the analysis carried out. By performing the analysis on the web system including all possible interaction modes the conditions for mode determination have been established. In regard to the limitation of the fundamental theory, the taut edge conditions have also been determined. Due to the complexity of the system analysis, no detailed derivation has been given. However all the relevant results have been listed. If one is interested in doing dynamic analysis on this type of system, this static analysis has provided a basic procedure on web mechanics needed in the dynamic analysis.

To circumvent the difficulty of modeling side loads on a web span due to an air-bar, the web system involving an air-bar unit has been experimentally investigated. This special web system is one of the type II interactive systems with an air-bar providing lateral loads. In Chapter V, the experimental study has been reported with the design consideration of air-bar systems included. In the parameter identification, it has been found that when there is no amplification of lateral web oscillation at the downstream end, the ARMA model structure is applicable. It is not applicable, however, if there is amplification. A unified approach to investigate the web system for both running states of with and without amplification is to use the concept of amplitude factor. Five important experimental parameters have been used to see the effect on the amplitude factor. Through the study , the amplification free condition is established using the concept of critical input ratio, which is a function of other four experimental parameters. The design considerations are provided based on the effect of experimental parameters on the amplitude factor. Some guidelines are given to keep the web systems involving air-bar units from going unstable in lateral web motion.

More understanding on the lateral dynamics has been gained through a variety of tests using a narrow web. The static test has proved that it is the transient air flow action that causes the amplification in lateral web oscillation when large lateral load disturbances are involved. The dynamic test has verified the results from the study with a wide web. The moving dam test has shown the recentering effect of the air-drum and dam combination. The negligibility of web mass effect on the lateral web dynamics has been further proved using the frequency test. With a narrow gap, the test system became a type III interactive system due to the moment transfer at the upstream roller. The limit cycle in lateral oscillation was found in such a system. Many ways have been found to eliminate the limit cycle.

Significant Contributions

In the theoretical analysis, the fundamental theory for lateral web motion has been extended to include considerable side loads on a moving web span. This work enables web handling researchers to analyze the lateral web motion of web systems involving a variety of web handling devices, which are capable of providing side loads on the web span. The requirement for disturbance related terms should also motivate web handling researchers to do more fundamental modeling on those process devices used in web handling.

The experimental study indicates that the model structure describing the lateral web motion are dramatically different for different running states. The investigation of the amplitude factor reveals that the input ratio can be used to specify the amplification free condition, which is a function of system and disturbance parameters. The guidelines in design consideration are based on the critical input ratio. The procedure developed in this study is applicable for investigation of lateral web motion with lateral loads provided by other types of process devices.

The application of a series of air-bar units with the same characteristics has been used in industry. If the web system is in the running state with amplification, the lateral web oscillation will be unstable at the downstream end. The system parameters thus must be adjusted so that the lateral stability is assured. When the web system is in the running state without amplification, the damping effect of air-bar units on lateral web displacement disturbances improves the controllability in lateral web position at the downstream end.

It is important to know that the lateral web motion in a web system with air-bar units has the same model structure as the one in the web system with contact handling. A similar control strategy as suggested by Young, Shelton, and Kardamilas [6] may be used to keep the web span at its desired lateral position. The parameters in the model not only involve uncertainty but also are dependent upon the web system and lateral load disturbances. Thus parameter estimation is an essential part of the control algorithm. The adaptive control is a good candidate for performing such a control task. Precautions must be taken in designing the controller to prevent the potential instability in lateral web motion.

In the running state with amplification, the transient air flow significantly affects the lateral web oscillation. Thus an adequate model for the air flotation system must include the effect of both the air dynamics at the air-drum and elastic web behavior. It is possible to use moving dams guiding the passing web at the location of the air-drum with a low web tension. It is less effective with a high tension, though, plus there may be an edge damage problem. The limit cycle in lateral web oscillation may exist for a type III interactive system. In the test system, the limit cycle was very sensitive to the system parameters. A variety of ways have been found by which the limit cycle can be eliminated if it does occur.

Suggestions for Further Research

In the theoretical analysis, the fundamental theory assumes that a web span can be adequately modeled as a Bernoulli-Euler beam. The shearing effect on lateral web motion is neglected through such an approach, which is appropriate for long web spans. When the shearing effect is significant, a web span should be modeled as a Timoshenko beam. Following the same procedure used in this thesis, this work can be readily carried out if there is an interest.

Similar to the dynamic analysis for the type I interactive system [13], the analysis on dynamics of the interactive systems of type III will need non-closed form solutions. The numerical technique or the fourier series approximation will be necessary to obtain those solutions. Due to the complexity of the web system, a huge amount of work is expected in making a detailed dynamic analysis. The limit cycle in lateral web oscillation has been found in this type of interactive system during the experimental study. A more complete control on the limit cycle is possible only after the system dynamics has been better understood.

One assumption for the theoretical analysis is that the web is kept taut or without wrinkling during its oscillation. The range for the steering from the guide roller, the disturbances at the upstream end, and the possible load disturbances on the web span is limited by this condition. In order to extend the applicability of the theory, the analysis including the slack edge or the wrinkling must be carried out. A more complicated mathematical manipulation is expected.

More fundamental modeling work needs to be done for lateral loads on a moving web span from devices in the process line. The air flotation problem exists in many web systems. More research should be done in modeling an air-bar and other types of air flotation devices. For over three decades, the theoretical modeling on the air-flotation problems is mainly limited in the foil bearing area. Even with this oversimplified case, the boundary conditions for the two-dimensional model still have not been established for a laminar flow. More efforts on the theoretical modeling should be completed for the air flotation problems encountered in web handling. After this mission is accomplished, some breakthrough in the lateral web dynamics involving air flotation devices can be expected.

In the experimental study of the web system with an air-bar unit, more types of air-bar patterns can be tested. Based on the information from those tests, a better air-bar design in terms of the stability in lateral web oscillation may be experimentally obtained. More extensive tests can be done on the amplitude factor using more experimental parameters in their discretized values. This way more reliable guidelines for the web system design related to the air-bar application will be provided. Instead of only one, many air-bar units are often found to be used in series in the application. The experimentation should be extended to the multiple air-bar units, in which the air-bar units may have the same or different characteristics. The air flotation application is widely used in the drying process, in which the high temperature is involved. The experimentation may be needed to understand the lateral web dynamics with air flotation and under the influence of high temperature. This of course can be extended to the case with multiple air-bar units. There are other types of air flotation devices used in the industry. The experimentation work should be done on those devices too so that their effect on the lateral web behavior can be better understood.

The modeling through experimental study should be parallel to the work in theoretical modeling. The important parameters and the boundary conditions in the air flotation effect on the lateral web dynamics may have to be identified experimentally. Then the theoretical modeling can be carried out concentrating on those limited parameters. Significant efforts must be put through before a reasonable model adequately representing the air flotation device can be constructed.

This investigation has provided a solid ground for designing controllers for lateral web motion control for web systems involving air-bar units. In order to make the web system operate properly it must always be maintained in the running state without amplification. The model structure for the lateral web motion has been confirmed to be the same as the one in the contact web handling. Work should be done in designing the controller so that the proper procedures are established, on which the running state with amplification can be detected and consequently prevented.

A SELECTED BIBLIOGRAPHY

1. Shelton, J. J., 1968, "Lateral dynamics of a moving web", Ph. D. thesis, Oklahoma State University, Stillwater, Oklahoma.

2. Shelton, J. J., and Reid, K. N., 1971, "Lateral dynamics of an idealized moving web", ASME Journal of Dynamic Systems, Measurement, and Control, Vol. 93, No. 3, Sept., pp. 187-192.

3. Shelton, J. J., and Reid, K. N., 1971, "Lateral dynamics of a real moving web", ASME Journal of Dynamic Systems, Measurement, and Control, Vol. 93, No. 3, Sept., pp. 180-186.

4. Soong, Tsai-Chen, Li, Chun, 1979, "An elastic analysis of multiroll endless web systems", ASME Journal of Dynamic Systems, Measurement, and Control, Vol. 101, No. 4, Dec., pp. 308-313.

5. Sievers, L. A., Balas, M. J., and von Flotow, A. H., "Modeling of web roller interactions and lateral web dynamics", 1987 American Control Conference.

6. Young, G. E., Shelton, J. J., and Kardamilas, C. E., 1989, "Modeling and control of multiple web spans using state estimation", ASME Journal of Dynamic Systems, Measurement, and Control., Vol. 111, No. 3, Sept., pp. 505-510.

7. Block, A., and Van Rossum, J. J., "The foil bearing - a new departure in hydrodynamic lubrication", Lubrication Engineering, Vol. 9, No. 6, Dec. 1953, pp. 310-320.

8. Eshel, A., and Elrod, H. G., Jr., "The theory of the infinitely wide, perfectly flexible, self-acting foil bearing", Journal of Basic Engineering, Trans. ASME, Series D, Vol. 87, No. 4, Dec. 1965, pp. 831-836.

9. Wildmann, M., "Foil bearings -- their general behavior with particular emphasis on the externally pressurized bearing", Proceedings of the Elastohydrodynamic Lubrication Conference, University of Leeds, England, 1965, pp. 9-16.

10. Barlow, E. J., "Externally pressurized, axisymmetrical foil gas bearings",. Ampex Report, No. RR65-n, AS&IA No. AD 625-762, 1966.

11. Basheer, M., 1988, "An experimental study of air entrainment", M.S. thesis, Oklahoma State University, Stillwater, Oklahoma.

12. Young, G. E., Shelton, J. J., Fang, B., 1989, "Interaction of web spans: part I - Statics," ASME Journal of Dynamic Systems, Measurement, and Control., Vol. 111, No. 3, Sept., pp. 490-496.

13. Young, G. E., Shelton, J. J., Fang, B., 1989, "Interaction of web spans: part II - dynamics," ASME Journal of Dynamic Systems, Measurement, and Control., Vol. 111, No. 3, Sept., pp. 497-504.

14. Kay, S. M., 1983, "Recursive maximum likelihood estimation of autoregressive processes", IEEE Transactions of Acoustics, Speech, and Signal Processing, Vol. ASSP 31, No. 1, Feb, pp. 56-65.

15. Åström, K. J., Söderström, T., 1974, "Uniqueness of the maximum likelihood estimates of the parameters of an ARMA model", IEEE Transactions on Automatic Control, Vol. 19, No. 6, Dec., pp. 769-774.

16. Kardamilas, C. E., Young, G. E., "Stochastic modeling of lateral web dynamics", Proceedings of the 1990 American Control Conference, pp. 474-480.

17. Freudenthal, A. M., 1966, Introduction to the mechanics of solids, John Wiley & Sons.

APPENDIXES

APPENDIX A

THE COMPUTER CODE FOR THE MODE DETERMINATION

The FORTRAN program, moddq3.f, is used for the interaction mode determination, which has been described in detail in Chapter 3. The computer code for this program is listed bellow. One sample input data file for this program along with the output data file are given in Appendix B.

```
      program moddq3f
cc
cc *************************************************************
cc  moddq3.f, March, 1989, written by Bin Fang
cc  mode determination program for interactive web system with lateral
cc  loads on pre-entering span,  given KLb, La/Lb,la/La, Q1, Q2, Q4,
cc  and Q5, and Q3i < Q3 < Q3f, find the range of Q3 for corresponding
cc  possible modes
cc *************************************************************
cc
      implicit real*8 (a-h,o-z)
      dimension x(35),y(35,2),md(35)
      character*3 ac(5)
      common /c1/chkla,chklam1,shkla,/c2/chklb,chklbm1,shklb
      common /c3/chklal,chklalm1,shklal,chkl,/c4/rn1,aq1,aq2,q4,q5
      common /c5/chklm1,/c6/ak,t,analn
      data  ac/'if','mo','so','ms','un'/,eps/1.0d-7/

      ni=11
      no=22
      open(unit=ni,file='moddq3.in')
      open(unit=no,file='moddq3.ou')

      read(ni,*)aklb,rab,ra,alb,t
      read(ni,*)aq1,aq2,q4,q5
```

```
      read(ni,*)q3i,q3f

      akla=aklb*rab
      ak=aklb/alb
      aklal=akla*ra
      akl=akla+aklb
      chkl=dcosh(akl)
      chklm1=chkl-1.0
      chkla=dcosh(akla)
      chklam1=chkla-1.0
      shkla=dsinh(akla)
      chklal=dcosh(akla*ra)
      chklalm1=chklal-1.0
      shklal=dsinh(akla*ra)
      chklb=dcosh(aklb)
      chklbm1=chklb-1.0
      shklb=dsinh(aklb)
cc
cc  analn=Nal/TK
cc
      analn=-1.0/chklam1*(q4*chklalm1-q5*shklal)
      rn1=1.0/aq1/chklam1*(q4*chklalm1-q5*shklal)
      write(6,*)'rn1=',rn1

      x(1)=q3i
      ii=2
      rm1=1.0
      x(ii)=-rm1*aq2*chklbm1/shklb
      if(x(ii).gt.q3i.and.x(ii).lt.q3f) ii=ii+1
      rm1=-1.0
      x(ii)=-rm1*aq2*chklbm1/shklb
      if(x(ii).gt.q3i.and.x(ii).lt.q3f) ii=ii+1

      rm2=1.0
      q1=aq1
      x(ii)=chklbm1/(chkl-chklb)*(-rm2*aq2*shkla+q1*chklam1-q4*
     &  chklalm1+q5*shklal)
      if(x(ii).gt.q3i.and.x(ii).lt.q3f) ii=ii+1
      q1=-q1
      x(ii)=chklbm1/(chkl-chklb)*(-rm2*aq2*shkla+q1*chklam1-q4*
     &  chklalm1+q5*shklal)
```

```
      if(x(ii).gt.q3i.and.x(ii).lt.q3f) ii=ii+1
      rm2=-1.0
      q1=aq1
      x(ii)=chklbm1/(chkl-chklb)*(-rm2*aq2*shkla+q1*chklam1-q4*
     &   chklalm1+q5*shklal)
      if(x(ii).gt.q3i.and.x(ii).lt.q3f) ii=ii+1
      q1=-q1
      x(ii)=chklbm1/(chkl-chklb)*(-rm2*aq2*shkla+q1*chklam1-q4*
     &   chklalm1+q5*shklal)
      if(x(ii).gt.q3i.and.x(ii).lt.q3f) ii=ii+1

      rn2=1.0
      x(ii)=(rn2-rn1)*aq1*chklbm1/chklb
      if(x(ii).gt.q3i.and.x(ii).lt.q3f) ii=ii+1
      rn2=-1.0
      x(ii)=(rn2-rn1)*aq1*chklbm1/chklb
      if(x(ii).gt.q3i.and.x(ii).lt.q3f) ii=ii+1

      rn3=1.0
      q2=aq2
      x(ii)=((rn3-rn1)*aq1*chklam1+q2*shkla)/(chkl-chklb)
     &   *chklbm1
      if(x(ii).gt.q3i.and.x(ii).lt.q3f) ii=ii+1
      q2=-q2
      x(ii)=((rn3-rn1)*aq1*chklam1+q2*shkla)/(chkl-chklb)
     &   *chklbm1
      if(x(ii).gt.q3i.and.x(ii).lt.q3f) ii=ii+1
      rn3=-1.0
      q2=aq2
      x(ii)=((rn3-rn1)*aq1*chklam1+q2*shkla)/(chkl-chklb)
     &   *chklbm1
      if(x(ii).gt.q3i.and.x(ii).lt.q3f) ii=ii+1
      q2=-q2
      x(ii)=((rn3-rn1)*aq1*chklam1+q2*shkla)/(chkl-chklb)
     &   *chklbm1
      if(x(ii).gt.q3i.and.x(ii).lt.q3f) ii=ii+1

      rn4=1.0
  x(ii)=-rn4*chklbm1/chklb/chklam1*(q4*chklalm1-q5*shklal)
      if(x(ii).gt.q3i.and.x(ii).lt.q3f) ii=ii+1
      rn4=-1.0
  x(ii)=-rn4*chklbm1/chklb/chklam1*(q4*chklalm1-q5*shklal)
```

```
      if(x(ii).gt.q3i.and.x(ii).lt.q3f) ii=ii+1

      q1=aq1
      x(ii)=chklbm1/chklb*(q1-1.0/chklam1*(q4*chklalm1-q5*shklal))
      if(x(ii).gt.q3i.and.x(ii).lt.q3f) ii=ii+1
      q1=-aq1
      x(ii)=chklbm1/chklb*(q1-1.0/chklam1*(q4*chklalm1-q5*shklal))
      if(x(ii).gt.q3i.and.x(ii).lt.q3f) ii=ii+1

      q1=aq1
      q2=aq2
      x(ii)=chklbm1/(chkl-chklb)*(q1*chklam1+q2*shkla-q4*chklalm1
     &  +q5*shklal)
      if(x(ii).gt.q3i.and.x(ii).lt.q3f) ii=ii+1
      q2=-aq2
      x(ii)=chklbm1/(chkl-chklb)*(q1*chklam1+q2*shkla-q4*chklalm1
     &  +q5*shklal)
      if(x(ii).gt.q3i.and.x(ii).lt.q3f) ii=ii+1
      q1=-aq1
      x(ii)=chklbm1/(chkl-chklb)*(q1*chklam1+q2*shkla-q4*chklalm1
     &  +q5*shklal)
      if(x(ii).gt.q3i.and.x(ii).lt.q3f) ii=ii+1
      q2=aq2
      x(ii)=chklbm1/(chkl-chklb)*(q1*chklam1+q2*shkla-q4*chklalm1
     &  +q5*shklal)
      if(x(ii).gt.q3i.and.x(ii).lt.q3f) ii=ii+1

      q1=aq1
      q2=aq2
      x(ii)=chklbm1*(chkla*chklb-1.0)/(chklb*chklam1*chklm1-shkla
     & *shklb*chklbm1)*(q1*chklam1+q2*shkla-q4*chklalm1
     2 +q5*shklal)
      if(x(ii).gt.q3i.and.x(ii).lt.q3f) ii=ii+1
      q2=-aq2
      x(ii)=chklbm1*(chkla*chklb-1.0)/(chklb*chklam1*chklm1-shkla
     & *shklb*chklbm1)*(q1*chklam1+q2*shkla-q4*chklalm1
     2 +q5*shklal)
      if(x(ii).gt.q3i.and.x(ii).lt.q3f) ii=ii+1
      q1=-aq1
      x(ii)=chklbm1*(chkla*chklb-1.0)/(chklb*chklam1*chklm1-shkla
     & *shklb*chklbm1)*(q1*chklam1+q2*shkla-q4*chklalm1
```

```
2    +q5*shklal)
      if(x(ii).gt.q3i.and.x(ii).lt.q3f) ii=ii+1
      q2=aq2
      x(ii)=chklbm1*(chkla*chklb-1.0)/(chklb*chklam1*chklm1-shkla
&    *shklb*chklbm1)*(q1*chklam1+q2*shkla-q4*chklalm1
2    +q5*shklal)
      if(x(ii).gt.q3i.and.x(ii).lt.q3f) ii=ii+1

      x(ii)=q3f
      if(ii.le.0) then
        write(6,*)'Q3i,Q3f=',q3i,q3f
        write(6,*)'Please check these values!'
        stop
      end if

      call sort(x,ii)
          do i=1,ii
            write(6,*)'i,x(i)=',i,x(i)
          end do
      k0=0
      k1=0
      do j=1,ii-1
        if(dabs(x(j+1)-x(j)).gt.eps) then
          q3=(x(j)+x(j+1))/2.0
          call dmode(q3,k)
            if(k.ne.k0) then
            k1=k1+1
            y(k1,1)=x(j)
            y(k1,2)=x(j+1)
            md(k1)=k
            k0=k
          else
            y(k1,2)=x(j+1)
          end if
        end if
      end do

      write(no,*)
      write(no,*)' Results for the given system from moddq3.f:'
      write(no,*)
      do j=1,k1
        write(no,100) y(j,1),y(j,2),ac(md(j))
```

```
100     format(1x,'(',f10.7,' < Q3 < ',f10.7,'),  mode=',a3)
        end do

        write(no,*)
        write(no,*)'  The ratios at the mid-point of each Q3 region:'
        write(no,*)
        write(no,103)
103     format(1x,7x,'q3',9x,'rm1',9x,'rm2',9x,'rn2',9x,'rn3')
        write(no,*)
        do j=1,k1
          q3=(y(j,1)+y(j,2))/2.0
          call dmodew(q3,no)
        end do


        stop
        end
cc
cc *************************************************************
cc  the subroutines
cc *************************************************************
cc
cc *************************************************************
cc  sort(), sorting from min. to max.
cc
        subroutine sort(x,ii)
        implicit real*8 (a-h,o-z)
        dimension x(35)

          do j=1,ii-1
            do k=j+1,ii
              if(x(k).lt.x(j)) then
                tem=x(k)
                x(k)=x(j)
                x(j)=tem
              end if
            end do
          end do

        return
        end
```

```
cc
cc ***************************************************************
cc  dmode(), determining the mode code
cc
        subroutine dmode(q3,k)
        implicit real*8 (a-h,o-z)
        common /c1/chkla,chklam1,shkla,/c2/chklb,chklbm1,shklb
     common /c3/chklal,chklalm1,shklal,chkl,/c4/rn1,aq1,aq2,q4,q5
        common /c5/chklm1,/c6/ak,t,analn

         iflag=0
         rm1=-q3/aq2*shklb/chklbm1
         arm1=dabs(rm1)
         rn2=q3*chklb/chklbm1/aq1+rn1
         arn2=dabs(rn2)
cc
cc      k = 1,  IF
c           2,  MO
cc          3,  SO
cc          4,  MS
cc          5,  UN
cc
         if(arm1.le.1.0d0.and.arn2.le.1.0d0) then
          k=1
          iflag=1
         else if(arm1.gt.1.0d0) then
          q2=aq2
          if(q3.lt.0.0d0) q2=-q2
            rn3=(-q2*shkla+q3*(chkl-chklb)/chklbm1)/aq1/chklam1+rn1
          arn3=dabs(rn3)
          if(arn3.le.1.0d0) then
           k=2
           iflag=1
          else
           k=4
           iflag=1
          end if
         else if(arn2.gt.1.0d0) then
          q1=aq1
          if(rn2.lt.0.0d0) q1=-q1
           rm2=1.0/aq2/shkla*(q1*chklam1-q3*(chkl-chklb)/chklbm1
  &      -q4*chklalm1+q5*shklal)
```

```
        arm2=dabs(rm2)
        if(arm2.le.1.0d0) then
         k=3
         iflag=1
        else
         q2=aq2
         if(rm2.gt.0.0d0) q2=-q2
           rn3=(-q2*shkla+q3*(chkl-chklb)/chklbm1)/aq1/chklam1+rn1
         arn3=dabs(rn3)
         if(arn3.le.1.0d0) then
          k=2
          iflag=1
         end if
        end if
       end if

       if(iflag.eq.1) return

       q1=aq1
       if(rn2.lt.0.0d0) q1=-q1
         rm2=1.0/aq2/shkla*(q1*chklam1-q3*(chkl-chklb)/chklbm1
     &    -q4*chklalm1+q5*shklal)
       arm2=dabs(rm2)
       if(arm2.le.1.0d0) then
        q2=aq2
        if(rm2.gt.0.0d0) q2=-q2
        rn3=(-q2*shkla+q3*(chkl-chklb)/chklbm1)/aq1/chklam1+rn1
        arn3=dabs(rn3)
        if(arn3.gt.1.0d0) then
         k=3
         iflag=1
        end if
       else if(arn2.gt.1.0d0) then
        k=4
        iflag=1
       end if

       if(iflag.eq.0) then
         write(6,*)'q3=',q3,' unknown mode!'
        k=5
       end if
```

```
      return
      end

cc
cc ***********************************************************
cc  dmodew(), output ratios
cc
      subroutine dmodew(q3,no)
      implicit real*8 (a-h,o-z)
      common /c1/chkla,chklam1,shkla,/c2/chklb,chklbm1,shklb
      common /c3/chklal,chklalm1,shklal,chkl,/c4/rn1,aq1,aq2,q4,q5
      common /c5/chklm1,/c6/ak,t,analn

       iflag=0
       rm1=-q3/aq2*shklb/chklbm1
       arm1=dabs(rm1)
       rn2=q3*chklb/chklbm1/aq1+rn1
       arn2=dabs(rn2)

       if(arm1.le.1.0d0.and.arn2.le.1.0d0) then
        q1=aq1
        q2=aq2
        if(rn2.lt.0.0d0) q1=-q1
        if(q3.lt.0.0d0) q2=-q2
        iflag=1
       else if(arm1.gt.1.0d0) then
        q2=aq2
        if(q3.lt.0.0d0) q2=-q2
          rn3=(-q2*shkla+q3*(chkl-chklb)/chklbm1)/aq1/chklam1+rn1
        arn3=dabs(rn3)
        q1=aq1
        if(rn3.lt.0.0d0) q1=-q1
        iflag=1
       else if(arn2.gt.1.0d0) then
        q1=aq1
        if(rn2.lt.0.0d0) q1=-q1
         rm2=1.0/aq2/shkla*(q1*chklam1-q3*(chkl-chklb)/chklbm1
     &  -q4*chklalm1+q5*shklal)
        arm2=dabs(rm2)
        if(arm2.le.1.0d0) then
```

```
        q2=aq2
        if(rm2.gt.0.0d0) q2=-q2
        iflag=1
      else
        q2=aq2
        if(rm2.gt.0.0d0) q2=-q2
         rn3=(-q2*shkla+q3*(chkl-chklb)/chklbm1)/aq1/chklam1+rn1
        arn3=dabs(rn3)
        if(arn3.le.1.0d0) then
         q1=aq1
         if(rn3.lt.0.0d0) q1=-q1
         iflag=1
        end if
      end if
     end if

     if(iflag.eq.1) goto 111

     q1=aq1
     if(rn2.lt.0.0d0) q1=-q1
     rm2=1.0/aq2/shkla*(q1*chklam1-q3*(chkl-chklb)/chklbm1
&    -q4*chklalm1+q5*shklal)
     arm2=dabs(rm2)
     if(arm2.le.1.0d0) then
      q2=aq2
      if(rm2.gt.0.0d0) q2=-q2
      rn3=(-q2*shkla+q3*(chkl-chklb)/chklbm1)/aq1/chklam1+rn1
      arn3=dabs(rn3)
      if(arn3.gt.1.0d0) then
       q1=aq1
       if(rn3.lt.0.0d0) q1=-q1
       iflag=1
      end if
     else if(arn2.gt.1.0d0) then
      q2=aq2
      if(q3.lt.0.0d0) q2=-q2
      iflag=1
     end if

111  continue

    rm2=1.0/aq2/shkla*(q1*chklam1-q3*(chkl-chklb)/chklbm1
```

```
     &    -q4*chklalm1+q5*shklal)
           rn3=(-q2*shkla+q3*(chkl-chklb)/chklbm1)/aq1/chklam1+rn1
          write(no,100)q3,rm1,rm2,rn2,rn3
100        format(1x,6(f11.6,1x))

          return
          end
```

APPENDIX B

THE SAMPLE INPUT AND OUTPUT FOR THE PROGRAM OF MODE DETERMINATION

Input file: moddq3.in

0.75, 1.4, 0.5, 100.0, 30.0, KLb, La/Lb, la/La, Lb (in.), T (lbf)
0.5, 0.25, 1.50, 0.85, |Q1|, |Q2|, Q4, Q5, (in.)
-0.2, 0.2, Q3i, Q3f, (in.)

Output file: moddq3.ou

Results for the given system from moddq3.f:

(-.2000000 < Q3 < -.0584945), mode=ms
(-.0584945 < Q3 < -.0174814), mode=so
(-.0174814 < Q3 < .0895893), mode=if
(.0895893 < Q3 < .1415692), mode=mo
(.1415692 < Q3 < .2000000), mode=ms

The ratios at the mid-point of each Q3 region:

q3	rm1	rm2	rn2	rn3
-0.129247	1.442663	2.388505	-1.982081	-2.441704
-0.037988	0.424023	0.597564	-1.180190	-0.582145
0.036054	-0.402436	-0.855490	-0.529587	-1.150047
.115579	-1.290100	-0.489955	0.169197	0.470413
.170785	-1.906305	-1.573345	.654283	1.595312

VITA

Bin Fang

Candidate for the Degree of

Doctor of Philosophy

Thesis: LATERAL WEB BEHAVIOR OF INTERACTIVE WEB SYSTEMS

Major Field: Mechanical Engineering

Biographical:

Personal Data: Born in Lanxi, Zhejiang, P. R. China, November 8, 1957, the son of Jiqiu Fang and Xiurong Dai.

Education: Graduated from Xinzhao High School, Heilongjiang, P. R. China, in June, 1975; received Bachelor of Science degree in Mechanical Engineering from Fuxin Mining College at Fuxin, Liaoning, P. R. China in June, 1982; received Master of Science degree in Mechanical Engineering from Oklahoma State University at Stillwater in December, 1985; completed requirements for the Doctor of Philosophy degree at Oklahoma State University in December, 1990.

Professional Experience: Research assistant, Department of Mechanical and Aerospace Engineering, Oklahoma State University, January, 1986 to August, 1990.